

# UC San Diego

## UC San Diego Electronic Theses and Dissertations

### Title

Metabolic Reprogramming and Interactions Underlying Bacillus subtilis Endospore Transition to and Emergence from Dormancy

### Permalink

<https://escholarship.org/uc/item/6s00x8fw>

### Author

Riley, Eammon Patrick

### Publication Date

2020

Peer reviewed|Thesis/dissertation

UNIVERSITY OF CALIFORNIA SAN DIEGO

Metabolic Reprogramming and Interactions Underlying *Bacillus subtilis* Endospore  
Transition to and Emergence from Dormancy

A dissertation submitted in partial satisfaction of the  
requirements for the degree Doctor of Philosophy

in

Biology

by

Eammon Patrick Riley

Committee in charge:

Professor Kit Pogliano, Chair  
Professor Rachel Dutton  
Professor Terence Hwa  
Professor James Wilhelm  
Professor Karsten Zengler

2020

Copyright

Eammon Patrick Riley, 2020

All rights reserved.

The dissertation of Eammon Patrick Riley is approved, and it is acceptable in quality and form for publication on microfilm and electronically:

---

---

---

---

---

Chair

University of California San Diego

2020

## DEDICATION

To my family: Alan and Heather Riley, Erin Goodell, Felicia Clark, Jake and Marcus LaCross, and to my San Diego family: Julie Ann, Theresa, Daniel, and Dante Alvarado, you have all blessed me beyond my wildest dreams. None of this would be possible without your continued support. I owe you all a debt of gratitude that can never be repaid.

## TABLE OF CONTENTS

Signature Page.....	iii
Dedication.....	iv
Table of Contents.....	v
List of Figures.....	vii
List of Tables.....	ix
Acknowledgements.....	x
Vita.....	xi
Abstract of the Dissertation.....	xii
Chapter I – Introduction.....	1
Brief overview of development and multicellularity in bacteria.....	1
Discovery of endospore formation.....	3
Developmental stages of endospore formation and spore revival.....	4
Genetic analysis of sporulation mutants.....	8
Sporulation initiation.....	12
Cell-specific gene expression.....	14
The future of sporulation research.....	20
Figures.....	24
References.....	26
Chapter II – Spatiotemporally regulated proteolysis to dissect the role of vegetative proteins during <i>Bacillus subtilis</i> sporulation: cell-specific requirement of $\sigma^H$ and $\sigma^A$ .....	34
Acknowledgements.....	52
Supplementary figures.....	53
Supplementary tables.....	61
Chapter III – Metabolic differentiation and intercellular nurturing underpin bacterial endospore formation.....	73
Abstract.....	73
Main text.....	73
Notes.....	86
Materials and methods.....	87
Strain construction.....	87
Culture conditions.....	87
Fluorescence microscopy.....	88
Batch culture microscopy.....	88
Timelapse microscopy.....	89
Spore titer assays.....	89
BONCAT.....	89
Fluorescence recovery after photobleaching (FRAP).....	92
Fluorescence loss in photobleaching (FLIP).....	93
Forespore to mother cell GFP fluorescence ratio quantification.....	93

Quantification of native CitZ-GFP depletion.....	94
Quantification of phase bright spores.....	94
Stable isotope labeling with amino acids in cell culture (SILAC).....	95
Spore purification.....	96
Extraction of spore coat proteins.....	96
Extraction of small acid soluble proteins.....	96
Sample preparation for mass spectrometry.....	97
LC-MS/MS Analysis.....	97
Statistical analysis.....	98
Acknowledgements.....	99
Figures.....	100
Tables.....	115
References.....	128
Chapter IV - A novel proteolytic pathway reprograms forespore metabolism to promote the transition to and exit from cellular dormancy.....	131
Abstract.....	131
Significance statement.....	131
Introduction.....	132
Results.....	134
Discussion.....	142
Materials and methods.....	144
Strain construction.....	144
Culture conditions.....	145
Fluorescence and phase-contrast microscopy.....	145
Batch culture microscopy.....	146
Forespore to mother cell GFP fluorescence ratio quantification.....	146
Fluorescence timelapse microscopy.....	147
Spore purification.....	148
Phase-contrast timelapse microscopy.....	148
Spore titers.....	149
Quantification of spore germination by loss of optical density.....	149
Acknowledgements.....	151
Figures.....	152
Tables.....	165
References.....	176
Chapter V – Conclusions and outlook.....	179
Novel approaches to study spore formation.....	179
Metabolic nurturing during spore formation.....	182
Mechanisms of metabolic differentiation during spore formation.....	187
References.....	190

## LIST OF FIGURES

Figure 1.1: Morphological stages of spore formation.....	24
Figure 1.2: Morphological stages of spore revival.....	25
Figure 2.1: The sporulation pathway in <i>B. subtilis</i> .....	35
Figure 2.2: Degradation of an abundant protein does not affect turnover of a native ClpXP substrate.....	36
Figure 2.3: Optimization of cell- and stage-specific protein degradation system.....	38
Figure 2.4: Cell- and stage-specific degradation of vegetative proteins.....	41
Figure 2.5: $\sigma^H$ activity is only required in predivisional cells.....	42
Figure 2.6: Cell-specific degradation of $\sigma^A$ .....	43
Figure 2.7: Forespore $\sigma^A$ contributes to spore germination and outgrowth.....	45
Figure 2.S1: Production of SspB <sup>Ec</sup> from a xylose-dependent promoter does not affect the progression of sporulation.....	53
Figure 2.S2: Expression pattern from the sustained and late promoters selected for further characterization.....	54
Figure 2.S3: Evidence that SspB <sup>Ec</sup> is not limiting for degradation during sporulation.....	55
Figure 2.S4: Cell-specific degradation of $\sigma^G$ -GFP-ssrA* and $\sigma^K$ -GFP-ssrA*.....	57
Figure 2.S5: Production of SspB <sup>Ec</sup> from a xylose inducible promoter triggers the efficient degradation of $\sigma^H$ -ssrA*.....	58
Figure 2.S6: Number of colonies upon extended incubation of spore titer plates at 30°C.....	59
Figure 2.S7: Germination assays by loss of O.D.....	60
Figure 3.1: Metabolic reprogramming during sporulation.....	100
Figure 3.2: Intercellular metabolic dependency during sporulation.....	101
Figure 3.3: Arginine is transported between the mother cell (MC) and the forespore (FS).....	102
Figure 3.4: A-Q is required for transport of small molecules between mother cell and forespore.....	103
Figure 3.S1: Metabolic asymmetry during spore formation.....	104



Figure 3.S2: Validation of <i>ssrA</i> *-tagged protein degradation.....	105
Figure 3.S3: Cell-specific degradation of all the metabolic proteins tested.....	107
Figure 3.S4: Visualization of cell-specific degradation of a ribosomal protein.....	109
Figure 3.S5: Reasoning for using a <i>SpoIVA</i> <sup>-</sup> mutant in BONCAT experiments.....	110
Figure 3.S6: Cell-specific SILAC experiments.....	111
Figure 3.S7: BONCAT experiments in <i>spolIIA</i> and <i>spolIQ</i> mutant sporangia.....	113
Figure 3.S8: FLIP and FRAP experiments in <i>spolIIA</i> and <i>spolIQ</i> mutant sporangia.....	114
Figure 4.1: Mother cell and forespore become metabolically differentiated during spore formation.....	152
Figure 4.2: Two mechanisms underlie the metabolic reprogramming of the forespore.....	153
Figure 4.3: ClpCP is required for proteolysis of CitZ in the forespore, but does not confer cell-specificity.....	154
Figure 4.4: YjbA is required for ClpCP-mediated proteolysis of CitZ in the forespore...	155
Figure 4.5: Spores lacking YjbA are sensitive to NaOCl-induced oxidative stress.....	156
Figure 4.6: Degrading CitZ via STRP does not suppress the NaOCl sensitivity of the $\Delta yjbA$ mutant.....	157
Figure 4.S1: Citrate synthase is depleted to a larger extent in the forespore than other metabolic enzymes.....	158
Figure 4.S2: Suppression of forespore growth through <i>spolIQ</i> inactivation does not stabilize citrate synthase in the forespore.....	159
Figure 4.S3: New protein synthesis is required in the forespore for the depletion of citrate synthase.....	160
Figure 4.S4: ClpCP is required for the depletion of citrate synthase in the forespore...	161
Figure 4.S5: ClpCP does not confer cell-specificity to the proteolysis of citrate synthase.....	162
Figure 4.S6: Screen identifying YjbA as the novel ClpCP adaptor protein.....	163
Figure 4.S7: Sporangia lacking YjbA suffer no severe defects in development.....	164

## LIST OF TABLES

Table 2.S1: Spore titers.....	61
Table 2.S2: Strains used in this study.....	63
Table 2.S3: Plasmids used in this study.....	67
Table 2.S4: Oligonucleotides used in this study.....	69
Table 3.S1: Spore titers.....	115
Table 3.S2: Strains used in this study.....	116
Table 3.S3: Plasmids used in this study.....	121
Table 3.S4: Oligonucleotides used in this study.....	123
Table 4.S1: Strains used in this study.....	165
Table 4.S2: Plasmids used in this study.....	171
Table 4.S3: Oligonucleotides used in this study.....	172

## ACKNOWLEDGEMENTS

I would like to acknowledge all the members of the Kit and Joe Pogliano labs that I have had the pleasure of working with over the past seven years. In particular, I would like to sincerely thank Javier Lopez-Garrido and Alan Derman for their unceasing support. Their insights and friendship have been absolutely instrumental to my development as a scientist. I would also like to thank my mentor, Kit Pogliano, for all of her encouragement throughout my dissertation. Her positivity and scientific rigor are certainly attributes to which I aspire. I would also like to graciously thank all the members of my cohort, my BGSE group, and my dissertation committee for their enlightening discussions. Finally, I would like to thank my family and friends, without whom none of this would be possible.

Chapter II, in full, is a reproduction of the material as it appears in *Molecular Microbiology* 2018. Riley, Eammon P.; Trinquier, Aude; Reilly, Madeline L.; Durchon, Marine; Perera, Varahenage R.; Pogliano, Kit; Lopez-Garrido, Javier, John Wiley & Sons Ltd, 2018. The dissertation author was the primary investigator and author of this paper.

Chapter III, in full, is currently being prepared for submission to *Science*. Riley, Eammon P.; Lopez-Garrido, Javier; Sugie, Joseph; Liu, Roland B.; Pogliano, Kit. The dissertation author was the primary investigator and author of this paper.

Chapter IV, in full, is currently being prepared for submission to *PNAS*. Riley, Eammon P.; Sugie, Joseph; Enustun, Eray; Armbruster, Emily; Ravishankar, Sumedha; Pogliano, Kit. The dissertation author was the primary investigator and author of this paper.

## VITA

- 2011 Bachelor of Science, Bates College
- 2011-2013 Research Assistant, Harvard Medical School
- 2020 Doctor of Philosophy, University of California San Diego

## PUBLICATIONS

Archambault, L., Linscott, J., Swerdlow, N., Boyland, K., Riley, E., and Schlax, P. (2013) Translational efficiency of *rpoS* mRNA from *Borrelia burgdorferi*: effects of the length and sequence of the mRNA leader region. *Biochem. Biophys. Res. Commun.* 433, 73–78.

Meeske, A. J., Riley, E. P., Robins, W. P., Uehara, T., Mekalanos, J. J., Kahne, D., Walker, S., Kruse, A.C., Bernhardt, T.G., Rudner, D.Z. (2016) SEDS proteins are a widespread family of bacterial cell wall polymerases. *Nature* 537, 634–638.

Lamsa, A., Lopez-Garrido, J., Quach, D., Riley, E.P., Pogliano, J., and Pogliano, K. (2016) Rapid Inhibition Profiling in *Bacillus subtilis* to identify the mechanism of action of new antimicrobials. *ACS Chem Biol* 11, 2222–2231.

Riley, E.P., Trinquier, A., Reilly, M.L., Durchon, M., Perera, V.R., Pogliano, K. and Lopez-Garrido, J. (2018) Spatiotemporally regulated proteolysis to dissect the role of vegetative proteins during *Bacillus subtilis* sporulation: cell-specific requirement of  $\sigma^H$  and  $\sigma^A$ . *Mol Microbiol*, 108, 45–62.

ABSTRACT OF THE DISSERTATION

Metabolic Reprogramming and Interactions Underlying *Bacillus subtilis* Endospore  
Transition to and Emergence from Dormancy

by

Eammon Patrick Riley

Doctor of Philosophy in Biology

University of California San Diego, 2020

Professor Kit Pogliano, Chair

Cellular differentiation is a crucial feature of developmental processes in diverse organisms. Endospore formation represents a developmental pathway entailing the transformation of rapidly dividing vegetative cells into metabolically dormant and highly resilient spores. Sporulation commences with polar cell division, which divides the sporangium into the mother cell (larger) and forespore (smaller). Despite initially having

similar molecular compositions, the two cells activate cell-autonomous programs of gene expression, causing their fates to diverge. The mother cell engulfs the forespore and lyses to liberate the mature spore. Upon sensing nutrient availability, spores readily escape dormancy, resuming growth within hours.

One of the few remaining deficiencies in the knowledge of sporulation is the developmental role played by proteins synthesized during vegetative growth. Although these proteins comprise the majority of the proteome, the lack of approaches to inactivate proteins in a spatiotemporally controlled manner without perturbing vegetative growth or sporulation initiation has prevented a systematic interrogation of their contribution to spore formation and revival.

We have developed a versatile genetic framework that harnesses cell-specific gene expression to target proteins for degradation in a spatiotemporally regulated manner, thereby allowing us to investigate the role of metabolic enzymes during development. We have employed this methodology to document the metabolic interactions underlying the spore's transition to dormancy, finding that the forespore becomes dependent on mother cell-derived metabolic precursors for biosynthesis. Our results empirically validate a long-standing model that the mother cell assumes the biosynthetic burden and nurtures the forespore with metabolites through a feeding tube-like apparatus connecting the two cells.

Our results also suggest that the metabolic capabilities of the forespore are drastically reprogrammed in preparation for dormancy, yielding a profound metabolic differentiation of the mother cell and forespore. Enzymes functioning in diverse biosynthetic pathways are rapidly depleted from the forespore. We have found that YjbA governs this pathway by targeting key metabolic enzymes for ClpCP-mediated proteolysis in the forespore, and that it is required for the efficient emergence from cellular dormancy under stress conditions. Altogether, our methodology has enabled the

dissection of many facets of spore formation and revival, and will be instrumental in future work.

## CHAPTER I

### Introduction

#### **Brief overview of development and multicellularity in bacteria**

Developmental processes occur throughout all domains of life and govern the transformation of single cells into tissues, organs, organisms, and even entire ecosystems. Defects in development are associated with a multitude of human pathologies ranging from spina bifida<sup>1</sup> to cancer<sup>2</sup>. Given the complexity of the human body plan, which is comprised of tens of trillions of cells, the quest to understand how single cells develop into complex, multicellular organisms began by studying cell lineages in simpler model organisms, such as *Caenorhabditis elegans*<sup>3</sup>. Although such studies have significantly advanced our understanding of the basic principles of development, the precise mechanisms by which simple units develop into complex systems remain enigmatic.

One of the hallmarks of development is differentiation, the process by which cells are reprogrammed to become functionally specialized from their ancestors. A crucial facet underlying differentiation is the generation of asymmetry, which allows two genetically identical cells to assume different fates as a product of development. Cells employ numerous strategies to achieve asymmetry including cell-to-cell signaling<sup>4</sup>, biochemical gradients<sup>5</sup>, and differential gene expression<sup>6</sup>. Because of the small size and relatively simple morphologies of bacterial cells, these complex behaviors were once thought to be restricted to eukaryotes. Recently, however, scientists have come to appreciate a myriad of developmental processes and intricate, multicellular behaviors in prokaryotes. Among these include heterocyst formation in *Anabaena nostoc*<sup>7</sup>, swarmer to stalk transition in *Caulobacter crescentus*<sup>8</sup>, fruiting body formation in *Myxococcus xanthus*<sup>9</sup>, quorum sensing in *Vibrio harveyi*<sup>10</sup>, multispecies biofilms<sup>11</sup>, and endospore formation<sup>12</sup>.



*Bacillus subtilis* cells can assume multiple different lifestyles when confronted with adverse environmental conditions, including competence<sup>13</sup>, biofilm formation<sup>14</sup>, and sporulation<sup>12</sup>, allowing this organism to flourish in diverse and fluctuating environments. Endospore formation (interchangeably referred to as spore formation or sporulation) constitutes one of the simplest developmental programs in all of biology, involving the differentiation of and interaction between just two cell-types. Although endospore formation is a feature common to several Gram (+) bacteria belonging to the genera *Bacillus* and *Clostridium*, this process is most extensively characterized in the bacterium *Bacillus subtilis*. The short doubling time, streamlined genome, genetic tractability, and abundance of molecular biological tools all render *Bacillus subtilis* an incredibly powerful model system to study developmental processes. Since endospore formation is not essential, it additionally represents an ideal platform to interrogate several fundamental cellular processes that are not ordinarily amenable to manipulation. Indeed, the study of endospore formation has illuminated the basic biology underpinning the phenomena of cell fate determination, membrane dynamics, signal transduction, and subcellular protein localization<sup>12</sup>.

The developmental program of spore formation is enacted in response to certain stimuli, including nutrient limitation and high cell density, and entails the transformation of an actively growing cell into a metabolically dormant spore with striking resistance properties<sup>15</sup>. This adaptation allows spore-forming bacteria to thrive and play crucial roles in complex and dynamic environments such as the mammalian gut and the soil. The process of spore formation involves the concerted action of hundreds of proteins that orchestrate a striking reorganization of cellular architecture, from a rod, to a cell-within-a-cell, and finally, to an ovoid spore possessing incredible resistance properties. This morphogenetic transformation is accompanied by dramatic changes in cellular physiology, all of which are completed within eight hours under standard conditions. The

end product of the sporulation pathway is a spore that is recalcitrant to a wide variety of environmental assaults, such as UV irradiation, desiccation, antibiotics, high temperatures, and bleach. These spores can persist in a dormant state for years, but the vegetative life cycle can be rapidly resumed when nutrient availability is restored through the process of germination<sup>16</sup>.

### **Discovery of endospore formation**

Endospores have long attracted the attention of researchers, and intermittently, the general public as well. One of the most notable features of endospores is the tremendous resistance properties they possess, which allow spores to survive long durations in harsh environments without nutrients<sup>17</sup>. It was the incredible resilience of spores that initially inspired their study by the scientific community. Although *Bacillus subtilis* spores had been observed as refractile bodies residing in bacterial cells by Christian Gottfried Ehrenberg as early as 1838<sup>18</sup>, Ferdinand Cohn was the first to perform studies characterizing their resistance properties in 1876<sup>19</sup>. He noted that the bacteria producing these bodies oscillated between two lifestyles, one of which was remarkably thermoresistant, surviving extended periods of boiling that killed most other microorganisms. This foundational discovery explained why microbial growth was observed in flasks that were boiled for prolonged periods of time, and proved critical to overturning the widely held belief of spontaneous generation. Cohn was thus the first to attribute the heat resistance properties of certain species of bacteria to endospore formation. Along with Robert Koch, he dedicated much of his time to further characterizing this process, documenting the transitions between the heat labile and heat resistant life cycles by microscopy<sup>20</sup>.

In the intervening decades, scientists pursued a cytological characterization of the process of spore formation with limited success<sup>21,22</sup>. The microscopes of that era lacked the resolution and contrast needed to achieve a detailed view of the architectural

changes occurring during spore development. It was not until the advent of electron microscopy and its application toward bacterial specimens that researchers were offered the first detailed glimpse of endospore formation at the cellular level<sup>23,24</sup>. Researchers used this technique to observe the cytological transformations that accompany spore formation in several different species, and quickly realized that the process of spore morphogenesis is highly conserved.

### **Developmental stages of endospore formation and spore revival**

The discovery that spore formation proceeds through a series of morphologically distinct stages that are highly conserved across species prompted researchers to formalize a system of nomenclature. In 1965, Antoinette Ryter defined six stages of spore formation based off her electron microscopy studies of *Bacillus subtilis*, which was subsequently refined to include an additional seventh stage<sup>25,26</sup>. The morphological stages of sporulation are briefly described below and are depicted in Figure 1. Also included below are the morphological stages of spore revival, though these were not outlined by the seminal work of Ryter, depicted in Figure 2.

The process of spore formation begins with vegetative cells, which comprise the developmental stage 0. When nutrients are replete, *Bacillus subtilis* cells enjoy a vegetative life cycle that is paradigmatic of the most comprehensively studied bacteria, such as *Escherichia coli*. During this phase of growth, cells double their length and cellular contents, segregate their genetic material to opposite poles of the cell, and then undergo binary fission at a medial position to produce two genetically identical offspring of equal size. Upon integrating numerous signals that indicate nutrient limitation, however, *Bacillus subtilis* cells exit the vegetative life cycle and embark on the developmental program of spore formation. The first observable feature of this transition is the remodeling of the chromosome into a structure spanning the entire length of the cell, called the axial filament<sup>27</sup>. The axial filament is composed of two complete copies of

the chromosome that are anchored to opposite cell poles at the origin of replication. Although axial filament formation defines stage I and is the first step unique to sporulation, no mutants have been isolated that arrest spore formation at this developmental stage.

In stage II of sporulation, the division machinery is repositioned from midcell to a single cell pole, where it directs the constriction of the cell envelope, thereby dividing the sporangium into two genetically identical sister cells that differ in size. The smaller cell forms the prospective spore and is known as the forespore, while the larger cell is called the mother cell. In addition to its polar localization, this septation event is also unique in the fact that it precedes chromosome segregation<sup>28</sup>. As a consequence, only an origin-proximal region containing about one-third of the chromosome is initially trapped in the forespore. The remaining two-thirds of the chromosome must be translocated into the forespore, a process, which occurs concomitantly with stage III<sup>29</sup>.

The next stage, denoted stage III, involves the engulfment of the forespore by the mother cell, in a dramatic process analogous to phagocytosis. During engulfment, the mother cell membranes migrate around the forespore, ultimately undergoing a fission event that releases the forespore as a free protoplast within the mother cell cytoplasm. It is important to note that following membrane fission, the forespore is surrounded by a thin layer of peptidoglycan sandwiched between two membranes, one mother cell-derived and the other forespore-derived. In this way, the layers surrounding the forespore resemble the Gram (-) cell envelope.

Following engulfment, layers of highly modified peptidoglycan, called cortex, are synthesized between the two membranes surrounding the forespore. A primordial germ cell wall is also assembled at this time, which serves as a scaffold for the synthesis of the vegetative cell wall following germination<sup>30</sup>. This developmental stage is

accompanied by a transition from phase-dark to phase-gray or phase-bright as assessed by phase-contrast microscopy.

The deposition of a multilayered, proteinaceous coat on the surface of the mother cell-derived outer forespore membrane constitutes stage V of sporulation. Coat assembly proceeds in multiple highly ordered and hierarchical stages<sup>31</sup>. First, a basement layer assembles at the surface of the outer forespore membrane, which is required to anchor the subsequent layers of the coat. Next comes encasement, where additional layers of coat are recruited to the outer forespore membrane and polymerize to form a complete shell that encompasses the developing spore<sup>32</sup>. This layer serves as a scaffold upon which the outer layers of the coat, including the crust, can assemble. The coat is impermeable to larger molecules, and therefore serves as a physical barrier to the spore core. The limited permeability of the coat also allows it to play a critical role in surveying the environment to ensure the proper timing of germination<sup>33</sup>. In addition to their structural functions, some coat proteins also have catalytic activities that help protect against oxidation and other environmental insults<sup>33</sup>. Both the cortex and the coat are essential to endowing the spore with its extreme resistance properties.

Stage VI of sporulation, known as maturation, is characterized not by readily apparent morphological changes, but rather by phenotypic changes in the resistance properties of the spore. During this stage, the calcium chelate of dipicolinate is synthesized in the mother cell and transported into the forespore, where it accumulates and results in the partial dehydration of the spore core<sup>34,35</sup>. Furthermore, a family of proteins, known as the small acid-soluble proteins (SASPs), assemble onto the forespore chromosome, causing it to adopt a unique, toroidal configuration<sup>36,37</sup>. Together, these processes are associated with the realization of the full suite of resistance properties that characterize *Bacillus subtilis* spores.

Stage VII represents the final stage of spore formation, and entails the production of cell wall degrading enzymes in the mother cell. The activity of these enzymes triggers the lysis of the mother cell, resulting in the liberation of the mature spore into the environment<sup>26</sup>. The spore can persist in its dormant state for millennia until favorable conditions return and vegetative growth is resumed through the processes of germination and outgrowth.

The processes governing the transformation of a dormant spore into a metabolically active, vegetatively growing cell are collectively referred to as spore revival, though this transformation can be subdivided into three distinct phases<sup>38</sup>. The first step in this process is germination, which involves the binding of germinants (alanine or a mixture of asparagine, glucose, fructose, and KCl) to their respective germination receptors embedded in the inner forespore membrane. This binding event commits the spores to the revival process and is likely to trigger a conformational change in proteins complexes involved in dipicolinic acid and monovalent cation efflux, though the exact mechanism remains unclear<sup>39</sup>. The release of dipicolinic acid coincides with the influx of water, which serves to partially rehydrate the spore core. These two processes activate the cortex lytic enzymes, CwlJ and SleB, which degrade the cortex, allowing a full rehydration of the germinating spore, ultimately resulting in a transition from phase-bright to phase-dark<sup>40,41</sup>. The entire process of germination is extraordinarily rapid, and is completed within seconds following germinant introduction. The prevailing model suggests that the process of germination is purely mechanical, occurring in the absence of any metabolic activity, though this model has been recently challenged<sup>38</sup>. The next phase of spore revival is called ripening, and in this stage, no morphological changes are evident, though the germinating spore becomes fully rehydrated, allowing the restoration of metabolic activity. During this period, protein synthesis resumes, sustained by precursors liberated from the proteolysis of the SASP proteins<sup>42</sup>. Outgrowth

constitutes the longest and final phase of spore revival. This stage involves the physical disruption of the spore integuments and the transition of the ovoid spore into an elongating rod, up until the time of the first medial cell division. Remarkably, the transition from a metabolically dormant spore to a fully functioning vegetative cell takes only an hour.

One of the main limitations of the classification system developed by Ryter is that the stages are defined solely by cell cytology, and represent discrete steps of a process that is truly continuous. Many of the processes underlying the observed morphological changes are gradual and occur concomitantly to one another. Therefore, sporulation can be interrupted at stages intermediate to those described by Ryter. Nonetheless, her work to formalize the landmark events of sporulation was crucial to providing a framework with which to characterize mutants compromised in spore formation.

### **Genetic analysis of sporulation mutants**

In the mid-20<sup>th</sup> century, the emergence of the field of molecular genetics allowed a thorough dissection of the gene products required for the morphological transformations occurring during spore formation. Mutants unable to form spores (asporogenous) or highly compromised in forming spores (oligosporogenous) were isolated in great numbers, and mapped using the classical genetic methods of transformation and transduction, which had recently been developed for *Bacillus subtilis*<sup>43,44,45,46</sup>. While electron microscopy allowed the foundations of sporulation research to be established, this technique is not amenable to the high throughput screening required to sift through the thousands of loci comprising the *Bacillus subtilis* chromosome. Thus, researchers developed forward genetic screens to isolate and characterize mutants en masse. One of the earliest and most efficient approaches developed to screen for genes involved in spore formation takes advantage of the fact that a constituent of the spore coat is pigmented, and therefore gives rise

characteristically dark colonies when sporogenous strains of *Bacillus subtilis* are plated on sporulation inducing media<sup>47</sup>. This assay allowed researchers to quickly screen mutant libraries for strains lacking the ability to produce this pigment. Since this pigment is produced during stage V of sporulation, however, mutants defective in subsequent stages of spore formation are not readily identified by this technique, leading to an overrepresentation of mutants compromised at early stages of development. Mapping these mutants, researchers quickly realized that there were multiple loci required for spore formation residing all throughout the chromosome<sup>43,44,48,49,50</sup>.

Ryter's definition of the developmental stages of sporulation provided an invaluable structure with which to evaluate mutant phenotypes. The cytological characterization of sporulation mutants led to the realization that the different mutants were blocked at different stages of spore formation. It immediately became useful to separate mutants into different classes, based on the stage at which morphogenesis is arrested<sup>26</sup>. Classically, these mutants were divided into two broad categories: *spo* and *ger*, though some genes escaped early screening techniques have been named directly after the molecular functions they encode, such as the genes encoding coat components (*cot*)<sup>51</sup> and the small acid soluble proteins (*ssp*)<sup>36</sup>.

The *spo* designation has traditionally been used to denote mutations that interfere with spore formation without affecting vegetative growth<sup>26</sup>. These mutants are classified according to the developmental stage beyond which sporulation is impaired when mutations are introduced at that given locus. Mutations that arrest sporulation at the same stage, but map to different loci, are distinguished by an additional capital letter. Thus, *spoIIIA* and *spoIIIE* represent mutations at two unique loci that both permit sporulation to proceed through engulfment, but prevent subsequent stages of sporulation such as the synthesis of cortex and coat assembly. It was subsequently discovered that certain *spo* loci were actually operons containing several genes. In these



cases, an additional uppercase letter is added to distinguish the different cistrons of the operon (for example, the *spoIIIA* locus consists of eight genes, named *spoIIIAA-spoIIIAH* in alphabetical order). The *ger* designation, on the other hand, is conventionally reserved for mutations that impede germination without affecting spore formation. The era of molecular genetics has allowed for the further refinement of *spo* and *ger* mutants, revealing that many of the loci implicated in spore formation and spore revival are in fact polycistronic.

Although this classification system has been instrumental in organizing research in the sporulation field for decades, the *spo* and *ger* classifications can also be problematic in certain cases. For instance, germination occurs in the absence of macromolecular synthesis, meaning that the proteins encoded by the *ger* loci are actually synthesized during sporulation<sup>52</sup>. The processes of spore formation and germination are so closely intertwined, it can be difficult to separate mutations that specifically block germination from ones that simply produce inviable, yet structurally sound, spores. Indeed, some of the *ger* mutants originally isolated have defects in spore formation<sup>53</sup>, while some of the *spo* mutants have been found to suffer germination defects<sup>54</sup>. Additionally, certain proteins may function at multiple stages of development, but defects in earlier stages may mask their involvement in later stages. Finally, mutants that compromise vegetative growth are by definition excluded from the *spo* designation, though it is possible that the products of these genes play crucial roles in development<sup>55</sup>. Nevertheless, the *spo* and *ger* nomenclature system has provided a remarkably effective framework within which to isolate and characterize mutants.

Other early screening techniques made use of biochemical assays to monitor the production of certain sporulation-specific enzymes. These include alkaline phosphatase, the activity of which is increased up to 40-fold during stage II in sporulation<sup>56</sup>, and glucose dehydrogenase<sup>57</sup>, which accumulates at the transition between stages III and

IV, among others. Although biochemical markers of several stages of sporulation have been discovered, screening a large volume of mutants by these methods is incredibly labor intensive. Therefore, plating techniques remained the gold standard to identify novel sporulation factors.

The development of new technologies has coincided with advancements in the knowledge of sporulation, with each technique offering higher sensitivity and spatiotemporal resolution. The introduction of *lacZ* containing transposons facilitated the mapping of sporulation mutants and enabled researchers to decipher the temporal pattern of gene expression through the measurement of  $\beta$ -galactosidase activity<sup>58</sup>. Work using these techniques made it clear that gene expression is spatiotemporally regulated in the sporangium. More recently, innovations in fluorescence microscopy have allowed dynamic processes of the cell to be visualized in vivo, providing insights into the functions of proteins produced during development. Techniques such as RNA-seq and microarrays have allowed for the elucidation and further refinement of the transcriptional profiles of sporulating cells<sup>59,60</sup>. Advances in whole genome sequencing have opened an entirely new field of comparative genomics, allowing researchers to infer new genes that are required for spore formation<sup>61</sup>. Finally, the advent of Tn-seq<sup>62</sup> and CRISPRi<sup>63</sup> methodologies has allowed the entire genome to be efficiently screened for novel factors acting during spore formation.

Altogether, these screens conducted over the past half-century have uncovered over 500 genes involved in sporulation and nearly 50 genes involved in germination, revealing that a significant fraction of the *Bacillus subtilis* genome is dedicated to the developmental processes of spore formation and spore revival. Strains harboring mutations in these genes suffer spore titer defects ranging over eight orders of magnitude. Thanks to the concerted effort of numerous researchers, a relatively

comprehensive understanding of how the *spo* and *ger* loci contribute to the processes of spore formation and spore revival, respectively, has been achieved.

### **Sporulation initiation**

The initiation of sporulation is tightly regulated and involves the integration of multiple signals indicative of nutrient exhaustion, chief among these being the depletion of guanosine triphosphate (GTP) levels, but also the replication state of the chromosome and cell density<sup>64</sup>. Upon sensing nutrient deprivation, cells execute a series of bet-hedging strategies before ultimately committing to the developmental program of spore formation<sup>65</sup>. This behavior results in an asynchronous activation of sporulation within a population, with only a fraction of the cells initially entering this energy intensive and time consuming pathway. Before initiating spore formation, a subset of the population begins to secrete toxins to cannibalize neighboring cells, thereby liberating nutrients and delaying the onset of sporulation<sup>66</sup>.

If starvation conditions persist, Spo0A, a transcription factor that serves as the master regulator of spore formation, is activated, which governs entry into the sporulation pathways, along with the stationary phase-specific sigma factor,  $\sigma^H$ . The activity of Spo0A is modulated by phosphorylation status, which is controlled by a phosphorelay system consisting of five autophosphorylating histidine kinases, KinA-KinE, and two phosphotransferases, Spo0F and Spo0B. This repertoire of histidine kinases senses the environment and responds to different stimuli indicating nutrient depletion<sup>67</sup>. Studies have implicated fermentation products as the ligands triggering kinase activity, but the exact ligands for each of the kinases have yet to be established. The phosphoryl group from the histidine kinases is ultimately transferred to Spo0A via two phosphotransferases that work in succession, Spo0F and Spo0B<sup>68</sup>. The phosphorylation of Spo0F and Spo0A can be reversed by a collection of Rap phosphatases and Spo0E, respectively<sup>69</sup>. The activity of the Rap phosphatases is

modulated by small pheromone peptides (Phr), which constitute a quorum-sensing module that signals and responds to high cell density<sup>70</sup>. Altogether, the phosphorelay system adds another robust layer of regulation to ensure that cells only commit to the sporulation pathway when certain environmental conditions are met.

Once activated, phosphorylated Spo0A (Spo0A~P) serves as both a transcriptional activator and a transcriptional repressor that governs the expression of over 100 genes involved in the entry into sporulation. The intracellular levels of Spo0A~P that accumulate mediate a decision between two different lifestyles, providing an additional bet-hedging opportunity where only a fraction of the population activates the sporulation pathway. Cells exhibiting lower levels of Spo0A~P differentiate into matrix producing cells, resulting in biofilm formation<sup>71</sup>. Alternatively, cells accumulating higher levels of Spo0A~P employ a feed forward loop to generate more Spo0A~P and proceed with spore formation<sup>72</sup>. The progressive accumulation of Spo0A is thought to provide temporal regulation over the expression of the Spo0A regulon<sup>73</sup>. The products of the Spo0A regulon promote the extensive remodeling of the chromosome into the axial filament, a structure that spans the entire length of the cell<sup>27</sup>. To build this structure, a protein called RacA anchors the origin regions of the chromosomes to opposite cell poles<sup>74</sup>. Spo0A blocks additional rounds of DNA replication both directly, by sterically occluding replication factors from the origin region of the chromosome, and indirectly, by directing the expression of *sirA* and *sda*<sup>75,76</sup>. These two factors survey the replication status of the chromosome, and ensure that sporulation is only initiated if there are exactly two copies present, one of which is destined for each of the two daughter cells.

The pre-divisional sporangium is prepared for cell division once the chromosome has assumed the axial filament conformation. Unlike vegetative cells, which undergo cytokinesis at a medial position, sporangia perform septation at a single cell pole, in a process known as polar septation. The proteins RefZ and SpoIIIE, which are produced

under the control of Spo0A, dictate the redistribution of the division machinery from midcell to the poles<sup>77,78</sup>. SpoIIIE interacts directly with the cell division protein FtsZ, and directs the polar assembly of the divisome. Interestingly, SpoIIIE preferentially localizes to the side of the division septum that ultimately becomes the spore<sup>79</sup>. Because of the extreme polar localization of the division septum, cytokinesis occurs over the chromosome and precedes chromosome segregation. As a result, only a stereotyped, origin-proximal region comprising one-third of the chromosome is initially trapped within the smaller compartment<sup>28</sup>. The SpoIIIE ATPase uses ATP hydrolysis to power the translocation of the remaining two-thirds of the chromosome into the smaller cell<sup>29</sup>. Thus, polar septation constitutes an asymmetric cell division in multiple senses: septation occurs toward a cell pole to generate progeny that differ in size, division takes place over the chromosome to create transient genetic asymmetry, and proteins are localized to a single side of the septum, causing them to be partitioned into only one of the daughter cells.

### **Cell-specific gene expression**

The completion of polar septation gives rise to two cells that differ in size and assume opposite fates as a product of development. The larger mother cell and smaller forespore are initially quite similar in terms of their molecular composition, but upon completing polar septation, the two cells activate cell autonomous programs of gene expression, which cause the fates of the two cells to diverge. Cell-specific gene expression is orchestrated by a cascade of spatiotemporally regulated sigma factors, proteins that initiate transcription by recruiting RNA polymerase to specific promoter sequences. Therefore, the mother cell and forespore produce distinct sets of proteins during spore formation.

The first sigma factor to be activated in this sequence is  $\sigma^F$ , which mediates early gene expression in the forespore. Although  $\sigma^F$  is produced under Spo0A control, prior to

compartmentalization, it is only activated in the forespore. This is due to the fact that  $\sigma^F$  is held in an inactive state by the anti- $\sigma$  factor, SpoIIAB.  $\sigma^F$  is freed from SpoIIAB repression by the anti-anti- $\sigma$  factor, SpoIIAA, a protein that is activated upon dephosphorylation by the SpoIIIE phosphatase<sup>80</sup>. By virtue of localizing preferentially to the forespore side of the polar division septum, the activity of SpoIIIE results in the derepression of  $\sigma^F$  only in the smaller forespore compartment.  $\sigma^F$  activation is further reinforced by the degradation of SpoIIAB by the ClpCP protease, once SpoIIAB is released from its  $\sigma^F$ -bound state<sup>81</sup>.

One of the principle functions of the  $\sigma^F$  regulon is to activate  $\sigma^E$ , which directs early gene expression in the mother cell.  $\sigma^E$  is initially produced in an inactive pro- $\sigma^E$  form and requires proteolytic processing for activation. SpoIIIGA, a membrane-bound protease, processes pro- $\sigma^E$  into its active form following the activation of the forespore line of gene expression<sup>82</sup>. This is signaled by the production of two factors, SpoIIIR and SpoIIIT, which are produced under the direction of  $\sigma^F$  in the forespore and secreted into the space between the mother cell and forespore membranes<sup>62</sup>. There, these factors bind to SpoIIIGA and induce a conformational change, stimulating its protease activity and prompting the cleavage of pro- $\sigma^E$ . Once  $\sigma^E$  is activated, sporulation cannot be reversed and sporangia become committed to the completing the pathway<sup>83</sup>.

The products of the  $\sigma^E$  and  $\sigma^F$  regulons function together to promote the engulfment of the forespore by the mother cell, which results in a striking reorganization of the cellular architecture of the sporangium. Engulfment is a phagocytosis-like process in which the mother cell membrane migrates around the forespore, transforming the sporangium from two cells lying side-by-side to a cell-within-a-cell. This process requires extensive remodeling of the peptidoglycan meshwork that surrounds the mother cell and forespore, which is mediated in part by the mother cell encoded proteins SpoIIID, SpoIIIM, and SpoIIP<sup>84</sup>. These proteins form a complex that thins the peptidoglycan at the polar

septum, thereby rendering the meshwork more flexible and removing the steric hindrance imposed on membrane migration<sup>85,86</sup>. The turgor pressure imparted to the forespore by chromosome translocation stretches this meshwork, providing a more navigable topology for the mother cell membrane to traverse<sup>86</sup>. Peptidoglycan degradation catalyzed by the mother cell is tightly coordinated with peptidoglycan synthesis catalyzed by the forespore<sup>87</sup>. The concerted action of cell wall polymerases and degradatory enzymes advance the mother cell membrane around the forespore in finger-like projections, ultimately creating a forespore compartment that is surrounded by two membranes sandwiching a thin layer of peptidoglycan<sup>85</sup>.

Forward migration of the mother cell membrane is further reinforced by a transmembrane complex comprised of the forespore encoded SpoIIQ and the mother cell encoded products of the *spoIIIA* operon, SpoIIAA-AH (the complex will hereafter be referred to as A-Q). This complex forms a zipper-like interaction that prevents the retraction of the advancing membrane<sup>88</sup>. SpoIIDMP activity results in the destruction of its own substrate, so the combination of SpoIIDMP and A-Q constitute a burnt bridge Brownian ratchet that ensures the directed movement of the mother cell membrane around the forespore<sup>89</sup>. When the advancing membrane meets at the tip of the forespore, the mother cell protein FisB catalyzes membrane fission, releasing the forespore into the mother cell cytoplasm, where it is sequestered away from the external environment<sup>90</sup>.

Interestingly, the A-Q transenvelope complex has been proposed to serve an additional role during spore formation. Several of the SpoIIIA proteins share structural homology with various components of bacterial secretion systems, and have been shown to assemble ring-like structures in vitro<sup>91,92,93</sup>. Further experiments have demonstrated that this complex bridges and physically connects the cytoplasm of the mother cell and forespore, as the soluble protein biotin ligase is able to modify SpoIIIAH

when produced only in the forespore<sup>91</sup>. A-Q is required to sustain gene expression in the forespore<sup>94</sup>. Mutants lacking A-Q produce small, collapsed forespores that fail to activate late gene expression and appear to lose their metabolic potential<sup>95</sup>. As such, A-Q has been proposed to serve as a feeding tube apparatus that delivers metabolic precursors to the forespore for assembly into macromolecules<sup>94</sup>. This model makes intuitive sense, as the forespore transitions to dormancy during spore formation and loses the ability to take up nutrients from the environment once engulfment is completed. A transport role for A-Q, however, has never been empirically demonstrated and the substrates it delivers to the forespore have yet to be identified.

Although the exact role of A-Q has not been established, it is known to be required for the activation of  $\sigma^G$ , the sigma factor that governs late gene expression in the forespore. It has been presumed that in the absence of A-Q, metabolic precursors are unable to be trafficked to the forespore, and thus,  $\sigma^G$ -directed biosynthetic activity does not commence<sup>94,95</sup>. The precise mechanisms by which  $\sigma^G$  is activated remain enigmatic, but it seems to be tightly coordinated with the completion of chromosome translocation and engulfment. Thus, sporangia appear to evaluate both the metabolic status of the cell and the completion of developmental milestones before activating late gene expression.

$\sigma^G$  activation results in the production of CtpB and SpoIVB, two proteases that are secreted into the intermembrane space between the forespore and mother cell<sup>96</sup>. There, these proteases process two mother cell-specific factors, BofA and SpoIVFA, which reside in a complex that holds an additional protease, SpoIVFB, in an inactive state<sup>97</sup>. The proteolytic processing of BofA and SpoIVFA frees SpoIVFB from inhibition, where it processes the inactive pro- $\sigma^K$  into active  $\sigma^K$ , thereby activating late mother cell gene expression<sup>96</sup>. Therefore, as is the case with  $\sigma^E$ , the activation of  $\sigma^K$  is coupled to the activation of gene expression in the forespore through regulated proteolysis.



Late gene expression helps the developing spore mature and assume its incredible resistance properties. During this time period, two structures encompassing the spore are built that confer protection from environmental assaults. The proteinaceous coat, synthesized by the mother cell and deposited on the surface of the outer forespore membrane, constitutes one of these protective structures. The coat is composed of four layers that form concentric rings around the developing spore. These layers are arranged in order from the furthest interior to furthest exterior as follows: basement, inner, outer, and crust<sup>31</sup>. Each of these layers is defined by one or two principal morphogenetic proteins that nucleate an entire network of binding events<sup>98</sup>. All told, the seventy plus proteins comprising the coat represent 25% of the total protein content of the spore and function to exclude enzymes and certain small molecules from the interior of the spore<sup>99</sup>.

The other major structure surrounding the spore is the cortex, which is a thick layer heavily modified peptidoglycan that is synthesized between the two forespore membranes. Even though the coat and cortex are spatially segregated, their synthesis is tightly coordinated. The cortex is composed of two layers that are chemically distinct. The inner layer, the germ cell wall, is a thin layer of peptidoglycan that is similar in composition to the vegetative cell wall<sup>30</sup>. This layer forms the template from which new peptidoglycan is synthesized upon germination. Peripheral to the germ cell wall lies the outer cortex, which is much thicker than the germ cell wall. The outer cortex exhibits a lower degree of peptide crosslinking, which is thought to confer flexibility to the spore core, allowing it to expand and contract in response to changing environmental conditions and core dehydration<sup>100</sup>. In addition, the outer cortex is distinguished by the presence of muramic lactam, which confers lysozyme resistance to the spore<sup>101</sup>. As opposed to the germ cell wall, the outer cortex is specifically recognized and degraded upon germination by the cortex-lytic enzymes SleB and CwlJ, thereby facilitating

outgrowth<sup>102</sup>. Mutants compromised in cortex synthesis fail to attain the full repertoire of resistance properties and are sensitive to heat and desiccation.

In addition to the coat and cortex, resistance is also mediated by the dehydration of the spore core. Multiple processes, including cortex synthesis, are required for proper spore dehydration<sup>103</sup>. The primary means by which the forespore achieves a dehydrated state, however, is through the accumulation of dipicolinic acid, which accounts for approximately 5-15% of the dry weight of the spore<sup>104</sup>. Dipicolinic acid dehydrates the spore core by complexing with  $\text{Ca}^{2+}$  and displacing water, which also serves to protect macromolecules from thermal stress<sup>105</sup>. In addition, the calcium chelate of dipicolinic acid protects the spore chromosome from damage<sup>106</sup>. Dipicolinic acid is synthesized from a precursor of the amino acid lysine, *meso*-diaminopimelic acid (mDAP), in a biosynthetic pathway that is activated only in the mother cell following engulfment. The conversion of mDAP into dipicolinic acid involves the mother cell encoded dipicolinic acid synthase comprised of SpoVFA and SpoVFB, and following synthesis, it is trafficked to the forespore by a two-step transport pathway<sup>34</sup>. First, dipicolinic acid is moved into the intermembrane space between the inner and outer forespore membrane by SpoVV, a mother cell encoded protein that resembles concentrative nucleoside transporters and localizes to the outer forespore membrane<sup>35</sup>. SpoVA, a forespore encoded protein that localizes to the inner forespore membrane, takes up the dipicolinic acid from the intermembrane space into the spore core<sup>107</sup>. Thus, dipicolinic acid is the only molecule known to be trafficked between the mother cell and forespore cytoplasm.

The integrity of the spore genome is further preserved by a collection of small acid-soluble spore proteins (SASPs) that decorate the spore chromosome in high abundance and help to package it into a distinct toroidal configuration<sup>36,37</sup>. The SASPs are generally less than 10 kDa and composed predominately of hydrophobic amino acids. There are three different classes of SASPs:  $\alpha$ ,  $\beta$ , and  $\gamma$ . The  $\gamma$ -SASPs are less

broadly conserved and their exact role is not clear. The  $\alpha$ - and  $\beta$ -SASPs, however, are known to provide protection against nucleases, wet heat, ultraviolet irradiation, and oxidative stress<sup>108</sup>. Furthermore, the processing of the SASPs by the germination protease, Gpr liberates the amino acids required to fuel early outgrowth until metabolic processes resume<sup>42</sup>.

Once the spore is equipped with its full armament of resistance properties, it is released into the environment through the activation of an autolysis program in the mother cell. The mature spore can persist through adverse conditions for thousands of years in a dormant state with no detectable macromolecular synthesis or metabolic activity, though there might exist a brief time period where RNA content is actively remodeled. Therefore, the mother cell and forespore assume opposite fates as a product of development: the mother cell undergoes an altruistic programmed cell death, while the spore becomes immortal.

### **The future of sporulation research**

The mother cell has long been thought to nurture the forespore to dormancy<sup>94</sup>. Indeed, the mother cell physically sequesters the forespore away from the dangers posed by the external environment and contributes to the resistance properties of the spore through dipicolinic acid export<sup>35</sup> and coat<sup>99</sup> and cortex deposition<sup>40</sup>. Examples of intercellular nurturing, however, have thus far been limited to the endowment of resistance properties to the spore. Although the mother cell line of gene expression is far vaster than that of the forespore, suggestive of nurturing, it remains unknown whether the mother cell nurtures the forespore in a fundamental metabolic capacity and to what extent<sup>59,60</sup>. Furthermore, the precise role of the A-Q transenvelope complex has remained elusive. Although this complex has been advanced as a putative feeding tube that allows the mother cell to nourish the forespore during its transition to dormancy, it is unclear whether A-Q forms a ring-like structure in vivo to facilitate the intercellular

trafficking of small molecules, and how the transport of its substrates is regulated<sup>59,60,92,93</sup>.

Research spanning the last six decades has illuminated many facets of spore formation, and has provided us with a relatively comprehensive understanding of how the products of cell-specific gene expression contribute to development. Scientists have come to appreciate the myriad of ways sporangia achieve asymmetry, including polar cell division that bisects the forespore chromosome<sup>28</sup>, differential partitioning of the cell-fate determinant SpoIIIE<sup>79</sup>, and the activation of cell-autonomous programs of gene expression<sup>59,60</sup>. Unfortunately, cell-specific gene expression offers no clues as to whether the mother cell and forespore become metabolically differentiated during spore formation, as very few core metabolic genes are under sporulation control. As most metabolic enzymes are produced during vegetative growth, prior to compartmentalization and the activation of cell-specific gene expression, one might presume that these enzymes are evenly partitioned into the mother cell and forespore following polar septation. This hypothesis, however, is difficult to reconcile with the fact that the forespore transitions to metabolic dormancy during the process of spore formation. This line of inquiry is further complicated by the fact that the biosynthesis pathways for many cellular macromolecules are required for either vegetative growth or efficient entry into sporulation, making the use of null mutants inviable. Although some of the first asporogenous mutants to be isolated were found to have lesions in genes encoding enzymes of the TCA cycle, metabolic enzymes have largely been excluded from the *spo* designation and intensive research, due to their role in supporting vegetative growth and the intractability of their study using existing genetic tools<sup>109,110</sup>.

All told, over a century of research dedicated toward understanding this process has made endospore formation in *Bacillus subtilis* one of the most intensively characterized developmental pathways in biology. One of the few remaining deficiencies

in the knowledge of sporulation is the developmental role played by proteins synthesized during vegetative growth, prior to sporulation initiation and the activation of cell-specific gene expression. Although these proteins constitute the vast majority of the proteome, the lack of suitable genetic and chemical genetic approaches to rapidly inactivate proteins in a cell- and stage-specific manner without perturbing vegetative growth or entry into sporulation has thus far prevented a systematic interrogation of the contribution of vegetatively synthesized proteins to spore formation. Furthermore, the exclusion of mutants causing vegetative growth defects from the *spo* nomenclature likely diverted the attention of researchers from studying how the products encoded by these genes contribute to spore formation. Therefore, the study of how metabolic processes are coordinated between the mother cell and forespore has largely been neglected, and represents one of the largest remaining challenges in the sporulation field.

Spore revival is a remarkable process that entails the rapid transition of a metabolically dormant spore into a fully metabolically active cell, but the study of this process poses significant challenges to researchers. Spore revival represents a highly intractable system, as spores are impervious to antibiotics and chemical genetic techniques. Additionally, and the processes of spore development and spore revival are often not genetically separable. Therefore, spore revival constitutes a rich source of further inquiry.

To overcome the challenges of studying spore formation and spore revival, we have developed a comprehensive framework, which allows us to dissect the manner in which vegetatively synthesized metabolic proteins contribute to these processes (Chapter II). This novel genetic approach, called STRP (spatiotemporallyregulated proteolysis) harnesses cell-specific gene expression to deplete target proteins in a spatiotemporally regulated manner. We have applied STRP to identify and characterize the metabolic interactions that underlie spore formation (Chapter III) and novel

mechanisms by which the mother cell and forespore become differentiated (Chapter IV). We are currently undertaking a genome-wide effort to deplete key metabolic enzymes from the mother cell or forespore using STRP, which will allow us to compile a comprehensive list of the cellular parts required for spore formation and revival (Chapter V). STRP provides an incredibly powerful and versatile framework to push beyond the longstanding limitations plaguing sporulation research, allowing a thorough understanding of the many facets of spore assembly and revival to be realized.

Figures

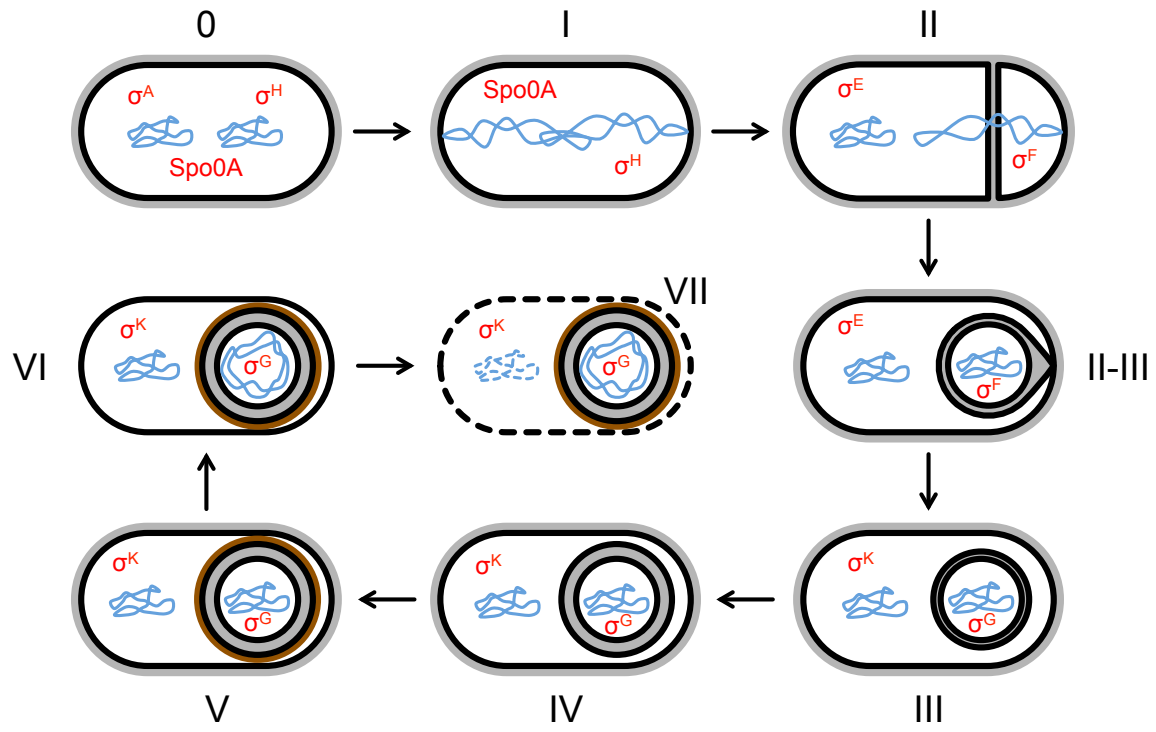


**Figure 1.1.** Morphological stages of spore formation. Stages are indicated by Roman numerals 0-VII. Membranes are indicated in black, peptidoglycan in gray, DNA in blue, spore coat in brown, and the transcription factors acting at each stage in red.

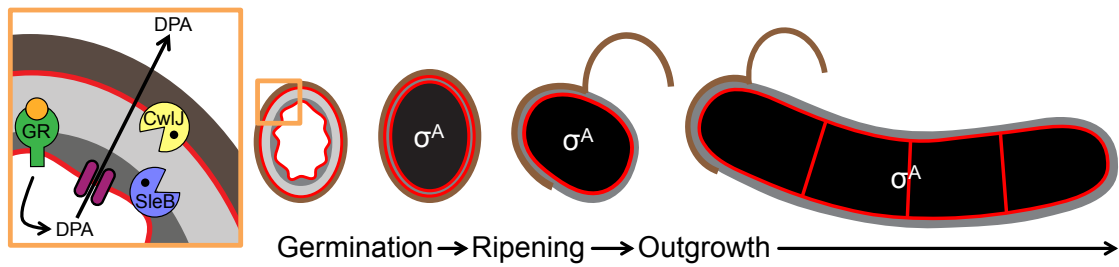


**Figure 1.2.** Morphological stages of spore revival. Phase transition indicated by change from white cytoplasm to black cytoplasm. Membranes are indicated in red, peptidoglycan in gray, and spore coat in brown. Orange inset: detailed view of germination. The binding of a germinant (orange circle) to its respective germinant receptor (GR, green) triggers the efflux of dipicolinic acid (DPA) from the spore core. This activates the cortex lytic enzyme SleB (purple Pac-Man) and the cell wall hydrolase CwlJ (yellow Pac-Man).



## References

1. Greene, N.D., and Copp, A.J. Development of the vertebrate central nervous system: formation of the neural tube. *Prenat Diagn.* **29**(4), 303-311 (2009).
2. Karin, M. Nuclear factor- $\kappa$ B in cancer development and progression. *Nature.* **441**(7092), 431-436 (2006).
3. Sulston, J.E., Schierenberg, E., White, J.G., and Thomson, J.N. The embryonic cell lineage of the nematode *Caenorhabditis elegans*. *Dev Biol.* **100**(1), 64-119 (1983).
4. A.E. Hofmeister, A. Londoño-Vallejo, E. Harry, P. Stragier, R. Losick, Extracellular signal protein triggering the proteolytic activation of a developmental transcription factor in *B. subtilis*. *Cell* **83**(2), 219–226 (1995).
5. W Driever, C. Nüsslein-Volhard, A gradient of bicoid protein in *Drosophila* embryos. *Cell* **54**(1), 83–93 (1988).
6. Dawid, I.B. Differential gene expression in vertebrate embryos. *J Biol Chem.* **284**(20), 13277-13283 (2009).
7. Wolk, C.P. Heterocyst formation. *Annu Rev Genet.* **30**, 59-78 (1996).
8. Shapiro, L., Agabian-Keshishian, N., and Bendis, I. Bacterial differentiation. *Science.* **173**(4000), 884-892 (1971).
9. Hodgkin, J., and Kaiser, D. Genetics of gliding motility in *Myxococcus xanthus* (Myxobacterales): two gene systems control movement. *Mol Gen Genet.* **171**, 177-191 (1979).
10. Waters, C.M., and Bassler, B.L. Quorum sensing: Cell-to-cell communication in bacteria. *Annu Rev Cell Dev. Biol.* **21**:319–346 (2005).
11. Lyons, N.A. and Kolter, R. On the evolution of bacterial multicellularity. *Curr Opin Microbiol.* **24**, 21-28 (2015).
12. Tan, I.S. and K. S. Ramamurthi, K.S. Spore formation in *Bacillus subtilis*. *Environ. Microbiol. Rep.* **6**, 212–225 (2014).
13. Dubanu, D. Genetic competence in *Bacillus subtilis*. *Microbiol Rev.* **55**(3), 395-424 (1991).
14. Stanley, N.R. and Lazazzera, B.A. Defining the genetic differences between wild and domestic strains of *Bacillus subtilis* that affect poly-gamma-dl-glutamic acid production and biofilm formation. *Mol Microbiol.* **57**(4), 1143-1158 (2005).
15. Grelet, N. Growth limitation and sporulation. *J Appl Bacteriol.* **20**, 315-324 (1957).
16. Paredes-Sabja, D., Setlow, P., and Sarker, M.R. Germination of spores of Bacillales and Clostridiales species: mechanisms and proteins involved. *Trends Microbiol* **19**, 85–94 (2011).

17. Cano, R.J., and Borucki, M.K. Revival and identification of bacterial spores in 25- to 40-million-year-old Dominican amber. *Science* **268**: 1060–1064 (1995).
18. Ehrenberg, C.G. Die Infusionstierchen als vollkommene Organismen. Leipzig: Verlag Leopold Voss. (1838).
19. Cohn, F. Untersuchungen über bakterien. *Beitr Biol Pflanz.* **2**, 249–276 (1876).
20. Koch, R. Über morphologie und entwicklungsgeschichte einiger endosporer bakterienformen. *Bot Zeit.* **46**, 227–287 (1888).
21. Knaysi, G. Cytology of bacteria. *Botan Rev.* **4**, 83-112 (1938).
22. Lewis, I. M. The cytology of bacteria. *Bact Revs.* **5**, 181-230 (1941).
23. Young, I.E. and Fitz-James, P. Chemical and morphological studies of bacterial spore formation. *J Cell Biol.* **12**(1), 115-133 (1962).
24. Kawata, T., Inoue, T., and Takagi, A. Electron microscopy of spore formation and germination in *Bacillus subtilis*. *Jpn J Microbiol.* **7**, 23-41 (1963).
25. Ryter, A. Morphologic study of the sporulation of *Bacillus subtilis*. *Ann Inst Pasteur (Paris)*. **108**, 40-60 (1965).
26. Piggot, P.J., and Coote, J.G. Genetic aspects of bacterial endospore formation. *Bacteriol Rev.* **40**(4), 908-962 (1976).
27. Ryter, A., Schaeffer, P., and Ionesco, H. Cytologic classification, by their blockage stage, of sporulation mutants of *Bacillus subtilis* Marburg. *Ann Inst Pasteur (Paris)*. **110**, 305–315 (1966).
28. Wu, L.J., and Errington, J. Use of asymmetric cell division and *spoIII*E mutants to probe chromosome orientation and organization in *Bacillus subtilis*. *Mol Microbiol.* **27**, 777–786 (1998).
29. Wu, L.J., and Errington, J. *Bacillus subtilis* SpoIII E protein required for DNA segregation during asymmetric cell division. *Science* **264**, 572–575 (1994).
30. Tipper, D.J., and Linnett, P.E. Distribution of peptidoglycan synthetase activities between sporangia and forespores in sporulating cells of *Bacillus sphaericus*. *J Bacteriol.* **126**, 213–221 (1976).
31. McKenney, P.T., Driks, A., Eskandarian, H.A., Grabowski, P., Guberman, J., Wang, K.H., Gitai, Z., and Eichenberegger, P. A distance-weighted interaction map reveals a previously uncharacterized layer of the *Bacillus subtilis* spore coat. *Curr Biol.* **20**, 934–938 (2010).
32. Wang, K.H., Isidro, A.L., Domingues, L., Eskandarian, H.A., McKenney, P.T., Drew, K., Grabowski, P., Chua, M.H., Barry, S.N., Guan, M., Bonneau, R., Henriques, A.O.,

Eichenberger, P. The coat morphogenetic protein SpoVID is necessary for spore encasement in *Bacillus subtilis*. *Mol Microbiol.* **74**, 634–649 (2009).

33. Driks, A. *Bacillus subtilis* spore coat. *Microbiol Mol Biol Rev.* **63**(1), 1-20 (1999).

34. Chen, N., Jiang, S., Klein, D., and Paulus, H. Organization and nucleotide sequence of the *Bacillus subtilis* diaminopimelate operon, a cluster of genes encoding the first three enzymes of diaminopimelate synthesis and dipicolinate synthase. *J Biol Chem.* **268**(13), 9448-9465 (1993).

35. Ramírez-Guadiana, F.H., Meeske, A.J., Rodrigues, C.D.A., Barajas-Orenlas, R.D.C., Kruse, A.C., and Rudner, D.Z. A two-step transport pathway allows the mother cell to nurture the developing spore in *Bacillus subtilis*. *PLoS Genet.* **13**(9), e1007015 (2017).

36. Connors, M. I., and Setlow, P. Cloning of a small, acid-soluble spore protein gene from *Bacillus subtilis* and determination of its complete nucleotide sequence. *J Bacteriol.* **161**, 333-39 (1985).

37. Pogliano, K., Harry, E., and Losick, R. Visualization of the subcellular location of sporulation proteins in *Bacillus subtilis* using immunofluorescence microscopy. *Mol Microbiol.* **18**, 459–470 (1995).

38. L. Sinai, A. Rosenberg, Y. Smith, E. Segev, S. Ben-Yehuda, The molecular timeline of a reviving bacterial spore. *Mol. Cell* **57**, 695–707 (2015).

39. Yi, X., and Setlow, P. Studies of the commitment step in the germination of spores of *Bacillus* species. *J Bacteriol.* **192**(13), 3424-3433 (2010).

40. Paidhungat, M. Ragkousi, K., and Setlow, P. Genetic requirements for induction of germination of spores of *Bacillus subtilis* by Ca(2+)-dipicolinate. *J Bacteriol.* **183**(16), 4886-4893 (2001).

41. Boland, F.M., Atrih, A., Chirakkal, H., Foster, S.J., Moir, A. Complete spore-cortex hydrolysis during germination of *Bacillus subtilis* 168 requires SleB and YpeB. *Microbiology.* **146**, 57-64 (2000).

42. Sanchez-Salas, J.L., Santiago-Lara, M.L., Setlow, B., Sussman, M.D., and Setlow, P. Properties of *Bacillus megaterium* and *Bacillus subtilis* mutants which lack the protease that degrades small, acid-soluble proteins during spore germination. *J Bacteriol.* **174**(3), 807-814 (1992).

43. Schaeffer, P., and Ionesco, H. Contribution to the genetic study of bacterial sporogenesis. *C R Hebd Seances Acad Sci.* **251**, 3125-3127 (1960).

44. Takahashi, I. Localization of spore markers on the chromosome of *Bacillus subtilis*. *J Bacteriol.* **89**, 1065-1067 (1965).

45. Spizizen, J. Transformation of biochemically deficient strains of *Bacillus subtilis* by deoxyribonucleate. *Proc Natl Acad Sci U S A.* **44**(10), 1072-1078 (1958).

46. Takahashi, I. Genetic transduction in *Bacillus subtilis*. *Biochem Biophys Res Commun.* **5**, 171-175 (1961).
47. Ilichinska, E. Some physiological features of asporogenous mutants of *Bacilli*. *Microbiol. USSR.* **29**, 147-50 (1960).
48. Michel, J.F., Millet, J. Physiological studies on early-blocked sporulation mutants of *Bacillus subtilis*. *J Appl Bacteriol.* **33**(1), 220-227 (1970).
49. Piggot, P. J. Mapping of asporogenous mutations of *Bacillus subtilis*: a minimum estimate of the number of sporulation operons. *J. Bacteriol.* **114**, 1241-1253 (1973).
50. Rogolsky, M. Genetic mapping of a locus which regulates the production of pigment associated with spores of *Bacillus subtilis*. *J Bacteriol.* **95**, 2426 (1968).
51. Donovan, W., L. Zheng, K. Sandman, and Losick, R. Genes encoding spore coat polypeptides from *Bacillus subtilis*. *J Mol Biol.* **196**, 1-10 (1987).
52. Cutting, S., and Mandelstam, J. The nucleotide sequence and the transcription during sporulation of the *gerE* gene of *Bacillus subtilis*. *J Gen Microbiol.* **132**, 3013-3024 (1986).
53. Jenkinson, H. F., and Lord, H. Protease deficiency and its association with defects in spore coat structure, germination and resistance properties in a mutant of *Bacillus subtilis*. *J Gen Microbiol.* **129**, 2727-2737 (1983).
54. Jenkinson, H. F. Germination and resistance defects in spores of a *Bacillus subtilis* mutant lacking a coat polypeptide. *J Gen Microbiol.* **127**, 81-91 (1981).
55. Young, M. Use of temperature-sensitive mutants to study gene expression during sporulation in *Bacillus subtilis*. *J Bacteriol.* **126**, 928-936 (1976).
56. Bookstein, C., C. W. Edwards, N. V. Kapp, and Hulett, F.M. The *Bacillus subtilis* 168 alkaline phosphatase III gene: impact of a *phoAIII* mutation on total alkaline phosphatase synthesis. *J Bacteriol.* **172**, 3730-3737 (1990).
57. Lampel, K. A., B. Uratani, G. R. Chaudhry, R. F. Ramaley, and Rudikoff, S. Characterization of the developmentally regulated *Bacillus subtilis* glucose dehydrogenase gene. *J Bacteriol.* **166**, 238-243 (1986).
58. Youngman, P., Zuber, P., Perkins, J.B., Sandman, K., Igo, M., Losick, R. New ways to study developmental genes in spore-forming bacteria. *Science* **228**, 285-91 (1985).
59. Eichenberger, P., Fujita, M., Jensen, S.T., Conlon, E.M., Rudner, D.Z., and Wang, S.T. The program of gene transcription for a single differentiating cell type during sporulation in *Bacillus subtilis*. *PLoS Biol.* **2**: e328 (2004).
60. Wang, S., Setlow, B., Conlon, E., Lyon, J., Imamura, D., Sato, T. Setlow, P., Losick, R., and Eichenberger, P. The forespore line of gene expression in *Bacillus subtilis*. *J Mol Biol.* **358**(1), 16-37 (2006).

61. Silvaggi JM, Popham DL, Driks A, Eichenberger P, and Losick R. Unmasking novel sporulation genes in *Bacillus subtilis*. *J Bacteriol.* **186**: 8089–8095 (2004).
62. Meeske, A.J., Rodrigues, C.D., Brady, J., Lim, H.C., Bernhardt, T.G., and Rudner, D.Z. High-throughput genetic screens identify a large and diverse collection of new sporulation genes in *Bacillus subtilis*. *PLoS Biol.* **14**(1), 1-33 (2016).
63. Peters, J.M., Colavin, A., Shi, H., Czarny, T.L., Larson, M.H., Wong, S., Hawkins, J.S., Lu, C.H.S., Koo, B.M., Marta, E., Shiver, A.L., Whitehead, E.H., Weissman, J.S., Brown, E.D., Qi, L.S., Huang, K.C., and C.A. Gross. A comprehensive, CRISPR-based functional Analysis of Essential Genes in Bacteria. *Cell.* **165**(6), 1493-1506 (2016).
64. Freese, E., Heinze, J. E., Galliers, E.M. Partial purine deprivation causes sporulation of *Bacillus subtilis* in the presence of excess ammonia, glucose and phosphate. *J Gen Microbiol.* **115**, 193-205 (1979).
65. Veening, J.W., Stewart, E.J., Berngruber, T.W., Taddei, F., Kuipers, O.P., and Hamoen, L.W. Bet-hedging and epigenetic inheritance in bacterial cell development. *Proc Natl Acad Sci USA.* **105**, 4393–4398 (2008).
66. Gonzalez-Pastor, J.E., Hobbs, E.C., and Losick, R. Cannibalism by sporulating bacteria. *Science.* **301**, 510–513 (2003).
67. LeDeaux, J.R., Yu, N., and Grossman, A.D. Different roles for KinA, KinB, and KinC in the initiation of sporulation in *Bacillus subtilis*. *J Bacteriol.* **177**, 861–863 (1995).
68. Burbulys, D., Trach, K.A., and Hoch, J.A. Initiation of sporulation in *B. subtilis* is controlled by a multicomponent phosphorelay. *Cell.* **64**, 545–552 (1991).
69. Perego, M., Hanstein, C., Welsh, K.M., Djavakhishvili, T., Glaser, P., and Hoch, J.A. Multiple protein-aspartate phosphatases provide a mechanism for the integration of diverse signals in the control of development in *B. subtilis*. *Cell.* **79**, 1047–1055 (1994).
70. Mueller, J.P., and Sonenshein, A.L. Role of the *Bacillus subtilis* *gsiA* gene in regulation of early sporulation gene expression. *J Bacteriol.* **174**, 4374–4383 (1992).
71. Fujita, M., and Losick, R. Evidence that entry into sporulation in *Bacillus subtilis* is governed by a gradual increase in the level and activity of the master regulator Spo0A. *Genes Dev.* **19**, 2236–2244 (2005).
72. Chai, Y., Kolter, R., and Losick, R. Reversal of an epigenetic switch governing cell chaining in *Bacillus subtilis* by protein instability. *Mol Microbiol.* **78**, 218–229 (2011).
73. Vishnoi, M., Narula, J., Devi, S.N., Dao, H.A., Igoshin, O.A., and Fujita, M. Triggering sporulation in *Bacillus subtilis* with artificial two-component systems reveals the importance of proper Spo0A activation dynamics. *Mol Microbiol.* **90**, 181–194 (2013).
74. Ben-Yehuda, S., Rudner, D.Z., and Losick, R. RacA, a bacterial protein that anchors chromosomes to the cell poles. *Science.* **299**, 532–536 (2003).

75. Rahn-Lee, L., Merrikh, H., Grossman, A.D., and Losick, R. The sporulation protein SirA inhibits the binding of DnaA to the origin of replication by contacting a patch of clustered amino acids. *J Bacteriol.* **193**, 1302–1307 (2011).
76. Cunningham, K.A., and Burkholder, W.F. The histidine kinase inhibitor Sda binds near the site of autophosphorylation and may sterically hinder autophosphorylation and phosphotransfer to Spo0F. *Mol Microbiol.* **71**, 659–677 (2009).
77. Miller, A.K., Brown, E.E., Mercado, B.T., and Herman, J.K. A DNA-binding protein defines the precise region of chromosome capture during *Bacillus* sporulation. *Mol Microbiol.* **99**(1), 111-122 (2016).
78. Carniol, K., Ben-Yehuda, S., King, N., and Losick, R. Genetic dissection of the sporulation protein SpoII<sub>E</sub> and its role in asymmetric division in *Bacillus subtilis*. *J Bacteriol.* **187**, 3511–3520 (2005).
79. Bradshaw, N., and Losick, R. Asymmetric division triggers cell-specific gene expression through coupled capture and stabilization of a phosphatase. *Elife.* **4**, e08145 (2015).
80. Duncan, L., Alper, S., Arigoni, F., Losick, R., and Stragier, P. Activation of cell-specific transcription by a serine phosphatase at the site of asymmetric division. *Science.* **270**, 641–644 (1995).
81. Pan, Q., Garsin, D., and Losick, R. Self-reinforcing activation of a cell-specific transcription factor by proteolysis of an anti-sigma factor in *B. subtilis*. *Mol Cell.* **8**(4), 873-883 (2001).
82. Stragier, P., Bonamy, C., and Karmazyn-Campelli, C. Processing of a sporulation sigma factor in *Bacillus subtilis*: how morphological structure could control gene expression. *Cell.* **52**, 697–704 (1988).
83. Dworkin, J. and Losick, R. Developmental commitment in a bacterium. *Cell.* **121**(3), 401-409 (2005).
84. Abanes-De Mello, A., Sun, Y.L., Aung, S., and Pogliano, K. A cytoskeleton-like role for the bacterial cell wall during engulfment of the *Bacillus subtilis* forespore. *Genes Dev.* **16**, 3253–3264 (2002).
85. Khanna, K., Lopez-Garrido, J., Zhao, Z., Watanabe, R., Yuan, Y., Sugie, J., Pogliano, K., and Villa, E. The molecular architecture of engulfment during *Bacillus subtilis* sporulation. *Elife.* **8**, e45257 (2019).
86. Lopez-Garrido, J., Ojkic, N., Khanna, K., Wagner, F.R., Villa, E., Endres, R.G., and Pogliano, K. Chromosome translocation inflates *Bacillus subtilis* forespores and impacts cellular morphology. *Cell.* **172**(4), 758-770 (2018).
87. Ojkic, N., López-Garrido, J., Pogliano, K. and Endres, R.G. Cell-wall remodeling drives engulfment during *Bacillus subtilis* sporulation. *Elife.* **5**, e18657 (2016).

88. Blaylock, B., Jiang, X., Rubio, A., Moran, C.P., Jr, and Pogliano, K. Zipper-like interaction between proteins in adjacent daughter cells mediates protein localization. *Genes Dev.* **18**, 2916–2928 (2004).
89. Broder, D.H., and Pogliano, K. Forespore engulfment mediated by a ratchet-like mechanism. *Cell.* **126**, 917–928 (2006).
90. Doan, T., Coleman, J., Marquis, K.A., Meeske, A.J., Burton, B.M., Karatekin, E., and Rudner, D.Z. FisB mediates membrane fission during sporulation in *Bacillus subtilis*. *Genes Dev.* **27**(3), 322-334 (2013).
91. Meisner, J., Wang, X., Serrano, M. Henriques, A., and Moran, C. A channel connecting the mother cell and forespore during bacterial endospore formation. *Proc. Natl. Acad. Sci.* **105**(39), 15100-15105 (2008).
92. Rodrigues, C.D., Henry, X., Neumann, E., Kurauskas, V., Bellard, L., Fichou, Y., Schanda, P., Schoehn, G., Rudner, D.Z., and Morlot, C. A ring-shaped conduit connects the mother cell and forespore during sporulation in *Bacillus subtilis*. *Proc Natl Acad Sci U.S.A.*, **113**, 11585–11590 (2016).
93. Zeytuni, N., Hong, C., Flanagan, K.A., Worrall, L.J., Theiltges, K.A., Vuckovic, M., Huang, R.K., Massoni, S.C., Camp, A.H., Yu, Z., and Strynadka, N.C. Near-atomic resolution cryoelectron microscopy structure of the 30-fold homooligomeric SpoIIAG channel essential to spore formation in *Bacillus subtilis*. *Proc Natl Acad Sci.* **114**(34), E7073-E7081 (2017).
94. Camp, A. and Losick, R. A feeding tube model for activation of a cell- specific transcription factor during sporulation in *Bacillus subtilis*. *Genes Dev.* **23**, 1014-1024 (2009).
95. Doan, T., Morlot, C., Meisner, J., Serrano, M., Henriques, A., Moran, C., and Rudner, D. Novel secretion apparatus maintains spore integrity and developmental gene expression in *Bacillus subtilis*. *PLoS Genet.* **5**(7), (2009).
96. Campo, N., and Rudner, D.Z. A branched pathway governing the activation of a developmental transcription factor by regulated intramembrane proteolysis. *Mol Cell.* **23**, 25–35 (2006).
97. Resnekov, O., and Losick, R. Negative regulation of the proteolytic activation of a developmental transcription factor in *Bacillus subtilis*. *Proc Natl Acad Sci USA.* **95**, 3162–3167 (1998).
98. Chada, V.G., Sanstad, E.A., Wang, R., and Driks, A. Morphogenesis of *Bacillus* spore surfaces. *J Bacteriol.* **185**, 6255–6261 (2003).
99. Munoz, L., Sadaie, Y., and Doi, R.H. Spore coat protein of *Bacillus subtilis*. Structure and precursor synthesis. *J Biol Chem.* **253**(19), 6694-6701 (1978).

100. Popham, D.L., and Setlow, P. The cortical peptidoglycan from spores of *Bacillus megaterium* and *Bacillus subtilis* is not highly cross-linked. *J Bacteriol.* **175**, 2767–2769 (1993).
101. Warth, A.D., and Strominger, J.L. Structure of the peptidoglycan from spores of *Bacillus subtilis*. *Biochemistry.* **11**, 1389–1396 (1972).
102. Ishikawa, S., Yamane, K., and Sekiguchi, J. Regulation and characterization of a newly deduced cell wall hydrolase gene (*cwlJ*) which affects germination of *Bacillus subtilis* spores. *J Bacteriol.* **180**, 1375–1380 (1998).
103. Meador-Parton, J., and Popham, D.L. Structural analysis of *Bacillus subtilis* spore peptidoglycan during sporulation. *J Bacteriol.* **182**, 4491–4499 (2000).
104. Orsburn, B.C., Melville, S.B., and Popham, D.L. EtfA catalyses the formation of dipicolinic acid in *Clostridium perfringens*. *Mol. Microbiol.* **75**(1), 178-186 (2010).
105. Balassa, G., Milhaud, P., Raulet, E., Silva, T., Sausa, J.C.F. A *Bacillus subtilis* mutant requiring dipicolinic acid for the development of heat-resistant spores. *J Gen Microbiol.* **110**, 365-79 (1979).
106. Setlow, B., Atluri, S., Kitchel, R., Koziol-Dube, K., and Setlow, P. Role of dipicolinic acid in resistance and stability of spores of *Bacillus subtilis* with or without DNA-protective alpha/beta-type small acid-soluble proteins. *J Bacteriol.* **188**, 3740–3747 (2006).
107. Tovar-Rojo, F., Chander, M., Setlow, B., and Setlow, P. The products of the *spoVA* operon are involved in dipicolinic acid uptake into developing spores of *Bacillus subtilis*. *J Bacteriol.* **184**(2), 584-587 (2002).
108. Mason, I. M., Setlow, P. Evidence for an essential role for small, acid-soluble spore proteins in the resistance of *Bacillus subtilis* spores to ultraviolet light. *J Bacteriol.* **167**, 174-78 (1986).
109. Fortnagel, P., and Freese, E. Analysis of sporulation mutants. II. Mutants blocked in the citric acid cycle. *J Bacteriol.* **95**, 1431-1438 (1968).
110. Hanson, R. S., J. Blicharska, and Szulmajster, J. Relationship between the tricarboxylic acid cycle enzymes and sporulation of *B. subtilis*. *Biochem Biophys Res Commun.* **17**, 1-7 (1964).



## CHAPTER II


### Spatiotemporally regulated proteolysis to dissect the role of vegetative proteins during

### *Bacillus subtilis* sporulation: cell-specific requirement of $\sigma^H$ and $\sigma^A$ .

Molecular Microbiology (2018) 108(1)

doi:10.1111/mmi.13916  
First published online 12 February 2018

## Spatiotemporally regulated proteolysis to dissect the role of vegetative proteins during *Bacillus subtilis* sporulation: cell-specific requirement of $\sigma^H$ and $\sigma^A$

Eammon P. Riley, Aude Trinquier,<sup>†</sup>  
Madeline L. Reilly, Marine Durchon,  
Varahenage R. Perera, Kit Pogliano and  
Javier Lopez-Garrido <sup>\*</sup>  
Division of Biological Sciences, University of  
California San Diego, La Jolla, CA, USA.

molecular dissection of every stage of sporulation,  
germination and outgrowth.

### Introduction

Cellular differentiation is a pivotal step in every developmental process, from human ontogeny to spore formation in certain bacteria. Sporulation in the bacterium *Bacillus subtilis* has become a paradigm for cell differentiation and development in bacteria (Errington, 2003; Hilbert and Piggot, 2004; Higgins and Dworkin, 2012; Tan and Ramamurthi, 2014; Narula *et al.*, 2016). Triggered by nutrient starvation, spore formation involves the close interaction between two cells that differ in both size and developmental fate: the smaller forespore, which becomes the dormant and highly resilient spore following maturation, and the larger mother cell, which lyses after contributing to the formation of the mature spore.

The sporulation process is depicted in Fig. 1. The forespore and the mother cell are the result of an asymmetrically positioned cell division event in which the septum is formed close to a single cell pole, in a process called polar septation. After polar septation, the membrane of the mother cell engulfs the forespore in a phagocytosis-like process that culminates with the forespore surrounded by two membranes and enclosed within the mother cell cytoplasm. The forespore subsequently matures inside the mother cell, where it is protected from the external medium. Spore maturation involves the formation of a peptidoglycan layer called the cortex between the inner and outer forespore membranes (Popham and Bernhards, 2015), the assembly of a proteinaceous coat around the outer membrane (McKenney *et al.*, 2013), and the dehydration of the forespore cytoplasm, which endows the spore with a bright appearance under phase-contrast microscopy. Once maturation is complete, the mother cell lyses and the spore is released into the environment, where it can remain dormant for years. Mature spores are resistant to a variety of environmental challenges (Setlow, 2006), including high temperature, desiccation, and a variety of

### Summary

Sporulation in *Bacillus subtilis* is a paradigm of bacterial development, which involves the interaction between a larger mother cell and a smaller forespore. The mother cell and the forespore activate different genetic programs, leading to the production of sporulation-specific proteins. A critical gap in our understanding of sporulation is how vegetative proteins, made before sporulation initiation, contribute to spore formation. Here we present a system, spatiotemporally regulated proteolysis (STRP), which enables the rapid, developmentally regulated degradation of target proteins, thereby providing a suitable method to dissect the cell- and developmental stage-specific role of vegetative proteins. STRP has been used to dissect the role of two major vegetative sigma factors,  $\sigma^H$  and  $\sigma^A$ , during sporulation. The results suggest that  $\sigma^H$  is only required in predivisional cells, where it is essential for sporulation initiation, but that it is dispensable during subsequent steps of spore formation. However, evidence has been provided that  $\sigma^A$  plays different roles in the mother cell, where it replenishes housekeeping functions, and in the forespore, where it plays an unexpected role in promoting spore germination and outgrowth. Altogether, the results demonstrate that STRP has the potential to provide a comprehensive

Accepted 21 January, 2018. \*For correspondence. E-mail jlopezgarrido@ucsd.edu; Tel. +1 858 822 1315; Fax +1 858 822 5740. <sup>†</sup>Present address: UMR 8261 (CNRS - Univ. Paris Diderot, Sorbonne Paris Cité), Institut de Biologie Physico-Chimique, 13 rue Pierre et Marie Curie, Paris, France.

© 2018 John Wiley & Sons Ltd

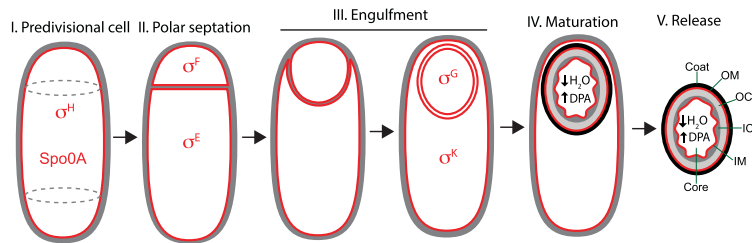


**Fig. 1.** The sporulation pathway in *B. subtilis*. Membranes are in red and peptidoglycan in gray. Transcription factors active in different cells and stages are shown red. I. In predivisional cells, the division sites (dotted ovals) are shifted to polar positions. II. Polar septation produces a small forespore and a large mother cell. III. After polar septation, the mother cell engulfs the forespore in a phagocytosis-like process. After engulfment, the forespore is enclosed within the mother cell cytoplasm and delimited by two membranes. IV. The forespore matures through the formation of a peptidoglycan cortex (gray) between the inner and outer forespore membranes, the assembly of a proteinaceous coat around the outer membrane (black), and the dehydration of the forespore core, which accumulates dipicolinic acid (DPA). V. Once maturation is completed, the mother cell lyses and the spore is released into the environment, where it remains dormant until conditions are appropriate for germination. OM, outer membrane; OC, outer cortex; IC, inner cortex; IM, inner membrane.

chemicals such as antibiotics, to which spores are impermeable. Spore germination is triggered in response to specific nutrients and other stimuli (Setlow, 2014). During germination the spore core is rehydrated, leading to the resumption of metabolic activities and vegetative growth.

The regulatory program that controls sporulation is relatively well understood (Errington, 2003; Hilbert and Piggot, 2004). Several transcriptional regulators are sequentially activated, which orchestrate distinct programs of gene expression in the mother cell and forespore at different developmental stages (Fig. 1). The entry into sporulation is controlled by the stationary phase-specific  $\sigma$  factor,  $\sigma^H$ , and the phosphorelay response regulator, Spo0A, which together govern gene expression in the predivisional cell. After polar septation, a cascade of cell-specific  $\sigma$  factors become active in the forespore and the mother cell. Immediately after polar septation,  $\sigma^F$  is activated in the forespore, followed by the activation of  $\sigma^E$  in the mother cell. Upon engulfment completion,  $\sigma^G$  becomes active in the forespore and  $\sigma^K$  in the mother cell. Together, the cell-specific  $\sigma$  factors control the transcription of approximately 560 genes (Eichenberger *et al.*, 2004; Wang *et al.*, 2006; Eichenberger, 2012), most of which are sporulation-specific and not transcribed in vegetative cells.

The study of sporulation has traditionally focused on deciphering the function of genes transcribed by sporulation-specific  $\sigma$  factors. Although there are still many questions to be answered, thanks to the concerted efforts of thousands of researchers over the past 50 years, we have achieved a relatively comprehensive understanding of the function of many sporulation-specific proteins. However, most *B. subtilis* proteins are produced during vegetative growth, before polar

septation, and the manner in which they contribute to sporulation remains largely unknown. This critical gap in our knowledge of sporulation is mainly due to the lack of suitable genetic tools to inhibit the function of specific proteins in a precise, cell- and developmental stage-specific manner during spore formation. The precisely regulated inactivation of target proteins is critical because many such proteins are important for growth, so null mutations may be nonviable or unable to initiate sporulation. Furthermore, because sporulating cells do not grow or divide following polar septation, methods based on inhibition of transcription or translation to deplete specific proteins have limited utility. Indeed, the average half-life of bacterial proteins is approximately 8–20 h in growing and stationary phase cells (Koch and Levy, 1955; Borek *et al.*, 1958; Mandelstam, 1958; Kock *et al.*, 2004), which, due to the absence of growth during sporulation, would produce a negligible reduction in the amount of protein in the approximately 3 h between polar septation and forespore maturation (at 37°C). Thus, there is a need for new systems to rapidly deplete proteins, preferably in a cell- and developmental stage-specific manner.

In 2008, Griffith and Grossman developed an inducible, targeted protein degradation system in *B. subtilis* (Griffith and Grossman, 2008), which provides an opportunity to circumvent these limitations. The system is based on the addition of a modified *ssrA* tag from *Escherichia coli* (hereafter *ssrA*<sup>\*</sup>) to the C-terminus of the target protein, and the expression of the *E. coli sspB* (*sspB*<sup>E<sub>c</sub></sup>) from inducible promoters. When SspB<sup>E<sub>c</sub></sup> is produced, it binds to the *ssrA*<sup>\*</sup> tag and delivers the target protein to the endogenous *B. subtilis* protease, ClpXP, for degradation. This system supports the degradation of target proteins within minutes after the induction of *sspB*<sup>E<sub>c</sub></sup> expression (Griffith and Grossman, 2008; Eswaramoorthy *et al.*,

2014; Yen Shin *et al.*, 2015; Lamsa *et al.*, 2016; Lopez-Garrido *et al.*, 2018), allowing for the rapid depletion of proteins in non-dividing cells.

We have previously shown that the expression of *sspB<sup>Ec</sup>* from sporulation-specific promoters dependent on  $\sigma^F$  and  $\sigma^E$  supports the efficient degradation of *ssrA*\*-tagged proteins in a cell-specific manner during sporulation (Yen Shin *et al.*, 2015; Lopez-Garrido *et al.*, 2018). Here, we expand on our previous study to build a comprehensive framework, called spatiotemporally regulated proteolysis (STRP), to rapidly deplete target proteins in a cell- and developmental stage-specific manner. We demonstrate that our framework is well suited to dissect the cell- and stage-specific requirement of target proteins during sporulation. First, we provide evidence that degradation of abundant target proteins does not affect the turnover of native ClpXP substrates. Second, we show that degradation of control proteins with well-documented roles in sporulation produce phenotypes equivalent to those of the null mutants. Third, we demonstrate that proteins produced before polar septation are rapidly degraded in a spatially and temporally controlled manner.

We have applied STRP to dissect the spatiotemporal requirement of the stationary-phase  $\sigma$  factor  $\sigma^H$ , and the essential vegetative  $\sigma$  factor  $\sigma^A$ , during sporulation. Our results indicate that  $\sigma^H$  is only required in predivisional cells, and does not play a major role once polar septation occurs. However, we present evidence that  $\sigma^A$  plays different roles in mother cell and forespore: in the mother cell, it may replenish housekeeping functions

needed to complete sporulation; in the forespore, it is required early in sporulation to produce spores that germinate efficiently and it is essential for spore outgrowth.

## Results

### Degradation of abundant *ssrA*\*-tagged proteins does not saturate ClpXP protease in *B. subtilis*

Targeted protein degradation systems based on modified *ssrA* tags have emerged as a powerful genetic tool in different bacteria, including *B. subtilis* (McGinness *et al.*, 2006; Griffith and Grossman, 2008; Wei *et al.*, 2011). Because those systems rely upon endogenous proteases (ClpXP in *B. subtilis*) to degrade target proteins, a potential caveat is that inducing the degradation of an abundant target protein could saturate the protease, preventing processing of its natural substrates (Cookson *et al.*, 2014). To test this possibility, we sought to develop an *in vivo* reporter for ClpXP saturation in *B. subtilis*. Toward this end, we constructed an N-terminal fusion of the green fluorescent protein (GFP) to the stress-related transcriptional regulator, Spx. A strain producing GFP-Spx as the only source of Spx was resistant to diamide (data not shown), suggesting that the fusion protein is functional (Nakano *et al.*, 2003). Under standard laboratory conditions, Spx is maintained at low levels due to proteolysis by ClpXP (Nakano *et al.*, 2002). Accordingly, no GFP-Spx is observed by fluorescence microscopy (Fig. 2A, +ClpXP). However, when

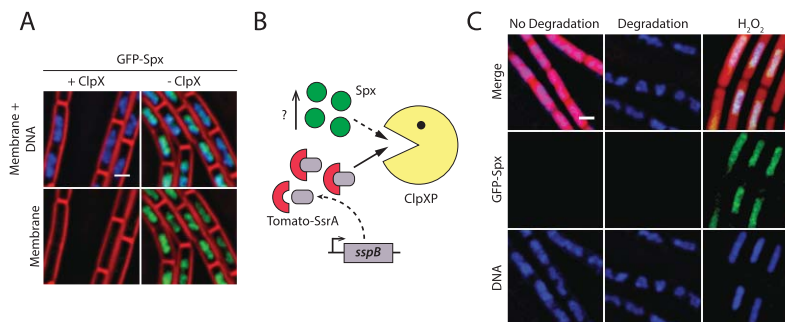


**Fig. 2.** Degradation of an abundant protein does not affect turnover of a native ClpXP substrate. A. Fluorescence microscopy of a strain carrying a GFP-Spx fusion that expresses ClpX under the control of an IPTG-inducible promoter (BER0552), grown in the presence (left, +ClpX) or absence (right, -ClpX) of 1 mM IPTG. When ClpX is limiting, GFP-Spx accumulates. Membranes are stained with FM4-64 (red) and DNA with DAPI (blue). Scale bar, 1  $\mu$ m. B. Inducing degradation of abundant *ssrA*\*-tagged proteins should cause accumulation of GFP-Spx if ClpXP is saturated. C. Fluorescence microscopy of a strain carrying a GFP-Spx fusion, producing the red fluorescent protein, tomato, from a strong promoter and *SspB<sup>Ec</sup>* from a xylose-inducible promoter (BER0577), grown in the absence (left, no degradation) or in the presence (middle, degradation) of 1% xylose, or with 2 mM  $H_2O_2$  (right) as a positive control. Imaging was performed 2 h after treatment. Inducing degradation does not yield an accumulation of GFP-Spx, but treatment with hydrogen peroxide, which is known to evoke the Spx response, does. Membranes are stained with FM4-64 (red) and DNA with DAPI (blue). Scale bar, 1  $\mu$ m.

the amount of ClpXP becomes limiting, GFP-Spx accumulates, yielding a clear fluorescent signal that co-localizes with the nucleoid (Fig 2A, -ClpXP). We reasoned that if inducing the degradation of *ssrA*\*-tagged proteins saturated ClpXP, we would observe an accumulation of GFP-Spx signal that co-localizes with the nucleoid. To test this idea, we induced the degradation of an *ssrA*\*-tagged derivative of the red fluorescent protein (Tomato-*ssrA*\*) produced at high levels from a strong constitutive promoter, and looked for the appearance of GFP-Spx (Fig. 2B). As a positive control, this strain was also treated with hydrogen peroxide, which has previously been shown to evoke the Spx response (Leelakriangsak *et al.*, 2007). Degradation of Tomato-*ssrA*\* did not result in the accumulation of GFP-Spx, whereas hydrogen peroxide treatment did (Fig. 2C). These data suggest that targeting abundant proteins for degradation by ClpXP has little or no effect on ClpXP housekeeping activity. Thus, the phenotypes observed upon degradation of target proteins are likely the result of target protein inactivation rather than a consequence of ClpXP saturation.

#### Development of a cell-specific protein degradation system during *B. subtilis* sporulation

To adapt targeted protein degradation to the study of sporulation in *B. subtilis*, we explored the possibility of using developmentally-regulated promoters to drive *sspB<sup>Ec</sup>* expression. We have previously employed  $\sigma^F$ - and  $\sigma^E$ -dependent promoters to produce *SspB<sup>Ec</sup>* and degrade the SpoIIIE DNA translocase after polar septation (Yen Shin *et al.*, 2015; Lopez-Garrido *et al.*, 2018).  $\sigma^F$  and  $\sigma^E$  are rapidly inactivated once engulfment is completed (Li and Piggot, 2001), which limits the ability of this approach to study proteins that are required throughout sporulation. Thus, we decided to expand the set of developmentally-regulated promoters to increase the versatility of the protein degradation system.

We designed a genetic strategy to screen for cell-specific promoters that triggered the efficient degradation of target proteins when driving the expression of *sspB<sup>Ec</sup>* (Fig. 3A). Specifically, we constructed strains producing *ssrA*\*-tagged versions of the essential sporulation proteins,  $\sigma^G$  and  $\sigma^K$ , which orchestrate cell-specific transcription after engulfment in the forespore and mother cell respectively (Fig. 1). *B. subtilis* mutants lacking  $\sigma^G$  or  $\sigma^K$  are unable to form spores (Supporting Information Table S1). However, the addition of the *ssrA*\* tags did not produce any observable defect in spore morphogenesis or titer (Fig. 3B–D; Supporting Information Table S1), suggesting that both tagged proteins are fully functional. Expression of *sspB<sup>Ec</sup>* from a

xylose-inducible promoter, however, yielded a dramatic reduction in spore titer for both strains (Fig. 3B; Supporting Information Table S1), indicating that  $\sigma^G$ -*ssrA*\* and  $\sigma^K$ -*ssrA*\* were efficiently degraded. Note that the addition of 1% of xylose alone to sporulating cultures did not reduce spore titers (Fig. 3B) nor affect the progression of sporulation (Supporting Information Fig. S1). We then chose sporulation cell-specific promoters to drive *sspB<sup>Ec</sup>* expression and tested if they triggered the efficient degradation of  $\sigma^G$ -*ssrA*\* and  $\sigma^K$ -*ssrA*\*. We selected promoters belonging to three different temporal classes:

- (i) Early promoters, active immediately after polar septation in the forespore ( $\sigma^F$ -dependent) or in the mother cell ( $\sigma^E$ -dependent), but inactive after engulfment. We selected the  $\sigma^F$ -dependent promoters *P<sub>spoIIIF</sub>* (Karow *et al.*, 1995) and *P<sub>spoIIQ</sub>* (Londoño-Vallejo *et al.*, 1997), and the  $\sigma^E$ -dependent promoters *P<sub>spoIID</sub>* (Clarke *et al.*, 1986; Rong *et al.*, 1986) and *P<sub>spoIVA</sub>* (Roels *et al.*, 1992).
- (ii) Late promoters, active in the forespore ( $\sigma^G$ -dependent) or the mother cell ( $\sigma^K$ -dependent) after engulfment. Here we used the  $\sigma^G$ -dependent promoters *P<sub>sspA</sub>* and *P<sub>sspB</sub>* (Nicholson *et al.*, 1989) and the  $\sigma^K$ -dependent promoters *P<sub>gerE</sub>* (Cutting *et al.*, 1989) and *P2<sub>cotE</sub>* (Zheng and Losick, 1990) for late forespore and mother cell expression respectively. Note that *P<sub>sspB</sub>* drives the expression of the *Bacillus sspB* gene, which encodes the major  $\beta$ -type small acid-soluble protein and is unrelated to the degradation adaptor protein *SspB<sup>Ec</sup>*.
- (iii) Sustained promoters, continuously active in the forespore ( $\sigma^F$ - and  $\sigma^G$ -dependent) or the mother cell ( $\sigma^E$ - and  $\sigma^K$ -dependent) during and after engulfment. The synthetic *P<sub>sspE(2G)</sub>* (Sun *et al.*, 1991), which is recognized by both  $\sigma^F$  and  $\sigma^G$ , was used to continuously transcribe *sspB<sup>Ec</sup>* in the forespore. To continuously transcribe *sspB<sup>Ec</sup>* in the mother cell, we used the two *cotE* promoters, the first of which is activated by  $\sigma^E$  (*P1<sub>cotE</sub>*), and the second by  $\sigma^K$  (*P2<sub>cotE</sub>*) (Zheng and Losick, 1990).

As shown in Fig. 3B, forespore expression of *sspB<sup>Ec</sup>* from *P<sub>spoIIQ</sub>*, *P<sub>sspE(2G)</sub>*, *P<sub>sspA</sub>* and *P<sub>sspB</sub>* resulted in significant spore titer defects in strains expressing  $\sigma^G$  tagged with *ssrA*\*. Similarly, mother cell expression of *sspB<sup>Ec</sup>* from *P<sub>spoIVA</sub>*, *P<sub>cotE</sub>*, *P<sub>gerE</sub>* and *P2<sub>cotE</sub>* significantly reduced the spore titer of the  $\sigma^K$ -*ssrA*\* strain. Importantly, no spore titer defects were observed in the  $\sigma^G$ -*ssrA*\* and  $\sigma^K$ -*ssrA*\* strains when *sspB<sup>Ec</sup>* was expressed in the cell in which the transcription factor is not active. Only the early promoters *P<sub>spoIIF</sub>* and *P<sub>spoIID</sub>* failed to trigger efficient degradation of  $\sigma^G$ -*ssrA*\* and  $\sigma^K$ -*ssrA*\* respectively. Both promoters are only transiently active during engulfment (Clarke *et al.*, 1986; Karow *et al.*,

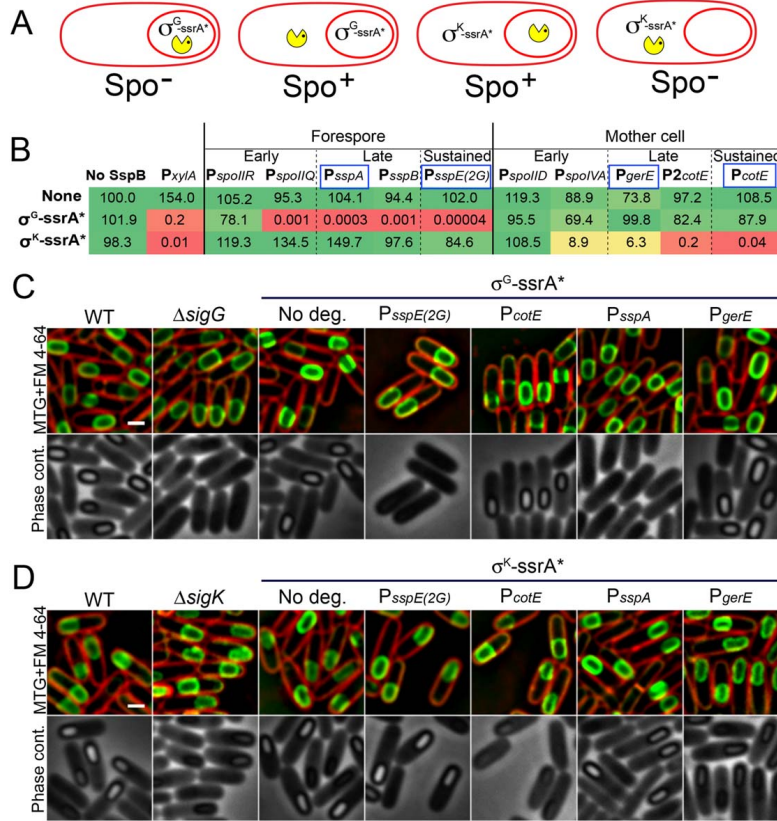


**Fig. 3.** Optimization of cell- and stage-specific protein degradation system.

**A.** Diagram representing the genetic strategy used to screen for cell-specific promoters that trigger the efficient degradation of target proteins when driving the expression of *sspB<sup>Ec</sup>*. We constructed *ssrA*\*-tagged versions of  $\sigma^G$  and  $\sigma^K$ , which are essential for sporulation and required in the forespore and mother cell, respectively. Degradation of either protein in the cell in which they are required should yield a strong sporulation defect (Spo<sup>-</sup>), while expression of *sspB<sup>Ec</sup>* in the opposite cell should have no effect (Spo<sup>+</sup>).

**B.** Relative spore titers of strains expressing *sspB<sup>Ec</sup>* from different cell-specific promoters (columns) in the absence of *ssrA*\*-tagged protein (none), when  $\sigma^G$  is tagged with *ssrA*\* ( $\sigma^G$ -*ssrA*\*) or when  $\sigma^K$  is tagged with *ssrA*\* ( $\sigma^K$ -*ssrA*\*) are shown. To facilitate data comparison, the spore titer of the wild type strain (no *ssrA*\*, no *SspB<sup>Ec</sup>*) was relativized to 100. The actual values are shown in Supporting Information Table S1. The color indicates the severity of the spore titer defect (green, no defect; yellow, moderate defect; red, severe defect). Expression from *P<sub>xyIA</sub>* was induced by the addition of 1% xylose. Sporulation-specific promoters were classified in three temporal classes according to their expression pattern: early promoters are activated shortly after polar septation, and inactivated after engulfment; late promoters are activated after engulfment; sustained promoters are continuously active throughout engulfment and forespore maturation. The promoters selected for further characterization are indicated by a blue box.

**C.** Micrographs of wild type sporangia (WT),  $\sigma^G$  mutant sporangia ( $\Delta sigG$ ) and sporangia in which  $\sigma^G$  is tagged with *ssrA*\* ( $\sigma^G$ -*ssrA*\*) in the absence of *SspB<sup>Ec</sup>* (No deg.) or when *SspB<sup>Ec</sup>* is produced from the sustained promoters *P<sub>sspE(2G)</sub>* and *P<sub>cotE</sub>* or the late promoters *P<sub>sspA</sub>* and *P<sub>gerE</sub>*. The top row shows membranes stained with FM 4-64 (red) and Mitotracker green (green). The bottom row shows phase contrast pictures. Pictures were taken 6 h after sporulation induction (t<sub>6</sub>). Scale bar, 1  $\mu$ m.

**D.** Micrographs of wild type sporangia (WT),  $\sigma^K$  mutant sporangia ( $\Delta sigK$ ) and sporangia in which  $\sigma^K$  is tagged with *ssrA*\* ( $\sigma^K$ -*ssrA*\*) in the absence of *SspB<sup>Ec</sup>* (No deg.) or when *SspB<sup>Ec</sup>* is produced from the sustained promoters *P<sub>sspE(2G)</sub>* and *P<sub>cotE</sub>* or the late promoters *P<sub>sspA</sub>* and *P<sub>gerE</sub>*. The top row shows membranes stained with FM 4-64 (red) and Mitotracker green (green). The bottom row shows phase contrast pictures. Pictures were taken 6 h after sporulation induction (t<sub>6</sub>). Scale bar, 1  $\mu$ m.

1995; Wu and Errington, 2000; Eichenberger *et al.*, 2004). In addition,  $P_{spoIII}$  is particularly weak (Sharp and Pogliano, 2002; Ojic *et al.*, 2016). Thus, it is possible these promoters do not yield enough SspB<sup>Ec</sup> to mediate the complete and/or sustained degradation of  $\sigma^G$ -ssrA\* and  $\sigma^K$ -ssrA\* once engulfment is complete. To avoid complications due to inactivation of promoters after engulfment, we focused on sustained and late promoters for further characterization. We specifically selected the sustained promoters  $P_{sspE(2G)}$  and  $P_{cotE}$  and the late promoters  $P_{sspA}$  and  $P_{gerE}$ . Although  $P_{2cotE}$  produced a stronger spore titer defect than  $P_{gerE}$  when  $\sigma^K$  was tagged with ssrA\* (Fig. 3B), we observed that its pattern of expression was variable, leading to premature degradation of target proteins in a fraction of the sporangia (not shown). We therefore decided to exclude  $P_{2cotE}$  from further studies. The sustained and late promoters that we selected for use in our system are indicated by a blue box in Fig. 3B.

#### Characterization of cell-specific degradation from sustained and late promoters

We next performed experiments to confirm that the selected promoters conferred the expected temporal and spatial regulation on  $sspB^{Ec}$  expression, and that they yielded enough SspB<sup>Ec</sup> to completely degrade target proteins. First, we made transcriptional fusions to *gfp* to confirm the expression pattern from the different promoters using fluorescence microscopy (Supporting Information Fig. S2). As expected,  $P_{sspE(2G)}$  and  $P_{cotE}$  conveyed sustained forespore- and mother cell-specific *gfp* expression that could be visualized shortly after polar septation, whereas  $P_{sspA}$  and  $P_{gerE}$  conveyed late expression in these cells. Expression of  $sspB^{Ec}$  from these promoters had no detectable effect on sporulation (Fig. 3B; Supporting Information Table S1). In addition, we compared the expression levels from the selected sustained or late promoters with the expression level of a xylose-inducible promoter ( $P_{xyIA}$ ) induced with a xylose concentration (0.01%) that we determined was enough to completely degrade abundant ssrA\* tagged proteins during vegetative growth (Supporting Information Fig. S3). As shown in Supporting Information Fig. S3E, expression from sustained and late promoters yielded intracellular GFP concentrations that were at least 20-fold higher than the concentration achieved when GFP was expressed from  $P_{xyIA}$  induced with 0.01% of xylose, suggesting that, when produced from the selected sustained and late promoters, SspB<sup>Ec</sup> is not limiting for degradation. Finally, we performed microscopy to determine if the cytological profiles obtained upon cell-specific degradation of  $\sigma^G$ -ssrA\* and  $\sigma^K$ -ssrA\* matched those of the

$\sigma^G$ - and  $\sigma^K$ - mutants. We used a combination of fluorescence and phase contrast microscopy to assess the completion of two developmental milestones: engulfment membrane fission, which depends on early cell-specific gene expression, and forespore dehydration, which depends on late cell-specific gene expression. To assess the completion of engulfment, we simultaneously stained sporangia with two membrane dyes: FM 4-64, which fluoresces red and is membrane-impermeable, and Mitotracker Green (MTG), which fluoresces green and is membrane-permeable (Sharp and Pogliano, 1999). During engulfment, the membrane of the forespore is exposed to the culture medium, and is accessible to both FM 4-64 and MTG. After engulfment culminates with membrane fission, the forespore is completely enclosed within the mother cell cytoplasm and the forespore membranes can only be stained by the membrane-permeable dye MTG, but not FM 4-64. This allows sporangia that have completed engulfment membrane fission to be easily distinguished from those that have not (Sharp and Pogliano, 1999). To assay forespore dehydration, we used phase-contrast microscopy and observed the appearance of phase-bright spores.

Degradation of  $\sigma^G$ -ssrA\* from the sustained promoter  $P_{sspE(2G)}$  or the late promoter  $P_{sspA}$  produced cytological profiles that phenocopied that of the  $\sigma^G$ - null mutant, with completion of engulfment membrane fission, but no forespore dehydration (Fig. 3C). Production of SspB<sup>Ec</sup> from the mother cell-specific promoters  $P_{cotE}$  or  $P_{gerE}$  in strains producing  $\sigma^G$ -ssrA\*, however, resulted in wild type profiles (Fig. 3C). Similarly, degradation of  $\sigma^K$ -ssrA\* from  $P_{cotE}$  or  $P_{gerE}$  allowed completion of engulfment membrane fission, but yielded less dehydrated, phase-gray forespores, similar to the  $\sigma^K$ - null mutant (Fig. 3D). As expected, production of SspB<sup>Ec</sup> from forespore-specific promoters did not trigger  $\sigma^K$ -ssrA\* degradation and resulted in wild-type cytological profiles (Fig. 3D). To confirm that  $\sigma^G$  and  $\sigma^K$  were efficiently degraded, we tagged each protein with GFP and ssrA\*. A clear GFP fluorescence signal was observed in the forespore and the mother cell in strains producing  $\sigma^G$ -GFP-ssrA\* and  $\sigma^K$ -GFP-ssrA\*, respectively (Supporting Information Fig. S4). The signal completely disappeared when  $sspB^{Ec}$  was expressed in the appropriate compartment from either sustained or late promoters (Supporting Information Fig. S4), indicating that both proteins were efficiently degraded. The cytological profiles and spore titers obtained after degradation of  $\sigma^G$ -GFP-ssrA\* and  $\sigma^K$ -GFP-ssrA\* were equivalent to those obtained after of  $\sigma^G$ -ssrA\* and  $\sigma^K$ -ssrA\* degradation (Supporting Information Fig. S4 and Supporting Information Table S1).

It is interesting to note that degradation of  $\sigma^G$  and  $\sigma^K$  from late promoters produced cytological profiles equivalent to those of the null mutants (Fig. 3C and D;

Supporting Information Fig. S4). Because transcription from late promoters depends on  $\sigma^G$  and  $\sigma^K$ , those  $\sigma$  factors must be initially activated, allowing a burst of expression of the genes under their control, including *sspB<sup>Ec</sup>*. Once enough SspB<sup>Ec</sup> has accumulated, it will trigger the degradation of  $\sigma^G$ -ssrA\* and  $\sigma^K$ -ssrA\*. Thus, these results suggest that  $\sigma^G$  and  $\sigma^K$  activity is required continuously during forespore maturation, and not just transiently after engulfment has been completed.

Overall, the above results demonstrate that production of SspB<sup>Ec</sup> from developmentally regulated promoters can be used to trigger the cell-specific degradation of sporulation-specific target proteins, yielding cytological profiles equivalent to the null mutants.

#### *Cell- and stage-specific degradation of vegetative proteins*

To assess whether expression of *sspB<sup>Ec</sup>* from the selected promoters led to an efficient, spatiotemporally-regulated degradation of target proteins made before polar septation, we studied the degradation of a YtsJ-GFP-ssrA\* fusion protein (Lamsa *et al.*, 2016). YtsJ is an abundant, non-essential cytoplasmic protein that is not required for sporulation. We visually evaluated degradation based on the disappearance of GFP fluorescence (Fig. 4A). The results obtained can be summarized as follows: (i) When *sspB<sup>Ec</sup>* was not expressed, a clear fluorescent signal was observed filling the cytoplasm of the mother cell and the forespore, as well as the cytoplasm of predivisional cells. (ii) Production of SspB<sup>Ec</sup> from sustained promoters triggered the continuous degradation of YtsJ-GFP-ssrA\* in the forespore ( $P_{sspE(2G)}$ ) or the mother cell ( $P_{cotE}$ ), starting shortly after polar septation. We also triggered degradation in both cells simultaneously by producing SspB<sup>Ec</sup> from  $P_{sspE(2G)}$  and  $P_{cotE}$  at the same time; in this case, fluorescence was only observed in cells before polar septation. (iii) Production of SspB<sup>Ec</sup> from the late promoters triggered degradation in the forespore ( $P_{ssrA}$ ), in the mother cell ( $P_{gerE}$ ) or in both ( $P_{ssrA} P_{gerE}$ ) only after engulfment completion. In every case, no fluorescence was detected in the cell types in which YtsJ-GFP-ssrA\* had been degraded, indicating that SspB<sup>Ec</sup> production led to the rapid and efficient degradation of the target protein.

Next, we performed timelapse microscopy to determine how quickly YtsJ-GFP-ssrA\* was degraded upon induction of *sspB<sup>Ec</sup>* expression. We specifically used sustained promoters, which are active immediately after polar septation, to drive the expression of *sspB<sup>Ec</sup>*, since polar septation provides a clear marker for the onset of degradation. We stained sporangia with the membrane

dye FM 4–64 and monitored the disappearance of YtsJ-GFP-ssrA\* fluorescence signal upon induction of *sspB<sup>Ec</sup>* expression in the mother cell or the forespore from  $P_{cotE}$  and  $P_{sspE(2G)}$ , respectively (Fig. 4B). To correct for GFP photobleaching due to continuous imaging, we calculated the ratio between the GFP intensity in the compartment in which degradation was induced and the other compartment. Once degradation started, the decrease in GFP fluorescence followed an exponential decay. Degradation was slightly faster in the forespore (protein half-life  $4.6 \pm 1.3$  min) than in the mother cell (protein half-life  $6.7 \pm 2.3$  min) (Fig. 4C). It has been reported that ClpXP is more active in the mother cell than in the forespore (Kain *et al.*, 2008). It seems therefore unlikely that the faster degradation kinetics in the forespore is due to differences in ClpXP activity between both cells, in which case we would expect degradation to happen faster in the mother cell. Instead, the difference might reflect a slower accumulation of SspB<sup>Ec</sup> in the mother cell due to its larger volume or differences in promoter strength. The kinetic data from cell-specific degradation are in good agreement with degradation speeds estimated at the population level in vegetative cells (Griffith and Grossman, 2008; Eswaramoorthy *et al.*, 2014; Lamsa *et al.*, 2016). Importantly, according to the estimated degradation rates, cell-specific expression of *sspB<sup>Ec</sup>* would allow complete depletion of target proteins within approximately 20–30 min, which is significantly less time than required for engulfment under these conditions (~ 90 min, Ojkic *et al.*, 2016).

These results show that expression of *sspB<sup>Ec</sup>* from sustained and late promoters allows the rapid degradation of proteins made before polar septation in a spatially and temporally controlled manner. Sustained promoters remain active in the forespore or mother cell throughout sporulation, while late promoters are active only after engulfment. Therefore, the use of both temporal classes of promoters to trigger degradation of target proteins, in combination with various assays to assess the completion of developmental milestones (Harwood *et al.*, 1990), allows for the dissection of the temporal and cell-specific requirement of target proteins during sporulation (Fig. 4D). We have named this experimental approach spatiotemporally regulated proteolysis (STRP). In the next sections, we have used STRP to dissect the cell-specific role that two key vegetative sigma factors,  $\sigma^H$  and  $\sigma^A$ , play during sporulation.

#### *The stationary phase sigma factor $\sigma^H$ is only required in predivisional cells*

The initiation of sporulation requires the activation of the stationary-phase sigma factor,  $\sigma^H$ , which is required

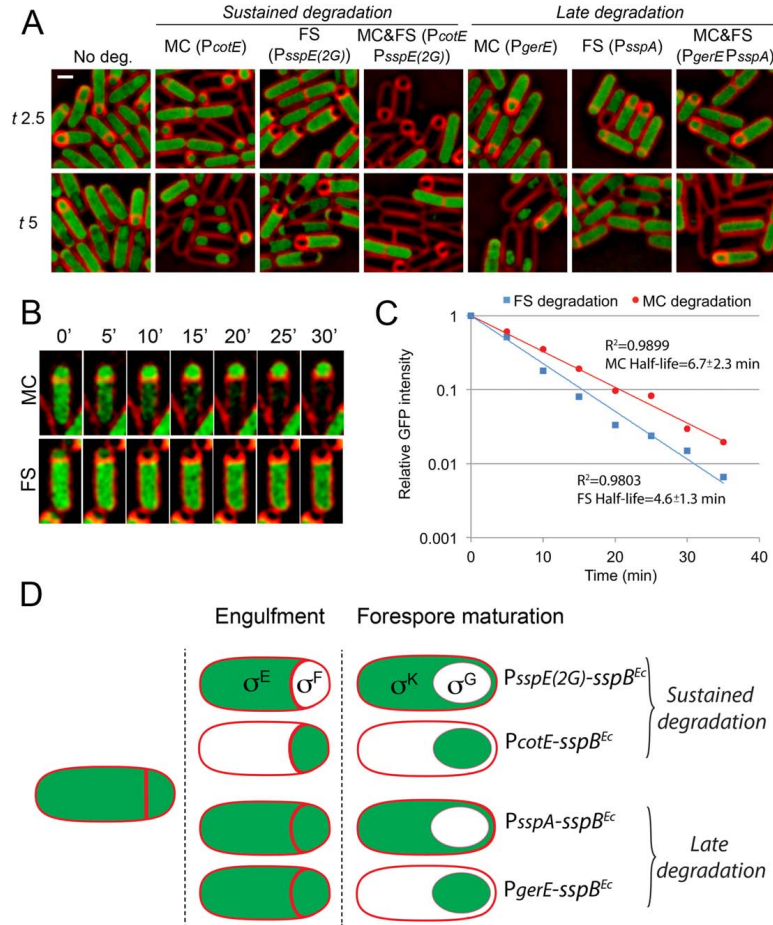


**Fig. 4.** Cell- and stage-specific degradation of vegetative proteins.

A. Fluorescence microscopy showing the cell-specific degradation of YtsJ-GFP-ssrA\*. SspB<sup>Ec</sup> was produced from sustained promoters (indicated in parentheses) in the mother cell (MC), forespore (FS) or both (MC&FS) to induce the sustained degradation of YtsJ-GFP-ssrA\*. To induce degradation only after engulfment (late degradation), sspB<sup>Ec</sup> was expressed from late promoters. Membranes were stained with FM 4-64. Scale bar, 1  $\mu$ m.

B. Timelapse microscopy showing the disappearance of YtsJ-GFP-ssrA\* fluorescence signal when degradation is induced in the mother cell (MC, sspB<sup>Ec</sup> expressed from  $P_{cotE}$ ) or in the forespore (FS, sspB<sup>Ec</sup> expressed from  $P_{sspE(2G)}$ ). Images taken every 5 min are shown. Membranes were stained with FM 4-64.

C. YtsJ-GFP-ssrA\* degradation kinetics when SspB<sup>Ec</sup> is produced in the forespore (blue squares and line) or in the mother cell (red circles and line). In both cases, the disappearance of the GFP signal follows an exponential decay. The coefficient of determination of the regression curves ( $R^2$ ), and the half-lives of YtsJ-GFP-ssrA\* when degradation is induced in the mother cell or the forespore are indicated in the graph. Data represent the average of 17 and 14 sporangia for forespore and mother cell degradation respectively.

D. STRP setup. The use of sustained promoters ( $P_{sspE(2G)}$  and  $P_{cotE}$ ) allows the sustained degradation of target proteins in the mother cell or the forespore. Expression of sspB<sup>Ec</sup> from late promoters ( $P_{sspA}$  and  $P_{gerE}$ ), however, triggers degradation of target proteins only after engulfment is completed. The combination of both classes of cell-specific promoters allows the evaluation of the spatial and temporal requirement of proteins made before polar septation.



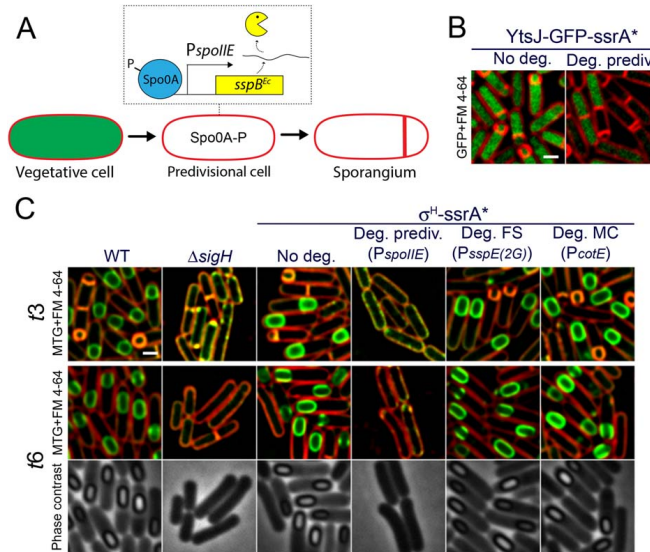


**Fig. 5.**  $\sigma^H$  activity is only required in predivisional cells.

A. Diagram representing the strategy used to induce the degradation of target proteins in predivisional cells about to undergo polar septation. Before polar septation, Spo0A becomes phosphorylated and controls the expression of several genes required for entry into sporulation. Expression of *sspB<sup>Ec</sup>* from promoters activated by Spo0A would trigger degradation in predivisional cells, before polar septation occurs. We specifically used the promoter of *spolIE* to drive *sspB<sup>Ec</sup>* expression.

B. Degradation of YtsJ-GFP-ssrA\* in predivisional cells. Membranes were stained with FM 4–64. Scale bar, 1  $\mu$ m.

C. Micrographs of wild type sporangia (WT),  $\sigma^H$  mutant sporangia ( $\Delta sigH$ ) and sporangia in which  $\sigma^H$  is tagged with ssrA\* ( $\sigma^H$ -ssrA\*) in the absence of SspB<sup>Ec</sup> (No deg.) or when SspB<sup>Ec</sup> is produced in predivisional cells from P<sub>spolIE</sub> (Deg. prediv.), in the forespore from P<sub>sspE(2G)</sub> (Deg. FS) or in the mother cell from P<sub>cotE</sub> (Deg. MC). Pictures were taken 3 (t3) and 6 (t6) hours after sporulation induction. Membranes stained with FM 4–64 (red) and Mitotracker green (green) are shown for t3 and t6. Phase contrast pictures are only shown for t6. Scale bar, 1  $\mu$ m.

for polar septation. Accordingly,  $\sigma^H$ - mutants are unable to undergo polar septation and do not initiate sporulation (Fig. 5C,  $\Delta sigH$ ). While its importance in sporulation initiation is well established, it is unclear if  $\sigma^H$  activity is required in the mother cell or forespore after polar septation. To evaluate this possibility, we constructed a  $\sigma^H$ -ssrA\* fusion protein, which supports sporulation at levels comparable to the wild type (Supporting Information Table S1). First, we validated that degradation of  $\sigma^H$ -ssrA\* prior to polar septation suppressed the formation of the polar septum. For this purpose we used two different strategies. First, we induced degradation of  $\sigma^H$ -ssrA\* by expressing *sspB<sup>Ec</sup>* from a xylose-inducible promoter (Supporting Information Fig. S5), which triggers  $\sigma^H$ -ssrA\* degradation continuously during the growth of the culture. Second, we expressed *sspB<sup>Ec</sup>* from the Spo0A-dependent promoter P<sub>spolIE</sub>, which becomes active in predivisional cells, shortly before polar septation (Fig. 5A). This second

strategy restricts degradation to predivisional cells that are about to commit to sporulation, a point that we confirmed by monitoring the disappearance of YtsJ-GFP-ssrA\* (Fig. 5B). In both cases, degradation of  $\sigma^H$ -ssrA\* prior to polar septation resulted in the inhibition of polar septum formation (Fig. 5C; Supporting Information Fig. S5), confirming the requirement of  $\sigma^H$ -dependent transcription in predivisional cells to start sporulation. We next determined the cytological profiles obtained upon cell-specific degradation of  $\sigma^H$ -ssrA\* from forespore- and mother cell-specific sustained promoters. As shown in Fig. 5C, degradation of  $\sigma^H$ -ssrA\* in the forespore or mother cell yielded cytological profiles equivalent to the control strain. These results suggest that  $\sigma^H$  does not play a critical role in either the forespore or the mother cell. Altogether, our results indicate that  $\sigma^H$ -dependent transcription is required in predivisional cells until the polar septum is formed, but that it is dispensable after polar septation.

### Effect of cell-specific degradation of $\sigma^A$ on spore formation

$\sigma^A$  is the only essential sigma factor in *B. subtilis*, and it controls the transcription of housekeeping genes in vegetative cells (Haldenwang, 1995). During sporulation,  $\sigma^A$  is present in both the mother cell and the forespore (Yen Shin *et al.*, 2015), and it is bound to a fraction of the core RNA polymerase (Ju *et al.*, 1999; Fujita, 2000). In addition, it has been shown that  $\sigma^A$  is active and that it mediates gene transcription in both cells (Li and Piggot, 2001). However, the actual relevance of  $\sigma^A$ -mediated transcription during sporulation is not known.

To address this question, we used a  $\sigma^A$ -ssrA\* version that supported a vegetative growth rate close to that of wild type in the absence of degradation, but did not support growth when *sspB<sup>Ec</sup>* expression was induced from a xylose-dependent promoter (Lamsa *et al.*, 2016). First, we studied the effect of cell-specific degradation of  $\sigma^A$ -ssrA\* from sustained and late promoters on spore titers, measured as the ability of heat-treated spores to form colonies in the presence of nutrients. In the absence of degradation, a strain containing  $\sigma^A$ -ssrA\* showed a mild spore titer reduction of approximately two- to threefold compared with the wild type (Fig. 6A), suggesting that the functionality of the tagged protein was somewhat impaired, but still enough to support spore formation. When degradation was induced in the mother cell from the sustained promoter *P<sub>cotE</sub>*, there was a modest additional threefold reduction in spore titer. No additional reduction was observed when *SspB<sup>Ec</sup>* was produced from the late mother cell-specific promoter *P<sub>gerE</sub>* (Fig. 6A). These results suggest that  $\sigma^A$ -dependent transcription does not play a major role in the mother cell during sporulation, although it might contribute to replenish the pool of housekeeping proteins early during development. When degradation was induced in the forespore from sustained (*P<sub>sspE(2G)</sub>*) or late (*P<sub>sspA</sub>*) promoters, however, there was a dramatic reduction in the spore titer of approximately five orders of magnitude (Fig. 6A). A similar reduction was observed when  $\sigma^A$ -ssrA\* was degraded simultaneously in the mother cell and in the forespore (Supporting Information Table S1).

To determine the specific sporulation steps affected by cell-specific degradation of  $\sigma^A$ -ssrA\*, we performed microscopy and observed the cytological profiles upon degradation of  $\sigma^A$ -ssrA\* from sustained promoters. As shown in Fig. 6B, tagging  $\sigma^A$  with ssrA\* had no detectable effect on engulfment or on the formation of phase bright spores, compared with the wild type. When degradation was induced in the mother cell, we observed occasional cell lysis, which might explain the mild spore titer defect obtained upon  $\sigma^A$ -ssrA\* degradation in the mother cell (Fig. 6A; Supporting Information Table S1).

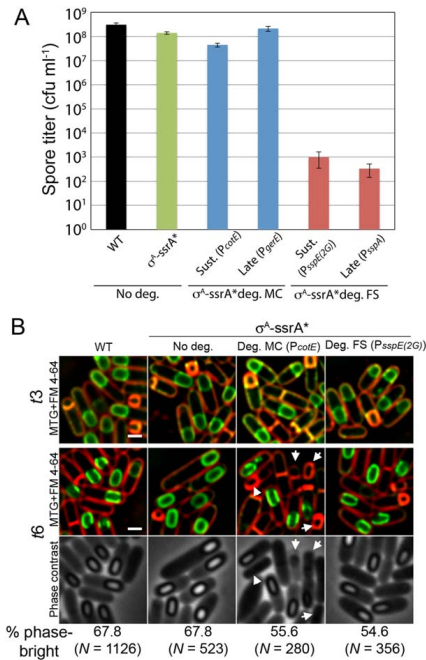


**Fig. 6.** Cell-specific degradation of  $\sigma^A$ . **A.** Spore titers, measured as the number of colony forming units per ml (cfu ml<sup>-1</sup>) in heat-killed sporulating cultures, of wild type (WT) and  $\sigma^A$ -ssrA\* strains, and strains in which  $\sigma^A$ -ssrA\* degradation is triggered in the mother cell ( $\sigma^A$ -ssrA\* deg. MC) or in the forespore ( $\sigma^A$ -ssrA\* deg. FS) from sustained (Sust.) or late promoters. The promoters used to drive the expression of *sspB<sup>Ec</sup>* are indicated in parentheses. Data represent the average and standard deviation of at least three independent experiments. **B.** Micrographs of wild type sporangia (WT) and  $\sigma^A$ -ssrA\* sporangia in the absence of degradation (No deg.) or when degradation is induced in the forespore (Deg. FS) or mother cell (Deg. MC) from sustained promoters (in parentheses). Pictures were taken 3 (t3) and 6 (t6) hours after sporulation induction. Lysed cells upon mother cell degradation at t6 are indicated by arrows. The percentage of sporangia containing phase-bright spores at t6 is shown at the bottom, including the number of sporangia (N) analyzed for each strain. Lysed sporangia were excluded from the quantification. Membranes stained with FM 4-64 (red) and Mitotracker green (green) for each time point. Phase contrast pictures are shown in the bottom row for t6. Scale bar, 1  $\mu$ m.

Nevertheless, a significant fraction of the forespores were phase bright by t6. Surprisingly, when  $\sigma^A$ -ssrA\* was degraded in the forespore there was no detectable defect in spore formation, indicating that  $\sigma^A$  is not required in the forespore for the production of phase-bright spores. Altogether, these results indicate that

$\sigma^A$ -dependent transcription is dispensable in both the forespore and the mother cell for the production of apparently mature spores.

#### *Forespore $\sigma^A$ is required for spore germination and outgrowth*

The above results suggest that the dramatic spore titer reduction observed when  $\sigma^A$ -ssrA\* is degraded in the forespore is not due to defects in forespore development. We noted that when  $\sigma^A$ -ssrA\* degradation was induced in the forespore from either sustained or late promoters, the few colonies formed by the germinating spores after overnight incubation at 30°C were remarkably small (not shown). We therefore reasoned that the spore titer defects observed after degradation of  $\sigma^A$ -ssrA\* in the forespore might be the result of deficient germination or outgrowth of spores devoid of  $\sigma^A$ , rather than the consequence of compromised spore development. In agreement with this idea, we observed the appearance of an increasing number of colonies after longer incubation of the plates at 30°C (Supporting Information Fig. S6).

To further explore this possibility, we monitored germination and outgrowth of individual spores over time using phase-contrast timelapse microscopy. During germination, the spore core is rehydrated, which causes the spores to transition from phase-bright to phase-dark. Simultaneously, the spore cortex is degraded and the coat is detached, allowing the germinated spore to resume vegetative growth during a process called outgrowth. We purified spores from the wild type strain,  $\sigma^A$ -ssrA\* (no degradation) strain, and from strains in which  $\sigma^A$ -ssrA\* degradation was induced in the forespore from either sustained or late promoters. We induced germination by placing the spores on an LB agarose pad supplemented with 10 mM of L-alanine, and used timelapse phase-contrast microscopy to monitor germination and outgrowth over time (Fig. 7A). We also estimated germination efficiency at the population level by monitoring the loss in optical density of spore suspensions upon addition of 10 mM of L-alanine (Supporting Information Fig. S7).  $\sigma^A$ -ssrA\* spores exhibited germination kinetics similar to that of wild-type spores (Supporting Information Movies S1 and S2; Supporting Information Fig. S7), with more than 90% phase-dark spores 80 minutes after imaging onset (Fig. 7B). Outgrowth was slightly delayed, however, compared with wild type (Fig. 7A), consistent with the idea that the  $\sigma^A$ -ssrA\* fusion protein is not completely functional. Spores from a strain in which  $\sigma^A$ -ssrA\* was degraded in the forespore from the late forespore promoter  $P_{sspA}$  (Fig. 7A and B; Supporting Information Movie S4; Supporting Information Fig. S7)

germinated normally, but showed no outgrowth, demonstrating that  $\sigma^A$  is required for the resumption of vegetative growth after germination, as expected. Surprisingly, spores from a strain in which  $\sigma^A$ -ssrA\* was degraded from the sustained promoter  $P_{sspE(2G)}$  showed a dramatic germination defect, with only approximately 50% of the spores transitioning to phase-dark 4 h after adding the germinant L-alanine (Fig. 7A and B; Supporting Information Movie S3; Supporting Information Fig. S7). Those spores that germinated showed no outgrowth. This suggests that  $\sigma^A$  activity is required early in sporulation to produce spores that germinate efficiently, and that  $\sigma^A$  activity in the spore is necessary for outgrowth. Potential models to explain these results are discussed below.

## Discussion

Here we present a method, called spatiotemporally regulated proteolysis (STRP), to rapidly deplete target proteins in a cell- and developmental stage-specific manner during sporulation in *B. subtilis*. STRP allows the first systematic evaluation of the cell- and developmental-stage specific requirement of proteins made before polar septation, and has the potential to complete the list of the cellular machineries required to assemble a spore. It also provides a versatile new tool to study proteins that play critical roles at several stages of sporulation, such as the peptidoglycan biosynthetic machinery, which is required for polar septation, engulfment and cortex biosynthesis.

A key feature of STRP is that it is based on the direct degradation of target proteins, rather than on the inhibition of transcription or translation. Our data indicate that target proteins are depleted within minutes after polar septation in the mother cell and in the forespore. This is critical to study the role of specific proteins during sporulation, when the lack of growth prevents the dilution of proteins and mRNAs that is required by other methods such as CRISPR interference.

An essential requirement to achieve the spatiotemporally controlled degradation of target proteins is the use of tightly regulated promoters to drive the expression of  $sspB^{Ec}$ . The sporulation regulatory program provides an excellent genetic framework for this purpose, since it includes a plethora of promoters that become active in specific cell types and developmental stages. Because these promoters show no ectopic expression, target protein degradation is only triggered in the cell and developmental stage in which the promoters are active. We have explored cell-specific promoters that are continuously active in the mother cell or the forespore after polar septation, which support the sustained degradation

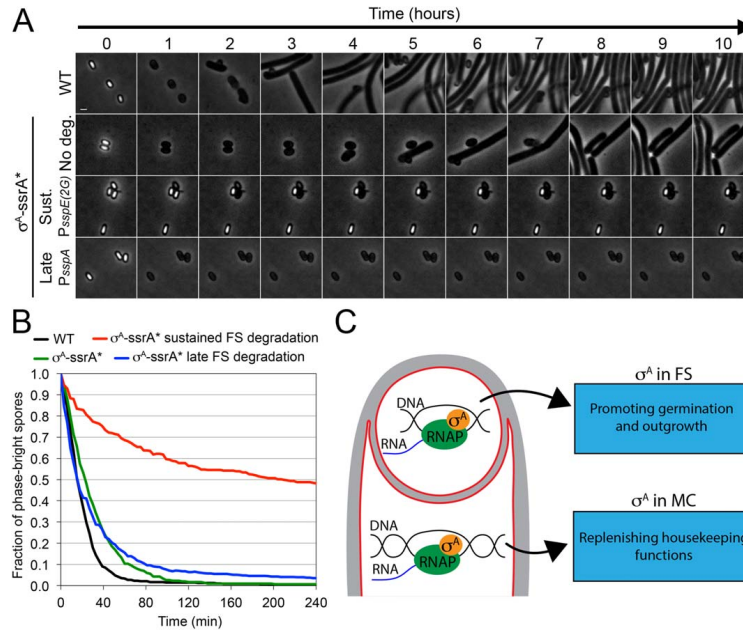


**Fig. 7.** Forespore  $\sigma^A$  contributes to spore germination and outgrowth. **A.** Phase-contrast timelapse microscopy of germinating spores from wild type (WT),  $\sigma^A$ -ssrA\* (No deg.),  $\sigma^A$ -ssrA\* sustained forespore degradation (Sust.) and  $\sigma^A$ -ssrA\* late forespore degradation (Late) strains. Images taken every hour for 10 h are shown. Complete time series of images taken every 3 min for 10 h are provided in Supporting Information Movies S1–S4. **B.** Fraction of phase-bright spores over time after germination induction, calculated from timelapse microscopy shown in **B.** Black line, wild type spores ( $N = 547$ ); green line,  $\sigma^A$ -ssrA\* spores ( $N = 318$ ); red line,  $\sigma^A$ -ssrA\* sustained forespore degradation spores ( $N = 434$ ); blue line,  $\sigma^A$ -ssrA\* late forespore degradation spores ( $N = 668$ ). The fraction of phase bright spores at the onset of imaging was relativized to 1 for every strain. More than 84% of the spores were phase-bright initially. **C.**  $\sigma^A$ -dependent transcription in the mother cell might contribute to replenish housekeeping functions during sporulation. In the forespore,  $\sigma^A$ -dependent transcription makes critical contributions to the germination and outgrowth of mature spores.

of target proteins throughout sporulation, and promoters that become active in either cell only when engulfment is completed, which trigger the late degradation of target proteins. This design provides a systematic method to determine the requirement of target proteins in the mother cell or the forespore at different developmental stages. Proteins required only during engulfment would cause sporulation defects only when subjected to sustained degradation, but not when subjected to late degradation. However, proteins required after engulfment would also produce sporulation defects upon late degradation. Altogether, our results show that STRP is well suited to dissect the spatiotemporal role of proteins made before polar septation, including essential proteins, during development. This opens new avenues in the study of sporulation, since it provides the possibility to investigate how vegetative cellular processes are

compartmentalized and coordinated between different cell types.

We here focus our efforts on the transcriptional machinery of sporulation, which provides an ideal system to test our methodology. In addition, there are key outstanding questions concerning the role played by vegetative transcription factors late in sporulation. We have used STRP to dissect the spatiotemporal requirement of two vegetative  $\sigma$  factors,  $\sigma^H$  and  $\sigma^A$ , during sporulation.  $\sigma^H$  controls gene expression upon entry into stationary phase, and some of the genes in the  $\sigma^H$  regulon are essential for sporulation initiation. Degradation of  $\sigma^H$ -ssrA\* in predivisional cells by expressing  $sspB^{Ec}$  from a high-threshold  $Spo0A$ - $P$  dependent promoter that is activated shortly before polar septation ( $P_{spoIIIE}$ ; Fujita *et al.*, 2005) blocks polar septation (Fig. 5C). This suggests that the initial  $\sigma^H$  activity after entry into

stationary phase is not sufficient for initiation of sporulation. However, degradation of  $\sigma^H$ -ssrA\* after polar septation in the mother cell, forespore or both does not produce any sporulation defects (Fig. 5C). Altogether, these results indicate that  $\sigma^H$  activity is required in pre-divisional cells until the polar septum is formed, but that after polar septation,  $\sigma^H$  activity is dispensable.

$\sigma^A$  is required for the transcription of housekeeping genes in vegetative cells, and is the only essential  $\sigma$  factor in *B. subtilis*. During sporulation,  $\sigma^A$  is found in both mother cell and forespore (Yen Shin *et al.*, 2015), and at least a fraction is bound to the core RNA polymerase (Ju *et al.*, 1999; Fujita, 2000). Accordingly,  $\sigma^A$ -dependent transcription has been demonstrated in both cells (Li and Piggot, 2001). However, our results show that  $\sigma^A$  activity is asymmetrically required in mother cell and forespore. The sustained degradation of  $\sigma^A$  in the mother cell produces only a mild spore titer defect, and no spore titer defect is observed after late degradation (Fig. 6A). These results suggest that  $\sigma^A$  plays a minor role in the mother cell, perhaps to replenish housekeeping functions in sporangia in which they become limiting. It is therefore possible that the  $\sigma^A$ -dependent functions provided before polar septation are enough to support sporulation in most sporangia, or that transcription of key genes under  $\sigma^A$ -control can be mediated by either  $\sigma^E$  or  $\sigma^K$  during sporulation, relieving the need for  $\sigma^A$ -dependent transcription in the mother cell. In support of this latter hypothesis, it has been shown that the transcription of genes involved in the synthesis of peptidoglycan precursors becomes dependent on mother cell-specific  $\sigma$  factors during sporulation (Eichenberger *et al.*, 2003, 2004), which leads to the accumulation of peptidoglycan precursors for cortex synthesis after engulfment (Vasudevan *et al.*, 2007).

Degradation of  $\sigma^A$  in the forespore produces a dramatic spore titer reduction (Fig. 6A) that our data suggest is the result of germination and outgrowth defects (Figs. 6 and 7). Germination of dormant, dehydrated spores is triggered by specific germinants that are recognized by receptors in the inner spore membrane. This triggers the release of dipicolinic acid, probably through channels made of SpoVA proteins, which leads to a partial rehydration of the spore core. Subsequently, cell wall lytic enzymes that degrade the cortex are activated, allowing the full expansion and rehydration of the spore core, in preparation for outgrowth (Setlow, 2014). During outgrowth, the germinated spore is transformed into a rod-shaped, growing, vegetative cell. Outgrowth is completely abolished when  $\sigma^A$  is degraded from either sustained or late promoters (Fig. 7; Supporting Information Movies S3 and S4). This is expected, since  $\sigma^A$ -mediated gene expression is likely required to resume growth after exiting dormancy. It seems reasonable to think that

degradation of  $\sigma^A$ -ssrA\* in the forespore results in mature spores devoid of  $\sigma^A$ . Therefore, when transcription restarts after germination,  $\sigma^A$ -dependent housekeeping transcripts will not be produced, preventing the growth of the reviving spore. Even if new  $\sigma^A$ -ssrA\* molecules are produced during outgrowth, they will be quickly degraded due to the presence of residual SspB<sup>Ec</sup> in the spores, which will target  $\sigma^A$ -ssrA\* for degradation by ClpXP.

The germination defect is only observed when  $\sigma^A$  is continuously degraded in the forespore, starting shortly after polar septation. We conceive of two potential models to explain this observation: First, it is possible that  $\sigma^A$ -dependent transcription is required in germinating spores to mediate the transition from phase-bright to phase-dark spores, which is consistent with recent results suggesting that translation happens during germination and that it is required to complete the germination process (Sinai *et al.*, 2015). However, we consider this possibility unlikely, since late degradation of  $\sigma^A$  in the forespore completely blocks outgrowth, but does not produce a significant germination defect (Fig. 7). Of course, it is possible that some intact  $\sigma^A$  remains in the spores after late degradation, and that this supports germination. However, the outgrowth defect after late  $\sigma^A$ -ssrA\* degradation argues against this possibility.

The second model to explain the germination defect observed when  $\sigma^A$  is continuously degraded in the forespore is that  $\sigma^A$ -dependent transcription is required in the developing forespore, early during spore formation, to produce germination-proficient spores. In this context, it is possible that specific factors produced in the forespore under  $\sigma^A$ -control are required for the germination of mature spores. Candidates for such factors are translation proteins that are required for efficient germination, which must be present in mature spores or quickly synthesized at the onset of germination (Sinai *et al.*, 2015). It is also possible that  $\sigma^A$ -dependent transcription plays a more general role in developing forespores, by providing housekeeping functions that confer to the forespore an optimal metabolic or structural state that promotes the formation of a functional germination machinery. Nevertheless, further experiments are required to clarify the requirement of  $\sigma^A$  in the forespore for germination.

Altogether, these results outline a potential application of STRP to identify cellular pathways involved in spore germination and outgrowth. This is particularly appealing, since it is unclear whether specific biosynthetic activities are required in the dehydrated, dormant spore to mediate germination (Sinai *et al.*, 2015; Boone *et al.*, 2016; Korza *et al.*, 2016; Sinai and Ben-Yehuda, 2016).

As discussed above, the use of targeted degradation to deplete proteins has key advantages compared with other methods. However, it also has limitations that are

important to consider. Perhaps the most apparent limitation is that not all proteins are suitable for degradation. The *ssrA*<sup>\*</sup>/*SspB*<sup>Ec</sup> degradation system requires that target proteins have an accessible cytoplasmic C-terminus for degradation, which excludes all extracellular proteins and membrane proteins with extracytoplasmic C-termini as potential targets, as well as cytoplasmic proteins in which the tag is sterically inaccessible due to the folding of the protein. The use of degradation systems based on N-terminal tags might provide an alternative to degrade some of the membrane proteins with extracytoplasmic C-termini (Sekar et al., 2016). Second, the inducible protein degradation system entails the modification of the target protein by adding the fifteen amino acid *ssrA*<sup>\*</sup> tag, which might significantly affect protein functionality. However, approximately 95% of the approximately 200 proteins we have tagged so far (see below) tolerate the addition of the tag, suggesting that the *ssrA*<sup>\*</sup> tag does not tend to significantly interfere with protein folding nor function.

Altogether, our results show that STRP holds great potential for providing a comprehensive molecular dissection of not only spore development, but also germination and outgrowth. We have undertaken a genome-wide approach to tag with *ssrA*<sup>\*</sup> every essential protein with cytoplasmic C-termini in *B. subtilis*. The systematic exploration of our collection will provide a comprehensive overview of the spatiotemporal role of essential vegetative cellular pathways during the different developmental stages in *B. subtilis*.

## Experimental procedures

### Strain construction

All the strains used in this study are derivatives of *B. subtilis* PY79, and are listed in Supporting Information Table S2. A list of plasmids and primers as long with detailed descriptions of plasmid construction, is provided in supplementary information (Supporting Information Tables S3 and S4). In every case, *ssrA*<sup>\*</sup> was added to the appropriate gene in its native locus. The amino acid sequence of the *ssrA*<sup>\*</sup> used in our constructs was AANDENYSENYALGG, and was previously described by Griffith and Grossman (2008). *sspB*<sup>Ec</sup> was inserted in different ectopic loci in *B. subtilis* chromosome, depending on the cell in which expression was taking place. For forespore-specific expression, we selected the *amyE* locus, which is trapped in the forespore after polar septation (Wu and Errington, 1998), allowing immediate expression before the forespore chromosome is fully translocated. For mother cell-specific expression, we inserted *sspB*<sup>Ec</sup> in the terminus-proximal *pebB* locus, which encodes a pectate lyase involved in polygalacturonic acid degradation. Because *pebB* (174<sup>o</sup>) is located in the chromosome close to the *dif* site (172<sup>o</sup>) (Sciochetti et al., 2001), it is one of the last loci to be translocated to the forespore

(Ptacin et al., 2008), which can transiently boost *sspB*<sup>Ec</sup> expression in the mother cell after polar septation. We previously inserted *sspB*<sup>Ec</sup> in the ectopic *thrC* locus for mother cell-specific expression. This creates a threonine auxotrophy, and therefore, the sporulation medium has to be supplemented with threonine. Under those conditions sporulation progress normally through engulfment, but we have observed that forespore maturation is delayed compared with threonine prototroph strains (not shown). For expression in predivisional cells, *sspB*<sup>Ec</sup> was inserted in the *lacA* locus. Xylose inducible expression was achieved by inserting *sspB*<sup>Ec</sup> in the *xyIA* locus (Lamsa et al., 2016), which simultaneously creates a mutant unable to use xylose as a carbon source, preventing the depletion of the inducer.

### Culture conditions

For microscopy experiments, sporulation was induced by resuspension (Sterlini and Mandelstam, 1969), except that the bacteria were grown in 25% LB prior to resuspension, rather than CH medium. Cultures were grown at 37°C for batch culture microscopy experiments, and at 30°C for timelapse fluorescence microscopy experiments.

For determination of heat-resistant spore titers and spore purification, cultures were grown and sporulated in DSM broth (Schaeffer et al., 1965).

To study YtsJ-GFP-*ssrA*<sup>\*</sup> degradation and P<sub>xyIA</sub> expression in vegetative cells (Supporting Information Fig. S3), cultures of the appropriate strains were grown in LB at 37°C until O.D.<sub>600</sub> 0.2. The cultures were then split into 2 ml aliquots and incubated for 45 min in LB or LB supplemented with different concentrations of xylose, at 37°C. Then 12 µl aliquots were used for microscopy, and 1 ml aliquots were used for protein extraction for Western blot.

### Spore titer assay

Strains were cultured in 2 ml of DSM for 24 h at 37°C. Cultures were then heated at 80°C for 20 min, serially diluted, and plated on LB. Spore titers were calculated based on colony counts.

### Spore purification

Sporulation was induced by exhaustion in 250 ml of DSM. Strains were grown for 72 h and then collected and washed with 4°C sterile water. The spores were incubated in sterile water at 4°C to lyse any remaining vegetative cells. Spores were further purified over a phosphate-polyethylene glycol aqueous biphasic gradient (Harrold et al., 2011). The top organic phase containing the spores was removed and extensively washed in at least 50 vol of 4°C sterile water. The spores were pelleted, resuspended in sterile water, and stored at 4°C. Sample purity was checked using phase contrast microscopy. Spore samples of >95% purity (phase-bright spores) were used in the studies.

#### Batch culture microscopy

Samples from sporulation cultures were taken at the indicated time points and transferred to 1.2% agarose pads for imaging. When appropriate, membranes were stained with  $0.5 \mu\text{g ml}^{-1}$  FM 4-64 (Life Technologies) and  $1 \mu\text{g ml}^{-1}$  Mitotracker green (Life Technologies). FM 4-64 was added to the agarose pad, whereas Mitotracker green was mixed with the cells before transferring them to the pad. Cells were visualized on an Applied Precision DV Elite optical sectioning microscope equipped with a Photometrics CoolSNAP-HQ<sup>2</sup> camera. Pictures were deconvolved using SoftWoRx v5.5.1 (Applied Precision). The median focal plane is shown.

#### Timelapse fluorescence microscopy to visualize YtsJ-GFP-ssrA\* degradation

Sporulation was induced at 30°C. About 1.5 h after sporulation induction,  $0.5 \mu\text{g ml}^{-1}$  FM 4-64 was added to the culture and incubation continued for another 1.5 h. Seven microliters of samples were taken 3 h after resuspension and transferred to agarose pads prepared as follows: 2/3 volume of supernatant from the sporulation culture; 1/3 volume 3.6% agarose in fresh A + B sporulation medium;  $0.17 \mu\text{g ml}^{-1}$  FM 4-64. Pads were partially dried, covered with a glass slide, and sealed with petroleum jelly to avoid dehydration during timelapse imaging. Pictures were taken in an environmental chamber at 30°C every 5 min for 5 h. To visualize FM 4-64 stained membranes, excitation/emission filters were TRITC/CY5, excitation light transmission was set to 5%, and exposure time was 0.1 s. To visualize GFP signal, excitation/emission filters were FITC/FITC, excitation light transmission was set to 50% and exposure time was 0.5 s.

#### Quantification of YtsJ-GFP-ssrA\* degradation kinetics

To calculate YtsJ-GFP-ssrA\* degradation kinetics, we measured the mean cytoplasmic GFP fluorescence in the mother cell and the forespore over time by drawing polygons encompassing either cell. After subtracting the mean background fluorescence, we calculated the mean fluorescence ratio between the cell in which degradation was triggered and the other cell of the same sporangium. This allowed us to correct for GFP photobleaching. We defined time zero as the time frame immediately before GFP degradation was first observed, and relativized the fluorescence ratios of subsequent time points with respect to time zero, that was arbitrarily given the value of one. The decrease in the fluorescence ratio over time followed an exponential decay curve. We fitted the data for each sporangia to an exponential decay function and determined the protein half-life upon degradation induction for individual sporangia. The reported half-lives are the averages  $\pm$  standard deviations of 17 and 14 sporangia for forespore and mother cell degradation respectively. The graph in Fig. 4C shows the average fluorescence ratio of the different sporangia over time.

© 2018 John Wiley & Sons Ltd, *Molecular Microbiology*, **108**, 45–62

#### Timelapse phase contrast microscopy to visualize spore germination and outgrowth

Purified spores were diluted in water to an O.D.<sub>600</sub> of 0.3, and  $10 \mu\text{l}$  of the spore suspension were placed on 1.2% agarose pads prepared in LB and supplemented with the germinant L-alanine (10 mM). Pads were partially dried, covered with a glass slide and sealed with petroleum jelly to avoid dehydration during timelapse imaging. Phase contrast pictures were taken at 30°C every 3 min for 10 h. Light transmission was set to 32% and exposure time was 0.1 s. Note that, after placing the spores in the agarose pads, there was a time lag of approximately 15 min until we started taking pictures. To minimize the number of spores that germinated during this time, spores were not heat-activated before timelapse microscopy. We quantified the number of spores that transitioned from phase-bright to phase-dark during the first 4 h of imaging, focusing only on spores that were phase bright at the onset of imaging.

#### Quantification of spore germination by loss of optical density

Germination assays by loss of O.D.<sub>580</sub> were performed as described in Harwood et al. (1990). Briefly, spores were heat activated at 70°C for 20 min in water, and resuspended in 10 mM Tris-HCl, pH 8.4, to obtain an O.D.<sub>580</sub> of 0.3. The resuspended spores were incubated at 37°C for 20 min, and then germination was induced by the addition of L-alanine 10 mM. O.D.<sub>580</sub> was measured every 5 min for an hour.

#### Protein extracts and Western blot analysis

Bacterial cultures were grown as described in 'Culture conditions'. Bacterial cells present in 1 ml aliquots of the cultures were collected by centrifugation (5000g, 2 min) and suspended in  $60 \mu\text{l}$  of Tris-sucrose buffer [33 mM Tris-HCl, pH 8.0; 40% sucrose; 1 mM EDTA] containing  $1 \text{ mg ml}^{-1}$  lysozyme,  $160 \mu\text{g ml}^{-1}$  PMSF and 1:100 diluted Sigma P2714 protease inhibitor cocktail, and incubated at 37°C for 10 min. Then, membranes were dissolved by adding  $2 \mu\text{l}$  of Triton X-100, samples were mixed with  $60 \mu\text{l}$  of Laemmli loading buffer [1.3% SDS; 10% (v/v) glycerol; 50 mM Tris-HCl; 1.8%  $\beta$ -mercaptoethanol; 0.02% bromophenol blue, pH 6.8] and boiled for 10 min. Proteins present in  $5 \mu\text{l}$  aliquots of each sample were resolved by Tris-Tricine-PAGE, using 12% gels. Conditions for protein transfer have been described elsewhere. Optimal dilutions of anti-SspB<sup>Ec</sup> and anti- $\sigma^A$  primary antibodies were 1:5000. Goat anti-rabbit horseradish peroxidase-conjugated antibody (1:20 000) was used as secondary antibody. Proteins recognized by the antibodies were visualized by chemoluminescence using the luciferin-luminol reagents, in a BioRad Gel Doc XR+ System. For quantification, the intensities of the bands were determined using ImageJ.  $\sigma^A$  was used as loading control.

#### Acknowledgements

We are thankful to Prof. Tania Baker for providing anti-SspB<sup>Ec</sup> antibody and to Prof. David Rudner for providing pDR110.

This work was supported by NIH Grant R01-GM57045. JLG was supported by an EMBO Long Term Fellowship (ALTF 1274–2011) during part of the duration of this project. AT, MLR and MD were part of the Magistère de Génétique Graduate Program, (Université Paris Diderot, 75013 Paris, France), which supported their stay in the lab. K. Pogliano is a co-founder of Linnaeus Bioscience Inc (La Jolla, CA), a shareholder, and a member of the Advisory Board. The terms of this arrangement have been reviewed and are managed by the University of California, San Diego in accordance with its conflict of interest policies.

### Author contributions

Conception and design of the study: EPR, KP and JLG; acquisition, analysis or interpretation of the data: all authors; writing of the manuscript: EPR, KP and JLG.

### References

- Boone, T., Driks, A., and Henkin, T.M. (2016) Protein synthesis during germination: shedding new light on a classical question. *J Bacteriol* **198**: 3251–3253.
- Borek, E., Ponticorvo, L., and Rittenberg, D. (1958) Protein turnover in micro-organisms. *Proc Natl Acad Sci U S A* **44**: 369–374.
- Clarke, S., Lopez-Diaz, I., and Mandelstam, J. (1986) Use of *lacZ* gene fusions to determine the dependence pattern of the sporulation gene *spoIID* in *spo* mutants of *Bacillus subtilis*. *J Gen Microbiol* **132**: 2987–2994.
- Cookson, N.A., Mather, W.H., Danino, T., Mondragón-Palomino, O., Williams, R.J., Tsimring, L.S., and Hastings, J. (2014) Queuing up for enzymatic processing: correlated signaling through coupled degradation. *Mol Syst Biol* **7**: 561.
- Cutting, S., Panzer, S., and Losick, R. (1989) Regulatory studies on the promoter for a gene governing synthesis and assembly of the spore coat in *Bacillus subtilis*. *J Mol Biol* **207**: 393–404.
- Eichenberger, P. (2012) Genomics and cellular biology of endospore formation. In *Bacillus: cellular and Molecular Biology*. Graumann, P.L. (ed). Norfolk, UK: Caister Academic Press, pp. 319–350.
- Eichenberger, P., Jensen, S.T., Conlon, E.M., Ooij, C., Van, Silvaggi, J., Gonzalez-Pastor, J.E., et al. (2003) The  $\sigma^E$  regulon and the identification of additional sporulation genes in *Bacillus subtilis*. *J Mol Biol* **327**: 945–972.
- Eichenberger, P., Fujita, M., Jensen, S.T., Conlon, E.M., Rudner, D.Z., and Wang, S.T. (2004) The program of gene transcription for a single differentiating cell type during sporulation in *Bacillus subtilis*. *PLoS Biol* **2**: e328.
- Errington, J. (2003) Regulation of endospore formation in *Bacillus subtilis*. *Nat Rev Microbiol* **1**: 117–126.
- Eswaramoorthy, P., Winter, P.W., Wawrzusin, P., York, A.G., Shroff, H., Ramamurthi, K.S., and Søgaard-Andersen, L. (2014) Asymmetric division and differential gene expression during a bacterial developmental program requires DivIVA. *PLoS Genet* **10**: e1004526.
- Fujita, M. (2000) Temporal and selective association of multiple sigma factors with RNA polymerase during sporulation in *Bacillus subtilis*. *Genes Cells* **5**: 79–88.
- Fujita, M., González-Pastor, J.E., and Losick, R. (2005) High- and low-threshold genes in the Spo0A regulon of *Bacillus subtilis*. *J Bacteriol* **187**: 1357–1368.
- Griffith, K.L., and Grossman, A.D. (2008) Inducible protein degradation in *Bacillus subtilis* using heterologous peptide tags and adaptor proteins to target substrates to the protease ClpXP. *Mol Microbiol* **70**: 1012–1025.
- Guérout-Fleury, A.M., Frandsen, N., and Stragier, P. (1996) Plasmids for ectopic integration in *Bacillus subtilis*. *Gene* **180**: 57–61.
- Haldenwang, W.G. (1995) The sigma factors of *Bacillus subtilis*. *Microbiol Rev* **59**: 1–30.
- Harrold, Z.R., Hertel, M.R., and Gorman-Lewis, D. (2011) Optimizing *Bacillus subtilis* spore isolation and quantifying spore harvest purity. *J Microbiol Methods* **87**: 325–329.
- Harwood, C.R., Cutting, S.M., Chambert, R., Galizzi, A., Gally, D., and Gruss, A.D. (1990) *Molecular Biological Methods for Bacillus*. Chichester, New York, Brisbane, Toronto, Singapore: John Wiley & Sons.
- Higgins, D., and Dworkin, J. (2012) Recent progress in *Bacillus subtilis* sporulation. *FEMS Microbiol Rev* **36**: 131–148.
- Hilbert, D.W., and Piggot, P.J. (2004) Compartmentalization of gene expression during *Bacillus subtilis* spore formation. *Microbiol Mol Biol Rev* **68**: 234–262.
- Ireton, K., Rudner, D.Z., Siranosian, K.J., and Grossman, A.D. (1993) Integration of multiple developmental signals in *Bacillus subtilis* through the Spo0A transcription factor. *Genes Dev* **7**: 283–294.
- Ju, J., Mitchell, T., Peters, H., and Haldenwang, W.G. (1999) Sigma factor displacement from RNA polymerase during *Bacillus subtilis* sporulation. *J Bacteriol* **181**: 4969–4977.
- Kain, J., He, G.G., and Losick, R. (2008) Polar localization and compartmentalization of ClpP proteases during growth and sporulation in *Bacillus subtilis*. *J Bacteriol* **190**: 6749–6757.
- Karow, L.M., Glaser, P., and Piggot, P.J. (1995) Identification of a gene, *spoIIIR*, which links the activation of  $\sigma^E$  to the transcriptional activity of  $\sigma^F$  during sporulation in *Bacillus subtilis*. *Proc Natl Acad Sci U S A* **92**: 2012–2016.
- Koch, A.L., and Levy, H.R. (1955) Protein turnover in growing cultures of *Escherichia coli*. *J Biol Chem* **217**: 947–957.
- Kock, H., Gerth, U., and Hecker, M. (2004) The ClpP peptidase is the major determinant of bulk protein turnover in *Bacillus subtilis*. *J Bacteriol* **186**: 5856–5864.
- Korza, G., Setlow, B., Rao, L., Li, Q., Setlow, P., and Henkin, T.M. (2016) Changes in *Bacillus* spore small molecules, rRNA, germination and outgrowth after extended sub-lethal exposure to various temperatures: evidence that protein synthesis is not essential for spore germination. *J Bacteriol* **198**: 3254–3264.
- Lamsa, A., Lopez-Garrido, J., Quach, D., Riley, E.P., Pogliano, J., and Pogliano, K. (2016) Rapid Inhibition Profiling in *Bacillus subtilis* to identify the mechanism of action of new antimicrobials. *ACS Chem Biol* **11**: 2222–2231.



- Leelakriangsak, M., Kobayashi, K., and Zuber, P. (2007) Dual negative control of *spx* transcription initiation from the P<sub>3</sub> promoter by repressors PerR and YodB in *Bacillus subtilis*. *J Bacteriol* **189**: 1736–1744.
- Li, Z., and Piggot, P.J. (2001) Development of a two-part transcription probe to determine the completeness of temporal and spatial compartmentalization of gene expression during bacterial development. *Proc Natl Acad Sci U S A* **98**: 12538–12543.
- Lopez-Garrido, J., Ojkic, N., Khanna, K., Wagner, F., Villa, E., Endres, R., and Pogliano, K. (2018) Chromosome translocation inflates *Bacillus* forespores and impacts cellular morphology. *Cell* **172**: 758–770.
- Londoño-Vallejo, J.A., Fréhel, C., and Stragier, P. (1997) *spoIIQ*, a forespore-expressed gene required for engulfment in *Bacillus subtilis*. *Mol Microbiol* **24**: 29–39.
- Mandelstam, J. (1958) Turnover of protein in growing and non-growing populations of *Escherichia coli*. *Biochem J* **69**: 110–119.
- McGinness, K.E., Baker, T. A., and Sauer, R.T. (2006) Engineering controllable protein degradation. *Mol Cell* **22**: 701–707.
- McKenney, P.T., Driks, A., and Eichenberger, P. (2013) The *Bacillus subtilis* endospore: assembly and functions of the multilayered coat. *Nat Rev Microbiol* **11**: 33–44.
- Nakano, S., Zheng, G., Nakano, M.M., and Zuber, P. (2002) Multiple pathways of Spx (YjbD) proteolysis in *Bacillus subtilis*. *J Bacteriol* **184**: 3664–3670.
- Nakano, S., Küster-Schöck, E., Grossman, A.D., and Zuber, P. (2003) Spx-dependent global transcriptional control is induced by thiol-specific oxidative stress in *Bacillus subtilis*. *Proc Natl Acad Sci U S A* **100**: 13603–13608.
- Narula, J., Fujita, M., and Igoshin, O.A. (2016) Functional requirements of cellular differentiation: lessons from *Bacillus subtilis*. *Curr Opin Microbiol* **34**: 38–46.
- Nicholson, W.L., Sun, D.X., Setlow, B., and Setlow, P. (1989) Promoter specificity of sigma G-containing RNA polymerase from sporulating cells of *Bacillus subtilis*: identification of a group of forespore-specific promoters. *J Bacteriol* **171**: 2708–2718.
- Ojkic, N., López-Garrido, J., Pogliano, K., and Endres, R.G. (2016) Cell-wall remodeling drives engulfment during *Bacillus subtilis* sporulation. *Elife* **5**: e18657.
- Popham, D.L., and Bernhards, C.B. (2015) Spore peptidoglycan. *Microbiol Spectr* **3**: TBS-0005-2012.
- Ptacin, J.L., Nollmann, M., Becker, E.C., Cozzarelli, N.R., Pogliano, K., and Bustamante, C. (2008) Sequence-directed DNA export guides chromosome translocation during sporulation in *Bacillus subtilis*. *Nat Struct Mol Biol* **15**: 485–493.
- Roels, S., Driks, A., and Losick, R. (1992) Characterization of *spoIVA*, a sporulation gene involved in coat morphogenesis in *Bacillus subtilis*. *J Bacteriol* **174**: 575–585.
- Rong, S., Rosenkrantz, M.S., and Sonenshein, A.L. (1986) Transcriptional control of the *Bacillus subtilis* *spoIID* gene. *J Bacteriol* **165**: 771–779.
- Ryguo, T., and Hillen, W. (1991) Inducible high-level expression of heterologous genes in *Bacillus megaterium* using the regulatory elements of the xylose-utilization operon. *Appl Microbiol Biotechnol* **35**: 594–599.
- Schaeffer, P., Millet, J., and Aubert, J.P. (1965) Catabolic repression of bacterial sporulation. *Proc Natl Acad Sci U S A* **54**: 704–711.
- Sciochetti, S., Piggot, P., and Blakely, G. (2001) Identification and characterization of the *dif* site from *Bacillus subtilis*. *J Bacteriol* **183**: 1058–1068.
- Sekar, K., Gentile, A.M., Bostick, J.W., Tyo, K.E.J., and Herman, C. (2016) N-terminal-based targeted, inducible protein degradation in *Escherichia coli*. *PLoS One* **11**: e0149746.
- Setlow, P. (2006) Spores of *Bacillus subtilis*: their resistance to and killing by radiation, heat and chemicals. *J Appl Microbiol* **101**: 514–525.
- Setlow, P. (2014) Germination of spores of *Bacillus* species: what we know and do not know. *J Bacteriol* **196**: 1297–1305.
- Sharp, M.D., and Pogliano, K. (1999) An *in vivo* membrane fusion assay implicates SpoIIIE in the final stages of engulfment during *Bacillus subtilis* sporulation. *Proc Natl Acad Sci U S A* **96**: 14553–14558.
- Sharp, M.D., and Pogliano, K. (2002) Role of cell-specific SpoIIIE assembly in polarity of DNA transfer. *Science* **295**: 137–139.
- Sinai, L., and Ben-Yehuda, S. (2016) Commentary: changes in *Bacillus* spore small molecules, rRNA, germination, and outgrowth after extended sublethal exposure to various temperatures: evidence that protein synthesis is not essential for spore germination. *Front Microbiol* **7**: 2043.
- Sinai, L., Rosenberg, A., Smith, Y., Segev, E., and Ben-Yehuda, S. (2015) The molecular timeline of a reviving bacterial spore. *Mol Cell* **57**: 695–707.
- Steinmetz, M., and Richter, R. (1994) Plasmids designed to alter the antibiotic resistance expressed by insertion mutations in *Bacillus subtilis*, through *in vivo* recombination. *Gene* **142**: 79–83.
- Sterlini, J.M., and Mandelstam, J. (1969) Commitment to sporulation in *Bacillus subtilis* and its relationship to development of actinomycin resistance. *Biochem J* **113**: 29–37.
- Sun, D., Fajardo-Cavazos, P., Sussman, M.D., Tovar-Rojo, F., Cabrera-Martinez, R.M., and Setlow, P. (1991) Effect of chromosome location of *Bacillus subtilis* forespore genes on their spo gene dependence and transcription by E sigma F: identification of features of good E sigma F-dependent promoters. *J Bacteriol* **173**: 7867–7874.
- Tan, I.S., and Ramamurthi, K.S. (2014) Spore formation in *Bacillus subtilis*. *Environ Microbiol Rep* **6**: 212–225.
- Vasudevan, P., Weaver, A., Reichert, E.D., Linnstaedt, S.D., and Popham, D.L. (2007) Spore cortex formation in *Bacillus subtilis* is regulated by accumulation of peptidoglycan precursors under the control of sigma K. *Mol Microbiol* **65**: 1582–1594.
- Wang, S.T., Setlow, B., Conlon, E.M., Lyon, J.L., Imamura, D., Sato, T., et al. (2006) The forespore line of gene expression in *Bacillus subtilis*. *J Mol Biol* **358**: 16–37.
- Wei, J.-R., Krishnamoorthy, V., Murphy, K., Kim, J.-H., Schnappinger, D., Alber, T., et al. (2011) Depletion of antibiotic targets has widely varying effects on growth. *Proc Natl Acad Sci U S A* **108**: 4176–4181.
- Wu, L.J., and Errington, J. (1998) Use of asymmetric cell division and *spoIIIE* mutants to probe chromosome

- orientation and organization in *Bacillus subtilis*. *Mol Microbiol* **27**: 777–786.
- Wu, L.J., and Errington, J. (2000) Identification and characterization of a new prespore-specific regulatory gene, *rsfA*, of *Bacillus subtilis*. *J Bacteriol* **182**: 418–424.
- Yen Shin, J., Lopez-Garrido, J., Lee, S.-H., Diaz-Celis, C., Fleming, T., Bustamante, C., and Pogliano, K. (2015) Visualization and functional dissection of coaxial paired SpoIIIE channels across the sporulation septum. *Elife* **4**: e06474.
- Youngman, P., Perkins, J.B., and Losick, R. (1984) A novel method for the rapid cloning in *Escherichia coli* of *Bacillus subtilis* chromosomal DNA adjacent to Tn917 insertions. *Mol Gen Genet* **195**: 424–433.
- Zheng, L., and Losick, R. (1990) Cascade regulation of spore coat gene expression in *Bacillus subtilis*. *J Mol Biol* **212**: 645–660.

#### Supporting information

Additional supporting information may be found in the online version of this article at the publisher's web-site.

## ACKNOWLEDGEMENTS

Chapter II, in full, is a reproduction of the material as it appears in *Molecular Microbiology* 2018. Riley, Eammon P.; Trinquier, Aude; Reilly, Madeline L.; Durchon, Marine; Perera, Varahenage R.; Pogliano, Kit; Lopez-Garrido, Javier, John Wiley & Sons Ltd, 2018. The dissertation author was the primary investigator and author of this paper. Permission from all authors has been obtained.

## Supplementary figures

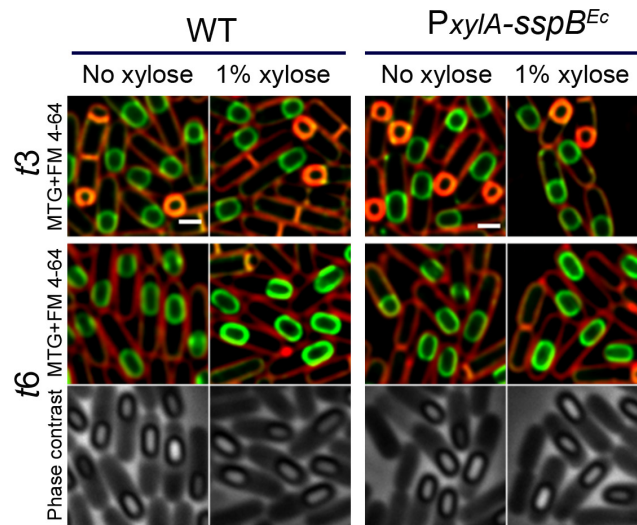


**Figure S1. Production of  $SspB^{Ec}$  from a xylose-dependent promoter does not affect the progression of sporulation**

Micrographs of wild type sporangia (WT) and of sporangia expressing  $sspB^{Ec}$  from a xylose-dependent promoter ( $P_{xyIA-sspB^{Ec}}$ ), in the absence of xylose or in the presence of 1% of xylose added upon resuspension. Pictures were taken 3 ( $t3$ ) and 6 ( $t6$ ) hours after sporulation induction. Membranes stained with FM 4-64 (red) and Mitotracker green (green). Phase contrast pictures are shown for in the bottom row for  $t6$ . Scale bar, 1  $\mu$ m.

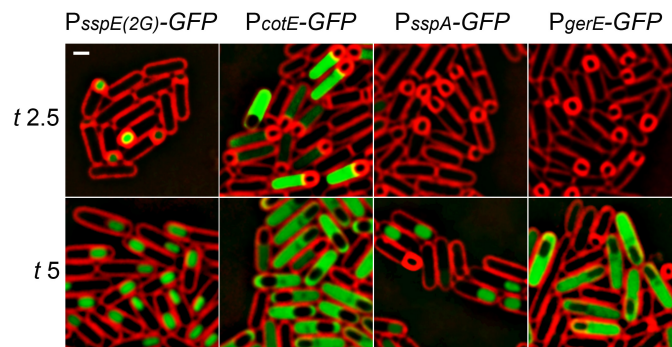


**Figure S2. Expression pattern from the sustained and late promoters selected for further characterization**

Micrographs showing the pattern of *gfp* expression from sustained ( $P_{sspE(2G)}$  and  $P_{cotE}$ ) and late ( $P_{sspA}$  and  $P_{gerE}$ ) promoters. Pictures taken 2.5 ( $t$  2.5) and 5 ( $t$  5) hours after resuspension in sporulation medium are shown. GFP brightness was adjusted for proper visualization, and the displayed intensities are not directly comparable. See Fig. S3E for a proper comparison of the intracellular GFP concentrations achieved in the different strains. Membranes were stained with FM 4-64. Scale bar, 1  $\mu$ m.

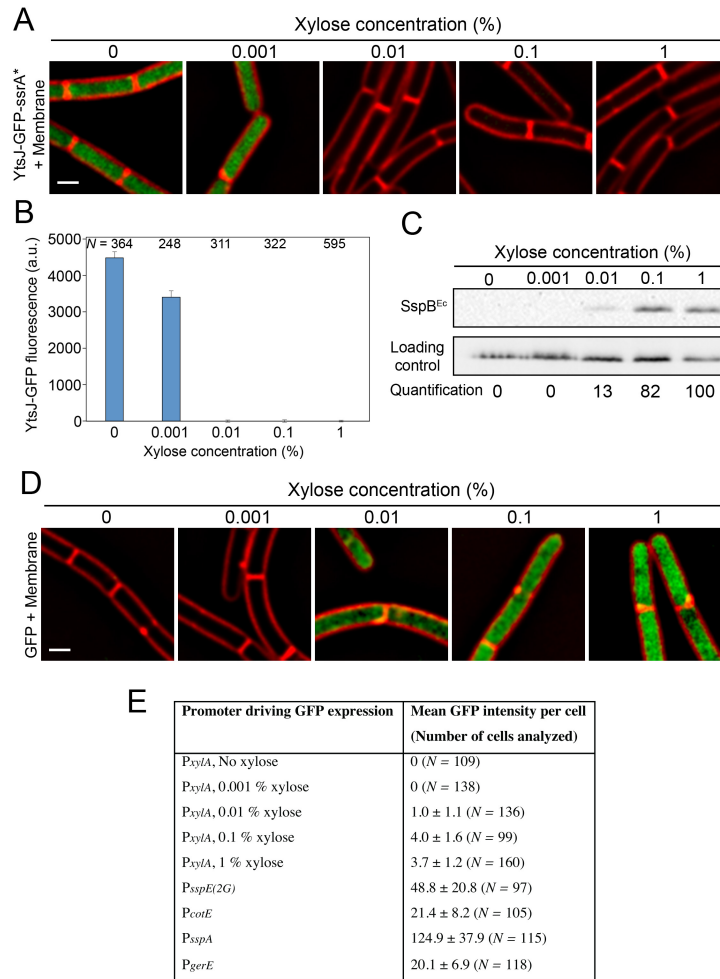


**Figure S3. Evidence that SspB<sup>Ec</sup> is not limiting for degradation during sporulation**

A. Degradation of YtsJ-GFP-ssrA\* in vegetative cells, when *sspB<sup>Ec</sup>* is expressed from a xylose-inducible promoter (*P<sub>xyIA</sub>*) in the presence of different concentrations of xylose. The cultures were grown in the presence of the

indicated percentage of xylose for 45 minutes before imaging. Membranes stained with FM 4-64. Scale bar, 1  $\mu$ m.

B. Quantification of the mean GFP intensity per cell from the microscopy shown in A. The average  $\pm$  SEM of  $N$  cells (indicated in the graph) is shown for every condition. No GFP signal is detected for xylose concentrations of 0.01% and above, suggesting that in the amount of SspB<sup>Ec</sup> produced using 0.01% of xylose is enough to efficiently degrade YtsJ-GFP-ssrA\*.

C. Levels of SspB<sup>Ec</sup> in protein extracts from the cultures used for the microscopy shown in A. SspB<sup>Ec</sup> was detected by Western blotting using an anti-SspB<sup>Ec</sup> antibody.  $\sigma^A$  was used as loading control. For quantification, the ratio SspB<sup>Ec</sup>/loading control was relativized to 100 in the 1% xylose culture.

D. Accumulation of GFP in a strain containing P<sub>xyIA</sub>-gfp transcriptional fusion, in the presence of different xylose concentrations. The cultures were grown in the presence of the indicated percentage of xylose for 45 min before imaging. All the images were adjusted in the same way. GFP signal is observed for xylose concentrations of 0.01% and above.

E. Table showing the mean GFP intensity per cell when GFP is produced from P<sub>xyIA</sub> in the presence of different concentrations of xylose in vegetative cells (microscopy shown in D), and when GFP is produced in mother cell or the forespore from sustained or late promoters (Fig. S2). The average  $\pm$  standard deviation of  $N$  cells is shown. Since P<sub>xyIA</sub> induced with 0.01% of xylose yields enough SspB<sup>Ec</sup> to completely degrade YtsJ-GFP-ssrA\* in vegetative cells (Fig. S3A-C), the average mean GFP intensity in this condition was used as reference and relativized to 1. The mean GFP intensities achieved when *gfp* is expressed from cell-specific promoters are at least 20-fold higher than the mean intensity in vegetative cells treated with 0.01% of xylose. Assuming that the intracellular concentration of GFP correlates with the concentration of SspB<sup>Ec</sup> achieved using the same promoters, and that protein degradation during sporulation requires a similar amount of SspB<sup>Ec</sup> as protein degradation in vegetative cells, these results provide evidence that, during sporulation, SspB<sup>Ec</sup> is in excess and therefore is not a limiting factor for the degradation of target proteins.

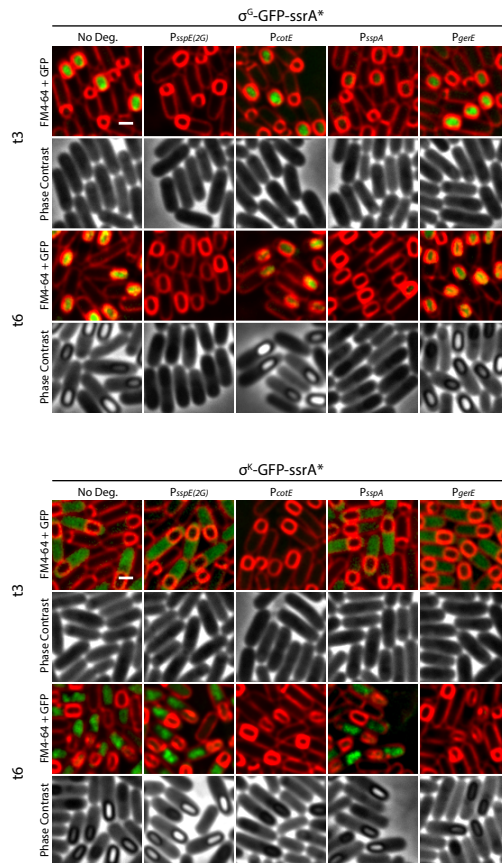


**Figure S4. Cell-specific degradation of  $\sigma^G$ -GFP-ssrA\* and  $\sigma^K$ -GFP-ssrA\***  
 Micrographs of sporangia in which  $\sigma^G$  (upper panel) or  $\sigma^K$  (lower panel) are tagged with GFP-ssrA\* in the absence of SspB<sup>Ec</sup> (No deg.) or when SspB<sup>Ec</sup> is produced from the sustained promoters  $P_{sspE(2G)}$  and  $P_{cotE}$  or the late promoters  $P_{sspA}$  and  $P_{gerE}$ . Cells from the different sporulating cultures were imaged 3 (*t3*) and 6 (*t6*) hours after resuspension in sporulation medium. The top row of each set shows membranes stained with FM 4-64 (red) and the GFP fluorescent signal emitted by the  $\sigma^G$ -GFP-ssrA\* and  $\sigma^K$ -GFP-ssrA\* fusion proteins. Phase-contrast images are shown in the bottom row of each set. To be able to visualize the forespore membranes after engulfment membrane fission, FM 4-64 was added to the sporulating cultures ~one hour after resuspension. Scale bar, 1  $\mu$ m.



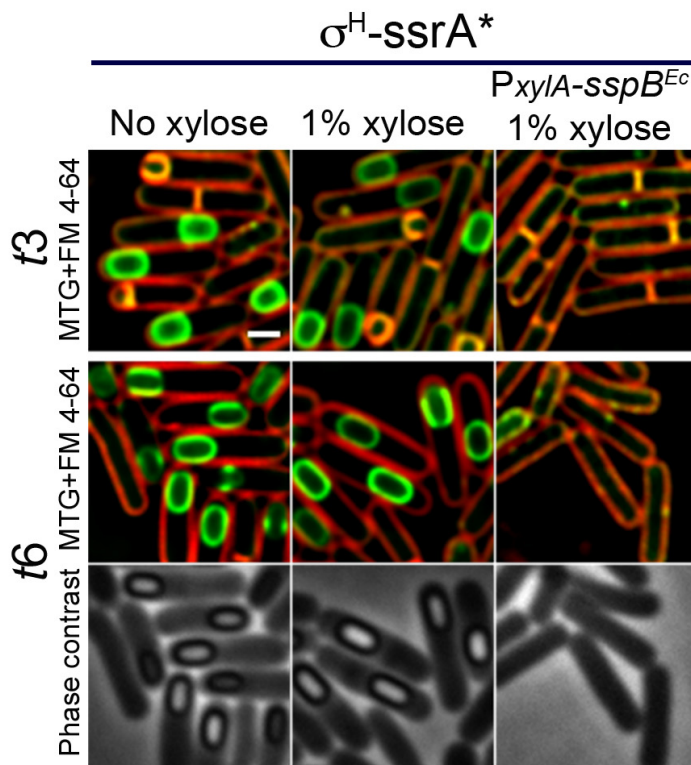


**Figure S5. Production of SspB<sup>Ec</sup> from a xylose inducible promoter triggers the efficient degradation of  $\sigma^H$ -ssrA\*.**

Micrographs of sporulating cultures of two different strains: a strain in which  $\sigma^H$  is tagged with ssrA\* ( $\sigma^H$ -ssrA\*) but no *sspB<sup>Ec</sup>* is present in the genome, with or without 1% xylose; and a  $\sigma^H$ -ssrA\* strain in which *sspB<sup>Ec</sup>* is under the control of a xylose dependent promoter ( $P_{xyIA}$ -*sspB<sup>Ec</sup>*), in the presence of 1% xylose, added upon resuspension of the culture in sporulation medium. Scale bar, 1  $\mu$ m.

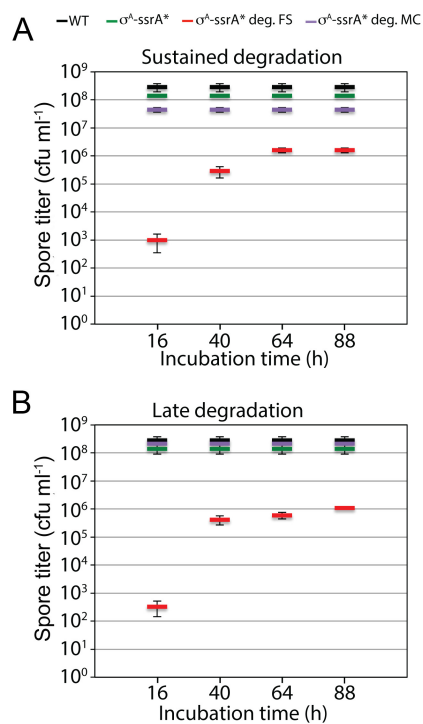


**Figure S6. Number of colonies upon extended incubation of spore titer plates at 30°C.**

Number of colony forming units per ml (cfu ml<sup>-1</sup>) in sporulating cultures from wild type and  $\sigma^A$ -ssrA\* cell-specific degradation strains after heat kill, when degradation is induced from sustained (A) or late (B) promoters. The number of colonies was determined after incubating the plates at 30°C for 16, 40, 64 and 88 hours. Data represents the average and standard deviation of at least three independent experiments.

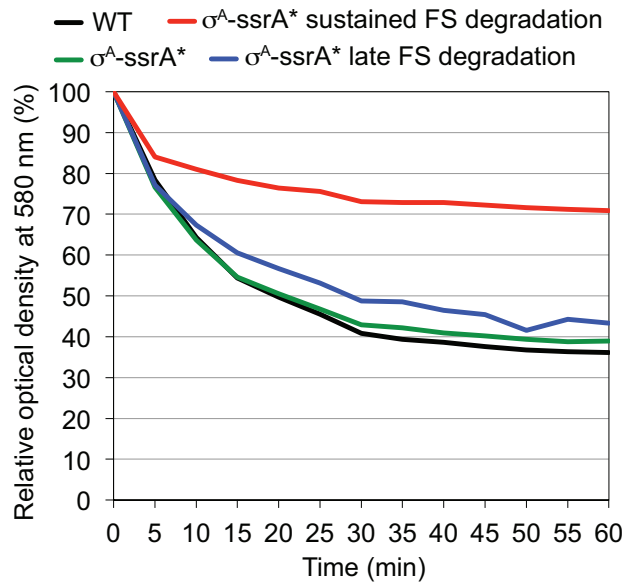


**Figure S7. Germination assays by loss of O.D.**

Loss of O.D.<sub>580</sub> upon induction of germination with 10 mM of L-alanine. The optical density at time zero was relativized to 100. Black line, wild type spores; green line,  $\sigma^A$ -ssrA<sup>+</sup> spores; red line,  $\sigma^A$ -ssrA<sup>+</sup> sustained forespore degradation spores; blue line,  $\sigma^A$ -ssrA<sup>+</sup> late forespore degradation spores. The experiment was performed twice, and a representative example is shown.

## Supplementary tables

<b>Tagged protein/mutation</b>	<b>Degradation</b>	<b>Strain</b>	<b>Spore titer (Spores/ml)<sup>a</sup></b>
None	None	PY79	3.07 x 10 <sup>8</sup>
	None + xylose 1%	PY79	4.73 x 10 <sup>8</sup>
	P <sub>xyIA</sub> (no xylose)	JLG364	3.40 x 10 <sup>8</sup>
	P <sub>xyIA</sub> + xylose 1%	JLG364	1.67 x 10 <sup>8</sup>
	P <sub>spolIR</sub>	JLG176	3.23 x 10 <sup>8</sup>
	P <sub>spolIQ</sub>	JLG170	2.93 x 10 <sup>8</sup>
	P <sub>sspA</sub>	JLG366	3.20 x 10 <sup>8</sup>
	P <sub>sspB</sub>	JLG367	2.90 x 10 <sup>8</sup>
	P <sub>sspE(2G)</sub>	JLG963	3.13 x 10 <sup>8</sup>
	P <sub>spolID</sub>	BER105	3.67 x 10 <sup>8</sup>
	P <sub>spolVA</sub>	BER100	2.73 x 10 <sup>8</sup>
	P <sub>gerE</sub>	BER101	2.27 x 10 <sup>8</sup>
	P2 <sub>cotE</sub>	JLG2145	2.99 x 10 <sup>8</sup>
	P <sub>cotE</sub>	BER131	3.33 x 10 <sup>8</sup>
	σ <sup>G</sup> -ssrA*	None	JLG314
None + xylose 1%		JLG314	5.27 x 10 <sup>8</sup>
P <sub>xyIA</sub> + xylose 1%		JLG2317	5.70 x 10 <sup>8</sup>
P <sub>spolIR</sub>		JLG1348	2.40 x 10 <sup>8</sup>
P <sub>spolIQ</sub>		JLG1315	3.33 x 10 <sup>8</sup>
P <sub>sspA</sub>		JLG518	1.07 x 10 <sup>8</sup>
P <sub>sspB</sub>		JLG1333	2.27 x 10 <sup>8</sup>
P <sub>sspE(2G)</sub>		JLG966	1.33 x 10 <sup>8</sup>
P <sub>spolID</sub>		JLG1321	2.93 x 10 <sup>8</sup>
P <sub>spolVA</sub>		JLG1338	2.13 x 10 <sup>8</sup>
P <sub>gerE</sub>		JLG1326	3.07 x 10 <sup>8</sup>
P2 <sub>cotE</sub>		JLG2329	2.53 x 10 <sup>8</sup>
P <sub>cotE</sub>		BER0189	2.70 x 10 <sup>8</sup>
σ <sup>K</sup> -ssrA*	None	JLG373	3.02 x 10 <sup>8</sup>
	None + xylose 1%	JLG373	5.93 x 10 <sup>8</sup>
	P <sub>xyIA</sub> + xylose 1%	JLG2318	4.53 x 10 <sup>8</sup>
	P <sub>spolIR</sub>	JLG1347	3.67 x 10 <sup>8</sup>
	P <sub>spolIQ</sub>	JLG409	4.13 x 10 <sup>8</sup>
	P <sub>sspA</sub>	JLG415	4.60 x 10 <sup>8</sup>
	P <sub>sspB</sub>	JLG436	3.00 x 10 <sup>8</sup>
	P <sub>sspE(2G)</sub>	JLG967	2.60 x 10 <sup>8</sup>
	P <sub>spolID</sub>	JLG1320	3.33 x 10 <sup>8</sup>
	P <sub>spolVA</sub>	JLG1337	2.73 x 10 <sup>7</sup>
	P <sub>gerE</sub>	JLG1325	1.93 x 10 <sup>7</sup>
	P2 <sub>cotE</sub>	JLG2330	6.13 x 10 <sup>5</sup>

	<i>P<sub>cotE</sub></i>	BER188	1.33 x 10 <sup>5</sup>
$\sigma^H$	N/A	BER657	0.00 x 10 <sup>0</sup>
$\sigma^H$ -ssrA*	None	BER666	1.03 x 10 <sup>8</sup>
	<i>P<sub>xyIA</sub></i> + xylose 1%	BER667	0.00 x 10 <sup>0</sup>
	<i>P<sub>spolIE</sub></i>	BER668	1.57 x 10 <sup>7</sup>
	<i>P<sub>cotE</sub></i>	BER669	1.02 x 10 <sup>8</sup>
	<i>P<sub>sspE(2G)</sub></i>	BER670	1.08 x 10 <sup>8</sup>
$\sigma^A$ -ssrA*	None	JLG370	1.40 x 10 <sup>8</sup>
	<i>P<sub>cotE</sub></i>	BER218	4.47 x 10 <sup>7</sup>
	<i>P<sub>sspE(2G)</sub></i> (16 h incubation)	BER219	1.00 x 10 <sup>3</sup>
	<i>P<sub>sspE(2G)</sub></i> (40 h incubation)	BER219	2.87 x 10 <sup>5</sup>
	<i>P<sub>sspE(2G)</sub></i> (64 h incubation)	BER219	1.60 x 10 <sup>6</sup>
	<i>P<sub>sspE(2G)</sub></i> (88 h incubation)	BER219	1.60 x 10 <sup>6</sup>
	<i>P<sub>gerE</sub></i>	JLG1322	2.13 x 10 <sup>8</sup>
	<i>P<sub>sspA</sub></i> (16 h incubation)	JLG413	3.33 x 10 <sup>2</sup>
	<i>P<sub>sspA</sub></i> (40 h incubation)	JLG413	4.13 x 10 <sup>5</sup>
	<i>P<sub>sspA</sub></i> (64 h incubation)	JLG413	6.00 x 10 <sup>5</sup>
	<i>P<sub>sspA</sub></i> (88 h incubation)	JLG413	1.07 x 10 <sup>6</sup>
$\sigma^G$ -GFP-ssrA*	None	BER1137	2.57 x 10 <sup>8</sup>
	<i>P<sub>xyIA</sub></i> + xylose 1%	BER1139	0.00 x 10 <sup>0</sup>
	<i>P<sub>cotE</sub></i>	BER1140	2.03 x 10 <sup>8</sup>
	<i>P<sub>sspE(2G)</sub></i>	BER1141	3.00 x 10 <sup>3</sup>
	<i>P<sub>gerE</sub></i>	BER1152	3.07 x 10 <sup>8</sup>
	<i>P<sub>sspA</sub></i>	BER1153	2.77 x 10 <sup>3</sup>
$\sigma^K$ -GFP-ssrA*	None	BER1138	3.55 x 10 <sup>8</sup>
	<i>P<sub>xyIA</sub></i> + xylose 1%	BER1143	0.00 x 10 <sup>0</sup>
	<i>P<sub>cotE</sub></i>	BER1144	4.53 x 10 <sup>3</sup>
	<i>P<sub>sspE(2G)</sub></i>	BER1145	2.63 x 10 <sup>8</sup>
	<i>P<sub>gerE</sub></i>	BER1155	3.53 x 10 <sup>6</sup>
	<i>P<sub>sspA</sub></i>	BER1156	1.33 x 10 <sup>8</sup>
<i>spo0A</i> <sup>-</sup>	N/A	KP648	0.00 x 10 <sup>0</sup>
<i>sigG</i> <sup>-</sup>	N/A	RP189	0.00 x 10 <sup>0</sup>
<i>sigK</i> <sup>-</sup>	N/A	RP190	0.00 x 10 <sup>0</sup>

<sup>a</sup>Spore titers were determined as the as the number of heat-treated spores able to form colonies. The average of at least three independent experiments is show for every strain.

<b>Table S2. Strains used in this study</b>		
<b>Strain</b>	<b>Genotype or description</b>	<b>Reference, source or construction<sup>a</sup></b>
PY79	Wild type	(Youngman <i>et al.</i> , 1984)
BER100	<i>pelB::PspolVA-sspB<sup>Ec</sup>Ωspc</i>	pJLG173→PY79 (Sp)
BER101	<i>pelB::PgerE-sspB<sup>Ec</sup>Ωspc</i>	pJLG171→PY79 (Sp)
BER105	<i>pelB::PspolD-sspB<sup>Ec</sup>Ωspc</i>	pJLG174→PY79 (Sp)
BER131	<i>pelB::PcotE-sspB<sup>Ec</sup>Ωspc</i>	pJLG172→PY79 (Sp)
BER174	<i>pelB::PcotE-sspB<sup>Ec</sup>Ωspc amyE::PsspE(2G)-sspB<sup>Ec</sup>Ωcat</i>	JLG963→BER131 (Cm)
BER188	<i>pelB::PcotE-sspB<sup>Ec</sup>Ωspc sigK-ssrA*Ωkan</i>	JLG373→BER131 (Km)
BER189	<i>pelB::PcotE-sspB<sup>Ec</sup>Ωspc sigG-ssrA*Ωkan</i>	JLG314→BER131 (Km)
BER206	<i>pelB::PgerE-sspB<sup>Ec</sup>Ωspc amyE::PsspA-sspB<sup>Ec</sup>Ωcat</i>	JLG366→BER101 (Cm)
BER218	<i>pelB::PcotE-sspB<sup>Ec</sup>Ωspc sigA-ssrA*Ωkan</i>	JLG370→BER131 (Km)
BER219	<i>amyE::PsspE(2G)-sspB<sup>Ec</sup>Ωcat sigA-ssrA*Ωkan</i>	JLG370→JLG963 (Km)
BER220	<i>pelB::PcotE-sspB<sup>Ec</sup>Ωspc amyE::PsspE(2G)-sspB<sup>Ec</sup>Ωcat sigA-ssrA*Ωkan</i>	JLG370→BER174 (Km)
BER461	<i>ytsJ-gfp-ssrA*Ωkan</i>	(Lamsa <i>et al.</i> , 2016)
BER468	<i>ytsJ-gfp-ssrA*Ωkan ΔxylA::sspB<sup>Ec</sup>Ωcat</i>	(Lamsa <i>et al.</i> , 2016)
BER469	<i>pelB::PcotE-sspB<sup>Ec</sup>Ωspc ytsJ-gfp-ssrA*Ωkan</i>	BER461→BER131 (Km)
BER470	<i>amyE::PsspE(2G)-sspB<sup>Ec</sup>Ωcat ytsJ-gfp-ssrA*Ωkan</i>	BER461→JLG963 (Km)
BER471	<i>pelB::PcotE-sspB<sup>Ec</sup>Ωspc amyE::PsspE(2G)-sspB<sup>Ec</sup>Ωcat ytsJ-gfp-ssrA*Ωkan</i>	BER461→BER174 (Km)
BER503	<i>amyE::Pspank-clpXΩspc</i>	pER104→PY79 (Sp)
BER504	<i>ΔclpX::tet</i>	pER106→PY79 (Tet)
BER505	<i>spxΩcat</i>	pER109→PY79 (Cm)
BER512	<i>pelB::PgerE-sspB<sup>Ec</sup>Ωspc ytsJ-gfp-ssrA*Ωkan</i>	BER461→BER101 (Km)
BER513	<i>amyE::PsspA-sspB<sup>Ec</sup>Ωcat ytsJ-gfp-ssrA*Ωkan</i>	BER461→JLG366 (Km)
BER514	<i>pelB::PgerE-sspB<sup>Ec</sup>Ωspc amyE::PsspA-sspB<sup>Ec</sup>Ωcat ytsJ-gfp-ssrA*Ωkan</i>	BER461→BER206 (Km)

BER516	$\Delta clpX::tet$ , $amyE::Pspank-clpX\Omega spc$	BER504→BER503
BER550	$gfp-spx\Omega cat$	pER122→PY79 (Cm)
BER552	$gfp-spx\Omega cat \Delta clpX::tet$ $amyE::Pspank-clpX\Omega spc$	BER550→BER516 (Cm)
BER555	$lacA::PspolIE-sspB^{Ec}\Omega erm$	pER128→PY79 (Em)
BER560	$lacA::PspolIE-sspB^{Ec}\Omega erm$ $ytsJ-gfp-ssrA*\Omega kan$	BER461→BER555 (Km)
BER575	$gfp-spx\Omega cm$ $xyIA::Pc-tomato-ssrA*\Omega kan$	JLG207→BER550 (Cm)
BER576	$xyIA::sspB\Omega erm$	pCm::Er (Steinmetz and Richter, 1994)→JLG364 (Em)
BER577	$gfp-spx\Omega cm$ $xyIA::Pc-tomato-ssrA*\Omega kan$ $xyIA::sspB\Omega erm$	BER576→BER575 (Em)
BER657	$\Delta sigH::kan$	pER157→PY79 (Km)
BER666	$sigH-ssrA*\Omega kan$	pER156→PY79 (Km)
BER667	$\Delta xyIA::sspB^{Ec}\Omega cat$ $sigH-ssrA*\Omega kan$	BER666→JLG364 (Km)
BER668	$lacA::PspolIE-sspB^{Ec}\Omega erm$ $sigH-ssrA*\Omega kan$	BER666→BER555 (Km)
BER669	$pelB::PcotE-sspB^{Ec}\Omega spc$ $sigH-ssrA*\Omega kan$	BER666→BER131 (Km)
BER670	$amyE::PsspE(2G)-sspB^{Ec}\Omega cat$ $sigH-ssrA*\Omega kan$	BER666→JLG963 (Km)
BER1137	$sigG-gfp-ssrA*\Omega kan$	pER286→PY79 (Km)
BER1138	$sigK-gfp-ssrA*\Omega kan$	pER287→PY79 (Km)
BER1139	$sigG-gfp-ssrA*\Omega kan$ $xyIA::sspB\Omega cat$	BER1137→JLG364 (Km)
BER1140	$sigG-gfp-ssrA*\Omega kan$ $pelB::PcotE-sspB\Omega spc$	BER1137→BER131 (Km)
BER1141	$sigG-gfp-ssrA*\Omega kan$ $amyE::PsspE(2G)-sspB\Omega cat$	BER1137→JLG963 (Km)
BER1143	$sigK-gfp-ssrA*\Omega kan$ $xyIA::sspB\Omega cat$	BER1138→JLG364 (Km)
BER1144	$sigK-gfp-ssrA*\Omega kan$ $pelB::PcotE-sspB\Omega spc$	BER1138→BER131 (Km)
BER1145	$sigK-gfp-ssrA*\Omega kan$ $amyE::PsspE(2G)-sspB\Omega cat$	BER1138→JLG963 (Km)
BER1152	$sigG-gfp-ssrA*\Omega kan$ , $pelB::PgerE-sspB\Omega spc$	BER1137→BER101 (Km)
BER1153	$sigG-gfp-ssrA*\Omega kan$ $amyE::PsspA-sspB\Omega cat$	BER1137→JLG366 (Km)
BER1155	$sigK-gfp-ssrA*\Omega kan$ $pelB::PgerE-sspB\Omega spc$	BER1138→BER101 (Km)
BER1156	$sigK-gfp-ssrA*\Omega kan$ $amyE::PsspA-sspB\Omega cat$	BER1138→JLG366 (Km)
JLG170	$amyE::PspolIQ-sspB^{Ec}\Omega cat$	(Yen Shin <i>et al.</i> , 2015)
JLG176	$amyE::PspolIR-sspB^{Ec}\Omega cat$	pJLG15→PY79 (Cm)

JLG207	<i>yxjA::Pc-tomato-ssrA*Ωkan</i>	pJLG41→PY79 (Km)
JLG314	<i>sigG-ssrA*Ωkan</i>	pJLG58→PY79 (Km)
JLG364	<i>ΔxylA::sspB<sup>Ec</sup>Ωcat</i>	(Lamsa <i>et al.</i> , 2016)
JLG366	<i>amyE::PsspA-sspB<sup>Ec</sup>Ωcat</i>	pJLG63→PY79 (Cm)
JLG367	<i>amyE::PsspB-sspB<sup>Ec</sup>Ωcat</i>	pJLG64→PY79 (Cm)
JLG370	<i>sigA-ssrA*Ωkan</i>	(Lamsa <i>et al.</i> , 2016)
JLG373	<i>sigK-ssrA*Ωkan</i>	pJLG68→PY79 (Km)
JLG409	<i>amyE::PspollQ-sspB<sup>Ec</sup>Ωcat sigK-ssrA*Ωkan</i>	JLG373→JLG170 (Km)
JLG413	<i>amyE::PsspA-sspB<sup>Ec</sup>Ωcat sigA-ssrA*Ωkan</i>	JLG370→JLG366 (Km)
JLG415	<i>amyE::PsspA-sspB<sup>Ec</sup>Ωcat sigK-ssrA*Ωkan</i>	JLG373→JLG366 (Km)
JLG436	<i>amyE::PsspB-sspB<sup>Ec</sup>Ωcat sigK-ssrA*Ωkan</i>	JLG373→JLG367 (Km)
JLG518	<i>amyE::PsspA-sspB<sup>Ec</sup>Ωcat sigG-ssrA*Ωkan</i>	JLG314→JLG366 (Km)
JLG931	<i>amyE::PsspE(2G)-gfpΩcat</i>	pJLG124→PY79 (Cm)
JLG963	<i>amyE::PsspE(2G)-sspB<sup>Ec</sup>Ωcat</i>	pJLG82→PY79 (Cm)
JLG966	<i>amyE::PsspE(2G)-sspB<sup>Ec</sup>Ωcat sigG-ssrA*Ωkan</i>	JLG314→JLG963 (Km)
JLG967	<i>amyE::PsspE(2G)-sspB<sup>Ec</sup>Ωcat sigK-ssrA*Ωkan</i>	JLG373→JLG963 (Km)
JLG1315	<i>amyE::PspollQ-sspB<sup>Ec</sup>Ωcat sigG-ssrA*Ωkan</i>	JLG314→JLG170 (Km)
JLG1320	<i>pelB::PspollD-sspB<sup>Ec</sup>ΩSpc sigK-ssrA*Ωkan</i>	JLG373→BER105 (Km)
JLG1321	<i>pelB::PspollD-sspB<sup>Ec</sup>ΩSpc sigG-ssrA*Ωkan</i>	JLG314→BER105 (Km)
JLG1322	<i>pelB::PgerE-sspB<sup>Ec</sup>Ωspc sigA-ssrA*Ωkan</i>	JLG370→BER101 (Km)
JLG1325	<i>pelB::PgerE-sspB<sup>Ec</sup>Ωspc sigK-ssrA*Ωkan</i>	JLG373→BER101 (Km)
JLG1326	<i>pelB::PgerE-sspB<sup>Ec</sup>Ωspc sigG-ssrA*Ωkan</i>	JLG314→BER101 (Km)
JLG1327	<i>pelB::PgerE-sspB<sup>Ec</sup>Ωspc amyE::PsspA-sspB<sup>Ec</sup>Ωcat sigA-ssrA*Ωkan</i>	JLG370→BER206 (Km)
JLG1333	<i>amyE::PsspB-sspBΩcat sigG-ssrA*Ωkan</i>	JLG314→JLG367 (Km)
JLG1337	<i>pelB::PspolVA-sspB<sup>Ec</sup>ΩSpc sigK-ssrA*Ωkan</i>	JLG373→BER100 (Km)
JLG1338	<i>pelB::PspolVA-sspB<sup>Ec</sup>ΩSpc sigG-ssrA*Ωkan</i>	JLG314→BER100 (Km)
JLG1347	<i>amyE::PspollR-sspB<sup>Ec</sup>Ωcat sigK-ssrA*Ωkan</i>	JLG373→JLG176 (Km)
JLG1348	<i>amyE::PspollR-sspB<sup>Ec</sup>Ωcat sigG-ssrA*Ωkan</i>	JLG314→JLG176 (Km)
JLG1371	<i>pelB::PgerE-gfpΩspc</i>	pJLG205→PY79 (Sp)
JLG1372	<i>pelB::PcotE-gfpΩspc</i>	pJLG206→PY79 (Sp)
JLG1376	<i>amyE::PsspA-gfpΩcat</i>	pJLG210→PY79 (Cm)
JLG2145	<i>pelB::P2cotE-sspB<sup>Ec</sup>Ωspc</i>	pJLG333→PY79 (Sp)



JLG2317	$\Delta xylA::sspB^{Ec}\Omega cat sigG-ssrA*\Omega kan$	JLG314→JLG364 (Km)
JLG2318	$\Delta xylA::sspB^{Ec}\Omega cat sigK-ssrA*\Omega kan$	JLG373→JLG364 (Km)
JLG2329	$pelB::P2cotE-sspB^{Ec}\Omega Spc sigG-ssrA*\Omega kan$	JLG314→JLG2145 (Km)
JLG2330	$pelB::P2cotE-sspB^{Ec}\Omega Spc sigK-ssrA*\Omega kan$	JLG373→JLG2145 (Km)
JLG2656	$xylA::gfp\Omega cat$	pJLG397→PY79 (Cm)
KP648	$\Delta spo0A::erm$	(Ireton <i>et al.</i> , 1993)
RP189	$\Delta sigG::spc$	pRP186→PY79 (Sp)
RP190	$\Delta sigK::spc$	pRP187→PY79 (Sp)

<sup>a</sup> Plasmid or genomic DNA employed (left side the arrow) to transform an existing strain (right side the arrow) to create a new strain are listed. The drug resistance is noted in parentheses.

<b>Table S3. Plasmid used in this study</b>	
<b>Plasmid</b>	<b>Description</b>
pER86	<i>lacA::MCS (multi-cloning site)</i>
pER96	<i>lacA::erm</i>
pER104	<i>amyE::Pspank-clpX<math>\Omega</math>spc</i>
pER106	$\Delta$ <i>clpX::tet</i>
pER109	<i>spx<math>\Omega</math>cat</i>
pER114	<i>ytsJ-gfp-ssrA*<math>\Omega</math>kan</i>
pER122	<i>gfp-spx<math>\Omega</math>cat</i>
pER128	<i>lacA::PspolIE-sspB<sup>EC</sup><math>\Omega</math>erm</i>
pER156	<i>sigH-ssrA*<math>\Omega</math>kan</i>
pER157	$\Delta$ <i>sigH::kan</i>
pER286	<i>sigG-gfp-ssrA*<math>\Omega</math>kan</i>
pER287	<i>sigK-gfp-ssrA*<math>\Omega</math>kan</i>
pJLG15	<i>amyE::PspolIR-sspB<sup>EC</sup><math>\Omega</math>cat</i>
pJLG24	<i>Pc-tomato-ssrA*<math>\Omega</math>kan</i>
pJLG58	<i>sigG-ssrA*<math>\Omega</math>kan</i>
pJLG41	<i>yxIA::Pc-tomato-ssrA*<math>\Omega</math>kan</i>
pJLG63	<i>amyE::PsspA-sspB<sup>EC</sup><math>\Omega</math>cat</i>
pJLG64	<i>amyE::PsspB-sspB<sup>EC</sup><math>\Omega</math>cat</i>
pJLG66	<i>thrC::PgerE-sspB<sup>EC</sup><math>\Omega</math>spc</i>
pJLG68	<i>sigK-ssrA*<math>\Omega</math>kan</i>
pJLG73	<i>thrC::PcotE-sspB<sup>EC</sup><math>\Omega</math>spc</i>
pJLG74	<i>thrC::PspolVA-sspB<sup>EC</sup><math>\Omega</math>spc</i>
pJLG82	<i>amyE::PsspE(2G)-sspB<sup>EC</sup><math>\Omega</math>cat</i>
pJLG124	<i>amyE::PsspE(2G)-gfp<math>\Omega</math>cat</i>
pJLG171	<i>pelB::PgerE-sspB<sup>EC</sup><math>\Omega</math>spc</i>
pJLG172	<i>pelB::PcotE-sspB<sup>EC</sup><math>\Omega</math>spc</i>
pJLG173	<i>pelB::PspolVA-sspB<sup>EC</sup><math>\Omega</math>spc</i>
pJLG174	<i>pelB::PspolID-sspB<sup>EC</sup><math>\Omega</math>spc</i>
pJLG205	<i>pelB::PgerE-gfp<math>\Omega</math>spc</i>
pJLG206	<i>pelB::PcotE-gfp<math>\Omega</math>spc</i>
pJLG210	<i>amyE::PsspA-gfp<math>\Omega</math>cat</i>

pJLG333	<i>pelB::P2cotE-sspB<sup>Ec</sup>Ωspc</i>
pJLG397	<i>xyIA::gfpΩcat</i>
pRP186	<i>ΔsigG::spc</i>
pRP187	<i>ΔsigK::spc</i>

<b>Table S4. Oligonucleotides used in this study</b>	
<b>Primer</b>	<b>Sequence<sup>a</sup></b>
JLG-7	AATTGGGACAACCTCCAGTG
JLG-16	<i>ttttgaattcggatcc</i> ATGGATTTGTACAGCTAACAC
JLG-32	<i>ttttcggccgctagc</i> TTACTTCACAACGCGTAATGC
JLG-36	<i>ttttgcatgcagttgtgactttatctacaagggtggcataatgtgt</i> TTAAGGAGGATTTAGATGGTG
JLG-38	<i>ttttactagf</i> TTTATACAGTTCATCCATGCC
JLG-63	CTTCCTGGACAGGGATATGG
JLG-64	<i>gttaccgtgtaagagccgc</i> GCCTTTAATCTCTCTCCAG
JLG-65	<i>ctgcaatgataccgcgagac</i> GTGTTGACGGGCAATCAG
JLG-66	AAGCCCGTTTTTCGGATTC
JLG-67	<i>atgaatccgaaaacgggctt</i> GCAACGTTGTTGCCATTGC
JLG-68	<i>ccatatccctgtccaggaag</i> TTCCGAATACCGCAAGCG
JLG-69	GCGGCTCTTACCAGCCTAAC
JLG-70	GTCTCGCGGTATCATTGCAG
JLG-77	<i>gctagc</i> AGCGCAAGCGC
JLG-95	CATGGATTACGCGTTAACCC
JLG-96	GCACTTTTCGGGGAAATGTG
JLG-138	CGAAGGCAGCAGTTTTTTGG
JLG-139	ATAGAGATCCGATCAGACCAG
JLG-178	<i>cactggagttgtccaattc</i> TGAAAAGCCTTTAAAACGATGTTG
JLG-179	<i>cacattccccgaaaagtgc</i> CCATAATACATGGATTGGCG
JLG-180	<i>catcatttgctgcgctagc</i> TTGATGAATATTTTATTCAATTTGTTG
JLG-181	<i>gggtaacgcgtaatccatg</i> ATAAAGTCGAAATCTGCGGG
JLG-184	GCTAGCGCAGCAAATGATG
JLG-187	TTTTCGCTACGCTCAAATCC
JLG-202	<i>cactggagttgtccaattc</i> TGCAGAAGAAGCCGGATC
JLG-203	<i>cacattccccgaaaagtgc</i> GCCGAAATGTCCTAATTGTG
JLG-204	<i>gggtaacgcgtaatccatg</i> CGGATTCATATCCATCTCC
JLG-205	<i>catcatttgctgcgctagc</i> TTTCCCCTTCGCCTTCTTC
JLG-213	GGATCCATGGATTTGTACAG
JLG-214	GCGATTTTCGTTTCGTGAATAC

JLG-215	AGATCCGAATTCTCATGTTTG
JLG-216	<i>caaacatgagaattcggatct</i> GGGAAATTGGCACATATGAG
JLG-217	<i>ctgtgacaaatccatggatcc</i> TGAGTTATTGTTAGCCATGTGTC
JLG-218	<i>caaacatgagaattcggatct</i> GCATCTATCATAAGAGCGGTG
JLG-219	<i>ctgtgacaaatccatggatcc</i> AGAGTTTTGGTTAGCCATGTG
JLG-222	<i>gtattcacgaacgaaatcgc</i> AACAGACCATGACAGTCGTG
JLG-223	<i>ctgtgacaaatccatggatcc</i> AAATCTTTCTCCTTCAAGTATTG
JLG-239	<i>gtattcacgaacgaaatcgc</i> AAATGGAAGTAAATGACCTACTGC
JLG-240	<i>ctgtgacaaatccatggatcc</i> CCTGTATTCAGACATTCCGG
JLG-241	<i>gtattcacgaacgaaatcgc</i> CTCTTACAGTGACAAGCCC
JLG-242	<i>ctgtgacaaatccatggatcc</i> ATCGACCTTTTCCAAGTGATC
JLG-253	TCCTTTAACTCTGGCAACCC
JLG-267	<i>ctgtgacaaatccatggatcc</i> GCTGAAGTTATTTGAGTTAGCC
JLG-268	<i>caaacatgagaattcggatct</i> CTAATGGAGAAGAACGGTGG
JLG-530	GCTGAAGTTATTTGAGTTAGCC
JLG-531	<i>ggctaactcaataacttcagc</i> GCTAAAGGCGAAGAAGTGTTC
JLG-532	<i>ctggtctgatcggatctctat</i> TCATTATTTATACAGTTCATCCATG
JLG-550	ATGTATACCTCCTTAAGCTTAATTGTTATC
JLG-696	GAGATCCCCCTATGCAAGG
JLG-697	ACTCAGTCAACCTTACCGC
JLG-850	<i>gggttgccagagttaagga</i> TGATGGTGCAGGTATAAAGAGG
JLG-851	<i>ccttgcataggggatctc</i> ACCAGGCGATTACAATTGC
JLG-852	<i>gcggttaagggtgactgagf</i> TCATCACAATATGCTTCCTTTC
JLG-853	<i>cacattccccgaaaagtgc</i> TACAAATGAACGAATGTGCAC
JLG-922	AAATCTTTCTCCTTCAAGTATTG
JLG-923	CCTGTATTCAGACATTCCGG
JLG-924	<i>caatactgaaggagaaagaattf</i> GCTAAAGGCGAAGAAGTGTTC
JLG-925	<i>ccggaatgtctgaatacagg</i> GCTAAAGGCGAAGAAGTGTTC
JLG-928	<i>ccaaaaactgctgccttcg</i> TCATTATTTATACAGTTCATCCATG
JLG-929	TGAGTTATTGTTAGCCATGTGTC
JLG-931	<i>gacacatggctaacaataactca</i> GCTAAAGGCGAAGAAGTGTTC
JLG-1237	P-TACAATGGAACAGAACTTTG
JLG-1238	P-CTGCAGTAGGTCATTTACTTCC

JLG-1404	<i>gataacaattaagcttaaggaggatatacatg</i> GCTAAAGGCGAAGAAGCTGTTTAC
JLG-1405	<i>ggattgagcgtagcgaaaa</i> TCATTATTTATACAGTTCATCCATGC
oER369	<i>gggtaacgcgtaatccatg</i> CCTTTCATCATTATGGCGTTC
oER372	<i>gcgcttgcgctgctagc</i> TTACCAATAATCGTAAGTTTTCTTG
oER373	<i>cactggagttgtcccaatt</i> TTTTAATTCATTCCAAAAATGGC
oER374	<i>cacattccccgaaaagtgc</i> GGATTGTTCCATCAAGC
oER417	<i>ttctgctccctgctcaggcggccgc</i> TTTTCGCTACGCTCAAATCC
oER418	<i>caggagcactggtcaacgctagc</i> GACTGTAAAAAGTACAGTCGGC
oER419	<i>ttctgctccctgctcaggcggccgc</i> TCCTTAACTCTGGCAACCC
oER420	<i>caggagcactggtcaacgctagc</i> ATGTGATAACTCGGCGTATG
oER421	<i>ttctgctccctgctcaggcggccgc</i> ATGAGAGAGGAAGAAAACGG
oER422	<i>caggagcactggtcaacgctagc</i> AATTGGGACAACCTCCAGTG
oER425	<i>ttctgctccctgctcaggcggccgc</i> TCCTTAACTCTGGCAACCC
oER426	<i>caggagcactggtcaacgctagc</i> ATGTGATAACTCGGCGTATG
oER439	<i>gttagctgtgacaaatccat</i> TCTTTCTGCTTTTTCCATTCTCTC
oER440	<i>gggtaacgcgtaatccatg</i> GTGATGTCAAAGCTTGAAAAACG
oER441	<i>aagcttgcctagcggatccgcccgcagctg</i> TCACAGTGGAATCTCCCC
oER442	<i>gcggatccgctagcaagctt</i> TCAAGCTATATTTGGAGTTGAGCC
oER443	<i>cacattccccgaaaagtgc</i> CTAATGTGTGTTTACGACAATTCTCAC
oER444	ATGGATTTGTCACAGCTAACACC
oER448	<i>gggtaacgcgtaatccatg</i> ATGGTTACACTATACACATACCAAG
oER449	<i>ctgagcagggagcagaa</i> AAGAAGGCTGATGACTCAGC
oER450	<i>gttgaccagtgtccctg</i> TTATTTTCAACCTGCTGG
oER451	<i>cacattccccgaaaagtgc</i> AGAATCGGATTAACAAGTGC
oER452	<i>ttgccactgtgacagctggc</i> TTACTTCACAACGCGTAATGC
oER453	<i>gttgccagagttaaggagc</i> GGTCAAGCGGTTAAGACACC
oER459	<i>gggtaacgcgtaatccatg</i> CCTGACTCTTGAGGCGATTG
oER460	<i>gcctgagcagggagcagaa</i> GTGTTTTTCCACAGAACGAGC
oER461	<i>gcgttgaccagtgtccctg</i> AAAGACGGCACTGAGGTAAGC
oER462	<i>cacattccccgaaaagtgc</i> ATCGAGTTCACAAAGACAGC
oER465	<i>acgacggtcgac</i> GTGAGACAAGATTAAGGGGTG
oER466	<i>gctgctgcatgc</i> TTATGCAGATGTTTTATCTTGGC
oER470	GCTAAAGGCGAAGAAGCTGTTTACAG

oER471	<i>tgcgcttgcgcttgcgctgctagc</i> TTTATACAGTTCATCCATGCCATG
oER472	<i>gcagcgcaagcgcaagcgca</i> ATGGTTACTACTATACACATCACCAAG
oER473	ATCAGAAGAAGAAATCTTGAAGCC
oER474	GTTCCGCTCCTCAGTCATTCG
oER665	<i>gggtaacgcgtaatccatg</i> CGAAGTACCGAACTTTGTTTCG
oER666	<i>catcattgctgctagc</i> CAACTGATTTTCGCGAATTC
oER667	<i>cactggagttgtccaatt</i> TAGGAATTTATGCTATATTGACAG
oER668	<i>cacattccccgaaaagtc</i> GATAACTTTTCATTTTAAGCCAC
oER672	<i>gggtaacgcgtaatccatg</i> CAGTTTTGAAGAGGCGAGAGAC
oER673	<i>gcctgagcgaggagcagaa</i> TGTTGAATTTCCCTTGTTGTTTC
oER674	<i>gcgttgaccagtgctccctg</i> CAGGAAGAATTTGATGATATTG
oVRP1	<i>taagatctgatcatatgcatc</i> AAGCCATCGAACAGCTCGATG
oVRP2	<i>ccgttttctcctctctcaf</i> TTTTTTCCCTCCCTACAGGAG
oVRP3	ATGAGAGAGGAAGAAAACGG
oVRP4	AATTGGGACAACCTCCAGTG
oVRP5	<i>cactggagttgtccaatt</i> TGAAAAGCCTTTAAAACGATGTTG
oVRP6	<i>cacattccccgaaaagtc</i> AAAGTCTCTCTCAGCTTCGCAAA
oVRP7	GATGCATATGATCAGATCTTA
oVRP8	<i>taagatctgatcatatgcatc</i> CTAACACTTCGTTTCCATAAC
oVRP9	<i>ccgttttctcctctctcaf</i> TTACAAAAGGGGGGCATAAATTT
oVRP10	<i>cactggagttgtccaatt</i> TGCAGAAGAAGCCGGATCTCATACT
oVRP11	<i>cacattccccgaaaagtc</i> GGCGATGGCCATTCTTGCAATGATT

<sup>a</sup>In capital letters are shown the regions of the primer that anneals to the template. Homology regions for Gibson assembly and restriction sites are shown in italics.

## CHAPTER III

Metabolic differentiation and intercellular nurturing underpin bacterial endospore formation.

### **Abstract**

Parent-to-progeny nurturing is critical for reproduction in higher eukaryotes, but analogous examples are undocumented in bacteria. Here, we demonstrate that sporulation in *Bacillus subtilis* entails a nourishing relationship between two cells arising from a single cell division: the forespore, which becomes the metabolically dormant spore, and the mother cell, which dies after sporulation. While both cells synthesize proteins throughout sporulation, the forespore rapidly downregulates central metabolism, amino acid, and nucleotide biosynthesis, and becomes dependent on mother cell-derived metabolic precursors for protein synthesis. We show that arginine moves between mother cell and forespore and we provide direct evidence that putative proteinaceous channels connecting the two cells mediate intercellular transport of small molecules. Our findings demonstrate that metabolic differentiation and intercellular nurturing underpin endospore formation.

### **Main text**

In multicellular organisms, such as animals and plants, reproduction typically involves the investment of metabolic resources from the parents to nurture the prospective progeny. This parent-to-progeny nurturing generally does not apply to unicellular bacteria, which usually reproduce by binary fission, generating two metabolically independent sister cells. However, bacterial sister cells sometimes remain together and differentiate after division, either as part of multicellular communities or during specific developmental pathways, and such cases might entail the formation of metabolic dependencies analogous to parent-to-progeny nurturing. Notwithstanding, the



few reported instances of metabolic dependency in bacteria entail the reciprocal nurturing among different cells<sup>1</sup> or among different cellular populations<sup>2</sup>, rather than the dedicated nourishment of “progeny” cells by “parental” counterparts. It has been speculated that a metabolic relationship analogous to parent-to-progeny nurturing emerges in the course of bacterial endospore formation<sup>3</sup>, during which two cells that arise from a single cell division collaborate to transform one cell into a metabolically dormant spore.

Endospore formation is a conserved process best characterized in *Bacillus subtilis*<sup>4,5,6</sup>. Sporulation begins with an asymmetrically positioned cell division event (polar septation), that gives rise to a sporangium consisting of two cells with different sizes: the smaller forespore and the larger mother cell (Fig. 1A). Following polar septation, the mother cell engulfs the forespore, which becomes enclosed within the mother cell cytoplasm, where it matures while protected from the extracellular medium. Once maturation is complete, the mother cell lyses, thereby releasing the resilient spore into the environment, where it remains dormant until the conditions are favorable for germination and the resumption of growth.

After polar septation, different genetic programs are activated in the mother cell and forespore, and both cells continue to synthesize new proteins until late stages of sporulation<sup>7,8,9</sup>. It remains unclear, however, whether each cell independently produces the metabolic intermediates required to sustain protein synthesis. It has been proposed that sporulation entails an intimate metabolic relationship between the mother cell and the forespore, in which the mother cell nurtures the forespore as it transitions to dormancy, providing the metabolic intermediates necessary to support forespore protein synthesis. This metabolic nurturing model is supported by the existence of sporulation-specific proteins, SpoIIIA and SpoIIQ (Note 2), which are proposed to form multimeric channels connecting the mother cell and forespore cytoplasm<sup>3,10,11,12,13,14,15,16,17</sup>

(hereafter referred to as A-Q channels). A-Q complexes are required for forespore transcription late in sporulation<sup>3,18</sup>, which has led to the proposal that the channel is a gap-junction-like feeding tube through which the mother cell nurtures the developing spore by providing small molecules needed for biosynthetic activity<sup>3</sup>. To date, however, there is no direct evidence that such channels mediate the intercellular transport of molecules.

To get insights into the metabolic relationship between the mother cell and the forespore, we first evaluated if enzymes functioning in different metabolic pathways are enriched in one cell compared to the other. For this purpose, we GFP-tagged key metabolic enzymes functioning in central carbon metabolism, in synthesis of amino acids and nucleotides, and in assembly of macromolecules (RNA and proteins), and quantified the fluorescence signals in the forespore and the mother cell during development (Fig. 1B to G; fig. S1). We found surprising differences between the fluorescence signal in the forespore and in the mother cell, which varied in magnitude depending on the pathway (Fig. 1E and G): enzymes belonging to central carbon metabolism exhibited a ~4- to >100-fold reduction in the forespore compared to the mother cell; amino acid and nucleotides biosynthetic proteins exhibited forespore reductions ranging from 2- to 12-fold; proteins directly involved in macromolecular assembly, however, were present at similar levels in the mother cell and the forespore, consistent with active protein synthesis occurring in both cells throughout sporulation.

The reduced forespore levels of proteins involved in central carbon metabolism and metabolic precursor synthesis seemed to be due to the specific disappearance of the proteins from the forespore rather than increased synthesis in the mother cell, since the proteins were present in vegetative cells prior to polar septation, and similar fluorescence signals were observed in the mother cell and the forespore shortly after polar septation (Fig. 1B; fig. S1). Timelapse microscopy further supported this point,

revealing that a CitZ-GFP fusion protein was rapidly and specifically depleted from the forespore to background levels, despite initially being present at high levels in both the mother cell and forespore immediately following polar septation (Fig 1C and D; movie S1). These results suggest that the forespore and mother cell rapidly become metabolically differentiated during sporulation: while proteins directly involved in macromolecular synthesis are retained by both cells, enzymes involved in central metabolism, in the synthesis of nucleotides, and in the synthesis of amino acids are quickly depleted in the forespore.

Together, the observations above outline a scenario for the metabolic interaction between the mother cell and the forespore compatible with the metabolic nurturing model: the mother cell assumes the burden of metabolic precursor biosynthesis to support macromolecular synthesis in both the mother cell and the forespore. For this model to be true, we reasoned that two premises should be fulfilled. First, enzymes involved in the synthesis of metabolic precursors should be required preferentially in the mother cell, while those involved in the assembly of macromolecules should be required in each cell individually. Although the asymmetric distribution of metabolic enzymes between the mother cell and the forespore is consistent with this premise, it remains possible that the forespore simply has a lower requirement for metabolic precursors. Second, the assembly of macromolecules in the forespore should depend on mother cell-derived metabolic precursors that are transported directly into the forespore.

To evaluate the first premise, we took advantage a recently developed technique called Spatiotemporally Regulated Proteolysis (STRP), which allows the rapid degradation of specific proteins in either the mother cell or the forespore after polar septation<sup>19</sup>. Briefly, a short degradation tag called *ssrA\** is fused to the C-terminus of target proteins, which are subsequently directed by the *SspB*<sup>Ec</sup> adaptor protein to the ClpXP protease for degradation<sup>20</sup> (Fig. 2A). Cell-specific degradation of target proteins is

achieved by expressing *sspB<sup>Ec</sup>* from promoters that are active exclusively in the mother cell or in the forespore after polar septation (Fig. 2B). We focused our efforts on metabolic pathways feeding into protein synthesis (Note 3) (Fig. 2C) by *ssrA*\*-tagging a panel of TCA cycle enzymes (OdhB, SucD, FumC, Mdh, CitZ, CitB (Note 4) and Icd), amino acid biosynthetic enzymes (ArgH, ThrB, and IlvD), and ribosomal proteins (RpsB and RplL). First, we confirmed that the tag did not interfere with protein functionality and that tagged proteins were efficiently degraded upon expression of *sspB<sup>Ec</sup>* (fig. S2A and B). Then, we assessed the requirement for each protein in the mother cell or in the forespore by taking advantage of a unique property of mature spores, namely, their resistance to high temperatures (of over 80 °C). We determined the heat-resistant spore titers of strains harboring the different *ssrA*\*-tagged proteins, and after degradation of each target protein in either the mother cell or in the forespore. Since the requirement for different target proteins can depend on the specific carbon source (Fig. 2D), we induced sporulation in either a defined medium with glutamate as sole carbon source, or in a complex, non-defined medium containing a variety of carbon sources (DSM (Note 1)).

The results can be summarized as follows (Fig. 2E and F; fig. S3C and D; table S1): (i) As expected, degradation of the ribosomal proteins RpsB or RplL in either cell individually produced dramatic spore titer reductions in both media, consistent with translation occurring independently in the mother cell and forespore. (ii) Amino acid biosynthetic proteins yielded mild spore titer reductions (~2-3 fold) when degraded in the mother cell in the glutamate defined medium. No spore titer defects were observed when degradation was induced in the forespore, suggesting that those pathways are dispensable in the forespore. (iii) Most TCA cycle enzymes also yielded significant spore titer defects when degraded in the mother cell, which varied in severity depending on the target protein and the medium. The strongest defects were caused by Icd degradation in DSM medium ( $8 \times 10^3$ -fold reduction), and by OdhB degradation in glutamate medium

(>10<sup>5</sup>-fold reduction). Importantly, degradation of most TCA cycle enzymes in the forespore did not produce spore titer defects in any medium. The lone exception was OdhB, whose forespore degradation reduced the spore titer ~100-fold in both media. Spore titer reductions, however, were up to 750-fold more severe when OdhB was degraded in the mother cell. In addition, further experiments suggested that the requirement of OdhB in the forespore was unrelated to the production of metabolic precursors for protein synthesis (see below). We further characterized the effects of cell-specific degradation of metabolic proteins using fluorescence and phase contrast microscopy to directly visualize sporulation progression. The cytological results are fully consistent with those of the spore titers (Fig. S3E and F).

The second premise that the metabolic nurturing model should fulfill is that forespore macromolecular assembly should depend on metabolic precursors that are synthesized in the mother cell and then subsequently transported to the forespore. To test this premise, we first investigated if forespore protein synthesis depended on mother cell metabolism. To this end, we developed a strategy to measure protein synthesis in the mother cell and forespore in strains in which metabolic enzymes were degraded in the mother cell. We quantified bulk protein synthesis in both cells using bio-orthogonal non-canonical amino acid tagging (BONCAT) and fluorescence microscopy<sup>21</sup>. Briefly, BONCAT involves the use of azide-alkyne click chemistry to fluorescently label cellular proteins (Fig. 2G). Cells are incubated with the L-methionine analog, L-azidohomoalanine (AHA), which is incorporated into newly synthesized proteins by the endogenous translation machinery, resulting in a general labeling of all newly synthesized proteins (Note 1). We used BONCAT in conjunction with STRP to measure new protein synthesis *in situ* in strains in which different proteins were degraded in either the mother cell or the forespore (Note 5).

We first validated this approach by degrading RpsB, the ribosomal protein S2, to induce a cell-specific global translation arrest (Fig. 2H and I, upper panels; fig. S4 and S5). Disabling translation in either cell individually produced a rapid, cell-specific inhibition of protein synthesis, illustrating the potential of STRP and BONCAT to dissect the metabolic interactions between cell-types during sporulation. We then focused on the TCA cycle, as blocking this process should produce a generalized metabolic shut down, affecting many downstream pathways. Specifically, we chose two enzymes whose cell-specific degradation produced strong sporulation defects: Icd, which caused sporulation defects only when degraded in the mother cell, and OdhB, which also impaired sporulation, albeit to a lesser degree, when degraded in the forespore. As shown in Fig. 2H and I (middle and lower panels), strains producing Icd-ssrA\* or OdhB-ssrA\* exhibited robust protein synthesis in both cells. When either protein was targeted for degradation in the forespore, protein synthesis levels in both the mother cell and forespore were similar to those observed in the absence of degradation, suggesting that TCA cycle activity in the forespore is not required to support protein synthesis in either cell. This result suggests that the sporulation defect observed when OdhB is degraded in the forespore is not due to a protein synthesis defect, and we speculate that it might be related to the maintenance of redox balance (Note 6). Degradation of Icd-ssrA\* or OdhB-ssrA\* in the mother cell, however, nearly completely abolished protein synthesis in both the mother cell and the forespore, demonstrating that both proteins are required in only the mother cell to support protein synthesis in both cells. Together, these data demonstrate that shortly after polar septation, forespore protein synthesis becomes dependent on mother cell central carbon metabolism, and suggest that the mother cell supplies the forespore with the metabolic building blocks required to support protein synthesis.

To directly test if the mother cell provides the forespore with substrates for protein synthesis, we devised a strategy to monitor the transport of amino acids between the two cells. The strategy is based upon the Stable Isotope Labeling with Amino Acids in Cell Culture (SILAC) technique<sup>22</sup>, in which cells are incubated with amino acids labeled with heavy stable isotopes of carbon (<sup>13</sup>C) and nitrogen (<sup>15</sup>N), whose incorporation into proteins can be detected by mass spectrometry (MS). Specifically, we engineered a cell-specific SILAC system in which labeled amino acids are imported by either the mother cell or the forespore (Fig. 3A). To achieve this, we expressed individual amino acid transporters from promoters that are active in only one of the cells, in strains genetically engineered to be otherwise unable to import that specific amino acid. This strategy, we reasoned, would restrict the uptake of the amino acid to the cell-type expressing the transporter, leading to incorporation of the label into proteins produced only in that cell. However, if the amino acid moved between the two cells, we would also observe incorporation into proteins produced in the cell not expressing the transporter (Fig. 3A). Note that the mother cell and forespore synthesize unique sets of abundant sporulation proteins that are not synthesized in non-sporulating cells, so proteins produced by each cell are easily distinguished using MS.

Based on our STRP results suggesting arginine as a likely candidate for intercellular transport (Fig. 2), we decided to focus on arginine importers. *Bacillus subtilis* encodes two predicted arginine permeases, RocC and RocE, and a high affinity arginine ABC transporter, ArtPQR<sup>23,24,25,26</sup>. An arginine auxotrophic strain lacking all three predicted transporters is only able to grow in the presence of high concentrations of arginine (Fig. S6A), indicating that RocC, RocE and ArtPQR actually participate in arginine uptake. In our design, we used strains lacking the RocC and RocE permeases, and in which the expression of *artPQR*, a major player in arginine uptake (Fig. S6A), is under the control of mother cell- or forespore-specific promoters, and therefore not

expressed during growth (Fig. S6B). We incubated sporulating cells of strains producing the transporter in either cell with a heavy version of arginine in which all the carbon and nitrogen atoms are replaced by their respective stable isotopes,  $^{13}\text{C}$  and  $^{15}\text{N}$ , which causes a +10 shift in molecular mass that is readily detected by MS (Note 7). To assess the background incorporation of heavy arginine into proteins, we used a strain lacking all three arginine transporters. We prepared protein extracts of spores produced by the different strains, digested them with trypsin to generate peptides suitable for MS analysis, and performed MS to detect the incorporation of heavy arginine in mother cell- and forespore-specific peptides. For every strain, we detected over 3000 sporulation-specific peptides containing at least one arginine residue, which were subsequently classified into mother cell- and forespore-specific to determine the percentage of heavy arginine incorporation in proteins from either cell.

The results were as follows (Fig. 3B): expression of *artPQR* in the mother cell led to heavy arginine incorporation in ~ 28 % of mother cell peptides, more than two-fold over background, indicating that the transporter was truly being produced and contributed to arginine uptake by the mother cell. Importantly, *artPQR* mother cell expression also produced an increase of similar magnitude in heavy arginine incorporation into forespore-specific peptides compared to the background, implying that arginine imported by the mother cell was subsequently transported to the forespore and incorporated into proteins in this cell. Expression of *artPQR* in the forespore produced only a slight increase (~1.35-fold over background) in the percentage of forespore peptides containing heavy arginine. This might be due to the fact that, after engulfment, the forespore becomes sequestered within the mother cell cytoplasm and loses access to the culture medium, leaving only a short window of opportunity for the forespore to import arginine. Actually, the fraction of forespore peptides that incorporate heavy arginine is higher for forespore proteins synthesized while the forespore is still exposed



to the medium (~2-fold over background) than for proteins synthesized afterwards (Fig. S6C). Interestingly, mother cell proteins also showed a mild increase in the incorporation of heavy arginine when *artPQR* is expressed in the forespore (Fig. 3B), which, as above, was more prominent for proteins synthesized during engulfment (Fig. S6C). Together, these results indicate that, in principle, arginine can be transported between the mother cell and the forespore bidirectionally. However, our findings that proteins involved in arginine biosynthesis are only required in the mother cell (Fig. 2) and disappear from the forespore after sporulation initiation (Fig. 1) suggest that, in the case of arginine, only mother cell to forespore transport might be physiologically relevant.

Next, we sought to investigate whether metabolic exchange between the mother cell and forespore could actually be mediated by A-Q channels, as previously proposed<sup>3</sup>. A-Q channels are required for sustained transcription in the forespore at late stages of development<sup>3,18</sup>, an observation that has been interpreted as evidence that they might mediate the intercellular transport of metabolic precursors from the mother cell to the forespore. To test and expand this observation, we used BONCAT and fluorescence microscopy to explore if the A-Q channel is also required for forespore protein synthesis. We performed BONCAT on wild-type sporangia, and on sporangia lacking A or Q, and measured protein synthesis in the mother cell and forespore (Fig. S7A and B). As expected, wild-type sporangia exhibited high levels of protein synthesis in both the mother cell and forespore. However, no protein synthesis was detected in the forespores of mutants lacking A or Q, while mother cells maintained levels of protein synthesis equivalent to that of the wild type. These results indicate that, in addition to forespore transcription, A-Q is required for forespore protein synthesis, but not for mother cell protein synthesis, reinforcing the proposal that A-Q constitutes a “feeding tube” through which nutrients or other molecules are transferred from the mother cell to the forespore<sup>3</sup>.

The inability of small proteins such as GFP to move between the mother cell and the forespore<sup>27</sup> suggests that, if A-Q does assemble into a channel, it might mediate intercellular transport of small molecules such as amino acids. The assessment of intercellular transport of amino acids in A-Q mutants using the cell-specific SILAC approach implemented above, however, is complicated by the fact that forespores lacking A-Q fail to synthesize new proteins (Fig. S7A and B). To determine directly if A-Q mediates the intercellular transport of small molecules *in vivo*, we employed an alternative strategy previously used to monitor small molecule transport between cells in filamentous cyanobacteria<sup>28</sup>. This strategy entails loading cells with fluorescent small molecules that cannot diffuse across membranes, followed by measuring fluorescence recovery after photobleaching (FRAP) in one cell (Fig. 4A) (Note 1). We sporulated *B. subtilis* cells in the presence of calcein AM, a non-fluorescent, membrane-permeant acetoxymethylester derivative of calcein used to label living cells. Upon being taken up by cells, the acetoxymethylester groups are hydrolyzed by non-specific cellular esterases, rendering the molecule both fluorescent and membrane-impermeable. With this treatment, we were able to achieve even fluorescent labeling of the mother cell and forespore cytoplasm (Fig. 4B). We then used a laser to specifically photobleach the forespores of calcein-labeled wild-type engulfing sporangia, and of engulfing sporangia lacking A or Q, and monitored recovery by fluorescence microscopy. As a negative control, we monitored the fluorescence recovery of vegetative cells separated by complete septa. If A-Q was required for small molecule intercellular transport, then photobleached forespores should recover in wild-type sporangia, but fail to recover in sporangia lacking A or Q (Fig. 4A). Bleached forespores of wild-type sporangia exhibited a rapid and significant recovery of fluorescence signal within 90 s (Fig. 4B and C; fig. S8A; movie S2), indicating that small molecules can move from the mother cell to the forespore under normal conditions. The fluorescent signal did not recover in forespores

of sporangia lacking either A or Q (Fig. 4B and C; fig. S8A; movies S3 and S4), indicating that both proteins are required to facilitate calcein movement from the mother cell to the forespore. Importantly, photobleached vegetative cells separated by fully formed septa failed to recover, indicating that transport does not occur across vegetative septa (Fig. 4B and C; fig. S8A; movie S5). This control also provides evidence that the recovery observed in wild-type sporangia is due to movement of calcein between cells, not the uptake of new calcein AM during the FRAP experiment.

The observation that arginine can move bidirectionally between the mother cell and the forespore prompted us to test whether A-Q could also mediate calcein transport from the forespore to the mother cell. For this purpose, we used the same strategy as above, but we photobleached calcein fluorescence in mother cells rather than in forespores (Fig. 4A, lower panel). Since the forespore is significantly smaller in volume than the mother cell, transport of fluorescent calcein from the forespore might not produce an obvious increase of fluorescence in the mother cell. Thus, to assess whether fluorescent calcein was transported from the forespore to the mother cell, we measured fluorescence loss in the forespore, rather than the fluorescence recovery in the mother cell. In wild-type sporangia, calcein fluorescence was rapidly lost in the forespore, reaching fluorescence levels not significantly different than those of bleached mother cells within 63 s (Fig. 4B and D; fig. S8B and C; movie S6). In mutants lacking A or Q, however, forespore fluorescence loss was markedly slower and fluorescence levels were still significantly higher than those in the mother cell after 90 s (Fig. 4B and D; fig. S8B and C; movies S7 and S8). Overall, these results show that A-Q channels allow the bidirectional movement of the small molecule calcein between the mother cell and the forespore. This opens the possibility that A-Q contributes to equilibrate the concentrations of small molecules between the two cells. Under physiological conditions, however, we presume that the transport of metabolic precursors from mother cell to

forespore predominates, since the forespore loses the ability to acquire nutrients from the environment once engulfment completes. Furthermore, the fact that synthesis pathways are downregulated in the forespore, and that the products of those pathways are quickly polymerized into final products, suggest that a concentration gradient could confer mother cell to forespore directionality. While this transport would allow the mother cell to nurture the metabolically disabled forespore, we speculate that forespore to mother cell transport might contribute to the clearance of metabolic byproducts from the developing spore. The larger volume of the mother cell could allow it to function as a reservoir for these byproducts, which could either be shunted into pathways that are active in the mother cell, or excreted into the environment. Further studies are required to fully define the nature by which metabolites and/or waste products are preferentially transported in one direction or the other.

The findings presented in this manuscript demonstrate that sporulation entails a nourishing relationship between two cells that become metabolically differentiated after a single cell division event (Fig. 4E): following polar septation, the forespore rapidly shuts down central and intermediary metabolism, becoming dependent on the mother cell for metabolic precursors, which are trafficked between the two cells and used for the synthesis of macromolecules. We provide evidence that A-Q functions as a non-specific metabolic conduit, allowing the mother cell to assume the burden of precursor biosynthesis, and to nurture the forespore as it transitions to dormancy. Altogether, our results outline the set of metabolic transformations and interactions that promote the development and maturation of an endospore. Elaborating the mechanisms that generate and maintain metabolic asymmetry and that mediate intercellular transport may provide a more comprehensive understanding of the nurturing interactions that underpin cellular transition to dormancy.

## Notes

NOTE1. Materials and methods are available as supplementary materials at the Science website.

NOTE2. SpoIIQ is produced in the forespore. The *spoIIIA* operon is transcribed only in the mother cell and encodes eight proteins, SpoIIIAA to SpoIIIAH. For simplicity, we globally referred to the proteins in the operon as “A”.

NOTE3. Here we provide a description of the proteins tagged with *ssrA\**. TCA cycle: CitZ, major citrate synthase (this protein was degraded in a background lacking the minor citrate synthase, CitA); CitB, aconitase; Icd, isocitrate dehydrogenase; OdhB, E2 subunit of 2-oxoglutarate dehydrogenase; SucD,  $\alpha$  subunit of succinyl-CoA synthetase; FumC; fumarase; Mdh, malate dehydrogenase. The addition of the *ssrA\** tag to components of the succinate dehydrogenase complex severely affected protein functionality, and they were excluded from this study. Amino acid biosynthetic proteins: ArgH, argininosuccinate lyase, required for arginine synthesis; IlvD, dihydroxy-acid hydratase, required for the synthesis of branched-chain amino acids (leucine, isoleucine and valine); ThrB, homoserine kinase, required for threonine synthesis. Ribosomal proteins: RpsB, ribosomal protein S2; RplL, ribosomal protein L12.

NOTE4. Aconitase (CitB) is both a TCA cycle enzyme and a regulatory RNA binding protein, and it has been shown that its regulatory role is important for sporulation<sup>29</sup>. Thus, the sporulation defects we observe after mother cell degradation of the aconitase (fig. S3) might be due to its regulatory role, rather than to its enzymatic activity.

NOTE5. An important fraction of the new proteins synthesized in the mother cell are coat proteins, which localize around the forespore, complicating the measurement of the fluorescence signals in both cells (fig. S5). To prevent the attachment of the coat to the forespore, we performed the BONCAT experiments in SpoIIV<sup>-</sup> background, in which the

coat proteins are not attached to the forespore surface and remain in the mother cell cytoplasm.

NOTE6. OdhB is part of the 2-oxoglutarate dehydrogenase complex, which catalyzes the conversion of 2-oxoglutarate to succinyl-CoA, a reaction that also entails the reduction of NAD<sup>+</sup> to NADH and H<sup>+</sup>. It is therefore possible that OdhB in the forespore is required to maintain an appropriate redox status, rather than to produce carbon skeletons for protein synthesis.

NOTE7. To maximize the incorporation of exogenous arginine into sporulation proteins, we used strains in which arginine synthesis was blocked in both the mother cell and the forespore by STRP-mediated degradation of ArgH-ssrA\*.

## **Materials and methods**

### **Strain construction**

All the strains used in this study are derivatives of *Bacillus subtilis* PY79. A complete list of strains is provided in Table S2. The plasmids and oligonucleotides used to construct the different strains are provided in Table S3 and S4, respectively. Detailed descriptions of plasmid construction can be found in the supplementary text.

### **Culture conditions**

*Bacillus subtilis* strains were routinely grown on LB plates at 30°C. We induced sporulation in two different ways: (i) By resuspension in A+B sporulation medium containing glutamate as the sole carbon source (Sterlini and Mandelstam, 1969), after growing the bacteria in ¼ diluted LB to O.D.<sub>600</sub> ~ 0.5 (Becker and Pogliano, 2007). Sporulation induction was considered to be the moment in which the cells were resuspended in A+B medium. (ii) By exhaustion in Difco Sporulation Medium (DSM) (Schaeffer et al., 1965), containing beef extract and peptones as carbon and nitrogen sources. In DSM the cells grow until the nutrients become limiting, and sporulation is induced at the onset of stationary phase, which is characterized by a plateau in the

growth curve. Sporulation cultures were grown at 37°C for batch culture experiments, and at 30°C for timelapse microscopy experiments. Arginine auxotrophic strains lacking either ArtPQR or RocC (or both) were cultured in LB medium supplemented with a high concentration of L-arginine (10 mM), which allowed for enough non-specific import of L-arginine to support growth.

### **Fluorescence microscopy**

Cells were visualized on an Applied Precision DV Elite optical sectioning microscope equipped with a Photometrics CoolSNAP-HQ2 camera. Images were deconvolved using SoftWoRx v5.5.1 (Applied Precision). The median focal planes are shown.

### **Batch culture microscopy**

We used microscopy to assay for the completion of two developmental milestones: engulfment and forespore maturation (fig. S3F). Engulfment completion was determined using a well-characterized membrane fission assay (Sharp and Pogliano, 1999). Briefly, cells are treated with a red membrane-impermeable membrane dye, FM 4-64, and a green membrane-permeable membrane dye, Mitotracker Green (MTG). During engulfment, forespore membranes are accessible to both the red and the green dyes. However, after engulfment forespore membranes cannot be stained by the red dye, and are clearly visible as green ovals inside the mother cells. Forespore maturation was assessed by phase contrast microscopy. Mature spores contain low water content, which endows them with a bright appearance under phase-contrast microscopy. This allows the extent to which developing spores become phase bright to be used as a proxy for spore maturation.

For batch culture microscopy, cells contained in 12  $\mu$ l of culture were transferred to 1.2% agarose pads, prepared using A+B medium or  $\frac{1}{4}$  diluted DSM, either 3 or 6 hours after sporulation induction. Membranes were stained with 0.5  $\mu$ g mL<sup>-1</sup> FM 4–64

(Life Technologies) and  $1 \mu\text{g mL}^{-1}$  Mitotracker green (Life Technologies). FM 4–64 was added to the agarose pad, whereas Mitotracker green was mixed with the cells before transferring them to the pad.

### **Timelapse microscopy**

For timelapse microscopy, sporulation was induced at  $30^{\circ}\text{C}$ . To visualize the membranes,  $0.5 \mu\text{g/mL}$  FM 4-64 was added to the culture one hour after sporulation induction and incubated for two additional hours under standard culturing conditions. Seven  $\mu\text{l}$  samples were taken 3 h after resuspension and transferred to agarose pads prepared as follows: 2/3 volume of supernatant from the sporulation culture; 1/3 volume of 3.6% agarose in fresh A+B sporulation medium;  $0.17 \mu\text{g/mL}$  FM 4-64. Pads were partially dried, covered with a glass slide and sealed with petroleum jelly to avoid dehydration during timelapse imaging (Ojkic et al., 2016). Pictures were taken in an environmental chamber at  $30^{\circ}\text{C}$  every 5 min for at least 2 h. Excitation/emission filters were TRITC/CY5 for membrane imaging, and FITC/FITC for GFP imaging. Excitation light transmission was set to 5% for membrane imaging and 32% for GFP imaging to minimize phototoxicity. Exposure time was 0.1 and 0.3 s for membrane and GFP imaging, respectively. For presentation purposes, sporangia were aligned vertically (with forespore on top) by rotating them using Photoshop.

### **Spore titer assays**

Sporulation was induced in 2 mL of DSM or in 10 mL of A+B resuspension medium, and was allowed to proceed at  $37^{\circ}\text{C}$  for 24 h. Two mL of culture was then heated at  $80^{\circ}\text{C}$  for 20 min, serially diluted in 1x T-base, plated on LB, and incubated overnight at  $30^{\circ}\text{C}$ . Spore titers were calculated based on colony counts.

### **BONCAT**

Sporulation was induced in either A+B medium or DSM, as indicated, at  $37^{\circ}\text{C}$ . One hour after sporulation induction,  $0.5 \mu\text{g/mL}$  FM 1-43FX (Thermo Fisher Scientific)



was added to cultures. 100  $\mu$ M of L-azidohomoalanine (Thermo Fisher Scientific) was added to cultures 3.75 hours following sporulation induction and incubated under standard culturing conditions for 15 minutes.

Cells were fixed and permeabilized as described previously (Perez et al., 2000). Briefly, 0.5 mL of culture was fixed at room temperature for 20 min in a solution containing 20 mM sodium phosphate pH 7.4, 2.6% (wt/vol) paraformaldehyde (EM Sciences), and 0.06% (wt/vol) glutaraldehyde (EM Sciences). Samples were washed three times with phosphate-buffered saline and once with GTE (50 mM glucose, 10 mM EDTA, 20 mM Tris, pH 7.4), and then resuspended in 200  $\mu$ L of GTE. Fixed cells were deposited on 15 well glass multitest slides (AP Biomedicals, L.L.C.) that were pretreated with 0.1% poly-L-lysine (Sigma-Aldrich) for 5 min and washed twice with sterile water. Fixed cells were permeabilized by adding 2 mg/mL lysozyme and incubating at room temperature for 4 min. Fixed cells on slides were washed three times with phosphate-buffered saline.

Strain-promoted click labeling was performed roughly in accordance with previously described methods (Hatzenpichler et al., 2014). All of the following incubations were performed in the dark to preserve the fluorescent signal. Fixed cells on multiwell slides were treated with 100 mM 2-chloroacetamide in Tris pH 7.4 and incubated at 37 °C for one hour to block free thiol functional groups. Following the one hour incubation, Alexa Fluor 647 DIBO Alkyne (Thermo Fisher Scientific) was added directly to the 2-chloroacetamide solution to a final concentration of 1  $\mu$ M and incubated at 37°C for an additional 30 min to promote click labeling. The 2-chloroacetamide dye mixture was then gently removed from the slide by aspiration. Unbound dye was removed through a series of washes, gently aspirating between each step. First, slides were treated with phosphate-buffered saline and incubated at 37°C for 10 min. Next, slides were treated with 50% DMSO in phosphate-buffered saline and incubated at room

temperature for 20 min. Then, slides were washed three times with phosphate-buffered saline, incubating for 3 min at room temperature for each wash. Finally, slides were washed and dehydrated with an increasing ethanol series, incubating three minutes at room temperature for each 50%, 80%, and 96% ethanol. Slides were air-dried and equilibrated in equilibration buffer (Life Technologies) for 5 min, then washed again with fresh equilibration buffer. Slides were treated with antifade reagent in glycerol/PBS (Life Technologies) and covered with a glass slide.

All BONCAT experiments were performed in a  $\Delta sigG$  and  $\Delta spoIVA$  genetic background. *sigG* encodes the sigma factor responsible for late forespore gene expression. Since some degradation strains fail to complete engulfment efficiently and since early forespore gene expression continues in the absence of SigG<sup>3</sup>, performing these experiments in a  $\Delta sigG$  background ensured that any observed differences in protein synthesis was not a consequence of the failure to activate late gene expression. To facilitate quantification of mother cell and forespore protein synthesis, all BONCAT experiments were performed in strains lacking SpoIVA to block coat assembly around the forespore (fig. S5). The spore coat consists of over 70 mother cell-synthesized proteins that encase the forespore and comprise 37% of the total spore protein (Munoz et al., 1978). SpoIVA is a protein that constitutes the basement layer of the spore coat and is required for the recruitment and anchoring of coat proteins to the surface of the forespore, but not for the assembly of other coat layers (Roels et al., 1992). Therefore,  $\Delta spoIVA$  mutants form aggregates of coat in the mother cell cytoplasm rather than at the forespore periphery, allowing mother cell protein synthesis to be easily distinguished from forespore protein synthesis.

Mother cell and forespore protein synthesis were quantified in sporangia from three microscopy fields using FIJI software. To determine protein synthesis levels, eight optical sections spanning 1.05  $\mu\text{m}$  from deconvolved images were summed using FIJI's

Z-project tool. Mean Alexa Fluor 647 fluorescence intensities of the forespore and mother cell were determined separately by drawing a polygon encompassing the entire cell and then subtracting the mean background intensity plus two standard deviations. Values for the mother cell and the forespore were made relative to the median fluorescence signal of the respective cell-type in an isogenic strain expressing only the –*ssrA\** tagged protein (for cell-specific inactivation of translation or the TCA cycle), or an isogenic wild-type strain (for Q-A mutants).

### **Fluorescence recovery after photobleaching (FRAP)**

Sporulation was induced in A+B medium. Two hours after resuspension, the medium was supplemented with 100  $\mu\text{g mL}^{-1}$  of calcein AM (Thermo Fisher Scientific), and the cells were incubated at 37°C for one extra hour. Then, cells were washed three times with 1 mL of fresh A+B medium without calcein AM and placed onto 1.2% agarose pads, supplemented with FM 4-64 to stain membranes. Before performing FRAP, a static membrane picture was taken (excitation/emission, TRITC/CY5; exposure time, 0.15 s), and was used as reference to determine the position of mother cells and forespores. The FRAP experiment was performed as follows: Prior to the photobleaching event, intracellular fluorescent calcein was imaged using FITC/FITC filters and 0.4 s exposure time. Subsequently, forespore calcein fluorescence was bleached with a 0.1 s pulse from a 488-nm argon laser set to 30% power, and calcein fluorescence images were collected every 3 s for 90 s, using the same filters and exposure time as the prebleach imaging. Quantification was performed as described previously (Fleming et al., 2010). Briefly, we calculated the corrected fluorescence recovery (cFR) by determining the relative intensity of the bleached cell to the unbleached cell, and defining the pre-bleaching ratio as  $\text{cFR} = 1$  and the ratio immediately following the bleaching event as  $\text{cFR} = 0$ . Average cFR curves were obtained by averaging fluorescence recovery values of different bleached cells at the same time points for each strain.

### **Fluorescence loss in photobleaching (FLIP)**

Sporulation was induced in A+B medium. Two hours after resuspension, the medium was supplemented with  $100 \mu\text{g mL}^{-1}$  of calcein AM (Thermo Fisher Scientific), and the cells were incubated at  $37^{\circ}\text{C}$  for one extra hour. Then, cells were washed three times with 1 mL of fresh A+B medium without calcein AM and placed onto 1.2% agarose pads, supplemented with FM 4-64 to stain membranes. Before performing FRAP, a static membrane picture was taken (excitation/emission, TRITC/CY5; exposure time, 0.15 s), and was used as reference to determine the position of mother cells and forespores. The FLIP experiment was performed as follows: Prior to the photobleaching event, intracellular fluorescent calcein was imaged using FITC/FITC filters 0.4 s exposure time. Subsequently, mother cell calcein fluorescence was bleached with a 0.1 s pulse from a 488-nm argon laser set to 70% power and calcein fluorescence images were collected every 3 s for 90 s, using the same filters and exposure time as the prebleach imaging. A standard curve was generated by measuring the average fluorescence loss of cells distal to the bleaching event (Fig. S7D), and this was used to correct for the loss of fluorescence caused by repeated image acquisition rather than intercellular transport (Fig. S7E). Fluorescence values were background subtracted and normalized such that the pre-bleach values were equal to 1 for both the mother cell and forespore, and such that the mother cell values immediately following the bleaching event were equal to zero. Following correction using the standard curve, average normalized fluorescence values for mother cell and forespore were obtained by averaging normalized fluorescence values of different bleached cells at the same time points for each strain.

### **Forespore to mother cell GFP fluorescence ratio quantification**

To be able to unambiguously distinguish if tagged proteins were present in the forespore or in the mother cell, we excluded membrane-associated proteins from the

analysis. The ratio of GFP intensity between forespore and mother cell was measured semi-automatically using a custom script in Matlab 2017b. Forespores and mother cell objects were identified and segmented from a single FM 4-64 channel by taking advantage of the increased fluorescence around the forespore. Thresholding high allowed for identification of forespores while thresholding low gave the whole cell outline. Subtracting the forespore image from the whole cell image allowed mother cells to be identified. Forespores were then paired to their corresponding mother cells first by filtering mother cell objects based on Euclidean distance, and then by the orientation of the mother cell. These filters were made strict to reduce false matches. GFP fluorescence ratio was calculated by using the paired forespore-mother cell objects to mask the GFP fluorescence image in order to obtain a mean fluorescence intensity for both.

#### **Quantification of native CitZ-GFP depletion**

Mean GFP fluorescence intensity of the median focal plane was quantified separately for the forespore and mother cell by drawing a polygon encompassing the entire area of each cell-type using FIJI. The mean background intensity was subtracted from each measurement. The mean fluorescence intensities for each cell-type were averaged, and the initial values were normalized to one.

#### **Quantification of phase bright spores**

Measurements of phase bright spore intensity were obtained in a semi-automated manner from images of sporulating cells at 6 hours post-induction using a custom script in Matlab 2017b, applied to the median focal plane. FM 4-64, which stained the outer cell membranes, provided a fluorescent image to threshold, segment and count the total number of cells present. The complement of the fluorescent FM 4-64 image provided a mask to segment the background for subsequent subtraction from the phase bright image. In addition, a second membrane dye, MitoTracker Green, capable

of diffusing into the cell, was used to stain fully engulfed forespore membranes. Thus, an image created from the difference in signals of both membrane dyes would only show fully engulfed forespores. Using this new image, and filtering out those forespores which contained objects from concurrent DAPI staining (as DAPI is unable to enter fully engulfed spores), ensured that all identified forespores were mature. For each forespore identified in this way, the average phase intensity was calculated with the average background phase intensity removed. A phase intensity threshold of 0.1 a.u. was used to constitute “phase bright”. This threshold was selected because it was the lowest value above which the majority of the engulfment completed wild-type population was found at six hours post sporulation induction. Additionally, the populations of known phase bright mutants failed to breach this threshold.

#### **Stable isotope labeling with amino acids in cell culture (SILAC)**

Sporulation was induced in A+B medium at 37°C. Cultures were supplemented with 0.1 mM L-arginine-<sup>13</sup>C<sub>6</sub>,<sup>15</sup>N<sub>4</sub> hydrochloride (Sigma-Aldrich) two hours after sporulation induction, and sporulation was allowed to proceed for 72 hours. Formation of mature spores was monitored by phase-contrast microscopy. To achieve arginine uptake by the mother cell, *artPQR* was expressed from *spolIM* or *spolVA* promoters. To achieve arginine uptake by the forespore, *artPQR* was expressed from *spolIQ* or *spolIR* promoters. To maximize the incorporation of exogenous arginine into sporulation proteins, we used strains in which arginine synthesis was blocked in both the mother cell and the forespore by STRP-mediated degradation of ArgH-ssrA\*. Additionally, wild-type cells were sporulated in the absence of 0.1 mM L-arginine-<sup>13</sup>C<sub>6</sub>,<sup>15</sup>N<sub>4</sub> hydrochloride to ensure that labeled peptides were only detected when the medium was supplemented with heavy arginine.

### **Spore purification**

72 hour sporulation cultures were pelleted and washed once with 4°C sterile water. To lyse remaining vegetative cells, spore samples were incubated overnight at 4°C in sterile water. The next day, the spores were pelleted by centrifugation, washed once with 4°C sterile water, and incubated again overnight at 4°C in sterile water. Spores were then further purified over a phosphate-polyethylene glycol aqueous biphasic gradient as previously described (Harrold et al., 2011). The spore-containing organic phase (top) was harvested and washed with 50 or more volumes of 4°C sterile water at least three times. The spores were pelleted, resuspended in fresh sterile water, and stored at 4°C. Sample purity was evaluated using phase contrast microscopy.

### **Extraction of spore coat proteins**

Purified intact spores were diluted to approximately  $5 \times 10^9$  spores mL<sup>-1</sup> in 0.1 M NaOH and incubated at 4°C for 15 minutes, vortexing periodically. Samples were pelleted by spinning at 10,000 x g for 10 minutes at 4°C. The supernatant was applied to a 2 mL 3.5K MWCO dialysis cassette (Thermo Fisher Scientific) and dialyzed against 1 L of 0.5M sodium acetate/acetic acid buffer (pH 5.0) and then against four changes of 1L of deionized water at 4°C over the course of 48 hours. Dialyzed material was harvested and submitted for mass spectrometry analysis.

### **Extraction of small acid soluble proteins**

Purified intact spores were diluted to approximately  $5 \times 10^9$  spores mL<sup>-1</sup> in 4°C 2 M HNO<sub>3</sub> and incubated on ice for 30 minutes. Samples were pelleted by spinning at 10,000 x g for 10 minutes at 4°C. The supernatant was applied to a 2 mL 3.5K MWCO dialysis cassette (Thermo Fisher Scientific) and dialyzed against five changes of 1 L of 1 % acetic acid at 4°C over the course of 48 hours. Dialyzed material was harvested and submitted for mass spectrometry analysis.

### **Sample preparation for mass spectrometry**

Mass spectrometry samples were prepared and analyzed by the University of California, San Diego Biomolecular and Proteomics Mass Spectrometry Facility (<http://bpmsf.ucsd.edu/>). An equal volume of 6 M guanidine solution was added to 100  $\mu$ L of protein extract and mixed. The samples were then boiled for 5 minutes followed by 5 minutes cooling at room temperature. The boiling and cooling cycle was repeated a total of 3 cycles. The proteins were precipitated with addition of methanol to final volume of 90% followed by vortexing and centrifugation at maximum speed on a benchtop microfuge (14000 rpm) for 10 minutes. The soluble fraction was removed by flipping the tube onto an absorbent surface and tapping to remove any liquid. The pellet was resuspended in 200  $\mu$ L of 8 M Urea made in 100mM Tris pH 8.0. To reduce and alkylate samples, TCEP (Tris (2-carboxyethyl) phosphine) was added to a final concentration of 10 mM and chloroacetamide was added to a final concentration of 40 mM and vortexed for 5 minutes. 3 volumes of 50 mM Tris pH 8.0 were added to the sample to reduce the final urea concentration to 2 M. Samples were digested with trypsin (trypsin:protein ratio of 1:50) and incubated at 37°C for 12 hours. The solution was then acidified using trifluoroacetic acid (TFA) (0.5% TFA final concentration) and mixed. Samples were desalted using 100 mg C18-StageTips (Thermo Fisher Scientific) as described by the manufacturer protocol. Samples were resuspended in sample loading buffer and the peptide concentration measured using BCA (Thermo Fisher Scientific). A total of 1  $\mu$ g was injected for each label free quantification run.

### **LC-MS/MS Analysis**

Trypsin-digested peptides were analyzed by ultra-high pressure liquid chromatography (UPLC) coupled with tandem mass spectroscopy (LC-MS/MS) using nanospray ionization. The nanospray ionization experiments were performed using an Orbitrap Fusion Lumos Hybrid mass spectrometer (Thermo Fisher Scientific) interfaced



with nano-scale reversed-phase UPLC (Thermo Dionex UltiMate™ 3000 RSLC nano System) using a 25 cm, 75-micron ID glass capillary packed with 1.7- $\mu$ m C18 (130) BEH™ beads (Waters Corporation). Peptides were eluted from the C18 column into the mass spectrometer using a linear gradient (5–80%) of ACN (acetonitrile) at a flow rate of 375  $\mu$ L min<sup>-1</sup> for 1h. The buffers used to create the ACN gradient were: Buffer A (98% H<sub>2</sub>O, 2% acetonitrile (ACN), 0.1% formic acid) and Buffer B (100% ACN, 0.1% formic acid). Mass spectrometer parameters were as follows: an MS1 survey scan using the Orbitrap detector [mass range (m/z): 400-1500 (using quadrupole isolation), 120000 resolution setting, spray voltage of 2200 V, ion transfer tube temperature of 275°C, automatic gain control (AGC) target of 400000, and maximum injection time of 50 ms] was followed by data dependent scans (top speed for most intense ions, with charge state set only to include +2-5 ions, and 5 second exclusion time), while selecting ions with minimal intensities of 50000 in which the collision event was carried out in the high energy collision cell (HCD Collision Energy of 30%), and the fragment masses were analyzed in the ion trap mass analyzer (with ion trap scan rate of turbo, first mass m/z was 100, AGC Target 5000 and maximum injection time of 35 ms). Protein identification and SILAC quantification was carried out using Peaks Studio 8.5 (Bioinformatics Solutions, Inc.) For modifications L-arginine-(<sup>13</sup>C<sub>6</sub>, <sup>15</sup>N<sub>4</sub>) was set as a variable modification and peptides with this modification were used for SILAC quantification. Regulon assignments were made in accordance with those found on the SubtiWiki databases (<http://subtiwiki.uni-goettingen.de/>). Genes expressed as part of the SigA, SigH, and/or Spo0A regulons were considered vegetative.

### **Statistical analysis**

Number of trials and error bars are described in figure legends.

## ACKNOWLEDGEMENTS

Chapter III, in full, is currently being prepared for submission to Science. Riley, Eammon P.; Lopez-Garrido, Javier; Sugie, Joseph; Liu, Roland B.; Pogliano, Kit. The dissertation author was the primary investigator and author of this paper. Permission from all authors has been obtained.

## Figures

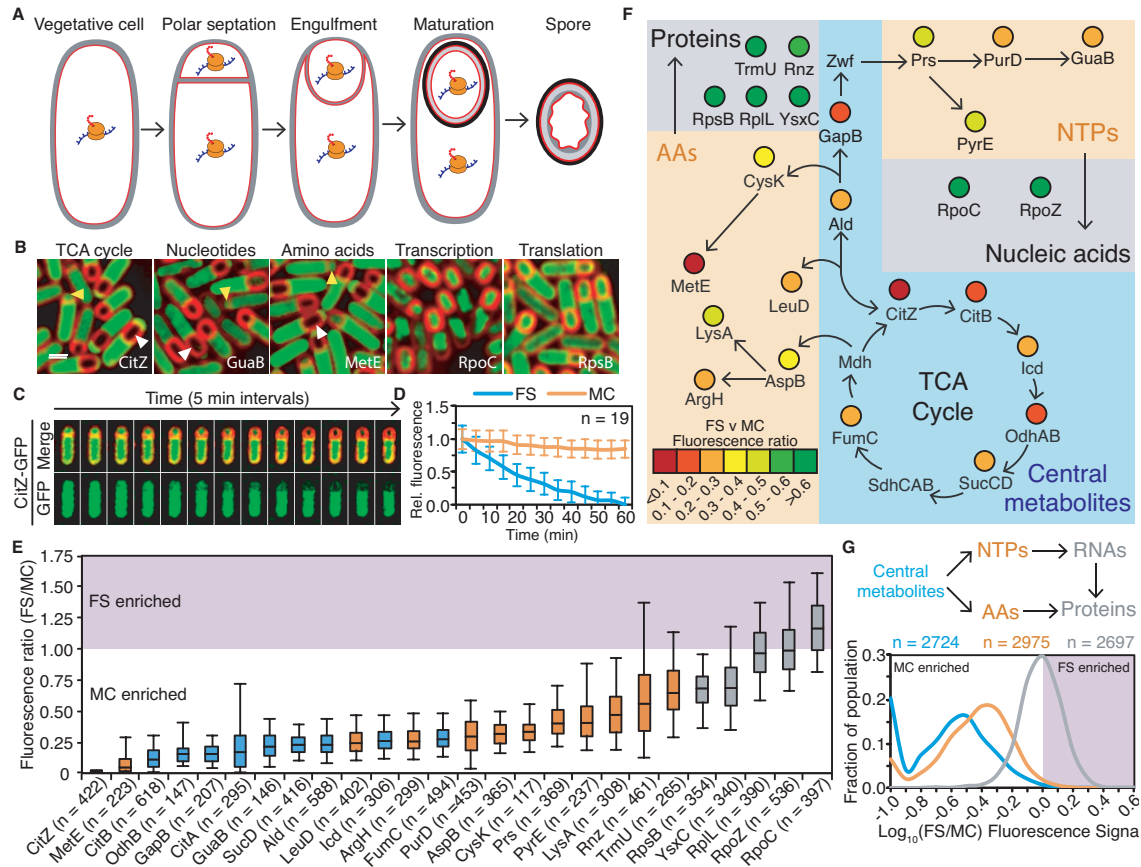


**Figure 3.1.** Metabolic reprogramming during sporulation. **(A)** Sporulation pathway in *Bacillus subtilis*. Membranes, red; spore integuments, gray and black. Active protein synthesis indicated by orange ribosomes. **(B)** Visualization of GFP fusions (green) to representative metabolic proteins. Membranes are in red. Yellow arrowheads denote sporangia that just completed polar septation. White arrowheads mark sporangia that have completed engulfment. Scale bar, 1  $\mu$ m. See fig. S1 for additional examples. **(C)** Timelapse fluorescence microscopy of a sporangium producing CitZ-GFP (green). Membranes are in red. See movie S1 for additional examples. **(D)** CitZ-GFP fluorescence signal in the mother cell (MC, orange) and in the forespore (FS, cyan) over time, relativized to the initial signal at  $t_0$ . Values represent the mean  $\pm$  SD. **(E)** Box and whisker plots showing forespore to mother cell fluorescence ratios for metabolic enzymes functioning in different metabolic pathways. The boxes represent the middle 75% of the data, and the vertical bars the middle 90%. Median values are indicated by the horizontal lines inside the boxes. **(F)** Results from **(E)** superimposed on a metabolic map. **(G)** Histogram of forespore to mother cell fluorescence ratios of the GFP fusions measured in **(E)**, grouped by tier in the metabolic hierarchy (blue, central metabolism; orange, precursor synthesis; gray, final product assembly).

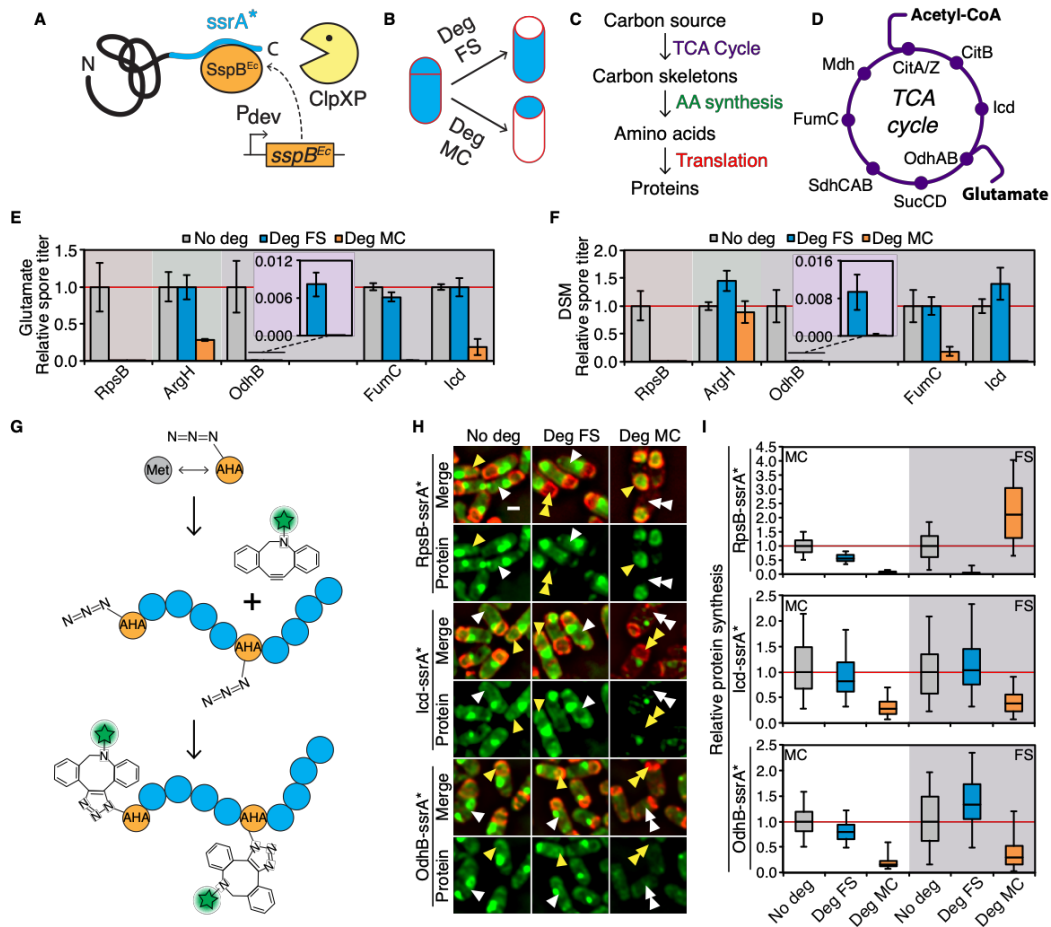


**Figure 3.2.** Intercellular metabolic dependency during sporulation. **(A)** and **(B)** STRP diagram. See main text for details. **(C)** Rationale for identifying cell-specific requirement of different metabolic pathways using STRP. **(D)** Diagram of the TCA cycle. Different carbon inputs indicated in bold. **(E)** and **(F)** Heat-resistant spore titers of strains in which different proteins are tagged with *ssrA\** and not degraded (gray), degraded in the forespore (FS, cyan) or in the mother cell (MC, orange), after sporulation in a glutamate defined medium **(E)** or in a complex medium (DSM) **(F)**. Titters of the non-degradation strains were normalized to one. Data represent the mean  $\pm$  SEM of at least three independent experiments. Insets, zoom of spore titers after cell-specific degradation of *OdhB-ssrA\**. **(G)** Diagram of BONCAT. See details in the main text. **(H)** Fluorescence micrographs of sporangia producing *RpsB-ssrA\**, *Icd-ssrA\** or *OdhB-ssrA\**, in the absence of degradation (No deg), or when degradation is induced in the forespore (Deg FS) or in the mother cell (Deg MC). Newly synthesized proteins (green) have been labeled using BONCAT. Membranes are in red. Representative forespores and mother cells are indicated with yellow and white arrowheads, respectively. Single and double arrowheads indicate high and low levels of protein synthesis, respectively. Scale bar, 1  $\mu$ m. **(I)** Protein synthesis in the mother cell (MC, left, white shading) and in the forespore (FS, right, purple shading) in *RpsB-ssrA\**, *Icd-ssrA\**, or *OdhB-ssrA\** strains, in the absence of degradation (Gray, No deg), or when degradation is induced in the forespore (Blue, Deg FS) or mother cell (Orange, Deg MC). At least 142 sporangia were quantified for each strain. Values were normalized to the median of tagged only strain (indicated by red line). See Fig 1E for description of box and whisker plot.

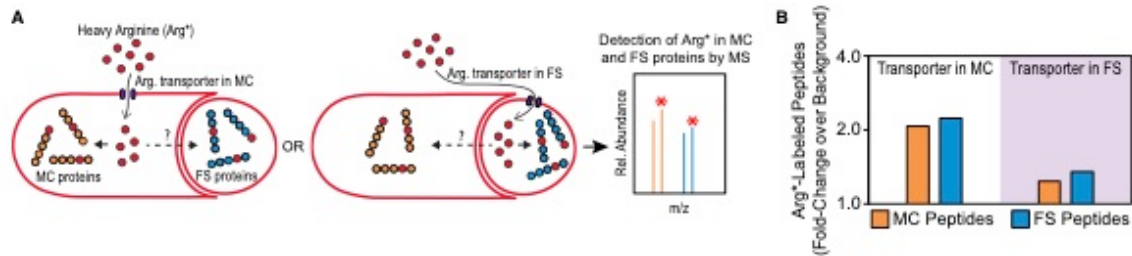


**Figure 3.3.** Arginine is transported between the mother cell (MC) and the forespore (FS). **(A)** Diagram of the cell-specific SILAC approach used to assess intercellular transport of arginine. See main text for details. **(B)** Fraction of mother cell (MC) peptides (orange) and forespore (FS) peptides (blue) containing heavy arginine (Arg\*) when the arginine transporter ArtPQR is produced in the MC (from *spoIIIM* promoter, white shading) or FS (from *spoIIQ* promoter, purple shading), compared to the background incorporation obtained when no arginine transporter is produced. More than 3000 MC and FS peptides were analyzed for every strain.

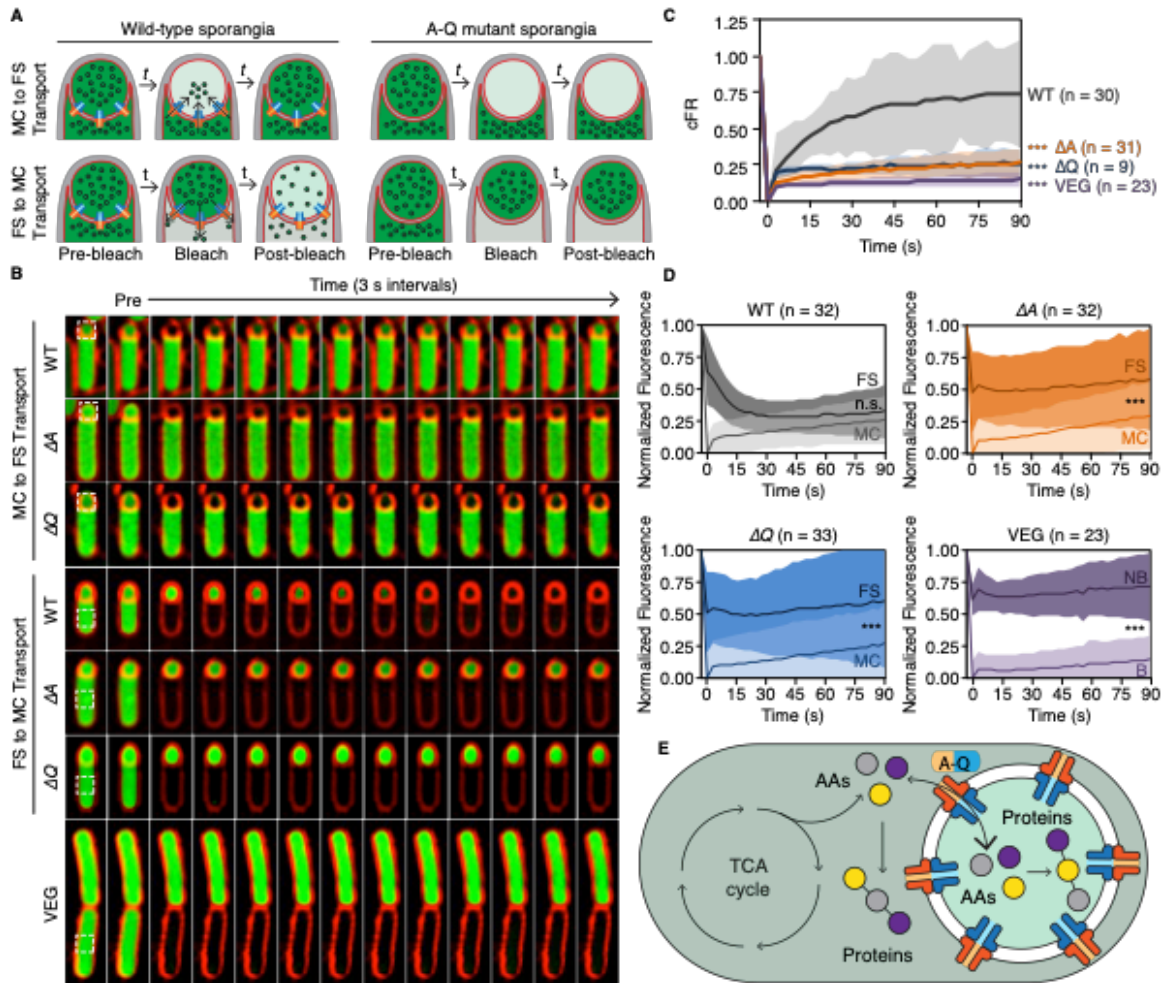


**Figure 3.4.** A-Q is required for transport of small molecules between mother cell and forespore. **(A)** Strategy to assay intercellular transport of small molecules using calcein labeling (green) and photobleaching. See main text for details. **(B)** Photobleaching experiments of calcein-loaded WT,  $\Delta A$  and  $\Delta Q$  sporangia, or vegetative cells (VEG). Photobleached spot indicated by white dotted square. See movies S2-S8 for additional examples. **(C)** Fluorescence recovery of WT (gray),  $\Delta A$  (orange), or  $\Delta Q$  (blue) forespores, or vegetative cells (purple), computed as described in the materials in methods section. The average recoveries of bleached cells are indicated by solid lines and standard deviations are indicated by shaded regions for each strain. The number of cells analyzed ( $n$ ) for each strain is indicated to the right of the graph and unpaired  $t$ -tests were used to determine the statistical significance of the difference between each strain compared to wild type at the final timepoint (\*\*\*,  $P \leq 0.001$ ). **(D)** Fluorescence loss of WT (gray),  $\Delta A$  (orange),  $\Delta Q$  (blue) sporangia, or vegetative cells (VEG) (purple), normalized and corrected as described in the materials and methods. Average fluorescence values of the forespore (dark) and mother cell (light) for each strain are indicated by solid lines and standard deviations are indicated by shaded regions. The number of cells analyzed ( $n$ ) for each strain is indicated above the respective graph and unpaired  $t$ -tests were used to determine the statistical significance of the difference between mother cell and forespore fluorescence values for each strain at the final timepoint (\*\*\*,  $P \leq 0.001$ ). **(E)** Model of metabolic coupling between mother cell and forespore.

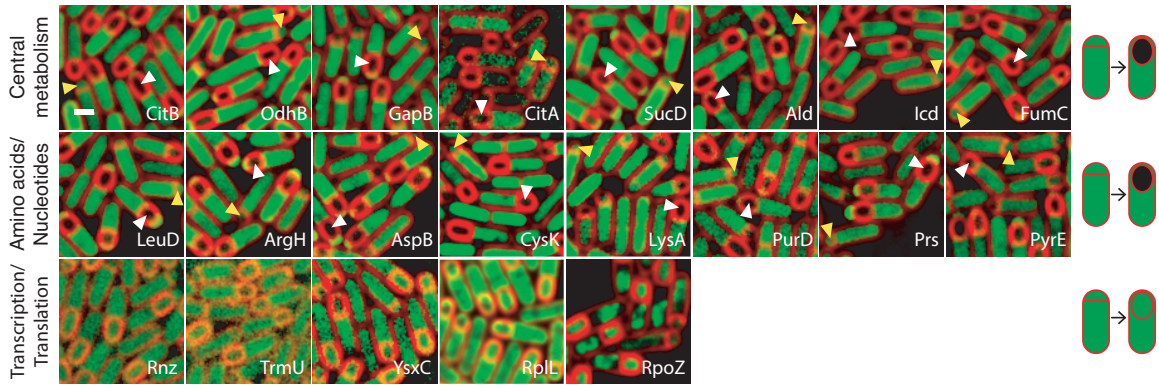


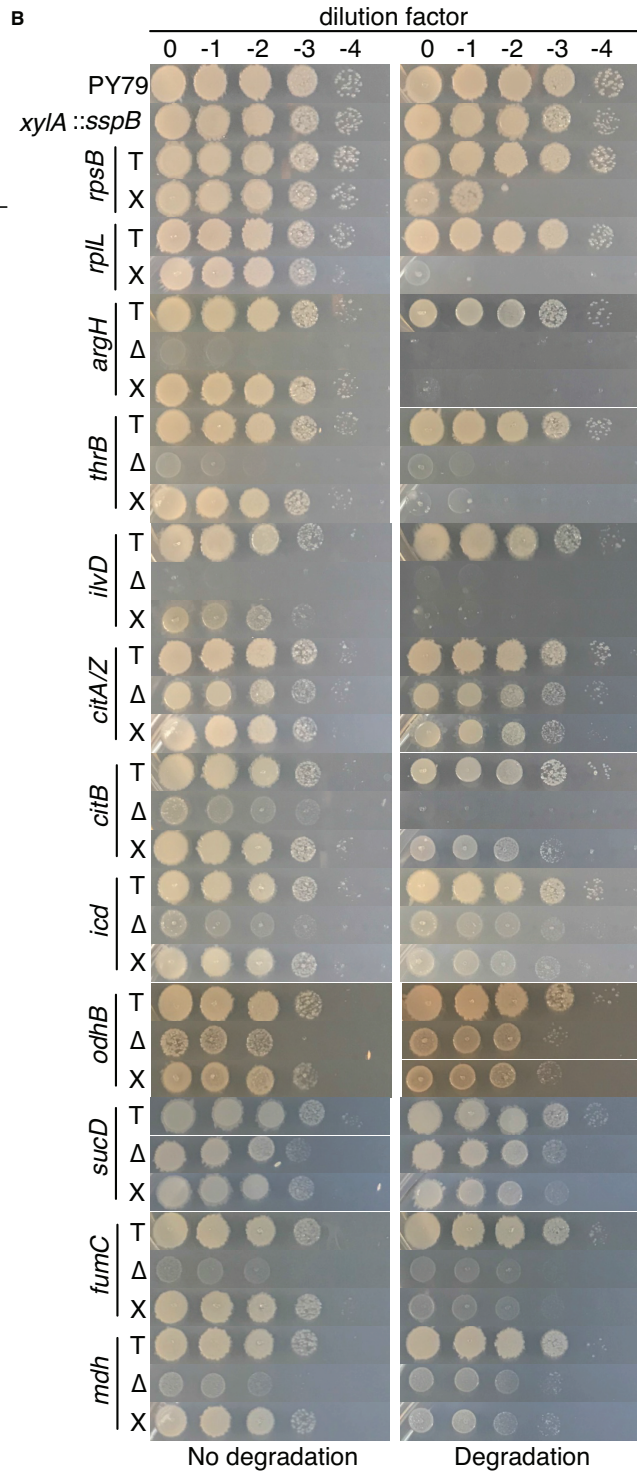
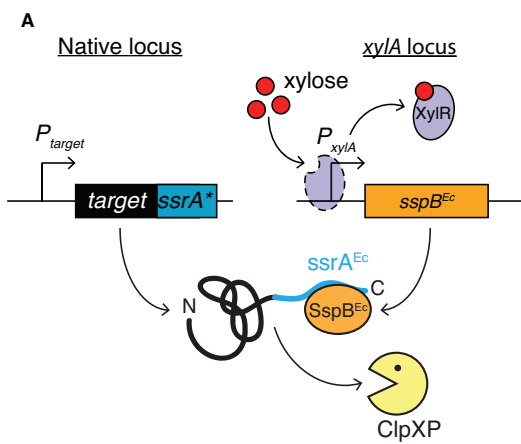
**Figure 3.S1. Metabolic asymmetry during spore formation**

A. Fluorescence micrographs sporangia producing of GFP fusions to metabolic proteins representative of different pathways. Membranes were stained with FM 4-64 (Red). Yellow arrows denote sporangia that have just completed polar septation. White arrows indicate sporangia that have completed engulfment. Scale bar, 1  $\mu$ m. The cartoons at the right illustrate the outcome of proteins in different metabolic categories in the mother cell and the forespore. Proteins involved in central carbon metabolism and synthesis of amino acids and nucleotides tend to disappear in the forespore as sporulation progresses, but are retained in the mother cell. Proteins directly involved in transcription and translation are retained in both cells.

### Figure 3.S2. Validation of *ssrA*\*-tagged protein degradation

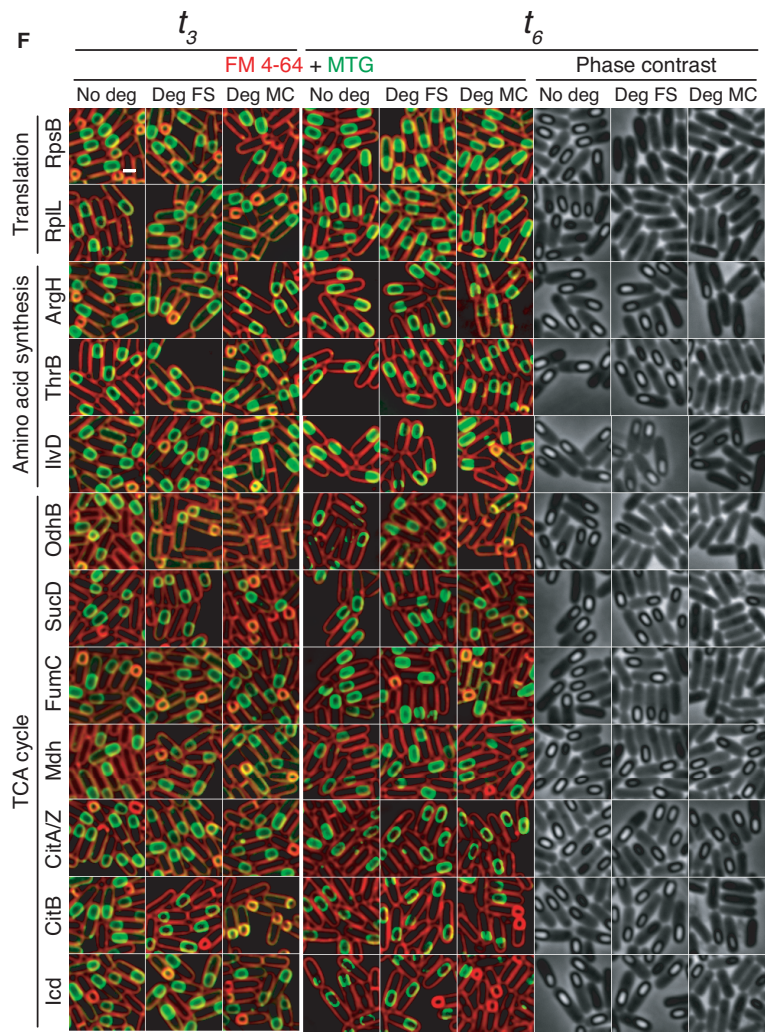
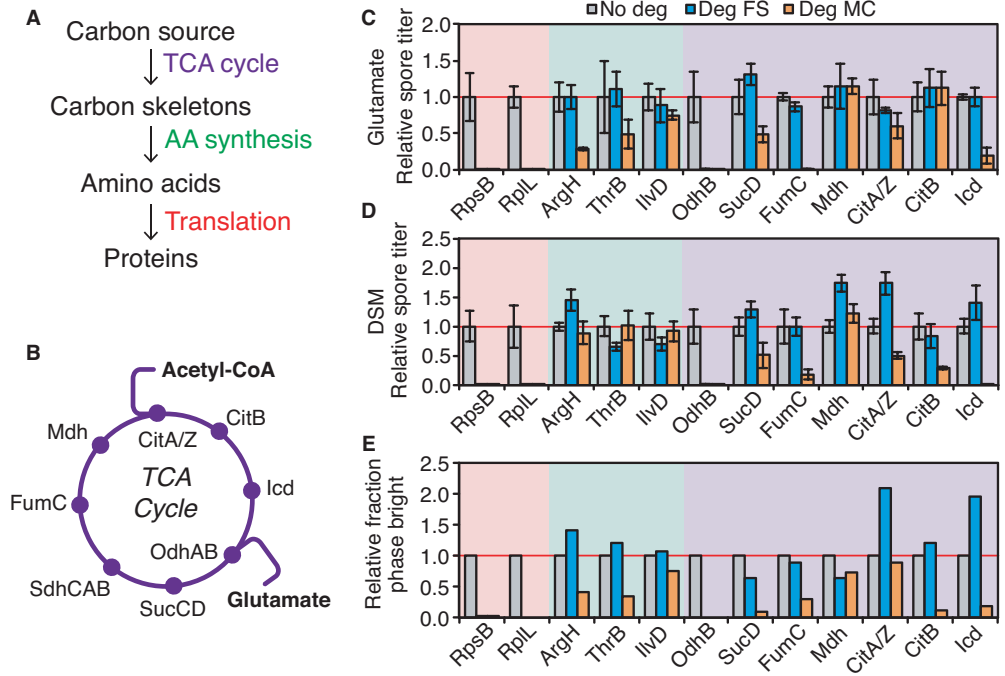
(A) Diagram illustrating xylose-induced protein degradation. The *sspB<sup>Ec</sup>* gene is inserted at the *xylA* locus in the chromosome, whose transcription is xylose-dependent. In the presence of xylose, SspB<sup>Ec</sup> is produced and *ssrA*\*-tagged proteins are delivered to ClpXP for degradation. (B) To determine if the metabolic proteins tagged with *ssrA*\* are efficiently degraded in the presence of SspB<sup>Ec</sup>, we plated spot dilutions of cultures of the different strains in minimal medium containing 1% of arabinose or glucose as carbon source, with or without 0.5% of xylose to induce degradation of the target protein (NOTE1). Although most of the proteins tested are not essential for growth in rich medium, many of them are important for growth in minimal medium. Therefore, strains lacking these proteins exhibit severe growth defects. For each target protein, we analyzed three different strains, denoted with the symbols T, Δ, and X. T, strain in which the indicated protein is tagged with *ssrA*\*, in the absence of xylose-inducible *sspB<sup>Ec</sup>*. Since the gene encoding SspB<sup>Ec</sup> is not present, this strain should grow equally well on plates with and without xylose. Δ, strain in which the gene encoding the indicated protein is deleted. No deletion strains were included for *rpsB* and *rplL*, since both genes are essential for growth in all conditions. X, strain in which the indicated protein is tagged with *ssrA*\*, in the presence of xylose-inducible *sspB<sup>Ec</sup>*. In this strain, the *ssrA*\* tagged protein is not degraded in the absence of xylose, but degradation should be induced in the presence of xylose. In all cases, growth of the X strain was impaired in the presence of xylose, usually to a level that was comparable to the growth of the deletion strain, suggesting that *sspB<sup>Ec</sup>* expression triggered the efficient degradation of the target proteins.

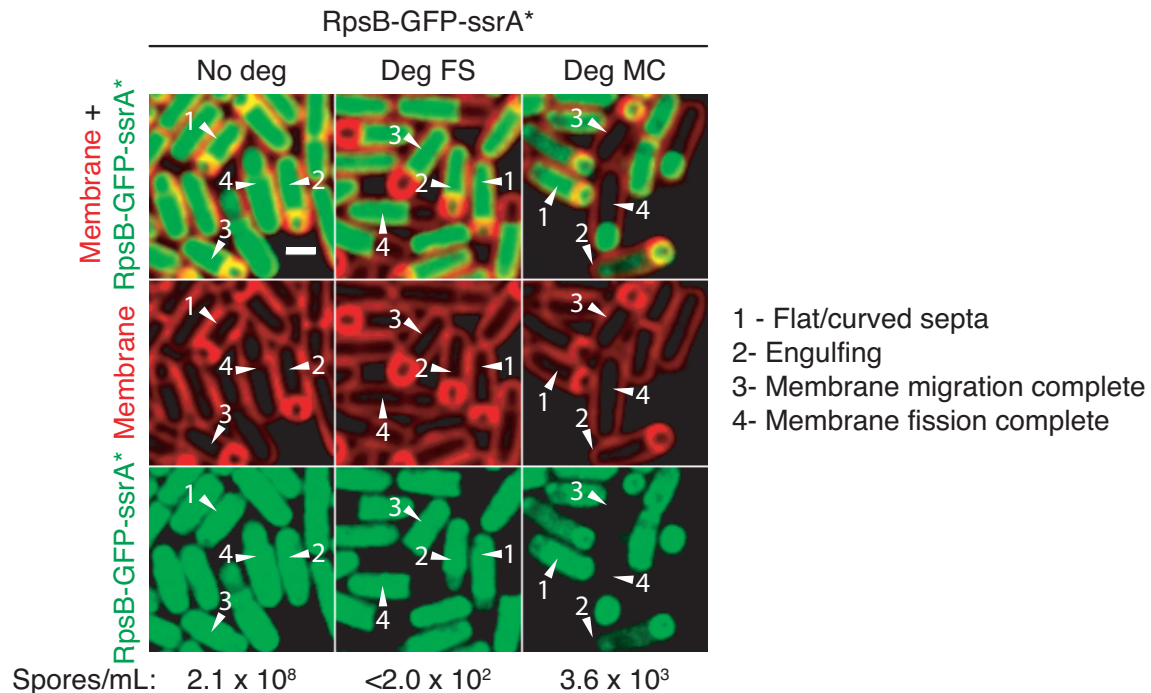




**Figure 3.S3. Cell-specific degradation of all the metabolic proteins tested**

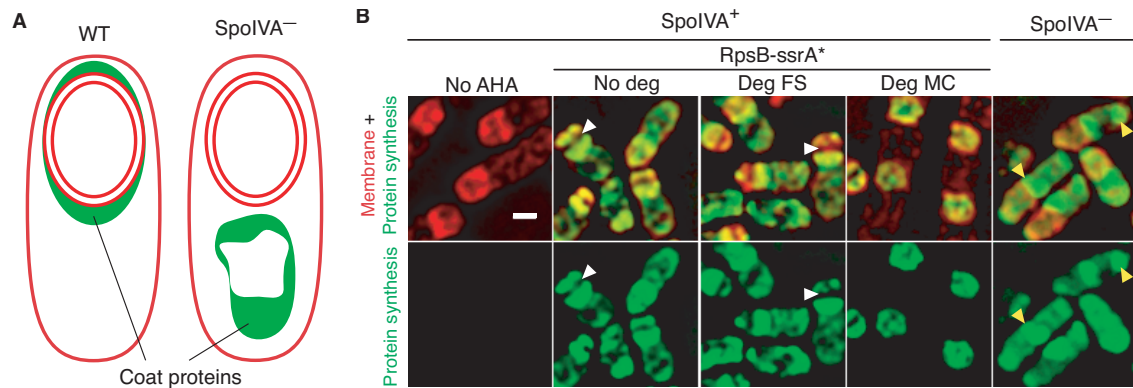
(A) Rationale for identifying cell-specific requirement of different metabolic pathways using STRP. (B) Diagram of the TCA cycle. Different carbon inputs are indicated in bold. (C) and (D) Heat-resistant spore titers of strains in which different proteins are tagged with *ssrA\** and not degraded (gray), degraded in the forespore (FS, cyan) or in the mother cell (MC, orange), after sporulating in a glutamate defined medium (C) or in a complex medium (DSM) (D). Titters of the non-degradation strains were normalized to one. Data represent the mean  $\pm$  SEM of at least three independent experiments. (E) Fraction of phase bright spores six hours after sporulation induction, relative to the wild type, after cell-specific degradation of the indicated *ssrA\**-tagged protein. At least 62 sporangia were analyzed for each strain. (F) Microscopy images of sporangia harboring *ssrA\**-fusions to the designated proteins in the absence of degradation (No deg), or when degradation is induced in the forespore (Deg FS) or in the mother cell (Deg MC). Fluorescence images of cells harvested 3 ( $t_3$ ) and 6 ( $t_6$ ) hours after sporulation induction are shown. Phase contrast microscopy images are only shown for  $t_6$ . Membranes are stained with FM 4-64 (red) and Mitotracker Green (MTG, green). During engulfment, forespore membranes are accessible to both the red and the green dyes. However, after engulfment forespore membranes cannot be stained by the red dye, and are clearly visible as green ovals inside the mother cells. Scale bar, 1  $\mu$ m.





**Figure 3.S4. Visualization of cell-specific degradation of a ribosomal protein**

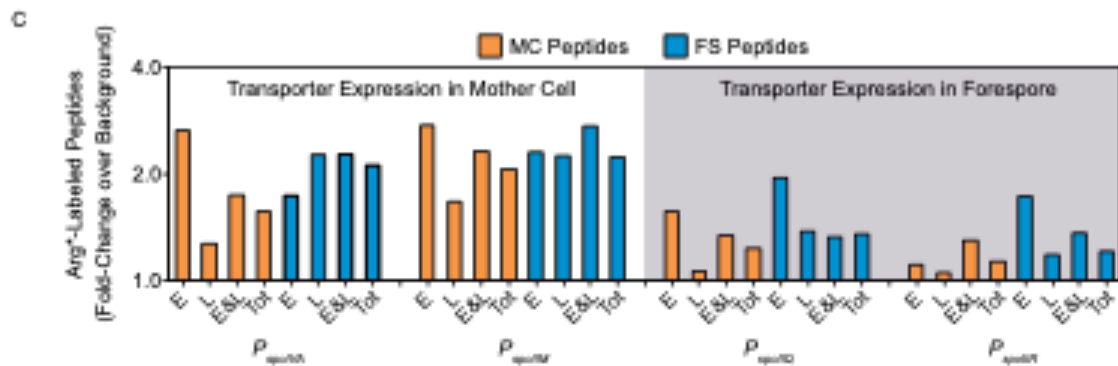
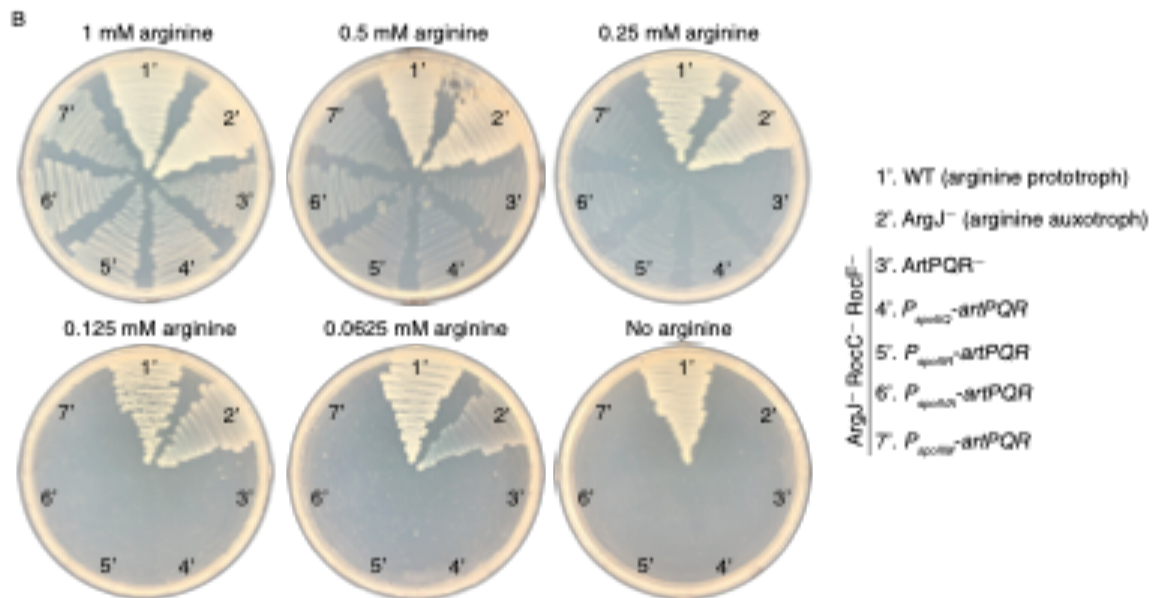
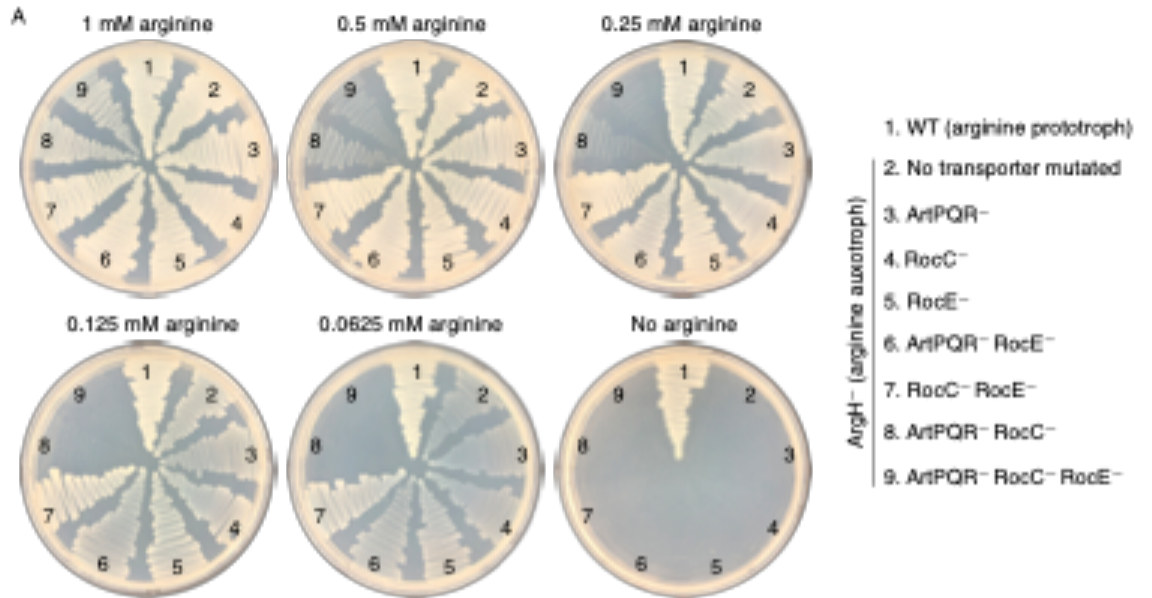
To directly assess the degradation of ribosomal proteins, we tagged the ribosomal protein S2 (RpsB) with GFP and *ssrA\**, and monitored the disappearance of the GFP signal by fluorescence microscopy. In the absence of degradation (No deg), the GFP signal was observed in both the forespore and the mother cell throughout sporulation. However, when degradation was induced in the forespore (Deg FS) or in the mother cell (Deg MC), the GFP signal disappeared in the appropriate cell throughout engulfment. Note that the disappearance of the GFP signal was gradual and some signal was detected until the completion of engulfment, suggesting that translation might not be completely blocked until after engulfment completion. Therefore, we focused on sporangia that have completed engulfment to quantify protein synthesis during BONCAT experiments described in Fig. 2 and Fig. S7. Membranes were stained with FM 4-64 (Red). The numbered arrowheads point at cells at different engulfment stages, with 1 indicating earlier stages and 4 later stages.



**Figure 3.S5. Reasoning for using a SpoIVA<sup>-</sup> mutant in BONCAT experiments**

**(A)** Diagram of the localization of coat proteins in wild-type (WT) sporangia and in sporangia lacking SpoIVA (SpoIVA<sup>-</sup>). Coat proteins are synthesized in the mother cell and localize around the forespore. In SpoIVA<sup>-</sup> mutants, however, coat proteins accumulate in the mother cell cytoplasm. **(B)** Fluorescence micrograph of sporangia in which newly synthesized proteins are fluorescently labeled using BONCAT, in strains containing SpoIVA (SpoIVA<sup>+</sup>) and lacking SpoIVA (SpoIVA<sup>-</sup>). Membranes are in red and newly synthesized proteins in green. The leftmost panel (No AHA) is a control in which newly synthesized proteins are not fluorescently labeled, to ensure specificity of labeling. The three middle panels are images of strains in which the RpsB (ribosomal protein S2) is tagged with *ssrA*<sup>\*</sup>, in the absence of degradation (No deg), when degradation is induced in the forespore (Deg FS) and when degradation is induced in the mother cell (Deg MC). In the absence of degradation, a significant fraction of newly synthesized proteins accumulated around the forespore, making it difficult to determine if they are forespore proteins or mother cell proteins. The bright signal around the forespore remains when RpsB-*ssrA*<sup>\*</sup> is degraded in the forespore, but is greatly reduced when RpsB-*ssrA*<sup>\*</sup> is degraded in the mother cell, suggesting that those proteins are actually synthesized in the mother cell. We reasoned that the bright signal around the forespore could correspond to the accumulation of mother cell-synthesized coat proteins around the forespore. In agreement with this idea, the signal is redistributed as protein clusters throughout the mother cell cytoplasm in sporangia lacking SpoIVA (SpoIVA<sup>-</sup>, rightmost panel). Therefore, to be able to reliably measure protein synthesis in the mother cell and in the forespore, BONCAT experiments were performed in SpoIVA<sup>-</sup> background.

**Figure 3.S6. Cell-specific SILAC experiments** (A) Indicated strains (right) were plated on S7<sub>50</sub> + 1 % glucose medium supplemented with the indicated concentration of L-arginine (above plates) and incubated at 37°C for 72 h, demonstrating the role of ArtPQR, RocC, and RocE in arginine import. (B) Indicated strains (right) were plated on S7<sub>50</sub> + 1 % glucose medium supplemented with the indicated concentration of L-arginine (above plates) and incubated at 37 °C for 72 h, demonstrating that ArtPQR is not produced to appreciable levels during vegetative growth when expressed from promoters active only during sporulation. (C) Fraction of mother cell (MC) peptides (orange) and forespore (FS) peptides (blue) containing heavy arginine (Arg\*) when the arginine transporter ArtPQR is produced in the MC (from *spoIVA* or *spoIIM* promoter, white shading) or FS (from *spoIIQ* or *spoIIR* promoter, purple shading), compared to the background incorporation obtained when no arginine transporter is produced. Peptides are separated into different temporal classes, depending on whether they are synthesized early (E, i.e. only during engulfment), late (L, i.e. only after engulfment completion), or early and late (E & L, i.e. both during and after engulfment) during spore formation. The sum of these three classes (Tot) represents a category encompassing all mother cell or forespore sporulation-specific peptides. More than 3000 MC and FS peptides were analyzed for every strain.



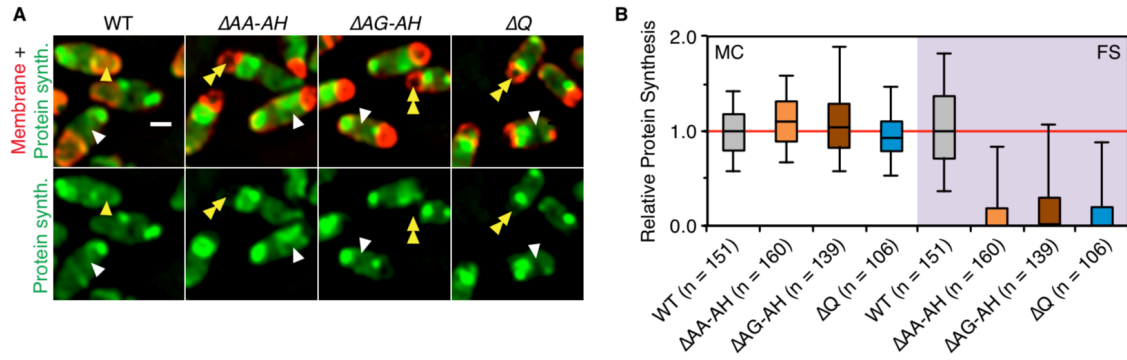


**Figure 3.S7. BONCAT experiments in *spollIA* and *spollQ* mutant sporangia (A)** BONCAT-labeled proteins (green) in WT,  $\Delta A$  and  $\Delta Q$  sporangia. Two different  $\Delta A$  strains were used, one containing a deletion of the entire *spollIA* operon ( $\Delta AA-AH$ ), and another lacking only the last two genes of the *spollIA* operon (*spollIAG* and *spollIAH*,  $\Delta AG-AH$ ). Membranes are in red. Representative forespores and mother cells indicated by yellow and white arrowheads, respectively. Single and double arrowheads, high and low levels of protein synthesis, respectively. Scale bar, 1  $\mu$ m. **(B)** Quantification of newly synthesized proteins in mother cell (MC, left, white shading) and forespore (FS, right, purple shading) from the microscopy shown in **(A)**. Values normalized to median of WT (indicated by red line). See Fig. 1E for description of box and whisker plots. The number of sporangia analyzed for each strain (n) are indicated by the labels in the x-axis.



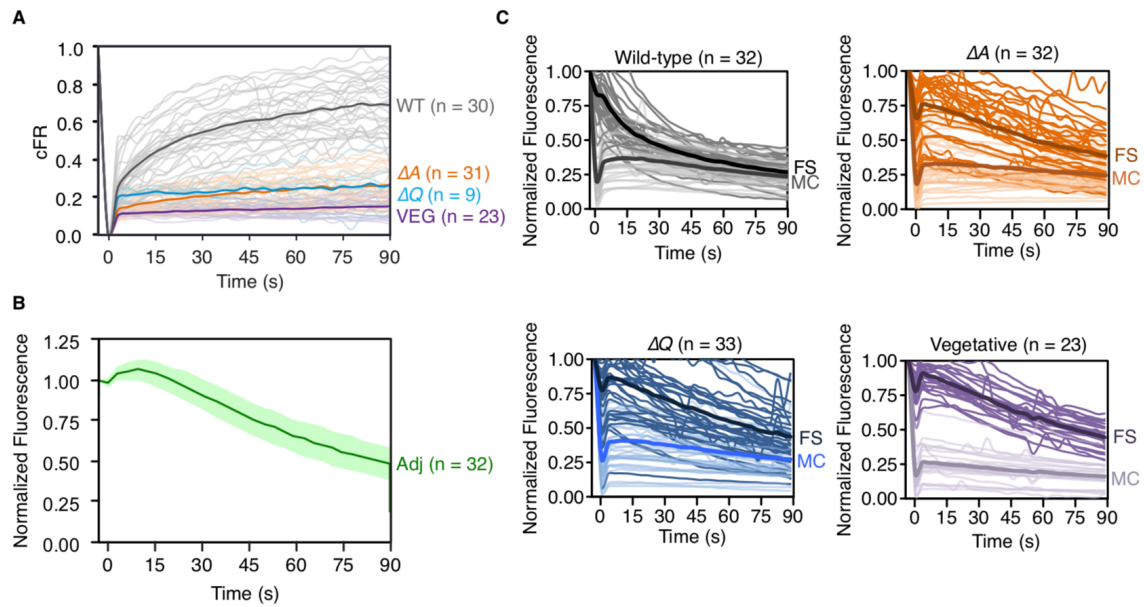


**Figure 3.S8. FLIP and FRAP experiments in *spollIA* and *spollQ* mutant sporangia**

**(A)** Fluorescence recovery of WT (gray),  $\Delta A$  (orange) or  $\Delta Q$  forespores (cyan) sporangia, or vegetative cells (purple). Each light line represents the recovery of a forespore from an individual sporangium. Darker bold lines represent the averages of each data set. The number of cells analyzed for each strain (n) is indicated to the right of the graph. **(B)** Standard curve of fluorescence loss of non-bleached cells caused by repeated imaging. Values are normalized to the pre-bleaching timepoint. The dark green line represents the average loss of fluorescence of 32 cells, and the light green shaded region indicates the standard deviation. **(C)** Non-corrected fluorescence loss of forespores and mother cells of wild-type (gray),  $\Delta A$  (orange),  $\Delta Q$  (blue) sporangia, or vegetative cells (purple). Each line represents the fluorescence loss of an individual forespore (darker lines) or mother cell (lighter lines). Bold lines represent the average of all individual traces for the forespore (darker) or mother cell (lighter) of each respective strain. All values were normalized to the pre-bleaching timepoint. Number of cells analyzed for each strain (n) is indicated above the graph. The curve in **(B)** was used to correct these values for fluorescence loss caused by repeated imaging, rather than intercellular transport.

Tables

Table 3.S1. Spore titers				
Tagged Protein	Degradation	Strain No.	Glutamate medium (spores/mL)	Complex medium (spores/mL)
RpsB	None	BER0621	$5.83 \times 10^8$	$2.10 \times 10^8$
	FS	BER0774	$1.60 \times 10^3$	$5.27 \times 10^3$
	MC	BER0773	$2.70 \times 10^4$	$1.56 \times 10^5$
RplL	None	BER0478	$2.93 \times 10^8$	$2.50 \times 10^8$
	FS	BER0780	$2.50 \times 10^3$	$2.37 \times 10^3$
	MC	BER0779	$5.57 \times 10^3$	$5.67 \times 10^5$
ArgH	None	BER0911	$4.12 \times 10^8$	$2.47 \times 10^8$
	FS	BER0946	$4.11 \times 10^8$	$3.57 \times 10^8$
	MC	BER0945	$1.17 \times 10^8$	$2.20 \times 10^8$
ThrB	None	BER1160	$2.85 \times 10^8$	$4.23 \times 10^8$
	FS	BER1177	$3.15 \times 10^8$	$2.77 \times 10^8$
	MC	BER1176	$1.40 \times 10^8$	$4.30 \times 10^8$
IivD	None	BER1182	$5.10 \times 10^8$	$3.20 \times 10^8$
	FS	BER1193	$4.50 \times 10^8$	$2.23 \times 10^8$
	MC	BER1192	$3.83 \times 10^8$	$2.93 \times 10^8$
OdhB	None	JLG1701	$5.53 \times 10^8$	$1.53 \times 10^8$
	FS	JLG1742	$4.53 \times 10^6$	$1.43 \times 10^6$
	MC	JLG1743	$3.43 \times 10^3$	$9.23 \times 10^3$
SucD	None	JLG1950	$1.71 \times 10^8$	$1.15 \times 10^8$
	FS	JLG2003	$2.24 \times 10^8$	$1.48 \times 10^8$
	MC	JLG2020	$8.27 \times 10^7$	$5.87 \times 10^7$
FumC	None	JLG1946	$4.67 \times 10^8$	$3.30 \times 10^8$
	FS	JLG1980	$4.03 \times 10^8$	$3.13 \times 10^8$
	MC	JLG2016	$6.17 \times 10^6$	$7.38 \times 10^7$
Mdh	None	JLG1947	$1.60 \times 10^8$	$7.63 \times 10^7$
	FS	JLG1981	$1.83 \times 10^8$	$1.33 \times 10^8$
	MC	JLG2017	$1.83 \times 10^8$	$9.33 \times 10^7$
CitZ ( $\Delta$ CitA)	None	BER0611	$3.03 \times 10^8$	$2.40 \times 10^8$
	FS	BER0618	$2.47 \times 10^8$	$4.17 \times 10^8$
	MC	BER0613	$1.82 \times 10^8$	$1.21 \times 10^8$
CitB	None	JLG1945	$5.90 \times 10^8$	$4.00 \times 10^8$
	FS	JLG1979	$6.63 \times 10^8$	$3.33 \times 10^8$
	MC	JLG2015	$6.60 \times 10^8$	$1.17 \times 10^8$
Icd	None	JLG1953	$3.90 \times 10^8$	$2.40 \times 10^8$
	FS	JLG2006	$3.90 \times 10^8$	$3.37 \times 10^8$
	MC	JLG2023	$7.47 \times 10^7$	$3.10 \times 10^4$

<b>Table 3.S2. Strains used in this study</b>		
<b>Strain</b>	<b>Genotype or description</b>	<b>Reference, source or construction<sup>a</sup></b>
PY79	Wild type	(Youngman et al., 1984)
BER1058	$\Delta$ spolIIAG-AH::kan $\Delta$ sigG::tet spolVA::Tn917 $\Omega$ erm	KP896→BER912 (Km)
BER1059	$\Delta$ spolIIAA-AH::kan $\Delta$ sigG::tet spolVA::Tn917 $\Omega$ erm	KP899→BER912 (Km)
BER1062	<i>icd-ssrA</i> * $\Omega$ kan $\Delta$ sigG::tet	BER888→JLG1953 (Tc)
BER1063	<i>icd-ssrA</i> * $\Omega$ kan <i>amyE</i> ::PsspE(2G)-sspB <sup>E<sub>c</sub></sup> $\Omega$ cat $\Delta$ sigG::tet	BER888→JLG2006 (Tc)
BER1064	<i>icd-ssrA</i> * $\Omega$ kan <i>pelB</i> ::PcotE-sspB <sup>E<sub>c</sub></sup> $\Omega$ spc $\Delta$ sigG::tet	BER888→JLG2023 (Tc)
BER1066	<i>icd-ssrA</i> * $\Omega$ kan $\Delta$ sigG::tet spolVA::Tn917 $\Omega$ erm	KP89→BER1062 (MLS)
BER1067	<i>icd-ssrA</i> * $\Omega$ kan <i>amyE</i> ::PsspE(2G)-sspB <sup>E<sub>c</sub></sup> $\Omega$ cat $\Delta$ sigG::tet spolVA::Tn917 $\Omega$ erm	KP89→BER1063 (MLS)
BER1068	<i>icd-ssrA</i> * $\Omega$ kan <i>pelB</i> ::PcotE-sspB <sup>E<sub>c</sub></sup> $\Omega$ spc $\Delta$ sigG::tet spolVA::Tn917 $\Omega$ erm	KP89→BER1064 (MLS)
BER1081	<i>rpsB-ssrA</i> * $\Omega$ kan spolVA::Tn917 $\Omega$ erm	KP89→BER621 (MLS)
BER1082	<i>rpsB-ssrA</i> * $\Omega$ kan <i>pelB</i> ::PcotE-sspB <sup>E<sub>c</sub></sup> $\Omega$ spc spolVA::Tn917 $\Omega$ erm	KP89→BER773 (MLS)
BER1083	<i>rpsB-ssrA</i> * $\Omega$ kan <i>amyE</i> ::PsspE(2G)- sspB <sup>E<sub>c</sub></sup> $\Omega$ cat spolVA::Tn917 $\Omega$ erm	KP89→BER774 (MLS)
BER1088	<i>rpsB-ssrA</i> * $\Omega$ kan $\Delta$ sigG::tet spolVA::Tn917 $\Omega$ erm	BER888→BER1081 (Tc)
BER1089	<i>rpsB-ssrA</i> * $\Omega$ kan <i>pelB</i> ::PcotE-sspB <sup>E<sub>c</sub></sup> $\Omega$ spc $\Delta$ sigG::tet spolVA::Tn917 $\Omega$ erm	BER888→BER1082 (Tc)
BER1090	<i>rpsB-ssrA</i> * $\Omega$ kan <i>amyE</i> ::PsspE(2G)- sspB <sup>E<sub>c</sub></sup> $\Omega$ cat $\Delta$ sigG::tet spolVA::Tn917 $\Omega$ erm	BER888→BER1083 (Tc)
BER1091	<i>guaB</i> -GFP $\Omega$ kan	pER261→PY79 (Km)
BER1093	<i>pyrE</i> -GFP $\Omega$ kan	pER263→PY79 (Km)
BER1094	<i>purD</i> -GFP $\Omega$ kan	pER264→PY79 (Km)
BER1095	<i>rpoZ</i> -GFP $\Omega$ kan	pER265→PY79 (Km)
BER1097	<i>lysA</i> -GFP $\Omega$ kan	pER267→PY79 (Km)
BER1098	<i>metE</i> -GFP $\Omega$ kan	pER268→PY79 (Km)
BER1099	<i>cysK</i> -GFP $\Omega$ kan	pER269→PY79 (Km)
BER1100	<i>aspB</i> -GFP $\Omega$ kan	pER270→PY79 (Km)
BER1101	<i>leuD</i> -GFP $\Omega$ kan	pER271→PY79 (Km)
BER1102	<i>argH</i> -GFP $\Omega$ kan	pER272→PY79 (Km)
BER1103	<i>rplL</i> -GFP $\Omega$ kan	pER273→PY79 (Km)
BER1104	<i>ysxC</i> -GFP $\Omega$ kan	pER274→PY79 (Km)
BER1106	<i>rnz</i> -GFP $\Omega$ kan	pER276→PY79 (Km)
BER1107	<i>gapB</i> -GFP $\Omega$ kan	pER277→PY79 (Km)
BER1110	<i>prs</i> -GFP $\Omega$ kan	pER280→PY79 (Km)
BER1112	<i>ald</i> -GFP $\Omega$ kan	pER282→PY79 (Km)
BER1113	<i>trmU</i> -GFP $\Omega$ kan	pER283→PY79 (Km)
BER1160	<i>thrB-ssrA</i> * $\Omega$ kan	pR288→PY79 (Km)
BER1162	$\Delta$ <i>thrB</i> ::tet	pER290→PY79 (Tc)

<b>Table 3.S2. Strains used in this study (continued)</b>		
<b>Strain</b>	<b>Genotype or description</b>	<b>Reference, source or construction<sup>a</sup></b>
BER1166	<i>thrB-ssrA*Ωkan ΔxylA::sspB<sup>Ec</sup>Ωcat</i>	BER1160→JLG364 (Km)
BER1176	<i>thrB-ssrA*Ωkan pelB::PcotE-sspB<sup>Ec</sup>Ωspc</i>	BER1160→BER131 (Km)
BER1177	<i>thrB-ssrA*Ωkan amyE::PsspE(2G)-sspB<sup>Ec</sup>Ωcat</i>	BER1160→JLG963 (Km)
BER1182	<i>ilvD-ssrA*Ωkan</i>	pER299→PY79 (Km)
BER1184	<i>ΔilvD::tet</i>	pER298→PY79 (Km)
BER1187	<i>ilvD-ssrA*Ωkan ΔxylA::sspB<sup>Ec</sup>Ωcat</i>	BER1182→JLG364 (Km)
BER1192	<i>ilvD-ssrA*Ωkan pelB::PcotE-sspB<sup>Ec</sup>Ωspc</i>	BER1182→BER131 (Km)
BER1193	<i>ilvD-ssrA*Ωkan amyE::PsspE(2G)-sspB<sup>Ec</sup>Ωcat</i>	BER1182→JLG963 (Km)
BER131	<i>pelB::PcotE-sspB<sup>Ec</sup>Ωspc</i>	(Riley et al., 2018)
BER478	<i>rplL-ssrA*Ωkan</i>	pER64→PY79 (Km)
BER548	<i>ΔodhAB::tet</i>	pER123→PY79 (Tc)
BER607	<i>citZ-ssrA*</i>	pCrePA→JLG1952 (Em)
BER611	<i>citZ-ssrA* ΔcitA::kan</i>	JLG1928→BER607 (Km)
BER613	<i>citZ-ssrA* ΔcitA::kan pelB::PcotE-sspB<sup>Ec</sup>Ωspc</i>	BER131→BER611 (Sp)
BER618	<i>citZ-ssrA* ΔcitA::kan amyE::PsspE(2G)-sspB<sup>Ec</sup>Ωcat</i>	JLG963→BER611 (Cm)
BER621	<i>rpsB-ssrA*Ωkan</i>	pER143→PY79 (Km)
BER749	<i>rpsB-ssrA*Ωkan ΔxylA::sspB<sup>Ec</sup>Ωcat</i>	BER621→JLG364 (Km)
BER751	<i>rplL-ssrA*Ωkan ΔxylA::sspB<sup>Ec</sup>Ωcat</i>	BER478→JLG364 (Km)
BER773	<i>rpsB-ssrA*Ωkan pelB::PcotE-sspB<sup>Ec</sup>Ωspc</i>	BER621→BER131 (Km)
BER774	<i>rpsB-ssrA*Ωkan amyE::PsspE(2G)-sspB<sup>Ec</sup>Ωcat</i>	BER621→JLG963 (Km)
BER779	<i>rplL-ssrA*Ωkan pelB::PcotE-sspB<sup>Ec</sup>Ωspc</i>	BER478→BER131 (Km)
BER780	<i>rplL-ssrA*Ωkan amyE::PsspE(2G)-sspB<sup>Ec</sup>Ωcat</i>	BER478→JLG963 (Km)
BER849	<i>ΔargH::tet</i>	pER183→PY79 (Tc)
BER858	<i>odhB-ssrA*Ωkan spoIVA::Tn917Ωerm</i>	KP89→JLG1701 (MLS)
BER859	<i>odhB-ssrA*Ωkan pelB::PcotE-sspB<sup>Ec</sup>Ωspc spoIVA::Tn917Ωerm</i>	KP89→JLG1743 (MLS)
BER860	<i>odhB-ssrA*Ωkan amyE::PsspE(2G)-sspB<sup>Ec</sup>Ωcat spoIVA::Tn917Ωerm</i>	KP89→JLG1742 (MLS)
BER888	<i>ΔsigG::tet</i>	pER187→RP189
BER896	<i>odhB-ssrA*Ωkan ΔsigG::tet spoIVA::Tn917Ωerm</i>	BER888→BER858 (Tc)
BER897	<i>odhB-ssrA*Ωkan pelB::PcotE-sspB<sup>Ec</sup>Ωspc ΔsigG::tet spoIVA::Tn917Ωerm</i>	BER888→BER859 (Tc)
BER898	<i>odhB-ssrA*Ωkan amyE::PsspE(2G)-sspB<sup>Ec</sup>Ωcat ΔsigG::tet spoIVA::Tn917Ωerm</i>	BER888→BER860 (Tc)
BER904	<i>ΔspollQ::erm ΔsigG::tet</i>	BER888→JLG626
BER911	<i>argH-ssrA*Ωkan</i>	pER195→PY79 (Km)
BER912	<i>ΔsigG::tet spoIVA::Tn917Ωerm</i>	KP89→BER888 (MLS)
BER913	<i>ΔspollQ::erm ΔsigG::tet spoIVA::Tn917Ωerm</i>	KP89→BER904 (MLS)
BER934	<i>argH-ssrA*Ωkan ΔxylA::sspB<sup>Ec</sup>Ωcat</i>	BER911→JLG364 (Km)
BER945	<i>argH-ssrA*Ωkan pelB::PcotE-sspB<sup>Ec</sup>Ωspc</i>	BER911→BER131 (Km)

<b>Table 3.S2. Strains used in this study (continued)</b>		
<b>Strain</b>	<b>Genotype or description</b>	<b>Reference, source or construction<sup>a</sup></b>
BER946	<i>argH-ssrA*Ωkan amyE::PsspE(2G)-sspB<sup>Ec</sup>Ωcat</i>	BER911→JLG963 (Km)
BER947	<i>pelB::PcotE-sspB<sup>Ec</sup>Ωspc amyE::PsspE(2G)-sspB<sup>Ec</sup>Ωcat argH-ssrA*Ωkan</i>	BER911→BER174 (Km)
BER961	<i>citB-GFPΩkan</i>	pER217→PY79 (Km)
BER969	<i>ΔcitZ::tet</i>	pER220→PY79 (Tc)
BER970	<i>ΔcitZ::tet ΔcitA::kan</i>	BER969→JLG1928 (Tc)
BER990	<i>rpoC-GFPΩkan</i>	pER227→PY79 (Km)
BER991	<i>rpsB-GFPΩkan</i>	(Lopez-Garrido et al., 2018)
BER1246	<i>ΔrocDEF::erm</i>	pER312→PY79 (Em)
BER1256	<i>ΔargJ::kan</i>	pER314→PY79 (Km)
BER1271	<i>ΔargJ</i>	pCrePA→BER1256
JLG1701	<i>odhB-ssrA*Ωkan</i>	pJLG256→PY79 (Km)
JLG1730	<i>odhB-ssrA*Ωkan ΔxylA::sspB<sup>Ec</sup>Ωcat</i>	JLG1701→JLG364 (Km)
JLG1742	<i>odhB-ssrA*Ωkan amyE::PsspE(2G)-sspB<sup>Ec</sup>Ωcat</i>	JLG1701→JLG963 (Km)
JLG1743	<i>odhB-ssrA*Ωkan pelB::PcotE-sspB<sup>Ec</sup>Ωspc</i>	JLG1701→BER131 (Km)
JLG1928	<i>ΔcitA::kan</i>	pJLG302→PY79 (Km)
JLG1929	<i>ΔcitB::kan</i>	pJLG303→PY79 (Km)
JLG1930	<i>ΔfumC::kan</i>	pJLG304→PY79 (Km)
JLG1931	<i>Δmdh::kan</i>	pJLG305→PY79 (Km)
JLG1933	<i>ΔsucD::kan</i>	pJLG307→PY79 (Km)
JLG1934	<i>Δicd::kan</i>	pJLG308→PY79 (Km)
JLG1945	<i>citB-ssrA*Ωkan</i>	pJLG319→PY79 (Km)
JLG1946	<i>fumC-ssrA*Ωkan</i>	pJLG320→PY79 (Km)
JLG1947	<i>mdh-ssrA*Ωkan</i>	pJLG312→PY79 (Km)
JLG1950	<i>sucD-ssrA*Ωkan</i>	pJLG324→PY79 (Km)
JLG1952	<i>citZ-ssrA*Ωkan</i>	pJLG326→PY79 (Km)
JLG1953	<i>icd-ssrA*Ωkan</i>	pJLG327→PY79 (Km)
JLG1962	<i>citB-ssrA*Ωkan ΔxylA::sspB<sup>Ec</sup>Ωcat</i>	JLG1945→JLG364 (Km)
JLG1963	<i>fumC-ssrA*Ωkan ΔxylA::sspB<sup>Ec</sup>Ωcat</i>	JLG1946→JLG364 (Km)
JLG1964	<i>mdh-ssrA*Ωkan ΔxylA::sspB<sup>Ec</sup>Ωcat</i>	JLG1947→JLG364 (Km)
JLG1967	<i>sucD-ssrA*Ωkan ΔxylA::sspB<sup>Ec</sup>Ωcat</i>	JLG1950→JLG364 (Km)
JLG1970	<i>icd-ssrA*Ωkan ΔxylA::sspB<sup>Ec</sup>Ωcat</i>	JLG1953→JLG364 (Km)
JLG1979	<i>citB-ssrA*Ωkan amyE::PsspE(2G)-sspB<sup>Ec</sup>Ωcat</i>	JLG1945→JLG963 (Km)
JLG1980	<i>fumC-ssrA*Ωkan amyE::PsspE(2G)-sspB<sup>Ec</sup>Ωcat</i>	JLG1946→JLG963 (Km)
JLG1981	<i>mdh-ssrA*Ωkan amyE::PsspE(2G)-sspB<sup>Ec</sup>Ωcat</i>	JLG1947→JLG963 (Km)
JLG2003	<i>sucD-ssrA*Ωkan amyE::PsspE(2G)-sspB<sup>Ec</sup>Ωcat</i>	JLG1950→JLG963 (Km)
JLG2006	<i>icd-ssrA*Ωkan amyE::PsspE(2G)-sspB<sup>Ec</sup>Ωcat</i>	JLG1953→JLG963 (Km)
JLG2015	<i>citB-ssrA*Ωkan pelB::PcotE-sspB<sup>Ec</sup>Ωspc</i>	JLG1945→BER131 (Km)
JLG2016	<i>fumC-ssrA*Ωkan pelB::PcotE-sspB<sup>Ec</sup>Ωspc</i>	JLG1946→BER131 (Km)
JLG2017	<i>mdh-ssrA*Ωkan pelB::PcotE-sspB<sup>Ec</sup>Ωspc</i>	JLG1947→BER131 (Km)

<b>Table 3.S2. Strains used in this study (continued)</b>		
<b>Strain</b>	<b>Genotype or description</b>	<b>Reference, source or construction<sup>a</sup></b>
JLG2020	<i>sucD-ssrA*Ωkan pelB::PcotE-sspB<sup>Ec</sup>Ωspc</i>	JLG1950→BER131 (Km)
JLG2023	<i>icd-ssrA*Ωkan pelB::PcotE-sspB<sup>Ec</sup>Ωspc</i>	JLG1953→BER131 (Km)
JLG2107	<i>odhB-GFPΩkan</i>	pJLG335→PY79 (Km)
JLG2108	<i>citA-GFPΩkan</i>	pJLG336→PY79 (Km)
JLG2109	<i>fumC-GFPΩkan</i>	pJLG337→PY79 (Km)
JLG2111	<i>sucD-GFPΩkan</i>	pJLG339→PY79 (Km)
JLG2113	<i>citZ-GFPΩkan</i>	pJLG341→PY79 (Km)
JLG2114	<i>icd-GFPΩkan</i>	pJLG342→PY79 (Km)
JLG2807	<i>ΔrocABC::kan</i>	pJLG408→PY79 (Km)
JLG2808	<i>ΔrocABC::cat</i>	pJLG409→PY79 (Cm)
JLG2811	<i>ΔartPQR::kan</i>	pJLG413→PY79 (Km)
JLG2881	<i>ΔartPQR::kan ΔargH::tet</i>	JLG2811→BER849 (Km)
JLG2901	<i>ΔrocABC::cat ΔargH::tet</i>	JLG2808→BER849 (Cm)
JLG2902	<i>ΔrocDEF::erm ΔargH::tet</i>	BER1246→BER849 (Em)
JLG2930	<i>ΔartPQR::kan ΔargH::tet ΔrocABC::cat</i>	JLG2808→JLG2881 (Cm)
JLG2931	<i>ΔrocABC::cat ΔargH::tet ΔrocDEF::erm</i>	BER1246→JLG2901 (Em)
JLG2935	<i>ΔrocDEF::erm ΔargH::tet ΔartPQR::kan</i>	JLG2811→JLG2902 (Km)
JLG2939	<i>ΔrocABC::cat ΔargH::tet ΔrocDEF::erm ΔartPQR::kan</i>	JLG2811→JLG2931 (Km)
JLG2947	<i>ΔargJ ΔrocDEF::erm</i>	BER1246→BER1271 (Em)
JLG2949	<i>ΔargJ ΔrocDEF::erm ΔrocABC::cat</i>	JLG2808→JLG2947 (Cm)
JLG2951	<i>ΔargJ ΔrocDEF::erm ΔrocABC::cat ΔartPQR::kan</i>	JLG2811→JLG2949 (Km)
JLG2956	<i>pelB::PcotE-sspBΩSp amyE::PsspE(2G)-sspBΩCm argH-ssrA*</i>	pCrePA→BER947
JLG2970	<i>PspolIQ-artPQRΩtet</i>	pJLG455→PY79 (Tc)
JLG2971	<i>PspolIR-artPQRΩtet</i>	pJLG456→PY79 (Tc)
JLG2974	<i>PspolVA-artPQRΩtet</i>	pJLG466→PY79 (Tc)
JLG2975	<i>PspolIM-artPQRΩtet</i>	pJLG459→PY79 (Tc)
JLG2976	<i>ΔartPQR::tet</i>	pJLG460→PY79 (Tc)
JLG3017	<i>pelB::PcotE-sspB<sup>Ec</sup>Ωspc amyE::PsspE(2G)-sspB<sup>Ec</sup>Ωcat argH-ssrA* ΔrocABC::kan</i>	JLG2807→JLG2956 (Km)
JLG3028	<i>pelB::PcotE-sspB<sup>Ec</sup>Ωspc amyE::PsspE(2G)-sspB<sup>Ec</sup>Ωcat argH-ssrA* ΔrocABC::cat ΔrocDEF::erm</i>	BER1246→JLG3017 (Em)
JLG3043	<i>pelB::PcotE-sspB<sup>Ec</sup>Ωspc amyE::PsspE(2G)-sspB<sup>Ec</sup>Ωcat argH-ssrA* ΔrocABC::kan ΔrocDEF::erm ΔartPQR::tet</i>	JLG2976→JLG3028 (Tc)

<b>Table 3.S2. Strains used in this study (continued)</b>		
<b>Strain</b>	<b>Genotype or description</b>	<b>Reference, source or construction<sup>a</sup></b>
JLG3044	<i>pelB::PcotE-sspB<sup>Ec</sup>Ωspc amyE::PsspE(2G)-sspB<sup>Ec</sup>Ωcat argH-ssrA* ΔrocABC::kan ΔrocDEF::erm PspollQ-artPQRΩtet</i>	JLG2970→JLG3028 (Tc)
JLG3045	<i>pelB::PcotE-sspB<sup>Ec</sup>Ωspc amyE::PsspE(2G)-sspB<sup>Ec</sup>Ωcat argH-ssrA* ΔrocABC::kan ΔrocDEF::erm PspollR-artPQRΩtet</i>	JLG2971→JLG3028 (Tc)
JLG3046	<i>pelB::PcotE-sspB<sup>Ec</sup>Ωspc amyE::PsspE(2G)-sspB<sup>Ec</sup>Ωcat argH-ssrA* ΔrocABC::kan ΔrocDEF::erm PspolVA-artPQRΩtet</i>	JLG2974→JLG3028 (Tc)
JLG3047	<i>pelB::PcotE-sspB<sup>Ec</sup>Ωspc amyE::PsspE(2G)-sspB<sup>Ec</sup>Ωcat argH-ssrA* ΔrocABC::kan ΔrocDEF::erm PspollM-artPQRΩtet</i>	JLG2975→JLG3028 (Tc)
JLGXXX	<i>ΔargJ ΔrocDEF::erm ΔrocABC::cat PspollQ-artPQRΩtet</i>	JLG2970→JLG2949 (Tc)
JLGXXX	<i>ΔargJ ΔrocDEF::erm ΔrocABC::cat PspollR-artPQRΩtet</i>	JLG2971→JLG2949 (Tc)
JLGXXX	<i>ΔargJ ΔrocDEF::erm ΔrocABC::cat PspolVA-artPQRΩtet</i>	JLG2974→JLG2949 (Tc)
JLGXXX	<i>ΔargJ ΔrocDEF::erm ΔrocABC::cat PspollM-artPQRΩtet</i>	JLG2975→JLG2949 (Tc)
JLG364	<i>ΔxylA::sspB<sup>Ec</sup>Ωcat</i>	(Lamsa et al., 2016)
JLG626	<i>ΔspollQ::erm</i>	(Ojkic et al., 2016)
JLG963	<i>amyE::PsspE(2G)-sspB<sup>Ec</sup>Ωcat</i>	(Lopez-Garrido et al., 2018)
KP89	<i>spoIVA::Tn917Ωerm</i>	KP laboratory stock
KP896	<i>ΔspollIAG-AH::kan</i>	(Blaylock et al., 2004)
KP899	<i>ΔspollIAA-AH::kan</i>	KP laboratory stock
RP189	<i>ΔsigG::spc</i>	(Riley et al., 2018)

<sup>a</sup> Plasmid or genomic DNA employed (right side the arrow) to transform an existing strain (left side the arrow) to create a new strain are listed. The drug resistance is noted in parentheses.

<b>Table 3.S3. Plasmids used in this study</b>	
<b>Plasmid</b>	<b>Description/Reference</b>
pCrePA	(Pomerantsev et al., 2006)
pDG1662	(Guérout-Fleury et al., 1996)
pDG1731	(Guérout-Fleury et al., 1996)
pER64	<i>rplL-ssrA*</i> Ωkan
pER123	<i>ΔodhAB::tet</i>
pER143	<i>rpsB-ssrA*</i> Ωkan
pER183	<i>ΔargH::tet</i>
pER187	<i>ΔsigG::tet</i>
pER195	<i>argH-ssrA*</i> Ωkan
pER217	<i>citB-GFP</i> Ωkan
pER220	<i>ΔcitZ::tet</i>
pER227	<i>rpoC-GFP</i> Ωkan
pER261	<i>guaB-GFP</i> Ωkan
pER263	<i>pyrE-GFP</i> Ωkan
pER264	<i>purD-GFP</i> Ωkan
pER265	<i>rpoZ-GFP</i> Ωkan
pER267	<i>lysA-GFP</i> Ωkan
pER268	<i>metE-GFP</i> Ωkan
pER269	<i>cysK-GFP</i> Ωkan
pER270	<i>aspB-GFP</i> Ωkan
pER271	<i>leuD-GFP</i> Ωkan
pER272	<i>argH-GFP</i> Ωkan
pER273	<i>rplL-GFP</i> Ωkan
pER274	<i>ysxC-GFP</i> Ωkan
pER276	<i>rnz-GFP</i> Ωkan
pER277	<i>gapB-GFP</i> Ωkan
pER280	<i>prs-GFP</i> Ωkan
pER282	<i>ald-GFP</i> Ωkan
pER283	<i>trmU-GFP</i> Ωkan
pER288	<i>thrB-ssrA*</i> Ωkan
pER290	<i>ΔthrB::tet</i>
pER298	<i>ΔilvD::tet</i>
pER299	<i>ilvD-ssrA*</i> Ωkan
pER312	<i>ΔrocDEF::erm</i>
pER314	<i>ΔargJ::kan</i>
pJLG256	<i>odhB-ssrA*</i> Ωkan
pJLG3	(Yen Shin et al., 2015)
pJLG302	<i>ΔcitA::kan</i>
pJLG303	<i>ΔcitB::kan</i>
pJLG304	<i>ΔfumC::kan</i>
pJLG305	<i>Δmdh::kan</i>
pJLG307	<i>ΔsucD::kan</i>
pJLG308	<i>Δicd::kan</i>
pJLG312	<i>mdh-ssrA*</i> Ωkan
pJLG319	<i>citB-ssrA*</i> Ωkan
pJLG320	<i>fumC-ssrA*</i> Ωkan
pJLG324	<i>sucD-ssrA*</i> Ωkan



<b>Table 3.S3. Plasmids used in this study (continued)</b>	
<b>Plasmid</b>	<b>Description/Reference</b>
pJLG326	<i>citZ-ssrA*Ωkan</i>
pJLG327	<i>icd-ssrA*Ωkan</i>
pJLG335	<i>odhB-GFPΩkan</i>
pJLG336	<i>citA-GFPΩkan</i>
pJLG337	<i>fumC-GFPΩkan</i>
pJLG339	<i>sucD-GFPΩkan</i>
pJLG341	<i>citZ-GFPΩkan</i>
pJLG342	<i>icd-GFPΩkan</i>
pJLG38	(Yen Shin et al., 2015)
pJLG408	<i>ΔrocABC::kan</i>
pJLG409	<i>ΔrocABC::cat</i>
pJLG413	<i>ΔartPQR::kan</i>
pJLG414	<i>PspollQ-artPQRΩcat</i>
pJLG415	<i>PspollR-artPQRΩcat</i>
pJLG445	<i>PspollM-artPQRΩcat</i>
pJLG455	<i>PspollQ-artPQRΩtet</i>
pJLG456	<i>PspollR-artPQRΩtet</i>
pJLG459	<i>PspollM-artPQRΩtet</i>
pJLG460	<i>ΔartPQR::tet</i>
pJLG465	<i>PspolVA-artPQRΩcat</i>
pJLG466	<i>PspolVA-artPQRΩtet</i>
pRP186	(Riley et al., 2018)
pWH1520	(Rygus and Hillen, 1991)

<b>Table 3.S4. Oligonucleotides used in this study</b>	
<b>Primer</b>	<b>Sequence<sup>a</sup></b>
JLG-7	AATTGGGACAACCTCCAGTG
JLG-77	GCTAGCAGCGCAAGCGC
JLG-95	CATGGATTACGCGTTAACCC
JLG-96	GCACTTTTCGGGGAAATGTG
JLG-153	GTTTTCTTCTCTCTCATTGTTTC
JLG-184	GCTAGCGCAGCAAATGATG
JLG-215	AGATCCGAATTCTCATGTTTG
JLG-297	TACTGTTTTTTTCATCGGTCC
JLG-712	<i>gggttaacgcgtaatccatg</i> TTGCAAAACGCCTTGTAGAG
JLG-713	<i>catcatttgctgcgctagc</i> TCCTTCTAATAAAAGCTGTTTCAGG
JLG-714	<i>cactggagttgtccaattc</i> TAAAAAAGGGTACATCACGATAAAG
JLG-715	<i>cacattccccgaaaagtgc</i> AAAGAGCTGGTCAGAAAGCC
JLG-732	<i>cttgcgcttgcgctgctagc</i> TCCTTCTAATAAAAGCTGTTTCAGG
JLG-735	<i>gggttaacgcgtaatccatg</i> ACAGCTGAAGCGACAAGAG
JLG-737	<i>cactggagttgtccaattc</i> TAAATTGTTACAAATTA AAAACATTTGACAG
JLG-738	<i>cacattccccgaaaagtgc</i> TCTTCATTTACGCTTGTCCC
JLG-739	<i>cttgcgcttgcgctgctagc</i> TGAAATTGTATAGTTAGGTGATTCTTTTG
JLG-786	<i>cactggagttgtccaattc</i> AAGATGAAAAACCTCAACACTGAG
JLG-787	<i>cacattccccgaaaagtgc</i> GTCTTGCTCTGTACAGCTG
JLG-788	<i>cttgcgcttgcgctgctagc</i> TACGTACCACAATTTTGTTCGG
JLG-885	<i>tccttaactctggcaacc</i> GAGTAGTTCAACAAACGGGC
JLG-886	<i>atgtgataactcggcgatg</i> AAATAGCGGTATCACGAGGC
JLG-961	<i>gggttaacgcgtaatccatg</i> GAGCATGCATTGTCACCTGG
JLG-1088	AACCTTCTTCAACTAACGGG
JLG-1114	<i>gggttaacgcgtaatccatg</i> CAAAGACATCGCACTGAATC
JLG-1116	<i>cttgcgcttgcgctgctagc</i> TGAAAGA ACTTCTCGGG
JLG-1117	<i>cactggagttgtccaattc</i> CATATTTTGGCGTTTATTCATTTT
JLG-1118	<i>cacattccccgaaaagtgc</i> AAACCAGCTCTTGAGCTGG
JLG-1122	<i>gggttaacgcgtaatccatg</i> GTATTGTTTCGAGCACCTCTTTG
JLG-1123	<i>ctgagcgagggagcagaaa</i> CAGTGCGATGTCTTTTGC
JLG-1124	<i>gttgaccagtgtccctg</i> TCAGCAAGCCGAATGGTAG
JLG-1125	<i>cacattccccgaaaagtgc</i> ACAATCGCACCTTTGTG
JLG-1126	<i>gggttaacgcgtaatccatg</i> GCAAGGATGGTCAAAACG
JLG-1127	<i>catcatttgctgcgctagc</i> GGA CTGCTTCATTTTTTTCACG
JLG-1128	<i>cttgcgcttgcgctgctagc</i> GGA CTGCTTCATTTTTTTCACG
JLG-1129	<i>cactggagttgtccaattc</i> TGAATCAATAGGAAGAGAAGGC
JLG-1130	<i>cacattccccgaaaagtgc</i> GCCGCTGTCTGAAGTATC
JLG-1134	<i>gggttaacgcgtaatccatg</i> TCGTTGCGTTTTGAATGG
JLG-1135	<i>ctgagcgagggagcagaaa</i> ATAAGGAAGCTTCGAAACCTTTT
JLG-1136	<i>gttgaccagtgtccctg</i> AATGAAGACGGCAATGTAACAAC
JLG-1137	<i>cacattccccgaaaagtgc</i> TTTCCATGACGAGCTCATG
JLG-1138	<i>gggttaacgcgtaatccatg</i> AAGCCAAAGCTCAAACGAC
JLG-1139	<i>catcatttgctgcgctagc</i> CGCCTTTGGTTTTTACCATG
JLG-1140	<i>cttgcgcttgcgctgctagc</i> CGCCTTTGGTTTTTACCATG
JLG-1141	<i>cactggagttgtccaattc</i> TAGGAAGAACGGCTGCTTTTTAAG
JLG-1142	<i>cacattccccgaaaagtgc</i> ATATCCTAGCAGGCCTCCG

<b>Table 3.S4. Oligonucleotides used in this study (continued)</b>	
<b>Primer</b>	<b>Sequence<sup>a</sup></b>
JLG-1146	<i>gggttaacgcgtaatccatg</i> CAATCCGTTGATAAACACAGC
JLG-1147	<i>ctgagcgagggagcagaaa</i> ATTCAGAACCGATCTTAAAGTTCTC
JLG-1148	<i>gttgaccagtgtccctg</i> GCCATAAAGAGGGATTGAC
JLG-1149	<i>cacatttccccgaaaagtgc</i> ACGGCTTACCGTAAACAGC
JLG-1150	<i>gggttaacgcgtaatccatg</i> GGGAAAAGCGCTTGATATG
JLG-1151	<i>catcatttgctgcgctagc</i> GGATAATACTTTCATGACATTTTTGAC
JLG-1153	<i>cactggagttgtccaattc</i> TAAAAAGAGAGAAAGGCTTGCTTAATAC
JLG-1154	<i>cacatttccccgaaaagtgc</i> ATTCCAGACTGCGCTCAG
JLG-1158	<i>gggttaacgcgtaatccatg</i> TATGCGATCGAGCATGG
JLG-1159	<i>ctgagcgagggagcagaaa</i> GTCAACAAGAACAACGTCTGC
JLG-1160	<i>gttgaccagtgtccctg</i> ACAATTGTAGGCGGCAAC
JLG-1161	<i>cacatttccccgaaaagtgc</i> TCGGTGTGAGTTCAAGCTG
JLG-1186	<i>gggttaacgcgtaatccatg</i> CGCTTTATTTTCATACGAAGCAG
JLG-1187	<i>catcatttgctgcgctagc</i> ATGCGTTTTACAAGTTTCGAAC
JLG-1188	<i>cttgcgcttgcgctgctagc</i> ATGCGTTTTACAAGTTTCGAAC
JLG-1189	<i>cactggagttgtccaattc</i> TAAAAAAGGGACAGCCGTC
JLG-1190	<i>cacatttccccgaaaagtgc</i> CCCCTTCGCTTAATACTTG
JLG-1194	<i>gggttaacgcgtaatccatg</i> GCCAGAGAAATTGCATTGG
JLG-1195	<i>ctgagcgagggagcagaaa</i> ACCGCCAACGATATTTGTG
JLG-1196	<i>gttgaccagtgtccctg</i> AAAACCCTTAATGCATGCG
JLG-1197	<i>cacatttccccgaaaagtgc</i> CCCCTTCGCTTAATACTTG
JLG-1210	<i>gggttaacgcgtaatccatg</i> CTCGAAAATGTTTCATCCCATG
JLG-1211	<i>catcatttgctgcgctagc</i> GGCTCTTTCTTCAATCGGAAC
JLG-1212	<i>cttgcgcttgcgctgctagc</i> GGCTCTTTCTTCAATCGGAAC
JLG-1213	<i>cactggagttgtccaattc</i> AGAACCATTGGAGGCTGG
JLG-1214	<i>cacatttccccgaaaagtgc</i> TCTGTGAAC TTCATGATGTTTCC
JLG-1218	<i>gggttaacgcgtaatccatg</i> TGCTCTTTGCTGTATCCGTC
JLG-1219	<i>ctgagcgagggagcagaaa</i> ATCATAACCCACATATGTAAGGG
JLG-1220	<i>gttgaccagtgtccctg</i> TGGCTCGCTCATATTCTTGAG
JLG-1221	<i>cacatttccccgaaaagtgc</i> CCGATACCTGATGTCTCAGG
JLG-1222	<i>gggttaacgcgtaatccatg</i> GATATTTACGCAGGCATCGAG
JLG-1223	<i>catcatttgctgcgctagc</i> GTCCATGTTTTTGATCAGTTCTTC
JLG-1224	<i>cttgcgcttgcgctgctagc</i> GTCCATGTTTTTGATCAGTTCTTC
JLG-1225	<i>cactggagttgtccaattc</i> GCAAGGAAAAAGCCTAAAAGTAGC
JLG-1226	<i>cacatttccccgaaaagtgc</i> GCAATTGTAGGAAGGACGC
JLG-1229	<i>ctgagcgagggagcagaaa</i> CGCGTTCCAAATATCAGGAC
JLG-1230	<i>gttgaccagtgtccctg</i> ATCGCTTCTAAAGTCGTAACCTTACG
JLG-1478	<i>gggttaacgcgtaatccatg</i> CATCACAATGAGGAGCTGC
JLG-1479	<i>gcctgagcgagggagcagaaa</i> ATCGGTAATGGTTCGTGCG
JLG-1480	<i>gcggtgaccagtgtccctg</i> TATGGCTGCGTGTTGATCAG
JLG-1481	<i>cacatttccccgaaaagtgc</i> GCCTAATGGAACCAAAGCG
JLG-1493	<i>gggttaacgcgtaatccatg</i> CAGCCTACCATTCCGTTTAC
JLG-1494	<i>gcctgagcgagggagcagaaa</i> AGGCTTATCTTTCCAGTGATCTC
JLG-1495	<i>gcggtgaccagtgtccctg</i> AATCCAAAAGAGCGCAGGAC
JLG-1496	<i>cacatttccccgaaaagtgc</i> CGATGCCAACCGTAATCAGC
JLG-1499	<i>cccgttagttgaagaaggtt</i> AGGCTTATCTTTCCAGTGATCTC
JLG-1500	<i>gaaacaatgagagaggaagaaac</i> ATGAAAAATGGCTTATTACTTGTGG

<b>Table 3.S4. Oligonucleotides used in this study (continued)</b>	
<b>Primer</b>	<b>Sequence<sup>a</sup></b>
JLG-1501	<i>ggaccgatgaaaaaacagta</i> ATGAAAAAATGGCTCTTATTACTTGTGG
JLG-1502	<i>cacattccccgaaaagtgc</i> GTCAGATTTGATTTCTGCACC
JLG-1566	ATGAAAAAATGGCTCTTATTACTTGTGG
JLG-1569	<i>caaacatgagaattcggatct</i> CTCTCTTACAGTGACAAGCCC
JLG-1572	<i>ccacaagtaataagagccatttttcat</i> ATCGACCTTTTCCAAGTGATC
JLG-1575	<i>caaacatgagaattcggatct</i> AGCCAAGCGAAAAAGAAGCG
JLG-1578	<i>ccacaagtaataagagccatttttcat</i> AGAGATTTTTCGCATACCGTTTC
JLG-1581	<i>gcctgagcgaggagcagaa</i> GTA ACTATTGCCGATGATAAGCTG
JLG-1582	<i>gcgttgaccagtgtccctg</i> CTAATGTCACTAACCTGCC
oER76	<i>gggtaacgcgtaatccatg</i> GTATTACGATGGCAACAGCGC
oER78	<i>cactggagttgtccaatt</i> AGGATCCTCTACCGTTTTATTATCG
oER79	<i>cacattccccgaaaagtgc</i> CCACAACAAGTATATGCATCGCTC
oER80	<i>gcgcttgcgctgctagc</i> CCGGTTTATCATTTTTTTGATCG
oER178	<i>gggtaacgcgtaatccatg</i> GAACTTCCATCACGCGAAGG
oER179	<i>catcatttgctgctagc</i> CTTAACTTCTACAGAAGCGCCAAC
oER180	<i>cactggagttgtccaatt</i> TCTTCACTTACCTGTAGGGGAAGC
oER181	<i>cacattccccgaaaagtgc</i> CATCGAACAGTTCCTCGAGC
oER182	<i>gcgcttgcgctgctagc</i> CTTAACTTCTACAGAAGCGCCAAC
oER276	<i>gggtaacgcgtaatccatg</i> GACATATCCGCTTGCGATCC
oER278	<i>cactggagttgtccaatt</i> AGGCGGAGCTCTTATTTGACAATTTG
oER279	<i>cacattccccgaaaagtgc</i> GTGTTGTCATCAGGAGAACGGAC
oER280	<i>gcgcttgcgctgctagc</i> GCCTCGCGGGACGTTTAC
oER304	<i>gggtaacgcgtaatccatg</i> GCTTGAAGCTGGTGTTCACTTC
oER305	<i>catcatttgctgctagc</i> CGCAGTTGTTGTTTCTGTTTCTG
oER306	<i>cactggagttgtccaatt</i> CCTATTCAAAGGTGATAAGAGGGAC
oER307	<i>cacattccccgaaaagtgc</i> GTTAATACACCGATGCGGCC
oER419	<i>ttctgctccctcgctcaggcggccgc</i> TCCTTTAACTCTGGCAACCC
oER420	<i>caggagcactggtcaacgctagc</i> ATGTGATAACTCGGCGTATG
oER421	<i>ttctgctccctcgctcaggcggccgc</i> ATGAGAGAGGAAGAAAACGG
oER422	<i>caggagcactggtcaacgctagc</i> AATTGGGACA ACTCCAGTG
oER425	<i>ttctgctccctcgctcaggcggccgc</i> TCCTTTAACTCTGGCAACCC
oER426	<i>caggagcactggtcaacgctagc</i> ATGTGATAACTCGGCGTATG
oER427	TTCTGCTCCCTCGCTCAG
oER428	CAGGGAGCACTGGTCAAC
oER475	<i>gggtaacgcgtaatccatg</i> CCAGCCAACTATTTCAATACG
oER476	<i>gcctgagcgaggagcagaa</i> CAACGATATTTTACCCTGTTTGC
oER477	<i>gcgttgaccagtgtccctg</i> TAAAAAAGGGTACATCACGATAAAG
oER478	<i>cacattccccgaaaagtgc</i> TTTATCTCAATCTTACAGGCGG
oER487	<i>gggtaacgcgtaatccatg</i> AATGGTATGAGATGTCGATTTCG
oER490	<i>cacattccccgaaaagtgc</i> CAACAGGATTTGTCAGCACC
oER565	<i>gggtaacgcgtaatccatg</i> GCGCCAGCTTGATGACATC
oER567	<i>cactggagttgtccaatt</i> TTCACAATAAGCTTGCAGAAAG
oER568	<i>cacattccccgaaaagtgc</i> TTATCTGCAGCCTGTTTCAGG
oER569	<i>gcgcttgcgctgctagc</i> AGCACCCGCCACAGATG
oER614	<i>gggtaacgcgtaatccatg</i> AAGTTAAAGCGCTTGAAGACG
oER616	<i>cactggagttgtccaatt</i> TTTGAAAAACCATCTGCATTTG
oER617	<i>cacattccccgaaaagtgc</i> GATCGTTCTTTCTTCAGCAGG

<b>Table 3.S4. Oligonucleotides used in this study (continued)</b>	
<b>Primer</b>	<b>Sequence<sup>a</sup></b>
oER618	<i>gcgcttgcgctgctagc</i> TACTAGCTGTGTCTGCTGTGC
oER749	<i>gggtaacgcgtaatccatg</i> CAGAAGGTTCAATCGATCCG
oER751	<i>cactggagttgtccaatt</i> CTGATTTAACTCTGCTGAAAGACTGC
oER752	<i>cacattccccgaaaagtgc</i> TAACCCACATACCCAGGTGG
oER753	<i>gcgcttgcgctgctagc</i> TTCAACCGGGACCATATCG
oER756	<i>gggtaacgcgtaatccatg</i> TCAAGGATTCTTTGATATACCG
oER758	<i>cactggagttgtccaatt</i> ACCATTTTTTCGAGGTTTAAATCC
oER759	<i>cacattccccgaaaagtgc</i> CTTGAAATATCAGCCTCAATCG
oER760	<i>gcgcttgcgctgctagc</i> GCTGAACAGATAGCTGACTG
oER794	<i>gggtaacgcgtaatccatg</i> AACAGGAAGCAGCATGATG
oER795	<i>catcatttgctgctgctagc</i> ACAAACTCCTGCTGCCAC
oER796	<i>cactggagttgtccaatt</i> AATTTCTTCATAAAATCCCG
oER797	<i>cacattccccgaaaagtgc</i> CAAATATGTATGGTCCAGCG
oER798	<i>gcgcttgcgctgctagc</i> ACAAACTCCTGCTGCCAC
oER801	<i>gggtaacgcgtaatccatg</i> CTTTCTGAGCTGATCTTGAAGC
oER802	<i>gcctgagcgagggagcagaa</i> TGGTCAAATGATATGGACGC
oER803	<i>gcgttgaccagtgtccctg</i> GTACACATGCATCGAAAGAGG
oER804	<i>cacattccccgaaaagtgc</i> CAAATATGTATGGTCCAGCG
oER818	<i>gggtaacgcgtaatccatg</i> GCCTGTTGTAAAAGTGCTGG
oER820	<i>cactggagttgtccaatt</i> AATAAGGTCATGGACACATTTTAAAG
oER821	<i>cacattccccgaaaagtgc</i> GCGACATTAGGATCTAAGTCTCC
oER822	<i>gcgcttgcgctgctagc</i> TACAGCAGACGGATGTTTCATTC
oER831	<i>gcgttgaccagtgtccctg</i> TGAAAAGCCTTTAAACGATGTTG
oER832	<i>gcctgagcgagggagcagaa</i> TTTTTCCCTCCCTACAGGAG
oER858	<i>gggtaacgcgtaatccatg</i> GCTTCATGCCACTGAATACG
oER860	<i>cactggagttgtccaatt</i> AAGAAAGCGCCGATTTTTC
oER861	<i>cacattccccgaaaagtgc</i> CGAAGGTGTATGTTACAGCACC
oER862	<i>gcgcttgcgctgctagc</i> TTGCTTTACACCCGTTTTAAATG
oER877	<i>gggtaacgcgtaatccatg</i> GGAAGGCATGAAAGGTGC
oER879	<i>cactggagttgtccaatt</i> AAAAAGCCAAAACCTCCCGG
oER880	<i>cacattccccgaaaagtgc</i> CTCTTCTTGATGGTCATAAACTGC
oER881	<i>gcgcttgcgctgctagc</i> ATCGAATTGGTACAGCGGC
oER931	<i>gggtaacgcgtaatccatg</i> GCACAGCTGTCAGACAGAC
oER933	<i>cactggagttgtccaatt</i> CAGATCAAAAAGCGGCTGAC
oER934	<i>cacattccccgaaaagtgc</i> CGCGAATGATTTTATTACGG
oER935	<i>gcgcttgcgctgctagc</i> GCTATGTTTTTCTACAAAACGC
oER966	<i>gggtaacgcgtaatccatg</i> GCTGTAGAAACGATCGTTAAGC
oER968	<i>cactggagttgtccaatt</i> GTGAGGAAAACCCGCAG
oER969	<i>cacattccccgaaaagtgc</i> TAAAGGAGCCAGACAAATGG
oER970	<i>gcgcttgcgctgctagc</i> TTTTTGGGCAGCCTTTAAAG
oER977	<i>gggtaacgcgtaatccatg</i> CCGCCTTACGCTATCTTTCC
oER979	<i>cactggagttgtccaatt</i> AAAATAAATTCAAATGATGTAAAGAGGC
oER980	<i>cacattccccgaaaagtgc</i> GCGCTCCTTTATAAGGATCG
oER981	<i>gcgcttgcgctgctagc</i> TTTTTTAAACCAATCTTTTGAICTCG
oER988	<i>gggtaacgcgtaatccatg</i> CACATACGGGGAAAGCAGC
oER990	<i>cactggagttgtccaatt</i> AAAAGCGGCCGGTATTTG
oER991	<i>cacattccccgaaaagtgc</i> GAGATTCATTTGCTCCTCAGGG

<b>Table 3.S4. Oligonucleotides used in this study (continued)</b>	
<b>Primer</b>	<b>Sequence<sup>a</sup></b>
oER992	<i>gcgcttgcgctgctagc</i> GGCTTGAAGCCAAGAGCTTC
oER999	<i>gggttaacgcgtaatccatg</i> GAACAGACGCTTCAAGATGG
oER1001	<i>cactggagttgtccaatt</i> TAGCACAAGTAGCAACCTATATCATG
oER1002	<i>cacatttccccgaaaagtgc</i> CGTAACCGCATGCTAAATAGC
oER1003	<i>gcgcttgcgctgctagc</i> TTCGCGGTCTTCCTTTTC
oER1026	<i>gggttaacgcgtaatccatg</i> TTATTCGGTAATCTAGCTCCGG
oER1027	<i>catcatttgctgcgctagc</i> GATTTTCATAATACCGCCGG
oER1028	<i>cactggagttgtccaatt</i> ATAGCTGGGGACACTTTC
oER1029	<i>cacatttccccgaaaagtgc</i> GATTTCTTCCATATCGTGTCC
oER1033	<i>gggttaacgcgtaatccatg</i> ACTCCAGCAAGCTTGTTTCG
oER1034	<i>gcctgagcgagggagcagaa</i> GGTGATCCTCCTAAATTCTTTC
oER1035	<i>gcgttgaccagtgtccctg</i> AAGTGCCAGAAGAAGAGTGG
oER1048	<i>gggttaacgcgtaatccatg</i> GTCTAGAAGAAGGACACCCG
oER1049	<i>catcatttgctgcgctagc</i> TACACTTTTTACTTGATATAAAGGATTTTC
oER1050	<i>cactggagttgtccaatt</i> ATCATGCCAAGCGTTCCTC
oER1051	<i>cacatttccccgaaaagtgc</i> CTCGGTCATCAATGCTTTCC
oER1055	<i>gggttaacgcgtaatccatg</i> ATGCTGGAAACATCACTGC
oER1056	<i>gcctgagcgagggagcagaa</i> ACACGGGCGCTCCTTTTAC
oER1057	<i>gcgttgaccagtgtccctg</i> AACGATTCTCGTCATGACC
oER1118	<i>gggttaacgcgtaatccatg</i> GAATCTTTCGTTATCGTTGACGC
oER1119	<i>gcctgagcgagggagcagaa</i> TCATGGTTCGATTCTCTCCCGTTC
oER1120	<i>gcgttgaccagtgtccctgtaa</i> TAAAGGGGAGCGAAATGAAG
oER1121	<i>cacatttccccgaaaagtgc</i> AGCTTATCGGCTTCAAGCG
oER1124	<i>gggttaacgcgtaatccatg</i> CCTTCCTGAAGAGCCTGTACC
oER1125	<i>gcctgagcgagggagcagaa</i> TCAGAAATAACAATCGGGAGCG
oER1126	<i>gcgttgaccagtgtccctg</i> TAAGAAAACCCCGCACCC
oER1127	<i>cacatttccccgaaaagtgc</i> ACATATGGATGACTTGTTGTCCG

<sup>a</sup>In capital letters are shown the regions of the primer that anneals to the template. Homology regions for Gibson assembly are shown in italics.

## References

1. Herrero, A., Stavans, J., and Flores, E. The multicellular nature of filamentous heterocyst-forming cyanobacteria. *FEMS Microbiol Rev.* **40**(6), 831–854 (2016).
2. Liu, J., Prindle, A., Humphries, J., Gabalda-Sagarra, M., Asally, M., Lee, D.Y., Ly, S., Carcia-Ojalvo, J., and Süel, G.M. Metabolic co-dependence gives rise to collective oscillations within biofilms. *Nature*, **523**(7562), 550–554 (2015).
3. Camp, A. and Losick, R. A feeding tube model for activation of a cell-specific transcription factor during sporulation in *Bacillus subtilis*. *Genes Dev.* **23**, 1014-1024 (2009).
4. Errington, J. Regulation of endospore formation in *Bacillus subtilis*. *Nat. Rev. Microbiol.* **1**(2), 117–26 (2003).
5. McKenney, P. T., Driks, A. and Eichenberger, P. The *Bacillus subtilis* endospore: assembly and functions of the multilayered coat. *Nat Rev Microbiol.* **11**(1), 33–44 (2013).
6. Tan, I. S., and Ramamurthi, K. S. Spore formation in *Bacillus subtilis*. *Environ Microbiol Rep.* **6**(3), 212–225 (2014).
7. Eaton, M. W. and Ellar, D. J. Protein synthesis and breakdown in the mother-cell and forespore compartments during spore morphogenesis in *Bacillus megaterium*. *Biochem J.* **144**(2), 327–337 (1974).
8. Watabe, K., Iida, S., Nakamura, K., Ichikawa, T., and Kondo, M. Protein synthesis in the isolated forespores from sporulating cells of *Bacillus subtilis*. *Microbiol Immunol.* **25**(6), 545–556 (1981).
9. Pereira, S. F. F., Gonzalez, R. L. and Dworkin, J. Protein synthesis during cellular quiescence is inhibited by phosphorylation of a translational elongation factor. *Proc. Natl. Acad. Sci.* **112**(25), E3274–E3281 (2015).
10. Meisner, J., Wang, X., Serrano, M., Henriques, A., and Moran, C. A channel connecting the mother cell and forespore during bacterial endospore formation. *Proc. Natl. Acad. Sci.* **105**(39), 15100-15105 (2008).
11. Meisner, J., Maehigashi, T., André, I., Dunham, C.M., and Moran, C.P. Structure of the basal components of a bacterial transporter. *Proc. Natl. Acad. Sci.* **109**(14), 5446–5451 (2012).
12. Doan, T., Morlot, C., Meisner, J., Serrano, M., Henriques, A., Moran, C., and Rudner, D. Novel secretion apparatus maintains spore integrity and developmental gene expression in *Bacillus subtilis*. *PLoS Genet.* **5**(7), (2009).
13. Levdikov, V. M., Blagova, E.V., McFeat, A., Fogg, M.J., Wilson, K.S., and Wilkinson, A.J. Structure of components of an intercellular channel complex in sporulating *Bacillus subtilis*. *Proc Natl Acad Sci.* **109**(14), 5441–5445 (2012).

14. Rodrigues, C.D., Henry, X., Neumann, E., Kurauskas, V., Bellard, L., Fichou, Y., Schanda, P., Schoehn, G., Rudner, D.Z., and Morlot, C. A ring-shaped conduit connects the mother cell and forespore during sporulation in *Bacillus subtilis*. *Proc Natl Acad Sci U.S.A.*, **113**, 11585–11590 (2016).
15. Zeytuni, N., Hong, C., Flanagan, K.A., Worrall, L.J., Theiltges, K.A., Vuckovic, M., Huang, R.K., Massoni, S.C., Camp, A.H., Yu, Z., and Strynadka, N.C. Near-atomic resolution cryoelectron microscopy structure of the 30-fold homooligomeric SpoIIAG channel essential to spore formation in *Bacillus subtilis*. *Proc Natl Acad Sci.* **114**(34), E7073-E7081 (2017).
16. Zeytuni, N., Flanagan, K.A., Worrall, L.J., Massoni, S.C., Camp, A.H., and Strynadka, N.C.J. Structural and biochemical characterization of SpoIIAF, a component of a sporulation-essential channel in *Bacillus subtilis*. *J Struct Biol.* **204**(1), 1–8 (2018).
17. Zeytuni, N., Flanagan, K.A., Worrall, L.J., Massoni, S.C., Camp, A.H., and Strynadka, N.C.J. Structural characterization of SpoIIAB sporulation-essential protein in *Bacillus subtilis*. *J Struct Biol.* **202**(2), 105–112 (2018).
18. Camp, A.H., and Losick, R. A novel pathway of intercellular signalling in *Bacillus subtilis* involves a protein with similarity to a component of type III secretion channels. *Mol Microbiol.* **69**(2), 402–417 (2008).
19. Riley, E.P., Trinquier, A., Reilly, M.L., Durchon, M., Perera, V.R., Pogliano, K. & Lopez-Garrido, J. Spatiotemporally regulated proteolysis to dissect the role of vegetative proteins during *Bacillus subtilis* sporulation: cell-specific requirement of  $\sigma^H$  and  $\sigma^A$ . *Mol. Microbiol.* **108**(1), 45-62 (2018).
20. Griffith, K. and Grossman, A. Inducible protein degradation in *Bacillus subtilis* using heterologous peptide tags and adaptor proteins to target substrates to the protease ClpXP. *Mol. Microbiol.* **70**(4), 1012-1025 (2008).
21. Dieterich, D.C., Link, A.J., Graumann, J., Tirrell, D.A., and Schuman, E.M. Selective identification of newly synthesized proteins in mammalian cells using bioorthogonal noncanonical amino acid tagging (BONCAT). *Proc Natl Acad Sci.* **103**(25), 9482–9487 (2006).
22. Ong, S. E., Blagoev, B., Kratchmarova, I., Kristensen, D.B., Steen, H., Pandey, A., and Mann, M. Stable isotope labeling by amino acids in cell culture, SILAC, as a simple and accurate approach to expression proteomics. *Mol Cell Proteomics.* **1**(5), 376–386 (2002).
23. Calogero, S., Gardan, R., Glaser, P., Schweizer, J., Rapoport, G., and Debarbouille, M. RocR, a novel regulatory protein controlling arginine utilization in *Bacillus subtilis*, belongs to the NtrC / NifA family of transcriptional activators. *J Bacteriol.* **176**(5), 1234–1241 (1994).
24. Gardan, R., Rapoport, G. and Debarbouille, M. Expression of the *rocDEF* operon involved in arginine catabolism in *Bacillus subtilis*. *J Mol Biol.* **249**(5), 843–856 (1995).
25. Quentin, Y., Fichant, G. and Denizot, F. Inventory, assembly and analysis of *Bacillus*



*subtilis* ABC transport systems. *J Mol Biol.* **287**(3), pp. 467–484 (1999).

26. Glekas, G. D., Mulhem, B.J., Kroc, A., Duelfer, K.A., Lei, V., Rao, C.V., and Ordal, G.W. The *Bacillus subtilis* chemoreceptor McpC senses multiple ligands using two discrete mechanisms. *J Biol Chem*, **287**(47), 39412–39418 (2012).

27. Liu, N.-J. L., Dutton, R. J., and Pogliano, K. Evidence that the SpoIIIE DNA translocase participates in membrane fusion during cytokinesis and engulfment. *Mol Microbiol.* **59**(4), 1097–1113 (2006).

28. Mullineaux, C. W., Mariscal, V., Nenninger, A., Khanum, H., Herrero, A., Flores, E., and Adams, D.G. Mechanism of intercellular molecular exchange in heterocyst-forming cyanobacteria. *EMBO J.* **27**(9), 1299–1308 (2008).

29. Serio, A. W., Pechter, K. B. and Sonenshein, A. L. *Bacillus subtilis* aconitase is required for efficient late-sporulation gene expression. *J Bacteriol.* **188**(17), 6396–6405 (2006).

## CHAPTER IV

A novel proteolytic pathway reprograms forespore metabolism to promote the transition to and exit from cellular dormancy.

### **Abstract**

Cellular differentiation is a key facet of developmental processes occurring in organisms ranging from bacteria to mammals. Endospore formation represents one of the simplest developmental pathways, and involves the differentiation of rapidly growing vegetative cells into highly resistant and metabolically dormant spores. Here, we show that the transition to dormancy entails a profound metabolic differentiation of the two cells that comprise the sporangium. Metabolic enzymes are depleted from the prospective spore through dilution by forespore growth and through the ClpCP-mediated proteolytic destruction of the key metabolic enzyme, citrate synthase. Proteolysis of citrate synthase is governed by YjbA, a novel ClpCP adaptor protein, which limits flux through central carbon metabolism as the spore prepares for dormancy. Mutant spores lacking this adaptor are highly sensitive to oxidative stress and fail to outgrow in the presence of nutrients. Taken together, our results constitute one of the first examples of a wholesale metabolic differentiation of genetically identical bacterial sister cells, and are compatible with a model suggesting that the robust reprogramming of the prospective spore's metabolic capabilities is required for the efficient transition to and exit from cellular dormancy.

### **Significance statement**

When confronted with nutrient limitation, *Bacillus subtilis* cells can differentiate into highly resistant and metabolically dormant spores that retain the ability to promptly resume vegetative growth when nutrients become available. Here, we show that the metabolism of the prospective spore is robustly reprogrammed during spore formation,

promoting the spore's efficient transition to and exit from dormancy under stress conditions. Our work illuminates the mechanisms underlying the transition between growth and cellular dormancy, which can potentially be harnessed to target spore-forming pathogens.

## **Introduction**

The generation of asymmetry is a hallmark of developmental processes in organisms ranging from bacteria to mammals, and represents a crucial facet underlying cellular differentiation. Cells employ numerous strategies to establish asymmetry in genetically identical offspring, including differential gene expression<sup>1</sup>, proteolysis or differential segregation of cell-fate determinants<sup>2</sup>, biochemical gradients<sup>3</sup>, and cell-to-cell signaling<sup>4</sup>. One striking example of cellular differentiation occurs during bacterial endospore formation, a highly conserved developmental program that involves the transformation of rapidly growing vegetative cells into metabolically dormant and highly resilient spores<sup>5</sup>. Although several species belonging to the Gram-positive genera *Bacillus* (aerobes) and *Clostridium* (anaerobes) possess the ability to form spores, the sporulation pathway is best characterized in *Bacillus subtilis*.

The process of spore formation is enacted in response to a myriad of environmental signals including nutrient limitation and high cell density. At the onset of sporulation, *Bacillus subtilis* cells undergo an asymmetric cell division toward a single cell pole, a process called polar septation, which divides the sporangium into a larger cell (the mother cell) and a smaller cell (the prospective spore or forespore) (Fig. 1A). The mother cell and forespore are initially highly similar in terms of molecular composition, but assume opposite fates as a product of development. Following polar septation, the mother cell and forespore activate cell-autonomous programs of gene expression, mediated by a series of cell- and stage-specific  $\sigma$  factors, which cause the developmental fates of the two cells to diverge. The mother cell engulfs the forespore to

produce a protoplast surrounded by two lipid bilayers that is sequestered away from the external medium within the mother cell cytoplasm, and then lyses after nurturing the forespore to dormancy, thereby liberating the mature and immortalized spore into the environment. Despite having no detectable metabolic activity, spores are able to survey the environment and quickly germinate in response to nutrient availability, resuming full metabolic activity within hours<sup>6</sup>.

Sporangia are therefore confronted with the tremendous challenge of transitioning to metabolic dormancy while simultaneously retaining the capacity to exit dormancy and rapidly resume full metabolic activity when environmental conditions become favorable. We recently demonstrated that the mother cell and forespore become metabolically differentiated during spore formation and that the forespore becomes dependent on mother cell-derived metabolic building blocks to sustain macromolecular synthesis<sup>7</sup> (Fig. 1B). Although sporangia are known to harness several fundamental principles of development to achieve the differentiation of the mother cell and forespore, including the proteolytic degradation of cell-fate determinants<sup>8</sup>, asymmetric cell division, and cell-specific gene expression<sup>9</sup>, the mechanisms underlying the metabolic reprogramming of the forespore remain unclear. The expression of only a select few genes encoding core metabolic enzymes are regulated under sporulation control, suggesting that sporangia possess alternative means of achieving the functional specialization of the mother cell and the forespore.

Here, we demonstrate that sporangia exploit multiple strategies to robustly reprogram the metabolism of the forespore. We show that key metabolic enzymes are depleted from the forespore passively by dilution and actively by proteolysis. We identify a post-translational layer to cell-specific gene expression in which YjbA promotes the ClpCP-mediated proteolysis of citrate synthase to inactivate the TCA cycle in the forespore. Finally, we show that spores lacking YjbA are sensitive to NaOCl-induced

oxidative stress and are slow to outgrow after exposure to oxidative stress. Altogether, our results suggest that the metabolic reprogramming of the forespore is crucial to the spore's transition to and exit from dormancy.

## Results

The recent finding that metabolic enzymes functioning in a variety of biosynthetic pathways are rapidly depleted from the forespore shortly following polar septation prompted us to identify the molecular mechanisms underlying this profound metabolic differentiation of the mother cell and forespore during spore formation<sup>7</sup>. We noted striking differences in the extent to which the levels of certain enzymes were reduced in the forespore (Fig. S1A). The levels of most metabolic enzymes in the forespore were only 2- to 5-fold reduced when compared to the corresponding levels in the mother cell. Citrate synthase (CitZ), however, exhibited a much more pronounced, 84-fold decrease in forespore levels with respect to the mother cell levels (Fig. 2A and B; Fig. S1B). To test whether transcriptional regulation could account for the differential expression of *citZ* in the mother cell and forespore, we placed the production of GFP under the control of  $P_{citZ}$  and used fluorescence microscopy to observe GFP levels in the mother cell and forespore. To our surprise, GFP levels in this strain were found to be only ~3-fold lower in the forespore than in the mother cell, consistent with the 2- to 5-fold reduction observed for several other GFP fusions (Fig. 2C and D). We therefore speculated that two unique pathways exist to govern the downregulation of metabolic activity in the forespore: (1) a general pathway that yields a global reduction in metabolic enzyme levels in the forespore, and (2) a specific pathway that mediates the more thorough clearance of CitZ from the forespore (Fig. 2E).

We surmised that the general differentiation pathway outlined above is not likely to be genetically encoded, given that numerous proteins, including heterologous ones, were found to be depleted from the forespore to a similar extent regardless of molecular

function. We happened to note that the extent of forespore depletion correlated with the volumetric ratio of the forespore to the mother cell, and reasoned that the exploitation of intrinsic properties of the cell could allow this system to function as broadly and uniformly as observed. Recent work demonstrated that the forespore roughly triples in volume during spore formation, yielding a corresponding decrease in mother cell volume, which would be consistent with the observed 2- to 5-fold reduction in the levels of metabolic enzymes in the forespore<sup>10</sup>. To test whether metabolic enzymes are diluted by increases in forespore volume, we partially suppressed the growth of the forespore by introducing a *spoIIQ* null mutation into strains producing GFP fusions to metabolic enzymes. Since GFP fluorescence in the mother cell remained relatively constant throughout engulfment for all fusions examined, the ratio of the forespore fluorescence signal to the mother cell fluorescence signal was used as an internally controlled measure of the extent of stabilization. The deletion of *spoIIQ* yielded sporangia with significantly smaller forespores than their wild type counterparts (Fig. S2A and B), and resulted in the stabilization of a wide array of metabolic enzymes, as well as GFP produced under the control of  $P_{citZ}$ , but not CitZ (Fig. 2A to D; Fig. S2C).

To ensure that the observed stabilization of metabolic enzymes in the forespore was due to the suppression of forespore growth, and not due directly to the lack of SpoIIQ activity, we manipulated forespore size independently of SpoIIQ. To do this, we treated sporangia with cerulenin to inhibit new membrane synthesis, which has been shown previously to block forespore growth, and monitored the behavior of GFP fusions to metabolic enzymes by timelapse microscopy<sup>10</sup>. We selected to use Icd-GFP for this purpose because it functions in the same metabolic pathway as CitZ, and is highly abundant, rendering it amenable to the repeated imaging that accompanies timelapse microscopy. In the absence of cerulenin treatment, Icd-GFP was diluted in the forespore to a minor extent as the forespore increased in size during engulfment (Fig. 2F and G).

In the presence of cerulenin, however, forespores failed to grow, and the Icd-GFP fusion remained completely stable. Importantly, blocking forespore growth via the inactivation of SpoIIQ or treatment with cerulenin did not yield the stabilization of CitZ-GFP in the forespore, indicating that CitZ is depleted from the forespore by other means. Taken together, these data indicate that the sporangium utilizes multiple strategies to achieve the metabolic reprogramming of the forespore, one of which acts generally to globally reduce metabolic enzyme levels in the forespore, and another that acts specifically to deplete the forespore of particular metabolic enzymes, such as CitZ.

We next sought to characterize the mechanism by which CitZ is depleted from the forespore. Since the reduction in CitZ levels in the forespore is not due to dilution by growth nor differential transcription, we hypothesized that CitZ is regulated at the level of degradation rather than synthesis. To rule out differential synthesis as the means driving the asymmetric accumulation of CitZ, we uncoupled synthesis from degradation by treating sporangia with chloramphenicol to inhibit new translation and monitored the levels of CitZ-GFP in the mother cell and forespore. We reasoned that if new synthesis is required to replenish CitZ in the mother cell, then translation inhibition should destabilize CitZ in the entire sporangium. Upon chloramphenicol treatment, however, CitZ-GFP levels remained high in both the mother cell and forespore (Fig. S3A and B). Since antibiotic treatment can have pleiotropic effects, we also induced a cell-specific translation arrest by using spatiotemporally regulated proteolysis (STRP) to deplete the mother cell or forespore of the sole isoleucyl tRNA synthetase, IleS, which has been previously shown to rapidly inhibit translation<sup>10</sup>. Briefly, STRP harnesses cell-specific gene expression to produce an SspB<sup>Ec</sup> adapter protein that directs –ssrA\* tagged target proteins for ClpXP-mediated proteolysis in a spatiotemporally regulated manner<sup>11</sup>. When we used STRP to induce a translation arrest in the mother cell through the degradation of IleS-ssrA\*, we did not notice any changes in the stability of CitZ-GFP compared to the

tagged-only control (Fig. S3C and D). On the other hand, when we blocked translation in the forespore, we noticed a marked increase in forespore levels of CitZ-GFP. Thus, our data indicate that new translation is not required to replenish CitZ-GFP levels in the mother cell, but rather to synthesize the proteolytic machinery that prompts the clearance of CitZ-GFP in the forespore.

Given that translation is required in the forespore for the clearance of CitZ-GFP, we reasoned that a CitZ-degrading protease is synthesized in the forespore shortly after polar septation. We therefore sought to identify the protease responsible for the depletion of CitZ-GFP from the forespore. We surveyed a panel of null mutants in genes encoding proteases or protease accessory factors, including the AAA+ ATPases *clpC*, *clpE*, *clpQY*, *clpX*, *ftsH*, and *lon*, the carboxy terminal peptidases *ctpA* and *ctpB*, the intracellular serine protease *ispA*, and the germination protease *gpr*. Of the ten null mutants tested, only the inactivation of *clpC* resulted in an appreciable stabilization of CitZ-GFP in the forespore (Fig. 3A and B; Fig. S4A and B).

Although *clpC* is expressed under the control of the early-acting forespore-specific sigma factor,  $\sigma^F$ , the ClpCP protease is required for the degradation of the anti- $\sigma$  factor, SpoIIAB, which allows for the efficient activation of the forespore line of gene expression<sup>12,13</sup>. As such, *clpC* mutants suffer severe defects in spore formation<sup>14</sup>. Therefore, we wanted to test whether the observed stabilization of CitZ-GFP in the forespores of *clpC* null mutants was an indirect consequence of the failure to robustly activate  $\sigma^F$ . To assess this, we made use of the STRP methodology to deplete ClpC-*ssrA*\* from the forespore. Since STRP requires the successful activation of cell-specific gene expression for function, it allows ClpC-*ssrA*\* to be depleted from the forespore only after  $\sigma^F$  activation<sup>11</sup>. We first ensured that the addition of the -*ssrA*\* tag did not affect ClpC function, and that ClpC-*ssrA*\* was efficiently degraded upon the production of SspB<sup>Ec</sup>. To do this, we expressed *sspB*<sup>Ec</sup> from a xylose-inducible promoter in strains



expressing *clpC-ssrA\** from the native locus, and measured heat resistant spore titers. In the absence of xylose induction, this strain sporulated at levels similar to that of wild type (Fig. S5C). In the presence of xylose induction, however, this strain suffered severe spore titer defects, phenocopying the *clpC* null mutant. Together, these data indicate that the tag does not interfere with ClpC function, and that ClpC-ssrA\* is readily degraded upon the production of SspB<sup>Ec</sup>. While expression of *clpC-ssrA\** alone had no effect on CitZ-GFP levels in the forespore, using STRP to deplete ClpC-ssrA\* from the forespore resulted in the marked stabilization of CitZ-GFP in the forespore (Fig. 3C and D; Fig. S5A and B). Thus, CitZ-GFP appears to accumulate in the forespores of ClpC-deficient strains because of the direct action of ClpCP, not because of the failure to efficiently activate  $\sigma^F$ .

Since CitZ-GFP is depleted specifically from the forespore in a ClpC-dependent manner and *clpC* expression is regulated in part by  $\sigma^F$ , we reasoned that ClpC levels might become enriched in the forespore during engulfment, thereby conferring cell-specificity to degradation. We constructed a ClpC-GFP fusion and used fluorescence microscopy to evaluate ClpC levels within the sporangium. Importantly, strains expressing *clpC-gfp* from the native locus sporulated to wild-type levels, suggesting that the addition of the GFP tag does not interfere with ClpC function (Fig. S5C). Interestingly, we found ClpC-GFP to be present in near equimolar amounts in the mother cell and forespore (Fig. S5D and E). Furthermore, placing *clpC* under the control of a xylose-inducible promoter to uncouple expression from the native promoter complemented the *clpC* null mutant and also resulted in the forespore-specific clearance of CitZ-GFP (Fig. S5A to C). Altogether, our results suggest that CitZ-GFP is subjected to ClpCP-mediated proteolysis in the forespore, but that the ClpCP protease does not itself confer the cell-specificity of proteolysis. Therefore, an additional mechanism must exist to promote the ClpCP-mediated proteolysis of CitZ in the forespore.

We next sought to identify the forespore-encoded factor responsible for targeting CitZ-GFP for ClpCP-mediated degradation. To narrow our screen, we took advantage of the transient genetic asymmetry that exists between the mother cell and forespore following polar septation<sup>15</sup>. As a consequence of undergoing polar septation at the onset of sporulation, cell division occurs over one of the daughter chromosomes, initially trapping only a stereotyped, origin-proximal one-third of the chromosome in the forespore (Fig. S6A). The SpoIIIE ATPase forms a complex that then translocates the remaining, terminus-proximal two-thirds of the forespore chromosome into the forespore<sup>16</sup>. Mutants of SpoIIIE lacking ATPase activity still undergo compartmentalization, but fail to translocate the terminus-proximal region of the chromosome into the forespore<sup>17</sup>. Therefore, if the locus encoding the unknown factor resides at an origin-proximal locus, then the forespore-specific depletion of CitZ should not require SpoIIIE ATPase activity. On the other hand, if the locus encoding the unknown factor resides at a terminus-proximal locus, then the abolition of SpoIIIE ATPase activity should inhibit the clearance of CitZ-GFP from the forespore. When we introduced a SpoIIIE ATPase mutation into strains harboring a CitZ-GFP fusion, we found that CitZ-GFP was notably stabilized in the forespore, suggesting the locus encoding the unknown factor lies in a terminus-proximal location (Fig. S6B to C).

To identify the factor, we screened for genes that satisfied the following criteria: (1) the gene is regulated by  $\sigma^F$ , (2) the locus encoding the gene resides in the origin-distal two-thirds of the chromosome, and (3) the product encoded by the gene has no known function. In total, we identified 28 candidates that fulfilled these criteria. We obtained null mutants of all 28 candidate genes from the *Bacillus* Genetic Stock Center and used fluorescence microscopy to screen for mutants in which CitZ-GFP was stabilized in the forespore to a similar extent as the *clpC* null. Of all the candidates, only a single null mutant, *yjbA*, resulted in the stabilization of CitZ-GFP (Fig. 4A). YjbA is a

DUF3603-containing protein of unknown function that is broadly conserved in the aerobic *Bacilli*, but largely absent in the anaerobic *Clostridia* (Fig. 4B). The gene encoding YjbA resides in a genetic neighborhood that is notably enriched in genes encoding other Clp adaptor proteins, including *mecA*<sup>18</sup> and *yjbH*<sup>19</sup> (Fig. 4C). Therefore, we reasoned that YjbA is the forespore-specific factor that prompts the ClpCP-mediated degradation of CitZ.

For this hypothesis to be true, *yjbA* should only be expressed in the forespore, and not in the mother cell. To test this, we constructed transcriptional and translational fusions to *yjbA* and performed fluorescence microscopy to observe expression levels within the sporangium. As expected, GFP fluorescence signals above background were only detected in the forespore in both *yjbA-gfp* and *P<sub>yjbA</sub>-gfp* strains, demonstrating that YjbA is only produced in the forespore (Fig. S6D). To discern whether YjbA functions in the same degradation pathway as ClpCP, we performed an epistasis experiment. We reasoned that if YjbA and ClpCP function in the same pathway, then the simultaneous inactivation of both *yjbA* and *clpC* should not stabilize CitZ-GFP in the forespore to a greater extent than either of the single mutants individually. On the other hand, if YjbA functions in a pathway independent of ClpCP, then inactivation of both *yjbA* and *clpC* in combination should confer additional stabilization to CitZ-GFP in the forespore compared to either of the single mutants individually. Using fluorescence microscopy, we found that CitZ-GFP was stabilized to a similar extent in  $\Delta yjbA$ ,  $\Delta clpC$ , and  $\Delta yjbA$ ,  $\Delta clpC$  genetic backgrounds, indicating that YjbA and ClpCP comprise a single proteolytic pathway (Fig. 4D and E). Taken together, our data indicate that YjbA stimulates ClpCP activity, promoting the degradation of CitZ to downregulate the metabolic capabilities of the forespore.

Sporangia lacking YjbA readily form phase bright spores and suffer no apparent defects in development or revival under standard conditions (Fig. S7A to C). Genes

encoding YjbA homologs are broadly distributed among the aerobic spore forming *Bacilli*, yet conspicuously absent from the genomes of the anaerobic spore forming *Clostridia*. Therefore, we reasoned that YjbA activity might be important in overcoming environmental challenges faced uniquely by *Bacillus* spores, such as oxidative stress. *Bacillus* spores are notoriously resistant to oxidative stress and can survive treatment with modest concentrations of hypochlorite<sup>20</sup>. To test the role of YjbA in mediating spore tolerance to oxidative stress, we subjected sporulating cultures to treatment with hypochlorite and quantified hypochlorite-resistant spore titers by the ability to form colonies on nutrient replete plates. Strains lacking YjbA were highly sensitive to oxidative stress, exhibiting a marked, 20-fold decrease in the ability to withstand hypochlorite treatment (Fig. 5A). Furthermore, we noted that the colonies formed by outgrowing spores lacking YjbA were appreciably smaller than their wild-type counterparts following hypochlorite treatment. Therefore, we subjected purified wild-type and  $\Delta yjbA$  spores to hypochlorite treatment, and performed timelapse microscopy to investigate this phenotype at the single-cell level. Consistent with our population level observations on plates, spores lacking YjbA were notably delayed and severely compromised in outgrowth (Fig. 5B). Altogether, our results indicate that YjbA-induced proteolysis is required to promote a metabolic environment in the spore conducive to overcoming oxidative stress during spore revival.

We next wished to determine whether the YjbA-ClpCP degradation pathway acts specifically on CitZ, or if it functions more broadly to target multiple substrates for proteolysis in the forespore. We reasoned that if CitZ is the sole target of this degradation pathway, then depleting CitZ from the forespore by other means should bypass the requirement for YjbA and suppress the sensitivity to hypochlorite treatment. On the other hand, if there are additional targets of the YjbA-ClpCP pathway, then spores depleted of CitZ in the absence of YjbA should remain sensitive to treatment with

hypochlorite. To test this, we used STRP to deplete CitZ-ssrA\* from the forespore of sporangia lacking YjbA, and subjected them to treatment with hypochlorite. Using STRP to deplete CitZ-ssrA\* from the forespore did not yield any discernable effect on hypochlorite-resistant spore titers and failed to suppress the defect associated with the *yjbA* null mutant (Fig. 6A and B). Therefore, YjbA has a function apart from inducing the ClpCP-mediated degradation of CitZ in the forespore, suggesting that this system acts more broadly to reprogram forespore metabolism.

## Discussion

Here, we have shown that sporulation entails the dramatic metabolic differentiation of the mother cell and forespore shortly after polar septation. Our findings demonstrate that sporangia utilize multiple strategies to robustly dampen the metabolic capacity of the forespore during its transition to dormancy. One of these strategies relies simply on the volumetric growth of the forespore during engulfment to broadly reduce the levels of metabolic enzymes in the forespore. In addition to metabolic downregulation, recent work suggests that forespore growth is also required to promote membrane migration during engulfment. Thus, we are coming to appreciate the number of ways in which the physical properties of the cell can be harnessed to mediate complex behaviors<sup>10</sup>. Since vast networks of genes regulate the intrinsic features of the cell, systems governed by the physical properties of the cell may be less susceptible to inactivation by single mutations.

In addition to the intrinsic pathway, we also identified a novel cellular differentiation pathway in which YjbA promotes the ClpCP-mediated proteolysis of key metabolic enzymes to reduce the metabolic capabilities of the forespore. Regulatory proteolysis is known to mediate the transition between several different developmental states in *Bacillus subtilis*, including competence<sup>21</sup>, biofilm formation<sup>22</sup>, and sporulation<sup>8,13</sup>. This generally involves the use of specific adaptor proteins to elicit the degradation of

cell-fate determinants or transcriptional regulators, thereby achieving differentiation indirectly through the modulation of transcription<sup>23</sup>. Here, we have shown that YjbA acts directly to govern the differentiation of the mother cell and forespore by inducing the ClpCP-mediated proteolysis of metabolic enzymes in the forespore, and that YjbA constitutes one of the founding members of a sporulation-specific family of Clp adaptor proteins along with CmpA<sup>24</sup>. Altogether, our results demonstrate that YjbA-induced proteolysis constitutes an additional layer to cell-specific gene expression during spore formation, and represents one of the few examples in microbes where the metabolic reprogramming of genetically identical sister cells is achieved through proteolysis<sup>25,26</sup>.

Sporangia face a unique challenge where they must transition to dormancy, but also remain equipped to rapidly respond to changes in the nutrient status of the environment. The sporangium appears to overcome the first hurdle of attaining dormancy by transferring biosynthetic responsibilities to the mother cell<sup>7</sup>. The second obstacle seems to be overcome by targeting critical metabolic enzymes for proteolytic destruction in the developing spore, thereby limiting the flux through certain pathways during the transition to dormancy. Citrate synthase acts at a crucial metabolic intersection that links glycolysis and gluconeogenesis with the TCA cycle, and represents the rate-limiting step of the TCA cycle<sup>27</sup>. As such, citrate synthase is one of the most heavily regulated enzymes in the cell<sup>28</sup>. Here, we demonstrate that the overall activity of citrate synthase is additionally regulated by proteolysis in the forespore. We speculate that the proteolytic removal of citrate synthase limits flux into the TCA cycle during spore formation, while enabling the reviving spore to quickly resume metabolic activity when conditions are favorable. It remains to be seen if this is a general principle, whereby enzymes situated at key metabolic junctions are specifically targeted for proteolytic removal in the forespore. This strategy could ease the exit from dormancy by allowing the synthesis of a small subset of enzymes to completely restore flux and

reinitiate metabolic activity in the reviving spore, obviating the need to fully reconstruct each biosynthetic pathway de novo.

Spores that fail to undergo YjbA-mediated proteolysis are highly sensitive to hypochlorite-induced oxidative stress. Previous work has demonstrated that germination and outgrowth place a tremendous oxidative burden on the reviving spore<sup>29</sup>. It is well documented that the electron transport chain serves as a major source of reactive oxygen species generation in the cell<sup>30</sup>. To protect against oxidative damage, sporangia appear to decrease flux through the electron transport chain by a number of means, including reducing the levels of dehydrogenases<sup>31</sup> and TCA cycle enzymes<sup>7</sup>. Despite accumulating large stores of 3-phosphoglycerate<sup>32</sup>, a glycolytic intermediate that could be readily funneled into the TCA cycle, reviving spores do not seem to resume oxidative metabolism until late stages of outgrowth, after stress responses have been activated<sup>33</sup>. Our work suggests that the activity of YjbA depletes the spore of citrate synthase, thereby alleviating flux through the TCA cycle and electron transport chain and reducing the oxidative burden until the cell is fully equipped to handle it.

Our results suggest that YjbA targets multiple substrates for ClpCP-mediated proteolysis. The identification of a comprehensive list of substrates using trapping approaches will reveal how extensively this pathway acts<sup>34</sup>. Cataloging substrates of this pathway may also prove critical to elucidating the signals that elicit the recognition and illuminate the metabolic junctions that are important to regulate during spore formation and revival.

## **Materials and methods**

### **Strain construction**

All strains used in this study are derivatives of *Bacillus subtilis* PY79. A comprehensive list of strains used in this study is provided in Table S1. The plasmids and oligonucleotides used in strain construction are provided in Table S2 and S3,

respectively. All BKE strains and strain 1S138 from the *Bacillus* Genetic Stock Center were back-crossed twice into *Bacillus subtilis* PY79. All plasmid integrations were confirmed by PCR. All *Bacillus subtilis* strains were constructed by transformation using genomic DNA and a 2-step competence protocol, unless otherwise noted. Antibiotic concentrations used for selection following transformation of *Bacillus subtilis*: 10 µg/mL kanamycin, 100 µg/mL spectinomycin, 5 µg/mL chloramphenicol, 10 µg/mL tetracycline, 1 µg/mL erythromycin and 25 µg/mL lincomycin.

### **Culture conditions**

*Bacillus subtilis* strains were generally grown on LB agar plates at 30°C for culturing. Sporulation was induced in two different ways. For fluorescence microscopy experiments, cells were grown to O.D.<sub>600</sub> ~ 0.6 in ¼ diluted LB, and sporulation was induced by resuspension in A+B sporulation medium containing glutamate as the sole carbon source (Sterlini and Mandelstam, 1969). Here, the induction of sporulation was considered to be the moment at which the cells were resuspended in A+B medium. For spore titers and spore purification, sporulation was induced by exhaustion in the undefined Difco Sporulation Medium (DSM) (Schaeffer et al., 1965). In DSM, cells grow until nutrients become limiting. Here, sporulation induction was considered to be the moment at which the growth curve plateaued. Sporulation cultures were grown at 37°C for batch culture experiments, spore titers, and spore purification, and at 30°C for timelapse microscopy experiments.

### **Fluorescence and phase-contrast microscopy**

Cells were visualized on an Applied Precision DV Elite optical sectioning microscope equipped with a Photometrics CoolSNAP-HQ2 camera. Images were deconvolved using SoftWoRx v5.5.1 (Applied Precision) and quantitative image analysis was performed using FIJI. The median focal planes are shown.



### **Batch culture microscopy**

To assess the GFP fluorescence signals in the mother cell and forespore, sporulation was induced by resuspension in A+B medium. To visualize the membranes, 0.5  $\mu\text{g}/\text{mL}$  FM 4-64 was added to the culture 1 hour after sporulation induction, and sporulation allowed to proceed for an additional 2 hours under standard culturing conditions. At three hours following sporulation induction, 12  $\mu\text{l}$  of culture was transferred to 1.2% agarose pads, prepared in A+B medium and supplemented with an additional 0.5  $\mu\text{g mL}^{-1}$  FM 4-64 (Life Technologies). Excitation/emission filters were TRITC/CY5 for membrane imaging (100 ms exposure time), and FITC/FITC for GFP imaging (600 ms exposure time), with excitation light transmission set to 100% for both filters.

We also used microscopy to assess the completion of two developmental milestones: engulfment completion and forespore maturation. Engulfment completion was monitored using a well-characterized membrane fission assay (Sharp and Pogliano, 1999). Briefly, cells are treated with a red membrane-impermeable membrane dye, FM 4-64, and a green membrane-permeable membrane dye, Mitotracker Green (MTG). During engulfment, forespore membranes are accessible to both dyes. Following membrane fission, however, the forespore membranes can no longer be stained by the red dye, and are therefore only labeled by the green dye. Forespore maturation was assessed by phase contrast microscopy. Mature spores become partially dehydrated, which confers upon them a bright appearance under phase-contrast microscopy. Thus, the extent to which developing spores become phase-bright can be used as a metric of spore maturation.

### **Forespore to mother cell GFP fluorescence ratio quantification**

We used the forespore:mother cell fluorescence ratio as a measure of the extent to which forespore enzymes were depleted from the forespore since the fluorescence signal in the mother cell remained more or less constant throughout engulfment for each

fusion. This allowed us to correct for any effects caused by photobleaching, and also allowed us to more readily compare across fusions, given the variability in the abundance of different proteins. The ratio of GFP intensity between forespore and mother cell was measured semi-automatically using a custom script in Matlab 2017b. Forespore and mother cell objects were identified and segmented from a single FM 4-64 z-stack by taking advantage of the increased fluorescence around the forespore. Thresholding high allowed for identification of forespores while thresholding low gave the whole cell outline. Subtracting the forespore image from the whole cell image allowed mother cells to be identified. Forespores were then paired to their corresponding mother cells first by filtering mother cell objects based on Euclidean distance, and then by the orientation of the mother cell. These filters were made strict to reduce false matches. GFP fluorescence ratio was calculated by using the paired forespore-mother cell objects to mask the GFP fluorescence image in order to obtain a mean fluorescence intensity for both.

### **Fluorescence timelapse microscopy**

For fluorescence timelapse microscopy, sporulation was induced by resuspension in A+B medium at 30°C. To visualize the membranes, 0.5 µg/mL FM 4-64 was added to the culture an hour after sporulation induction and incubated for an additional two hours under standard culturing conditions. 10 µL samples of culture were taken 2 h after resuspension and transferred to agarose pads prepared as follows: 2/3 volume of sporulation culture supernatant; 1/3 volume of 3.6% agarose prepared in fresh A+B sporulation medium; 0.17 µg/mL FM 4-64. For antibiotic experiments, pads were additionally supplemented with either 30 µg/mL cerulenin or 100 µg/mL chloramphenicol. Pads were partially dried at 30°C, covered with a glass coverslip, and sealed with petroleum jelly to avoid dehydration during timelapse imaging (Ojkic et al., 2016). Pictures were taken in an environmental chamber at 30°C every 5 min for at least 2 h.

Excitation/emission filters were TRITC/CY5 for membrane imaging (100 ms exposure), and FITC/FITC for GFP imaging (300 ms exposure). Excitation light transmission was set to 5% for membrane imaging and 32% for GFP imaging to minimize phototoxicity. For presentation purposes, sporangia were aligned vertically (with forespore on top) using Photoshop to rotate the images. To quantify depletion kinetics, we measured the mean GFP fluorescence signal in the mother cell and the forespore cytoplasm over time by drawing polygons encompassing either cell in FIJI. After subtracting the mean background fluorescence, we calculated the mean fluorescence ratio between the forespore and the corresponding mother cell, allowing us to correct for photobleaching. We relativized the fluorescence ratios of all time points to the initial time point, which was arbitrarily given the value of one.

### **Spore purification**

Sporulation was induced in DSM and allowed to proceed for 72 hours at 37°C. Cultures were pelleted and washed once with 4°C sterile water. To lyse remaining vegetative cells, spore samples were incubated overnight at 4°C in sterile water. The following day, the spore samples were pelleted by centrifugation, washed once with 4°C sterile water, and incubated again overnight at 4°C in sterile water. Spores were then further purified over a phosphate-polyethylene glycol aqueous biphasic gradient as previously described (Harrold et al., 2011). The organic phase (top) containing the purified spores was harvested and washed with 50 or more volumes of 4°C sterile water at least three times. The spores were pelleted, resuspended in fresh sterile water, and stored at 4°C. Sample purity was evaluated using phase-contrast microscopy.

### **Phase-contrast timelapse microscopy**

Purified spores were diluted to an O.D.<sub>600</sub> of 0.3 in sterile water, and 10 µL of the spore suspension was applied to 1.2% agarose pads prepared in LB and supplemented with the 10 mM of the germinant, L-alanine. Pads were partially dried, covered with a

glass cover slip, and sealed with petroleum jelly to avoid dehydration during timelapse imaging. Phase-contrast imaging was performed in an environmental chamber set to 30°C. Images were acquired every 3 min for 10 hours using POL/POL filters. Light transmission was set to 32% and exposure time was 0.1 s. Note that, due to sample preparation, there was a time lag of approximately 15 min before imaging commenced. To minimize the germination of spores on the pads during this time, spores were not heat-activated before performing timelapse microscopy. We focused on spores that were phase-bright at the onset of imaging. For NaOCl experiments, purified spores were first treated with 0.25 % (v/v) NaOCl for 18 min. Samples were pelleted by gentle centrifugation, and washed 3 times with phosphate-buffered saline before diluting to an O.D.<sub>600</sub> of 0.3 in sterile water.

### **Spore titers**

Strains were cultured in 2 mL of DSM for 24 hours at 37°C. To test the efficiency of ClpC-ssrA\* degradation, *sspB<sup>Ec</sup>* expression was induced by supplementing DSM cultures with 1 % xylose or an equivalent volume of vehicle (sterile water). After 24 hours, cultures were either heated at 80°C for 20 min, or subjected to treatment with 0.25 % NaOCl for 18 min, serially diluted in 1x T-Base, and plated on LB. Spore titers were calculated based on the number of colony forming units (CFU).

### **Quantification of spore germination by loss of optical density**

Germination assays by loss of O.D.<sub>580</sub> were performed as described in *Harwood et al. (1990)*. Briefly, spores were heat activated at 70°C for 20 min in water, and resuspended to a final O.D.<sub>580</sub> of 0.3 in 10 mM Tris-HCl, pH 8.4. The resuspended spores were incubated for 20 min at 37°C, and then germination was induced by the addition of 10 mM L-alanine. The O.D.<sub>580</sub> was measured every 5 min for an hour. For NaOCl experiments, purified spores were first treated with 0.25 % (v/v) NaOCl for 18

min, pelleted by gentle centrifugation, and washed 3 times with phosphate-buffered saline before diluting to an O.D.<sub>600</sub> of 0.3 in sterile water.

## ACKNOWLEDGEMENTS

Chapter IV, in full, is currently being prepared for submission to PNAS. Riley, Eammon P.; Sugie, Joseph; Enustun, Eray; Armbruster, Emily; Ravishankar, Sumedha; Pogliano, Kit. The dissertation author was the primary investigator and author of this paper. Permission from all authors has been obtained.

## Figures

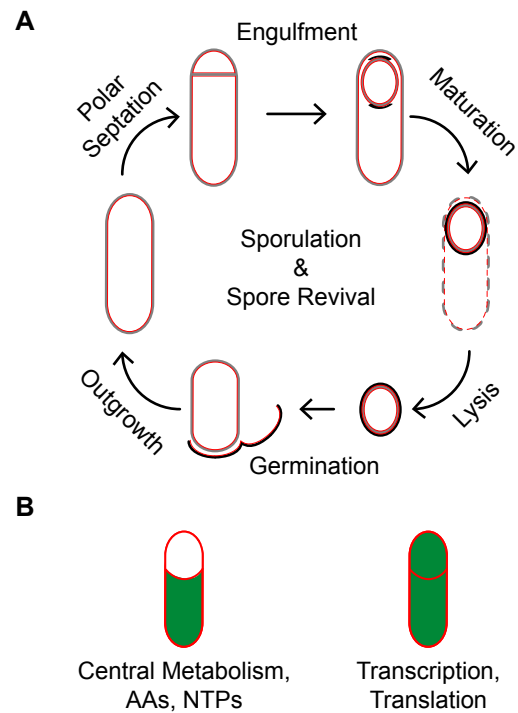


**Figure 4.1.** Mother cell and forespore become metabolically differentiated during spore formation. (A) Diagram of spore formation and revival pathways in *Bacillus subtilis*. Membranes are represented in red, peptidoglycan is represented in gray, and the spore coat is represented in black. (B) Diagram representing the division of metabolic responsibilities during spore formation. Central carbon metabolism, amino acid synthesis, and nucleotide synthesis all become mother cell specific, whereas transcription and translation are performed in both the mother cell and the forespore.

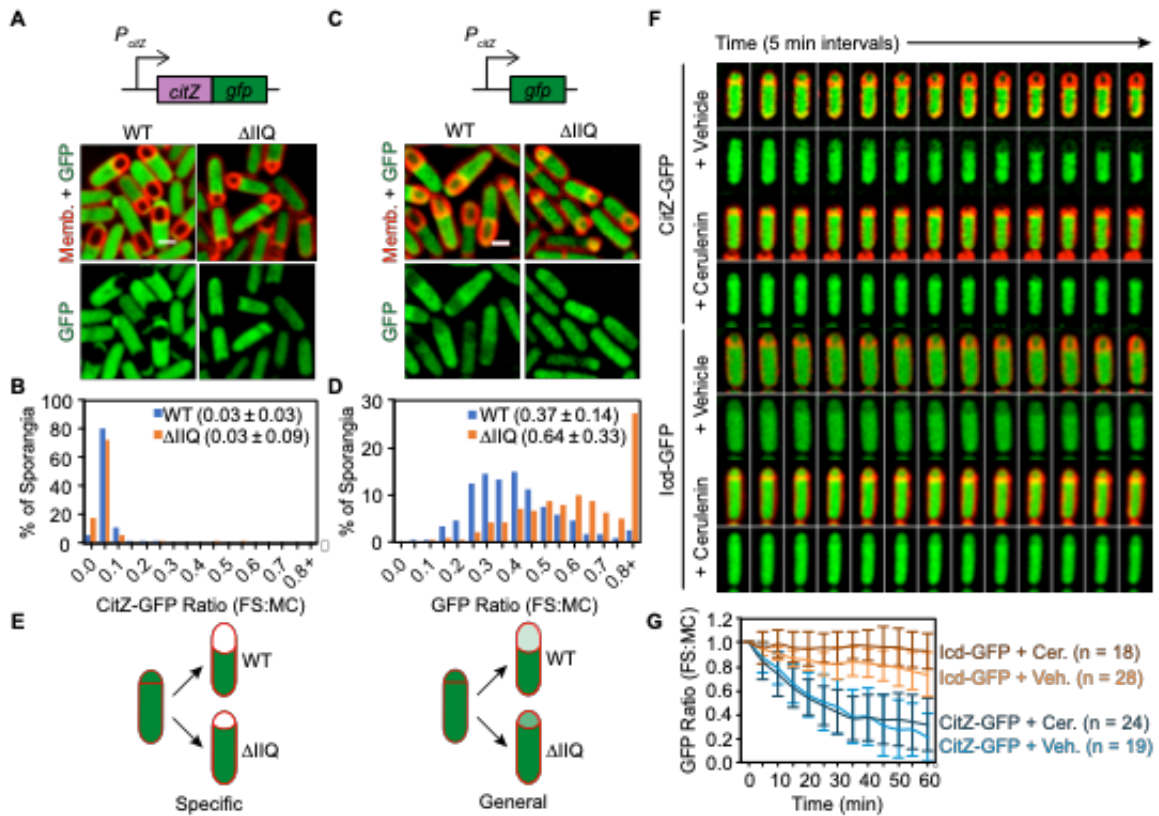


**Figure 4.2.** Two mechanisms underlie the metabolic reprogramming of the forespore. (A) Fluorescence micrographs of a translational fusion of GFP to CitZ (green) in wild-type (WT) and  $\Delta spolIQ$  ( $\Delta IIQ$ ) genetic backgrounds. Membranes are in red. Scale bar,  $1\mu\text{m}$ . (B) Histogram of forespore to mother cell CitZ-GFP fluorescence ratios when produced in wild-type (WT, blue) or  $\Delta spolIQ$  ( $\Delta IIQ$ , orange) genetic backgrounds. Mean ratios  $\pm$  standard deviations of at least 69 sporangia are indicated in parentheses. (C) Fluorescence micrographs of a transcriptional fusion of GFP to  $P_{citZ}$  (green) in wild-type (WT) and  $\Delta spolIQ$  ( $\Delta IIQ$ ) genetic backgrounds. Membranes are in red. Scale bar,  $1\mu\text{m}$ . (D) Histogram of forespore to mother cell GFP fluorescence ratios when produced from  $P_{citZ}$  in wild-type (WT, blue) or  $\Delta spolIQ$  ( $\Delta IIQ$ , orange) genetic backgrounds. Mean ratios  $\pm$  standard deviations of at least 224 sporangia are indicated in parentheses. (E) Model showing specific (left) and general (right) mechanisms of forespore metabolic reprogramming. Red represents membranes, and green represents high (darker shades) or low (lighter shades) levels of metabolic enzymes predicted under each regime in wild-type (WT) or  $\Delta spolIQ$  ( $\Delta IIQ$ ) genetic backgrounds. (F) Timelapse fluorescence microscopy of sporangia producing either CitZ-GFP or Icd-GFP (green), treated with vehicle or with cerulenin ( $30\ \mu\text{g/mL}$ ). Membranes are in red. Images acquired every 5 min are shown. (G) Forespore to mother cell GFP fluorescence ratios over time for strains described in (F) during treatment with vehicle or cerulenin ( $30\ \mu\text{g/mL}$ ). Values were relativized to the respective initial ratio at  $t_0$ . Values represent the mean  $\pm$  SD of at least 18 sporangia per condition.



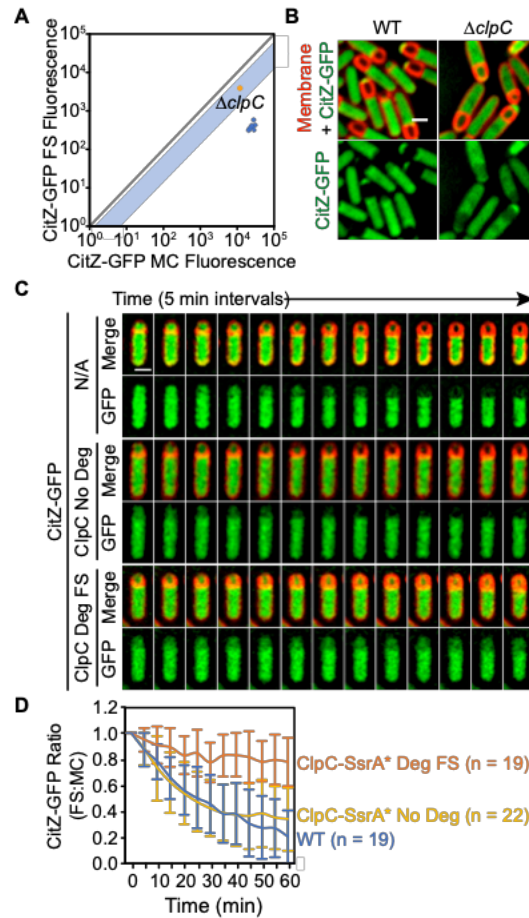


**Figure 4.3.** ClpCP is required for proteolysis of CitZ in the forespore, but does not confer cell-specificity. (A) Background subtracted mean fluorescence signal in arbitrary units of CitZ-GFP in the mother cell and forespore of different protease null mutants. The gray diagonal line represents values where the fluorescence signal of the mother cell is equal to the fluorescence signal of the forespore, and divides the regions of the graphs in which the signal is enriched in the forespore (left) or in the mother cell (right). The blue stripe indicates the region where values are expected to fall given the dilution caused by forespore growth. Each dot represents mean reading from an individual null mutant expressing *citZ-gfp*. The null mutant in which CitZ-GFP was stabilized in the forespore is indicated in orange ( $\Delta clpC$ ). (B) Fluorescence micrographs of CitZ-GFP (green) in indicated genetic backgrounds. Membranes are in red. Scale bar, 1  $\mu$ m. (C) Fluorescence timelapse microscopy of strains producing CitZ-GFP in the wild-type background (N/A), in a background in which ClpC-ssrA\* is produced in the absence of degradation (No Deg), or in a background in which ClpC-ssrA\* is produced and degradation is induced through SspB production in the forespore (Deg FS). Membranes are in red. Scale bar, 1  $\mu$ m. (D) Forespore to mother cell CitZ-GFP fluorescence ratio over time in strains described in (C), relativized to the initial ratio at  $t_0$ . Values represent the mean  $\pm$  SD.

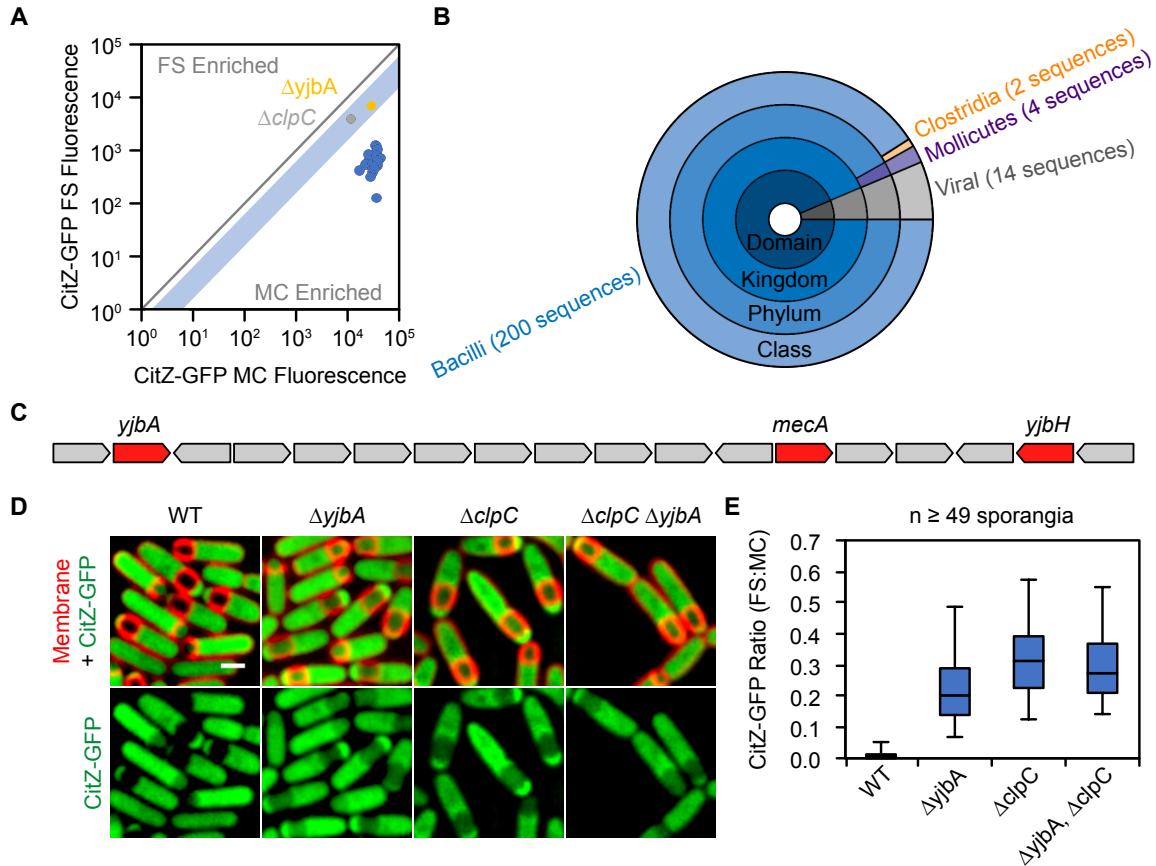


**Figure 4.4.** YjbA is required for ClpCP-mediated proteolysis of CitZ in the forespore. (A) Background subtracted mean fluorescence signal in arbitrary units of CitZ-GFP in the mother cell and forespore of different  $\sigma^F$  regulon null mutants. The gray diagonal line represents values where the fluorescence signal of the mother cell is equal to the fluorescence signal of the forespore, and divides the regions of the graphs in which the signal is enriched in the forespore (left) or in the mother cell (right). The blue stripe indicates the region where values are expected to fall given the dilution caused by forespore growth. Each dot represents mean reading from an individual null mutant expressing *citZ-gfp*. The two null mutants in which CitZ-GFP was stabilized in the forespore are indicated in gray ( $\Delta clpC$ ) and yellow ( $\Delta yjbA$ ). (B) Phylogenetic tree representing the distribution of YjbA homologs across different taxa. Blue represents *Bacilli* homologs, orange represents *Clostridia* homologs, purple represents *Mollicute* homologs, and gray represents viral homologs. Tree was adapted from the sunburst depiction found on the Pfam database (<http://pfam.xfam.org/family/PF12227>). (C) Diagram depicting the genetic context of *yjbA* in the *Bacillus subtilis* genome. Genes encoding Clp adaptor proteins are indicated in red, and intervening genes in gray. Diagram is not to scale. (D) Fluorescence micrographs of CitZ-GFP (green) in indicated genetic backgrounds. Membranes are in red. Scale bar, 1  $\mu$ m. (E) Box and whisker plot showing forespore to mother cell fluorescence ratio of CitZ-GFP in indicated genetic backgrounds. The boxes represent the middle 75% of the data, and the vertical bars the middle 90%. Median values are indicated by horizontal lines inside the boxes. At least 49 sporangia were assayed for each strain.

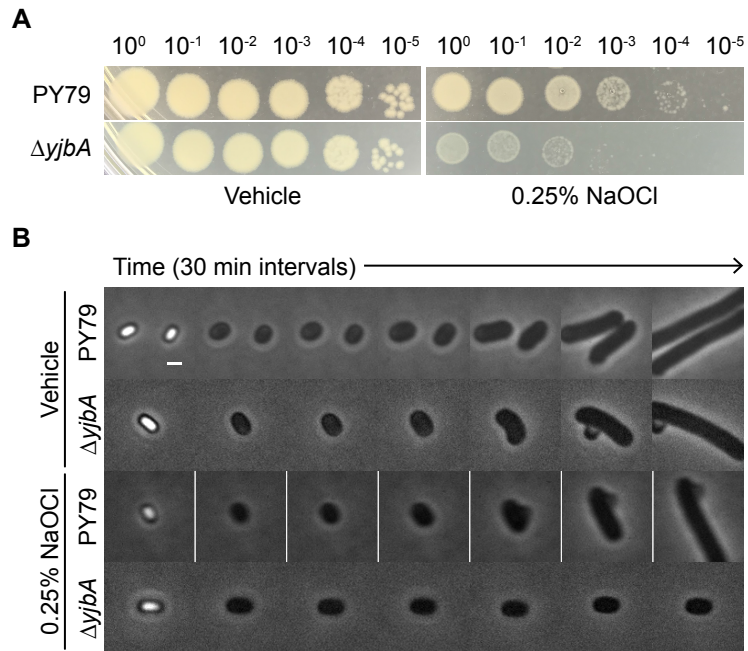


**Figure 4.5.** Spores lacking YjbA are sensitive to NaOCl-induced oxidative stress. (A) Spot dilutions of the indicated strains after overnight sporulating cultures in DSM were subjected to treatment with either 0.25% NaOCl or vehicle for 18 min. Samples were serially diluted in 10-fold increments in 1x T-Base. 5  $\mu$ L of each dilution was spotted on an LB agar plate. (B) Phase-contrast timelapse microscopy of reviving spores from the indicated strains that were either treated with 0.25% NaOCl or vehicle for 18 min. Spore samples were washed three times and diluted to an O.D.<sub>580</sub> of 0.3 in phosphate-buffered saline following treatment. Images acquired every 30 min for 3 h are shown. Scale bar, 1  $\mu$ m.

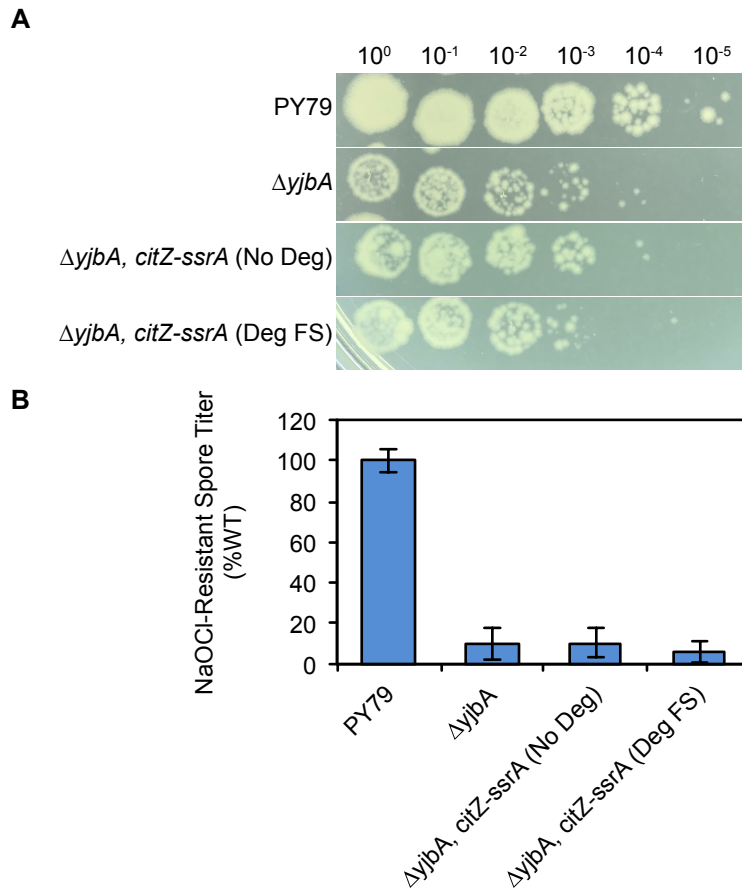


**Figure 4.6.** Degrading CitZ via STRP does not suppress the NaOCl sensitivity of the  $\Delta yjbA$  mutant. (A) Spot dilutions of the indicated strains after overnight sporulating cultures in DSM were subjected to treatment with 0.25% NaOCl for 18 min. Samples were serially diluted in 10-fold increments in 1x T-Base. 5  $\mu$ L of each dilution was spotted on an LB agar plate. (B) NaOCl-resistant spore titers of the indicated strains, relative to the PY79 wild-type strain. Overnight sporulating cultures in DSM were subjected to treatment with 0.25% NaOCl for 18 min. Data represent the mean  $\pm$  the standard deviations from three independent biological replicates.

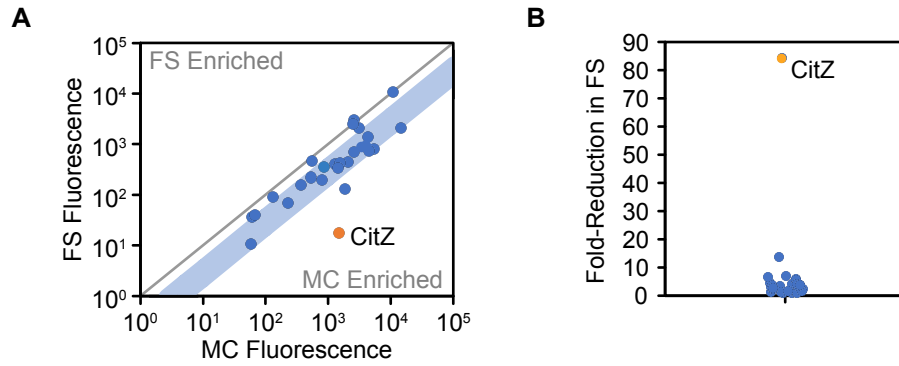


**Figure 4.S1.** Citrate synthase is depleted to a larger extent in the forespore than other metabolic enzymes. (A) Background subtracted mean fluorescence signal in arbitrary units of GFP fusions to different metabolic enzymes in the mother cell and forespore. The gray diagonal line represents values where the fluorescence signal of the mother cell is equal to the fluorescence signal of the forespore, and divides the regions of the graphs in which the signal is enriched in the forespore (left) or in the mother cell (right). The blue stripe indicates the region where values are expected to fall given the dilution caused by forespore growth. Each dot represents mean reading of an individual metabolic enzyme fused to GFP. CitZ-GFP is indicated in orange. (B) Plot showing the fold-reduction of the fluorescence signal in the forespore compared to the mother cell of different GFP fusions to metabolic enzymes. Each dot represents a GFP fusion to a different metabolic enzyme, with CitZ-GFP indicated in orange.

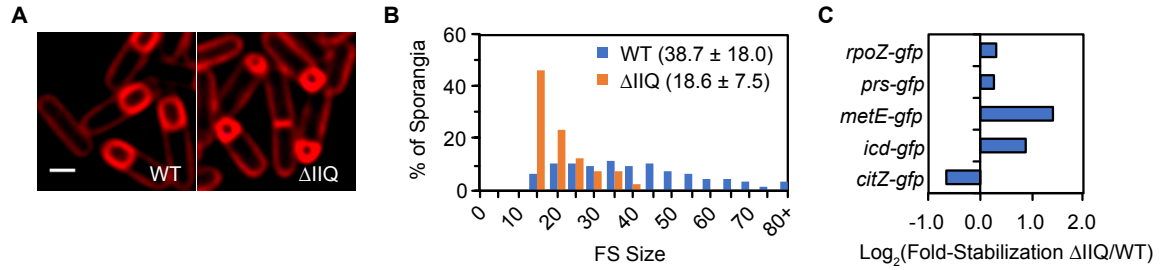


**Figure 4.S2.** Suppression of forespore growth through *spoIIQ* inactivation does not stabilize citrate synthase in the forespore. (A) Fluorescence micrographs of wild-type and  $\Delta spoIIQ$  sporangia. Membranes are in red. Scale bar, 1  $\mu$ m. (B) Histogram of forespore sizes of wild-type (WT, blue) and  $\Delta spoIIQ$  ( $\Delta IIQ$ , orange) sporangia. Mean sizes  $\pm$  standard deviations of at least 235 forespores measured for each strain are indicated in parentheses. (C) Plot showing stabilization of GFP fusions to different metabolic enzymes in a  $\Delta spoIIQ$  background. The x-axis compares the forespore to mother cell fluorescence ratio of each respective fusion in a  $\Delta spoIIQ$  genetic background to the respective forespore to mother cell fluorescence ratio in the wild-type background and represents the  $\log_2(FS^{\Delta spoIIQ}:MC^{\Delta spoIIQ}/FS^{WT}:MC^{WT})$ .

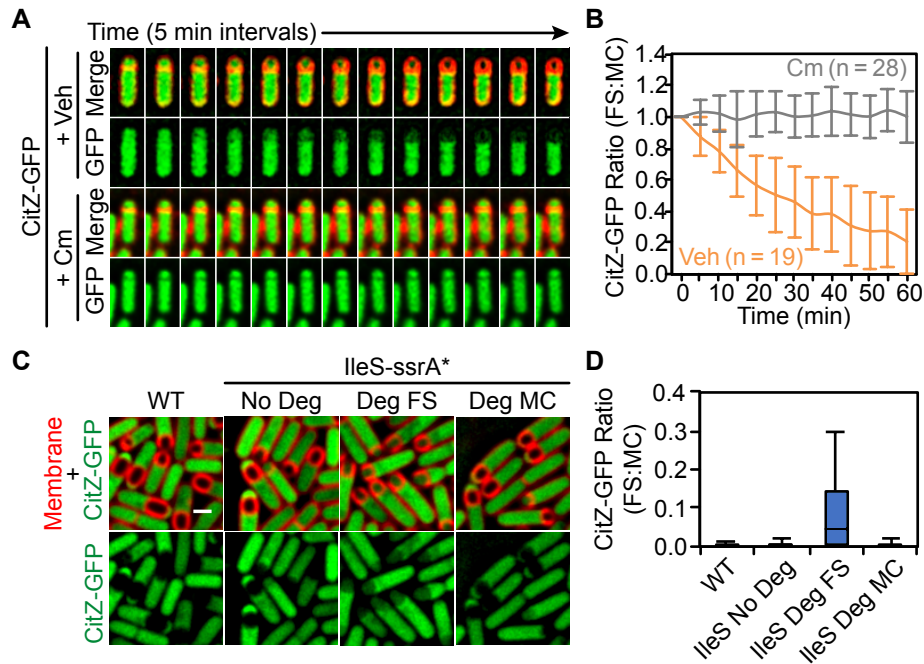


**Figure 4.S3.** New protein synthesis is required in the forespore for the depletion of citrate synthase. (A) Timelapse fluorescence microscopy of a strain producing CitZ-GFP (green) subjected to treatment with vehicle or with chloramphenicol (100  $\mu\text{g}/\text{mL}$ ). Membranes are in red. Images acquired every 5 min are shown. (B) Forespore to mother cell fluorescence ratio of CitZ-GFP over time in sporangia treated with vehicle or with chloramphenicol (100  $\mu\text{g}/\text{mL}$ ), relativized to the initial ratio at  $t_0$ . Values represent the mean  $\pm$  SD for at least 19 sporangia per condition. (C) Fluorescence micrographs of CitZ-GFP (green) in wild-type sporangia, in sporangia producing IleS-ssrA\* (No Deg), in sporangia in which IleS-ssrA\* is produced and subjected to degradation in the forespore (Deg FS), or in sporangia in which IleS-ssrA\* is produced and subjected to degradation in the mother cell (Deg MC). Membranes are in red. Scale bar, 1  $\mu\text{m}$ . (D) Box and whisker plots of the forespore to mother cell CitZ-GFP ratio in strains described in (C). The boxes represent the middle 75% of the data, and the vertical bars the middle 90%. Median values are indicated by horizontal lines inside the boxes. At least 234 sporangia were assayed for each strain.

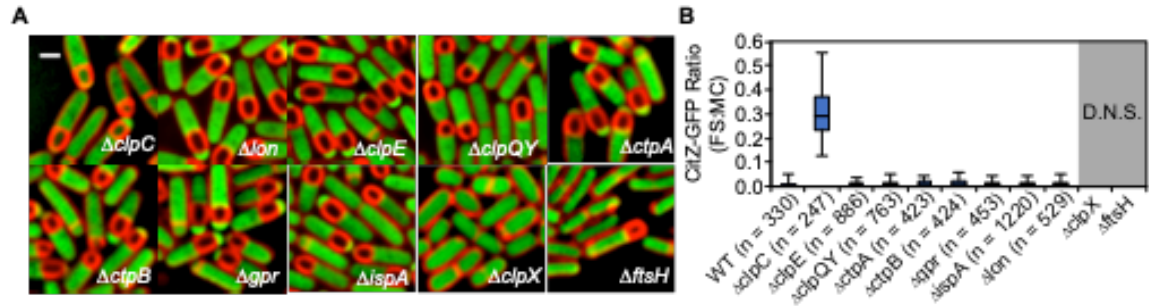


**Figure 4.S4.** ClpCP is required for the depletion of citrate synthase in the forespore. (A) Fluorescence micrographs of CitZ-GFP (green) produced in the indicated genetic backgrounds. Membranes are in red. Scale bar, 1  $\mu m$ . (B) Box and whisker plots of the forespore to mother cell CitZ-GFP ratio in the indicated genetic background. The boxes represent the middle 75% of the data, and the vertical bars the middle 90%. Median values are indicated by horizontal lines inside the boxes. At least 247 sporangia were assayed for each genetic background, except for  $\Delta clpX$  and  $\Delta ftsH$ , which did not sporulate efficiently (D.N.S.).



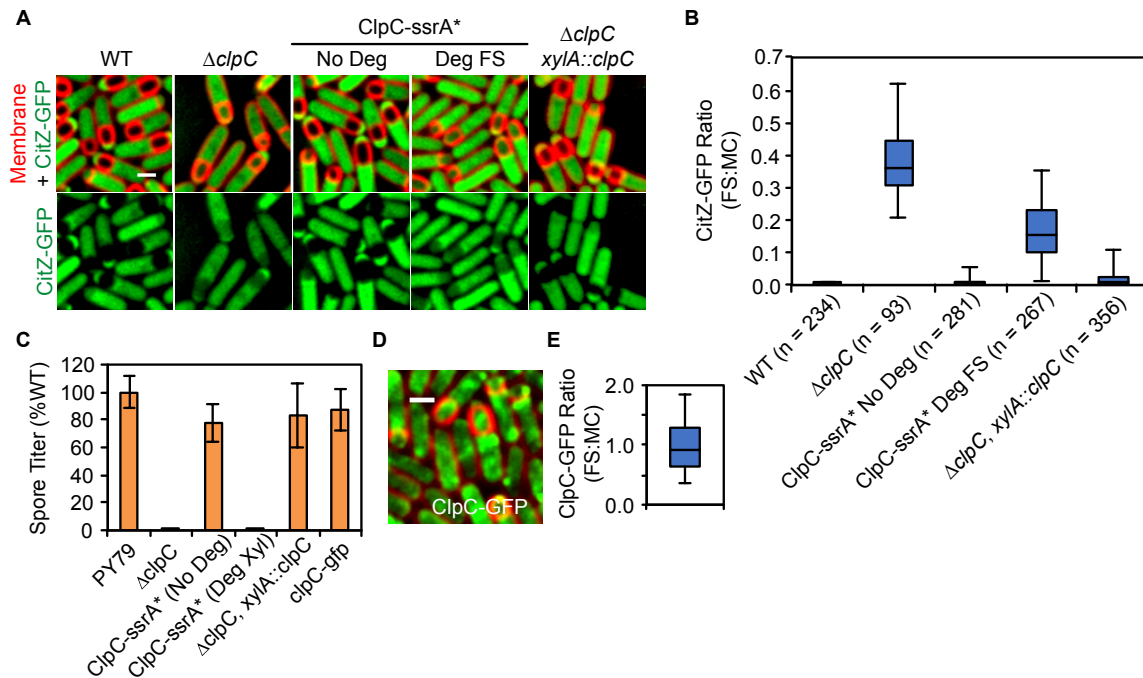


**Figure 4.S5.** ClpCP does not confer cell-specificity to the proteolysis of citrate synthase. (A) Fluorescence micrographs of CitZ-GFP (green) in wild-type sporangia,  $\Delta clpC$  mutant sporangia, in sporangia producing ClpC-ssrA\* (No Deg), in sporangia producing ClpC-ssrA\* in which degradation is induced in the forespore (Deg FS), or in  $\Delta clpC$  mutant sporangia producing ClpC under the control of a xylose-inducible promoter in the presence of 0.1% xylose. Membranes are in red. Scale bar, 1  $\mu$ m. (B) Box and whisker plots of the forespore to mother cell CitZ-GFP ratio in the genetic backgrounds described in (A). The boxes represent the middle 75% of the data, and the vertical bars the middle 90%. Median values are indicated by horizontal lines inside the boxes. At least 93 sporangia were assayed for each genetic background. (C) Heat-resistant spore titers of wild-type sporangia (PY79), of sporangia lacking ClpC ( $\Delta clpC$ ), of sporangia producing ClpC-ssrA\* without inducing degradation (No Deg), of sporangia producing ClpC-ssrA\* inducing degradation with 1 % xylose (Deg Xyl), of  $\Delta clpC$  sporangia producing ClpC from a xylose-inducible promoter with induction of 0.1% xylose, and of sporangia producing ClpC-GFP. The data are normalized to the wild-type strain (PY79) and represent the mean  $\pm$  SD of at least three independent biological replicates. (D) Fluorescence micrograph of sporangia producing ClpC-GFP (green). Membranes are in red. Scale bar, 1  $\mu$ m. (E) Forespore to mother cell fluorescence ratio of ClpC-GFP. The boxes represent the middle 75% of the data, and the vertical bars the middle 90%. Median values are indicated by horizontal lines inside the boxes. At least 100 sporangia were analyzed.

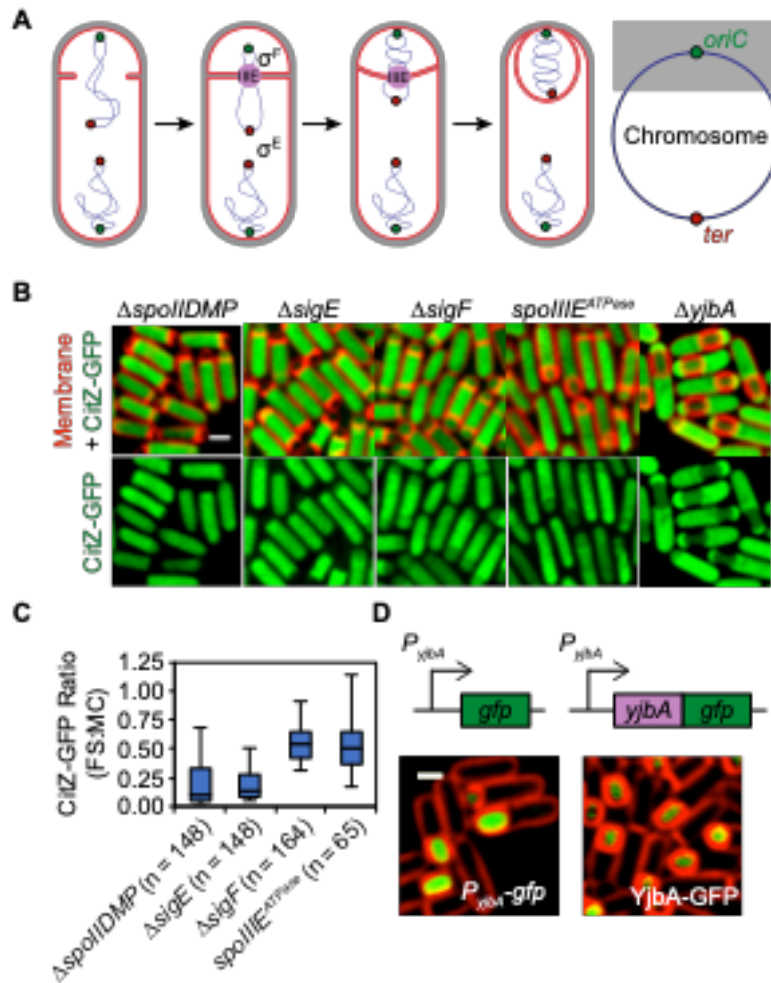


**Figure 4.S6.** Screen identifying YjbA as the novel ClpCP adaptor protein. (A) Diagram representing polar septation, chromosome translocation, and engulfment (left), showing the chromosomes (indigo), *oriC* (green circle), terminus (red circle), SpoIIIE (lavender), membranes (red), and peptidoglycan (gray). Arrows indicate passage of time. The region of the chromosome initially trapped in the forespore is indicated by gray shading (right). (B) Fluorescence micrographs of CitZ-GFP (green) produced in sporangia lacking SpoIIDMP ( $\Delta spoIIDMP$ ), lacking  $\sigma^E$  ( $\Delta sigE$ ), lacking  $\sigma^F$  ( $\Delta sigF$ ), producing an ATPase mutant of SpoIIIE ( $spoIIIE^{ATPase}$ ), or lacking YjbA ( $\Delta yjbA$ ). Membranes are in red. Scale bar, 1  $\mu$ m. (C) Box and whisker plots of the forespore to mother cell CitZ-GFP ratio in the genetic backgrounds described in (B). The boxes represent the middle 75% of the data, and the vertical bars the middle 90%. Median values are indicated by horizontal lines inside the boxes. At least 65 sporangia were assayed for each genetic background. (D) Transcriptional and translational fusions of GFP to  $P_{citZ}$  and CitZ, respectively, shown in green. Membranes are in red. Scale bar, 1  $\mu$ m.

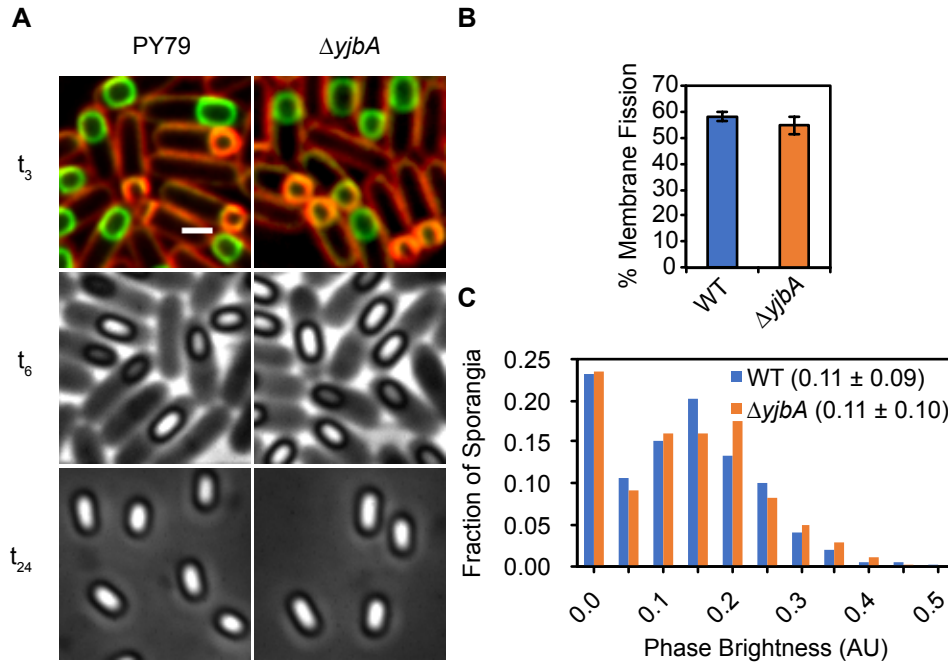


**Figure 4.S7.** Sporangia lacking YjbA suffer no severe defects in development. (A) Micrographs of wild-type and  $\Delta yjbA$  sporangia. Fluorescence micrographs of cells harvested 3 hours after sporulation induction ( $t_3$ ) are shown. Phase-contrast micrographs of cells harvested 6 hours ( $t_6$ ) or 24 hours ( $t_{24}$ ) after sporulation induction. Membranes are stained with FM 4-64 (red) and Mitotracker Green (MTG, green). During engulfment, forespore membranes are accessible to both the red and the green dyes. Following engulfment completion, however, forespore membranes cannot be stained by the red dye, and are clearly visible as green ovals inside the mother cells. Scale bar, 1  $\mu$ m. (B) Percent of wild-type (blue) and  $\Delta yjbA$  (orange) sporangia completing membrane fission 3 hours after sporulation induction. Means  $\pm$  SEM for three independent experiments are shown. (C) Histogram showing extent of phase-bright spore formation of wild-type (blue) and  $\Delta yjbA$  (orange) sporangia 6 hours following sporulation induction. Over 937 sporangia were analyzed for each strain. Mean phase-brightness  $\pm$  SD are given for each strain in parentheses.

## Tables

<b>Table 4.S1. Strains used in this study</b>		
<b>Strain</b>	<b>Genotype or description</b>	<b>Reference, source or construction<sup>a</sup></b>
1S138	$\Delta csfG::kan$	(Koo et al., 2017)
BER0100	$pelB::P_{spolVA}-sspB^{Ec}\Omega spc$	(Riley et al., 2018)
BER0131	$pelB::P_{cotE}-sspB^{Ec}\Omega spc$	(Riley et al., 2018)
BER0504	$\Delta clpX::tet$	(Riley et al., 2018)
BER0607	$citZ-ssrA^*$	pCrePA→JLG1952 (Em)
BER0707	$\Delta clpC::tet$	pER161→PY79 (Tc)
BER0715	$\Delta clpX::tet, citZ-GFP\Omega kan$	BER0504→JLG2113 (Tc)
BER0716	$\Delta clpC::tet, citZ-GFP\Omega kan$	BER0707→JLG2113 (Tc)
BER0717	$\Delta lon::cat, citZ-GFP\Omega kan$	KP419→JLG2113 (Cm)
BER0835	$clpC-ssrA^*\Omega kan$	pER179→PY79 (Km)
BER0889	$clpC-ssrA^*\Omega kan, \Delta xylA::sspB^{Ec}\Omega cat$	BER0835→JLG364 (Km)
BER0905	$citZ-gfp$	pCrePA→JLG2113 (Em)
BER0906	$icd-gfp$	pCrePA→JLG2114 (Em)
BER0920	$clpC-ssrA^*\Omega kan, citZ-gfp$	BER0835→BER0905 (Km)
BER0961	$citB-GFP\Omega kan$	pER217→PY79 (Km)
BER0990	$rpoC-GFP\Omega kan$	pER227→PY79 (Km)
BER0991	$rpsB-GFP\Omega kan$	(Lopez-Garrido et al., 2018)
BER1091	$guaB-GFP\Omega kan$	pER261→PY79 (Km)
BER1093	$pyrE-GFP\Omega kan$	pER263→PY79 (Km)
BER1094	$purD-GFP\Omega kan$	pER264→PY79 (Km)
BER1095	$rpoZ-GFP\Omega kan$	pER265→PY79 (Km)
BER1097	$lysA-GFP\Omega kan$	pER267→PY79 (Km)
BER1098	$metE-GFP\Omega kan$	pER268→PY79 (Km)
BER1099	$cysK-GFP\Omega kan$	pER269→PY79 (Km)

**Table 4.S1. Strains used in this study (continued)**

Strain	Genotype or description	Reference, source or construction <sup>a</sup>
BER1100	<i>aspB-GFP</i> $\Omega$ <i>kan</i>	pER270→PY79 (Km)
BER1101	<i>leuD-GFP</i> $\Omega$ <i>kan</i>	pER271→PY79 (Km)
BER1102	<i>argH-GFP</i> $\Omega$ <i>kan</i>	pER272→PY79 (Km)
BER1103	<i>rplL-GFP</i> $\Omega$ <i>kan</i>	pER273→PY79 (Km)
BER1104	<i>ysxC-GFP</i> $\Omega$ <i>kan</i>	pER274→PY79 (Km)
BER1106	<i>rnz-GFP</i> $\Omega$ <i>kan</i>	pER276→PY79 (Km)
BER1107	<i>gapB-GFP</i> $\Omega$ <i>kan</i>	pER277→PY79 (Km)
BER1110	<i>prs-GFP</i> $\Omega$ <i>kan</i>	pER280→PY79 (Km)
BER1112	<i>ald-GFP</i> $\Omega$ <i>kan</i>	pER282→PY79 (Km)
BER1113	<i>trmU-GFP</i> $\Omega$ <i>kan</i>	pER283→PY79 (Km)
BER1215	<i>clpC-ssrA*</i> $\Omega$ <i>kan</i> , <i>amyE::P<sub>spolIQ</sub>-sspB<sup>Ec</sup></i> $\Omega$ <i>cat</i>	BER0835→JLG170 (Km)
BER1216	<i>clpC-ssrA*</i> $\Omega$ <i>kan</i> , <i>pelB::P<sub>spolVA</sub>-sspB<sup>Ec</sup></i> $\Omega$ <i>sps</i>	BER0835→BER0100 (Km)
BER1222	$\Delta$ <i>spolIQ::sps</i> , <i>citZ-GFP</i>	KP575→BER0905 (Sp)
BER1224	<i>amyE::P<sub>spolIQ</sub>-sspB<sup>Ec</sup></i> $\Omega$ <i>cat</i> , <i>citZ-gfp</i>	JLG170→BER0905 (Cm)
BER1225	<i>pelB::P<sub>spolVA</sub>-sspB<sup>Ec</sup></i> $\Omega$ <i>sps</i> , <i>citZ-gfp</i>	BER0100→BER0905 (Sp)
BER1228	$\Delta$ <i>spolIQ::sps</i> , <i>icd-GFP</i>	KP575→BER0906 (Sp)
BER1232	<i>amyE::P<sub>spolIQ</sub>-sspB<sup>Ec</sup></i> $\Omega$ <i>cat</i> , <i>clpC-ssrA*</i> $\Omega$ <i>kan</i> , <i>citZ-gfp</i>	JLG170→BER0920 (Cm)
BER1233	<i>pelB::P<sub>spolVA</sub>-sspB<sup>Ec</sup></i> $\Omega$ <i>sps</i> , <i>clpC-ssrA*</i> $\Omega$ <i>kan</i> , <i>citZ-gfp</i>	BER0100→BER0920 (Sp)
BER1234	<i>ileS-ssrA*</i> $\Omega$ <i>kan</i> , <i>citZ-gfp</i>	JLG680→BER0905 (Km)
BER1235	<i>ileS-ssrA*</i> $\Omega$ <i>kan</i> , <i>amyE::P<sub>spolIQ</sub>-sspB<sup>Ec</sup></i> $\Omega$ <i>cat</i> , <i>citZ-gfp</i>	JLG680→BER1224 (Km)
BER1236	<i>ileS-ssrA*</i> $\Omega$ <i>kan</i> , <i>pelB::P<sub>spolVA</sub>-sspB<sup>Ec</sup></i> $\Omega$ <i>sps</i> , <i>citZ-gfp</i>	JLG680→BER1225 (Km)
BER1320	<i>clpC-GFP</i> $\Omega$ <i>kan</i>	pER320→PY79 (Km)
BER1375	<i>citZ-GFP</i> $\Omega$ <i>kan</i> , <i>spolIII</i> EATP- (G467S; ATPase mutant)	JLG2113→KP541 (Km)
BER1385	$\Delta$ <i>clpE::cat</i>	pER324→PY79 (Cm)
BER1386	$\Delta$ <i>clpQY::kan</i>	pER325→PY79 (Km)

**Table 4.S1. Strains used in this study (continued)**

<b>Strain</b>	<b>Genotype or description</b>	<b>Reference, source or construction<sup>a</sup></b>
BER1387	<i>ΔispA::erm</i>	pER326→PY79 (Em)
BER1395	<i>ΔispA::erm, citZ-GFPΩkan</i>	BER1387→JLG2113 (Tc)
BER1396	<i>ΔclpE::cat, citZ-GFPΩkan</i>	BER1385→JLG2113 (Cm)
BER1426	<i>ΔclpQY</i>	pCrePA→BER1386 (Em)
BER1428	<i>citZ-GFPΩkan, ΔclpQY</i>	JLG2113→BER1426 (Km)
BER1431	<i>ΔyetF::erm, citZ-GFPΩkan</i>	BKE07140→JLG2113 (Em)
BER1432	<i>ΔyfhF::erm, citZ-GFPΩkan</i>	BKE08510→JLG2113 (Em)
BER1433	<i>ΔyfhE::erm, citZ-GFPΩkan</i>	BKE08500→JLG2113 (Em)
BER1434	<i>ΔyfhD::erm, citZ-GFPΩkan</i>	BKE08490→JLG2113 (Em)
BER1435	<i>Δyhcm::erm, citZ-GFPΩkan</i>	BKE09140→JLG2113 (Em)
BER1436	<i>Δyhcn::erm, citZ-GFPΩkan</i>	BKE09150→JLG2113 (Em)
BER1437	<i>ΔyhfM::erm, citZ-GFPΩkan</i>	BKE10280→JLG2113 (Em)
BER1438	<i>ΔyjbA::erm, citZ-GFPΩkan</i>	BKE11410→JLG2113 (Em)
BER1438	<i>ΔyjbA::erm, citZ-GFPΩkan</i>	BKE11410→JLG2113 (Em)
BER1439	<i>ΔcsfG::kan, citZ-GFPΩkan</i>	1S138→JLG2113 (Em)
BER1440	<i>ΔyIbB::erm, citZ-GFPΩkan</i>	BKE14950→JLG2113 (Em)
BER1441	<i>ΔyIbC::erm, citZ-GFPΩkan</i>	BKE14960→JLG2113 (Em)
BER1442	<i>ΔyIoc::erm, citZ-GFPΩkan</i>	BKE15660→JLG2113 (Em)
BER1443	<i>ΔymfJ::erm, citZ-GFPΩkan</i>	BKE16880→JLG2113 (Em)
BER1444	<i>ΔyphB::erm, citZ-GFPΩkan</i>	BKE22900→JLG2113 (Em)
BER1445	<i>ΔyphA::erm, citZ-GFPΩkan</i>	BKE22860→JLG2113 (Em)
BER1446	<i>ΔypzI::erm, citZ-GFPΩkan</i>	BKE22869→JLG2113 (Em)
BER1447	<i>ΔyqhQ::erm, citZ-GFPΩkan</i>	BKE24490→JLG2113 (Em)

**Table 4.S1. Strains used in this study (continued)**

<b>Strain</b>	<b>Genotype or description</b>	<b>Reference, source or construction<sup>a</sup></b>
BER1448	<i>ΔyqhP::erm, citZ-GFPΩkan</i>	BKE24500→JLG2113 (Em)
BER1449	<i>ΔyqhG::erm, citZ-GFPΩkan</i>	BKE24590→JLG2113 (Em)
BER1450	<i>ΔyqzG::erm, citZ-GFPΩkan</i>	BKE24650→JLG2113 (Em)
BER1451	<i>ΔyrdR::erm, citZ-GFPΩkan</i>	BKE26620→JLG2113 (Em)
BER1452	<i>Δyzo::erm, citZ-GFPΩkan</i>	BKE26619→JLG2113 (Em)
BER1453	<i>ΔyzzR::erm, citZ-GFPΩkan</i>	BKE27469→JLG2113 (Em)
BER1454	<i>ΔyzzQ::erm, citZ-GFPΩkan</i>	BKE27468→JLG2113 (Em)
BER1455	<i>ΔytfI::erm, citZ-GFPΩkan</i>	BKE29510→JLG2113 (Em)
BER1456	<i>ΔytcC::erm, citZ-GFPΩkan</i>	BKE30470→JLG2113 (Em)
BER1457	<i>ΔytlL::erm, citZ-GFPΩkan</i>	BKE30739→JLG2113 (Em)
BER1458	<i>ΔyuiC::erm, citZ-GFPΩkan</i>	BKE32070→JLG2113 (Em)
BER1461	<i>ΔclpC::tet, ΔyjbA::erm, citZ-GFPΩkan</i>	BER0707→BER1438
BER1486	<i>yjbA-gfpΩkan</i>	pER344→PY79 (Km)
BER1506	<i>xylA::clpCΩcat, ΔclpC::tet</i>	pER342→BER0707 (Cm)
BER1519	<i>citZ-GFPΩkan, xylA::clpCΩcat, ΔclpC::tet</i>	JLG2113→BER1506 (Km)
BER1530	<i>P<sub>yjbA</sub>-gfpΩkan</i>	pER351→PY79 (Km)
BER1541	<i>ΔctpA::tet</i>	pER354→PY79 (Tc)
BER1542	<i>ΔctpB::tet</i>	pER355→PY79 (Tc)
BER1543	<i>ΔftsH::tet</i>	pER356→PY79 (Tc)
BER1544	<i>Δgpr::tet</i>	pER357→PY79 (Tc)
BER1551	<i>ΔctpA::tet, citZ-GFPΩkan</i>	BER1541→JLG2113 (Tc)
BER1552	<i>ΔctpB::tet, citZ-GFPΩkan</i>	BER1542→JLG2113 (Tc)
BER1553	<i>ΔftsH::tet, citZ-GFPΩkan</i>	BER1543→JLG2113 (Tc)
BER1554	<i>Δgpr::tet, citZ-GFPΩkan</i>	BER1544→JLG2113 (Tc)

**Table 4.S1. Strains used in this study (continued)**

<b>Strain</b>	<b>Genotype or description</b>	<b>Reference, source or construction<sup>a</sup></b>
BER1576	<i>metE-GFP</i> $\Omega$ <i>kan</i> , $\Delta$ <i>spolIQ::spc</i>	BER1098→KP575 (Km)
BER1577	<i>prs-GFP</i> $\Omega$ <i>kan</i> , $\Delta$ <i>spolIQ::spc</i>	BER1110→KP575 (Km)
BER1578	<i>rpoZ-GFP</i> $\Omega$ <i>kan</i> , $\Delta$ <i>spolIQ::spc</i>	BER1095→KP575 (Km)
BER1615	$\Delta$ <i>yjbA::erm</i> , <i>citZ-ssrA*</i> $\Omega$ <i>kan</i>	BKE11410→JLG1952 (Em)
BER1616	$\Delta$ <i>yjbA::erm</i> , <i>citZ-ssrA*</i> $\Omega$ <i>kan</i> , <i>amyE::PsspE(2G)-sspB<sup>Ec</sup></i> $\Omega$ <i>cat</i>	BKE11410→JLG2005 (Em)
BER1637	<i>P<sub>citZ</sub>-gfp</i> $\Omega$ <i>kan</i>	pER375→PY79 (Km)
BER1640	<i>P<sub>citZ</sub>-gfp</i> $\Omega$ <i>kan</i> , $\Delta$ <i>spolIQ::spc</i>	BER1637→KP575 (Km)
BKE07140	$\Delta$ <i>yetF::erm</i>	(Koo et al., 2017)
BKE08490	$\Delta$ <i>yfhD::erm</i>	(Koo et al., 2017)
BKE08500	$\Delta$ <i>yfhE::erm</i>	(Koo et al., 2017)
BKE08510	$\Delta$ <i>yfhF::erm</i>	(Koo et al., 2017)
BKE09140	$\Delta$ <i>yhcM::erm</i>	(Koo et al., 2017)
BKE09150	$\Delta$ <i>yhcN::erm</i>	(Koo et al., 2017)
BKE10280	$\Delta$ <i>yhfM::erm</i>	(Koo et al., 2017)
BKE11410	$\Delta$ <i>yjbA::erm</i>	(Koo et al., 2017)
BKE14950	$\Delta$ <i>ylbB::erm</i>	(Koo et al., 2017)
BKE14960	$\Delta$ <i>ylbC::erm</i>	(Koo et al., 2017)
BKE15660	$\Delta$ <i>yloC::erm</i>	(Koo et al., 2017)
BKE16880	$\Delta$ <i>ymfJ::erm</i>	(Koo et al., 2017)
BKE22860	$\Delta$ <i>yphA::erm</i>	(Koo et al., 2017)
BKE22869	$\Delta$ <i>ypzI::erm</i>	(Koo et al., 2017)
BKE22900	$\Delta$ <i>ypfB::erm</i>	(Koo et al., 2017)
BKE24490	$\Delta$ <i>yqhQ::erm</i>	(Koo et al., 2017)
BKE24500	$\Delta$ <i>yqhP::erm</i>	(Koo et al., 2017)
BKE24590	$\Delta$ <i>yqhG::erm</i>	(Koo et al., 2017)
BKE24650	$\Delta$ <i>yqzG::erm</i>	(Koo et al., 2017)



**Table 4.S1. Strains used in this study (continued)**

Strain	Genotype or description	Reference, source or construction <sup>a</sup>
BKE26619	$\Delta yzO::erm$	(Koo et al., 2017)
BKE26620	$\Delta yrdR::erm$	(Koo et al., 2017)
BKE27468	$\Delta yzQ::erm$	(Koo et al., 2017)
BKE27469	$\Delta yzR::erm$	(Koo et al., 2017)
BKE29510	$\Delta ytfI::erm$	(Koo et al., 2017)
BKE30470	$\Delta yzC::erm$	(Koo et al., 2017)
BKE30739	$\Delta yzL::erm$	(Koo et al., 2017)
BKE32070	$\Delta yuiC::erm$	(Koo et al., 2017)
JLG170	$amyE::P_{spollQ}-sspB^{Ec}\Omega cat$	(Yen Shin et al., 2015)
JLG1952	$citZ-ssrA*\Omega kan$	pJLG326→PY79 (Km)
JLG2107	$odhB-GFP\Omega kan$	pJLG335→PY79 (Km)
JLG2108	$citA-GFP\Omega kan$	pJLG336→PY79 (Km)
JLG2109	$fumC-GFP\Omega kan$	pJLG337→PY79 (Km)
JLG2111	$sucD-GFP\Omega kan$	pJLG339→PY79 (Km)
JLG2113	$citZ-GFP\Omega kan$	pJLG341→PY79 (Km)
JLG2114	$icd-GFP\Omega kan$	pJLG342→PY79 (Km)
JLG364	$\Delta xylA::sspB^{Ec}\Omega cat$	(Lamsa et al., 2016)
JLG626	$\Delta spollQ::erm$	(Ojkic et al., 2016)
JLG680	$ileS-ssrA*\Omega kan$	(Lopez-Garrido et al., 2018)
JLG963	$amyE::P_{sspE(2G)}-sspB^{Ec}\Omega cat$	(Lopez-Garrido et al., 2018)
KP419	$\Delta lon::cat$	REFERENCE
KP541	$spollIEATP-$ (G467S; ATPase mutant)	(Sharp and Pogliano, 1999)
KP575	$\Delta spollQ::spc$	(Londono-Vallejo et al., 1997)
PY79	Wild type	(Youngman et al., 1984)

<sup>a</sup> Plasmid or genomic DNA used (right side the arrow) to transform an existing strain (left side the arrow) to create a new strain are listed. The drug resistance is noted in parentheses.

<b>Table 4.S2. Plasmids used in this study</b>	
<b>Plasmid</b>	<b>Description/Reference</b>
pCrePA	(Pomerantsev et al., 2006)
pDG1662	(Guérout-Fleury et al., 1996)
pDG1731	(Guérout-Fleury et al., 1996)
pER161	$\Delta clpC::tet$
pER179	<i>clpC-ssrA*</i> $\Omega kan$
pER217	<i>citB-GFP</i> $\Omega kan$
pER227	<i>rpoC-GFP</i> $\Omega kan$
pER261	<i>guaB-GFP</i> $\Omega kan$
pER263	<i>pyrE-GFP</i> $\Omega kan$
pER264	<i>purD-GFP</i> $\Omega kan$
pER265	<i>rpoZ-GFP</i> $\Omega kan$
pER267	<i>lysA-GFP</i> $\Omega kan$
pER268	<i>metE-GFP</i> $\Omega kan$
pER269	<i>cysK-GFP</i> $\Omega kan$
pER270	<i>aspB-GFP</i> $\Omega kan$
pER271	<i>leuD-GFP</i> $\Omega kan$
pER272	<i>argH-GFP</i> $\Omega kan$
pER273	<i>rplL-GFP</i> $\Omega kan$
pER274	<i>ysxC-GFP</i> $\Omega kan$
pER276	<i>rnz-GFP</i> $\Omega kan$
pER277	<i>gapB-GFP</i> $\Omega kan$
pER280	<i>prs-GFP</i> $\Omega kan$
pER282	<i>ald-GFP</i> $\Omega kan$
pER283	<i>trmU-GFP</i> $\Omega kan$
pER320	<i>clpC-GFP</i> $\Omega kan$
pER324	$\Delta clpE::cat$
pER325	$\Delta clpQY::kan$
pER326	$\Delta ispA::erm$
pER342	<i>xylA::clpC</i> $\Omega cat$
pER344	<i>yjbA-GFP</i> $\Omega kan$
pER351	<i>P<sub>yjbA</sub>-GFP</i> $\Omega kan$
pER354	$\Delta ctpA::tet$
pER355	$\Delta ctpB::tet$
pER356	$\Delta ftsH::tet$
pER357	$\Delta gpr::tet$
pER375	<i>P<sub>citZ-gfp</sub></i> $\Omega kan$
pJLG3	(Yen Shin et al., 2015)
pJLG38	(Yen Shin et al., 2015)
pJLG67	(Lamsa et al., 2016)
pJLG326	<i>citZ-ssrA*</i> $\Omega kan$
pJLG335	<i>odhB-GFP</i> $\Omega kan$
pJLG336	<i>citA-GFP</i> $\Omega kan$
pJLG337	<i>fumC-GFP</i> $\Omega kan$
pJLG339	<i>sucD-GFP</i> $\Omega kan$
pJLG341	<i>citZ-GFP</i> $\Omega kan$
pJLG342	<i>icd-GFP</i> $\Omega kan$
pWH1520	(Ryguis and Hillen, 1991)

<b>Table 4.S3. Oligonucleotides used in this study</b>	
<b>Primer</b>	<b>Sequence<sup>a</sup></b>
JLG-7	AATTGGGACAACCTCCAGTG
JLG-77	GCTAGCAGCGCAAGCGC
JLG-95	CATGGATTACGCGTTAACCC
JLG-96	GCACTTTTCGGGGAAATGTG
JLG-184	GCTAGCGCAGCAAATGATG
JLG-187	TTTTCGCTACGCTCAAATCC
JLG-188	<i>cccttcagtaaagctg</i> cggtGACTGTAAAAAGTACAGTCGGC
JLG-550	<i>atgtatacctcctt</i> AAGCTTAATTGTTATC
JLG-712	<i>gggttaacgcgtaatccatg</i> TTGCAAACGCCTTGTAGAG
JLG-714	<i>cactggagttgtcccaattc</i> TAAAAAGGGTACATCACGATAAAG
JLG-715	<i>cacatttccccgaaaagtgc</i> AAAGAGCTGGTCAGAAAGCC
JLG-732	<i>cttgcgcttgcgctgctagc</i> TCTTCTAATAAAAGCTGTTTCAGG
JLG-735	<i>gggttaacgcgtaatccatg</i> ACAGCTGAAGCGACAAGAG
JLG-737	<i>cactggagttgtcccaattc</i> TAAATTGTTACAAATTAACATTTGACAG
JLG-738	<i>cacatttccccgaaaagtgc</i> TCTTCATTTACGCTTGTCCC
JLG-739	<i>cttgcgcttgcgctgctagc</i> TGAAATTGTATAGTTAGGTGATTCTTTTG
JLG-786	<i>cactggagttgtcccaattc</i> AAGATGAAAACCTCAACACTGAG
JLG-787	<i>cacatttccccgaaaagtgc</i> GTCTTGCTCTGTACAGCTG
JLG-788	<i>cttgcgcttgcgctgctagc</i> TACGTACCACAATTTTGTTCGG
JLG-885	<i>tcctttaactctggcaaccc</i> GAGTAGTTCAACAAACGGGC
JLG-886	<i>atgtgataactcggcgtatg</i> AAATAGGCGTATCACGAGGC
JLG-961	<i>gggttaacgcgtaatccatg</i> GAGCATGCATTGTCACTTGG
JLG-1114	<i>gggttaacgcgtaatccatg</i> CAAAGACATCGCACTGAATC
JLG-1116	<i>cttgcgcttgcgctgctagc</i> TGAAAGAACTTCTCCTCGGG
JLG-1117	<i>cactggagttgtcccaattc</i> CATATTTTGGCGTTTATTCATTTT
JLG-1118	<i>cacatttccccgaaaagtgc</i> AAACCAGCTCTTGAGCTGG
JLG-1126	<i>gggttaacgcgtaatccatg</i> GCAAGGATGGTCAAACG
JLG-1128	<i>cttgcgcttgcgctgctagc</i> GGACTGCTTCATTTTTTTCACG
JLG-1129	<i>cactggagttgtcccaattc</i> TGAATCAATAGGAAGAGAAGGC
JLG-1130	<i>cacatttccccgaaaagtgc</i> GCCGCTGTCCTGAAGTATC
JLG-1138	<i>gggttaacgcgtaatccatg</i> AAGCCAAAGCTCAAACGAC
JLG-1140	<i>cttgcgcttgcgctgctagc</i> CGCCTTTGGTTTTACCATG
JLG-1142	<i>cacatttccccgaaaagtgc</i> ATATCCTAGCAGGCCTCCG
JLG-1186	<i>gggttaacgcgtaatccatg</i> CGCTTTATTTTACATACGAAGCAG
JLG-1188	<i>cttgcgcttgcgctgctagc</i> ATGCGTTTTACAAGTTTCGAAC
JLG-1189	<i>cactggagttgtcccaattc</i> TAAAAAGGGACAGCCGTC
JLG-1190	<i>cacatttccccgaaaagtgc</i> CCCCTTCGCCTTAATACTTG
JLG-1210	<i>gggttaacgcgtaatccatg</i> CTCGAAAATGTTTCATCCCATG
JLG-1211	<i>catcatttgctgcgctagc</i> GGCTCTTTCTTCAATCGGAAC
JLG-1212	<i>cttgcgcttgcgctgctagc</i> GGCTCTTTCTTCAATCGGAAC
JLG-1213	<i>cactggagttgtcccaattc</i> AGAACCATTGGAGGCTGG
JLG-1214	<i>cacatttccccgaaaagtgc</i> TCTGTGAACTTCATGATGTTTCC
JLG-1218	<i>gggttaacgcgtaatccatg</i> TGCTCTTTGCTGTATCCGTC
JLG-1222	<i>gggttaacgcgtaatccatg</i> GATATTTACGCAGGCATCGAG
JLG-1224	<i>cttgcgcttgcgctgctagc</i> GTCCATGTTTTTGTATCAGTTCTTC
JLG-1225	<i>cactggagttgtcccaattc</i> GCAAGGAAAAAGCCTAAAACCTAGC
JLG-1226	<i>cacatttccccgaaaagtgc</i> GCAATTGTAGGAAGGACGC

<b>Table 4.S3. Oligonucleotides used in this study (continued)</b>	
<b>Primer</b>	<b>Sequence<sup>a</sup></b>
oER76	<i>gggtaacgcgtaatccatg</i> GTATTACGATGGCAACAGCGC
oER78	<i>cactggagttgtcccaatt</i> AGGATCCTCTACCGGTTTTATTATCG
oER79	<i>cacatttccccgaaaagtg</i> cCCACAACAAGTATATGCATCGCTC
oER80	<i>gcgcttgcgctgctagc</i> CCGGTTTATCATTTTTTTGGATCG
oER178	<i>gggtaacgcgtaatccatg</i> GAACTTCCATCACGCGAAGG
oER180	<i>cactggagttgtcccaatt</i> TCTTCACTTACCTGTAGGGGAAGC
oER181	<i>cacatttccccgaaaagtg</i> cCATCGAACAGTTCCTCGAGC
oER182	<i>gcgcttgcgctgctagc</i> CTTAACTTCTACAGAAGCGCCAAC
oER276	<i>gggtaacgcgtaatccatg</i> GACATATCCGCTTGCGATCC
oER278	<i>cactggagttgtcccaatt</i> AGGCGGAGCTCTTATTTGACAATTTG
oER279	<i>cacatttccccgaaaagtg</i> cGTGTTGTCATCAGGAGAACGGAC
oER280	<i>gcgcttgcgctgctagc</i> GCCTCGCGGGACGTTTAC
oER417	<i>ttctgctccctcgctcaggcggccgc</i> TTTTCGCTACGCTCAAATCC
oER418	<i>cagggagcactggtcaacgctagc</i> GACTGTAAAAAGTACAGTCGGC
oER419	<i>ttctgctccctcgctcaggcggccgc</i> TCCTTTAACTCTGGCAACCC
oER420	<i>cagggagcactggtcaacgctagc</i> ATGTGATAACTCGGCGTATG
oER421	<i>ttctgctccctcgctcaggcggccgc</i> ATGAGAGAGGAAGAAAACGG
oER422	<i>cagggagcactggtcaacgctagc</i> AATTGGGACAACCTCCAGTG
oER425	<i>ttctgctccctcgctcaggcggccgc</i> TCCTTTAACTCTGGCAACCC
oER426	<i>cagggagcactggtcaacgctagc</i> ATGTGATAACTCGGCGTATG
oER470	GCTAAAGGCGAAGAAGCTGTTTACAG
oER565	<i>gggtaacgcgtaatccatg</i> GCGCCAGCTTGATGACATC
oER567	<i>cactggagttgtcccaatt</i> TTCAACAATAAGCTTGCAGAAAG
oER568	<i>cacatttccccgaaaagtg</i> cTTATCTGCAGCCTGTTCCAGG
oER569	<i>gcgcttgcgctgctagc</i> AGCACCCGCCACAGATG
oER614	<i>gggtaacgcgtaatccatg</i> AAGTTAAAGCGCTTGAAGACG
oER616	<i>cactggagttgtcccaatt</i> TTTGAAAAACCATCTGCATTTG
oER617	<i>cacatttccccgaaaagtg</i> cGATCGTTCTTTCTTCAGCAGG
oER618	<i>gcgcttgcgctgctagc</i> TACTAGCTGTGTCTGCTGTGC
oER718	<i>gggtaacgcgtaatccatg</i> CTTTTGGCGGCTGTTTGC
oER719	<i>gcctgagcgaggagcagaa</i> AGCAGCAATGCCCTCTCCTTC
oER720	<i>gcgcttgaccagtgctccctg</i> CGGTGCCCGTCCGTTAAG
oER721	<i>cacatttccccgaaaagtg</i> cCCTGTGACACACTGCCTGGAG
oER749	<i>gggtaacgcgtaatccatg</i> CAGAAGGTTCAATCGATCCG
oER751	<i>cactggagttgtcccaatt</i> CTGATTTAACTCTGCTGAAAGACTGC
oER752	<i>cacatttccccgaaaagtg</i> cTAACCCACATAACCCAGGTGG
oER753	<i>gcgcttgcgctgctagc</i> TCAACCGGGACCATATCG
oER756	<i>gggtaacgcgtaatccatg</i> TCAAGGATTCTTTGATATACCG
oER760	<i>gcgcttgcgctgctagc</i> GCTGAACAGATAGCTGACTG
oER775	<i>gggtaacgcgtaatccatg</i> CAAGTTCTTGAAGACGGACG
oER776	<i>catcatttgctgcgctagc</i> ATTCGTTTTAGCAGTCGTTTTTACG
oER777	<i>cactggagttgtcccaatt</i> TATAGAAGACGGAAATGAGGC
oER778	<i>cacatttccccgaaaagtg</i> cGTGACGGATTATTAATGCCG
oER779	<i>gcgcttgcgctgctagc</i> ATTCGTTTTAGCAGTCGTTTTTACG
oER794	<i>gggtaacgcgtaatccatg</i> AACAGGAAGCAGCATGATG
oER796	<i>cactggagttgtcccaatt</i> AATTTCTTCATAAAATCCCG
oER797	<i>cacatttccccgaaaagtg</i> cCAAATATGTATGGTCCAGCG

<b>Table 4.S3. Oligonucleotides used in this study (continued)</b>	
<b>Primer</b>	<b>Sequence<sup>a</sup></b>
oER798	<i>gcgcttgcgctgctagc</i> ACAAACTCCTGCTGCCAC
oER818	<i>gggtaacgcgtaatccatg</i> GCCTGTTGTAAAAGTGCTGG
oER820	<i>cactggagttgtcccaatt</i> AATAAGGTCATGGACACATTTTAAAG
oER821	<i>cacatttccccgaaaagtc</i> GCGACATTAGGATCTAAGTCTCC
oER822	<i>gcgcttgcgctgctagc</i> TACAGCAGACGGATGTTTCATTC
oER858	<i>gggtaacgcgtaatccatg</i> GCTTCATGCCACTGAATACG
oER860	<i>cactggagttgtcccaatt</i> AAGAAAGCGCCGATTTTTC
oER861	<i>cacatttccccgaaaagtc</i> CGAAGGTGTATGTTACAGCACC
oER862	<i>gcgcttgcgctgctagc</i> TTGCTTTACACCCGTTTTAAATG
oER877	<i>gggtaacgcgtaatccatg</i> GGAAGGCATGAAAGGTGC
oER879	<i>cactggagttgtcccaatt</i> AAAAAGCCAAAACCTCCCGG
oER880	<i>cacatttccccgaaaagtc</i> CTCTTCTTGATGTCATAAACTGC
oER881	<i>gcgcttgcgctgctagc</i> ATCGAATTGGTACAGCGGC
oER931	<i>gggtaacgcgtaatccatg</i> GCACAGCTGTCAGACAGAC
oER933	<i>cactggagttgtcccaatt</i> CAGATCAAAAAGCGGCTGAC
oER934	<i>cacatttccccgaaaagtc</i> CGCGAATGATTTCAATTACGG
oER966	<i>gggtaacgcgtaatccatg</i> GCTGTAGAAACGATCGTTAAGC
oER968	<i>cactggagttgtcccaatt</i> GTGAGGAAAACCCGCAG
oER969	<i>cacatttccccgaaaagtc</i> TAAAGGAGCCAGACAAATGG
oER970	<i>gcgcttgcgctgctagc</i> TTTTTGGGCAGCCTTTAAAG
oER977	<i>gggtaacgcgtaatccatg</i> CCGCCTTACGCTATCTTTCC
oER979	<i>cactggagttgtcccaatt</i> AAAATAAATTCAAATGATGTAAAGAGGC
oER980	<i>cacatttccccgaaaagtc</i> GCGCTCCTTTATAAGGATCG
oER981	<i>gcgcttgcgctgctagc</i> TTTTTTAAACCAATCTTTTGA CT CG
oER988	<i>gggtaacgcgtaatccatg</i> CACATACGGGGAAAGCAGC
oER990	<i>cactggagttgtcccaatt</i> AAAAGCGGCCGGTATTTG
oER991	<i>cacatttccccgaaaagtc</i> GAGATTCATTTGCTCCTCAGGG
oER992	<i>gcgcttgcgctgctagc</i> GGCTTGAAGCCAAGAGCTTC
oER999	<i>gggtaacgcgtaatccatg</i> GAACAGACGCTTCAAGATGG
oER1001	<i>cactggagttgtcccaatt</i> TAGCACAAGTAGCAACCTATATCATG
oER1002	<i>cacatttccccgaaaagtc</i> CGTAACCGCATGCTAAATAGC
oER1003	<i>gcgcttgcgctgctagc</i> TTCGCGGTCTTCCTTTTC
oER1156	<i>gggtaacgcgtaatccatg</i> GATATGACTTGGCATTGATTTCG
oER1157	<i>gcctgagcgaggagcagaa</i> CAATGTTGACAACGCATTTGC
oER1158	<i>gcgttgaccagtgtcccctg</i> CGAGCAAATAACAATCAGCG
oER1159	<i>cacatttccccgaaaagtc</i> TACGACTGCTGAGATTGTCC
oER1162	<i>gggtaacgcgtaatccatg</i> CTGTTAGAGCTGCTCTATGC
oER1163	<i>gcctgagcgaggagcagaa</i> AAGATGACATAAAGGGCCTCC
oER1164	<i>gcgttgaccagtgtcccctg</i> GAAAAGCTCGGAACGATAGC
oER1165	<i>cacatttccccgaaaagtc</i> CCATTCCGACA ACT GTTGC
oER1168	<i>gggtaacgcgtaatccatg</i> CTCCTGTTTCTCATAAACTCC
oER1169	<i>gcctgagcgaggagcagaa</i> CTGCTCATTGCTCACATACG
oER1170	<i>gcgttgaccagtgtcccctg</i> GCAATCACATTTGTTGACCC
oER1171	<i>cacatttccccgaaaagtc</i> TTCCAATACGCTTCAAGTGC
oER1190	<i>aagcttaaggaggtatacat</i> ATGATGTTTGAAGATTTACAG
oER1191	<i>ggatttgagcgtagcgaaaa</i> TTAATTCGTTTTAGCAGTCC
oER1198	<i>gggtaacgcgtaatccatg</i> TGTTTTGTCGTAACAGACGG

<b>Table 4.S3. Oligonucleotides used in this study (continued)</b>	
<b>Primer</b>	<b>Sequence<sup>a</sup></b>
oER1199	<i>gcgcttgcgctgctagc</i> GTTGACCTTTGATTTCGTTTTCC
oER1200	<i>cactggagttgtcccaatt</i> AAAAAACCGCTCTTTGCAAAG
oER1201	<i>cacatttccccgaaaagtgc</i> CAACGACATCTTTACGATTCC
oER1203	CATATATAACATCTCCTTTTTCAATAAATTTCC
oER1233	<i>aacagttcttcgccttagc</i> CATCTCTAACCCCTCAC
oER1234	<i>gggtaacgcgtaatccatg</i> CTTGCTGCTAAAACAATTGG
oER1235	<i>gggtaacgcgtaatccatg</i> CTCTTGAAATTTCTTGAAGAGAGG
oER1236	<i>gcctgagcgaggagcagaa</i> TAAACACCACCTTTTTCTTCTTAC
oER1237	<i>gcgctgaccagtgtccctg</i> AAAAAACCATACGCGGCTG
oER1238	<i>cacatttccccgaaaagtgc</i> CCTTGTTCCATTATGGCAATCG
oER1241	<i>gggtaacgcgtaatccatg</i> CCGTTTGTAAAGTGGTGC
oER1242	<i>gcctgagcgaggagcagaa</i> CCTTACTCCTCCTGTATGC
oER1243	<i>gcgctgaccagtgtccctg</i> AGGAGATGGTATTTTCTCCTG
oER1244	<i>cacatttccccgaaaagtgc</i> GACCAAATATCTGCTGAACAGC
oER1247	<i>gggtaacgcgtaatccatg</i> ACATTTCCGTTGGCAATCG
oER1248	<i>gcctgagcgaggagcagaa</i> TCCTTACCTCCTCCCACAG
oER1249	<i>gcgctgaccagtgtccctg</i> TTCGCTTTCTTTCTAAAAAAC
oER1250	<i>cacatttccccgaaaagtgc</i> GCATTTACGATTCTGTCTGC
oER1253	<i>gggtaacgcgtaatccatg</i> ATCCCATTATTGAGGATCG
oER1254	<i>gcctgagcgaggagcagaa</i> CTCACTCTTTTTCATACAGGG
oER1255	<i>gcgctgaccagtgtccctg</i> ACAGTTCTACTTCTCTAGC
oER1256	<i>cacatttccccgaaaagtgc</i> CTCTTTCTTCTCCTCCATCACC
oER1316	GAAGAACTGTTTACAGGCG

<sup>a</sup>In capital letters are shown the regions of the primer that anneals to the template. Homology regions for Gibson assembly are shown in italics.

## References

1. S.H. Orkin, D. Swan, P. Leder, Differential expression of  $\alpha$ - and  $\beta$ -globin genes during differentiation of cultured erythroleukemic cells. *Proc. Natl. Acad. Sci. U.S.A.* **72**, 98-102 (1975).
2. S. Strome, W.B. Wood, Immunofluorescence visualization of germ-line-specific cytoplasmic granules in embryos, larvae, and adults of *Caenorhabditis elegans*. *Proc. Natl. Acad. Sci. U.S.A.* **79**(5), 1558–1562 (1982).
3. W Driever, C. Nüsslein-Volhard, A gradient of bicoid protein in *Drosophila* embryos. *Cell* **54**, 83–93 (1988).
4. A.E. Hofmeister, A. Londoño-Vallejo, E. Harry, P. Stragier, R. Losick, Extracellular signal protein triggering the proteolytic activation of a developmental transcription factor in *B. subtilis*. *Cell* **83**(2), 219–226 (1995).
5. I. S. Tan, K. S. Ramamurthi, Spore formation in *Bacillus subtilis*. *Environ. Microbiol. Rep.* **6**, 212–225 (2014).
6. P. Setlow, Spore germination. *Curr. Opin. Microbiol.* **6**, 550–556 (2003).
7. Chapter III of this dissertation.
8. N. Bradshaw, R. Losick, Asymmetric division triggers cell-specific gene expression through coupled capture and stabilization of a phosphatase. *eLife* **4**, e08145 (2015).
9. P. Margolis P, A, Driks, R. Losick, Establishment of cell type by compartmentalized activation of a transcription factor. *Science* **254**, 562–565 (1991).
10. J. Lopez-Garrido, N. Ojkic, K. Khanna, F.R. Wagner, E. Villa, R.G. Endres, K. Pogliano, Chromosome translocation inflates *Bacillus* forespores and impacts cellular morphology. *Cell* **172**(4), 758-770 (2018).
11. E. P. Riley, A. Trinquier, M.L. Reilly, M. Durchon, V.R. Perera, K. Pogliano, J. Lopez-Garrido, Spatiotemporally regulated proteolysis to dissect the role of vegetative proteins during *Bacillus subtilis* sporulation: cell-specific requirement of  $\sigma^H$  and  $\sigma^A$ . *Mol. Microbiol.* **108**, 45–62 (2018).
12. S.T. Wang, B. Setlow, E.M. Conlon, J.L. Lyon, D. Imamura, T. Sato, P. Setlow, R. Losick, P. Eichenberger, The forespore line of gene expression in *Bacillus subtilis*. *J. Mol. Biol.* **358**(1), 16–37 (2006).
13. Q. Pan, D.A. Garsin, R. Losick, Self-Reinforcing activation of a cell-specific transcription factor by proteolysis of an anti- $\sigma$  factor in *B. subtilis*. *Mol. Cell* **8**, 873–883 (2001).
14. A.J. Meeske, C.D. Rodrigues, J. Brady, H.C. Lim, T.G. Bernhardt, D.Z. Rudner, High-throughput genetic screens identify a large and diverse collection of new sporulation genes in *Bacillus subtilis*. *PLoS Biol.* **14**(1), e1002341 (2016).

15. L.J. Wu, J. Errington, Use of asymmetric cell division and *spoIIIE* mutants to probe chromosome orientation and organization in *Bacillus subtilis*. *Mol. Microbiol.* **27**, 777–786 (1998).
16. M.D. Sharp, K. Pogliano, Role of cell-specific SpoIIIE assembly in polarity of DNA transfer. *Science* **295**, 137–139 (2002).
17. N.J. Liu NJ, R.J. Dutton, K. Pogliano, Evidence that the SpoIIIE DNA translocase participates in membrane fusion during cytokinesis and engulfment. *Mol. Microbiol.* **59**(4), 1097–1113 (2006).
18. L. Kong, K. Siranosian, A. Grossman, D. Dubnau, Sequence and properties of *mecA*, a negative regulator of genetic competence in *Bacillus subtilis*. *Mol. Microbiol.* **9**(2), 365-73 (1993).
19. S.K. Garg, S. Kommineni, L. Henslee, Y. Zhang, P. Zuber, The YjbH protein of *Bacillus subtilis* enhances ClpXP-catalyzed proteolysis of Spx. *J. Bacteriol.* **191**(4), 1268-77 (2009).
20. S.B. Young, P. Setlow, Mechanisms of killing of *Bacillus subtilis* spores by hypochlorite and chlorine dioxide. *J. Appl. Microbiol.* **95**, 54–67 (2003).
21. K. Turgay K, J. Hahn, J. Burghoorn, D. Dubnau, Competence in *Bacillus subtilis* is controlled by regulated proteolysis of a transcription factor. *EMBO J.* **17**, 6730–6738 (1998).
22. S. Mukherjee, A.C. Bree, J. Liu, J.E. Patrick, P. Chien, D.B. Kearns, Adaptor-mediated Lon proteolysis restricts *Bacillus subtilis* hyperflagellation. *Proc. Natl. Acad. Sci. U.S.A.* **112**, 250–255 (2015).
23. J. Kirstein, N. Molière, D. A. Dougan, K. Turgay, Adapting the machine: Adaptor proteins for Hsp100/Clp and AAA+ proteases. *Nat. Rev. Microbiol.* **7**, 589–599 (2009).
24. I.S. Tan, C.A. Weiss, D.L. Popham, K.S. Ramamurthi, A quality-control mechanism removes unfit cells from a population of sporulating bacteria. *Dev. Cell* **34**(6), 682-693 (2015).
25. N.B. Wood, R. Haselkorn, Control of phycobiliprotein proteolysis and heterocyst differentiation in *Anabaena*. *J. Bacteriol.* **141**(3), 1375-85 (1980).
26. M.C. Mutomba, C.C Wang, The role of proteolysis during differentiation of *Trypanosoma brucei* from the bloodstream to the procyclic form. *Mol. Biochem. Parasitol.* **93**(1), 11-22 (1998).
27. A.L. Sonenshein, Control of key metabolic intersections in *Bacillus subtilis*. *Nat. Rev. Microbiol.* **5**(12), 917–927 (2007).
28. D.E. Johnson, R.S. Hanson. Bacterial citrate synthases: purification, molecular weight and kinetic mechanism. *Biochim. Biophys. Acta.* **350**(2), 336-53 (1974).



29. J.R. Ibarra, A.D. Orozco, J.A. Rojas, K. López, P. Setlow, R.E. Yasbin, M. Pedraza-Reyes, The Nfo and ExoA apurinic/aprimidinic endonucleases in repair of DNA damage during outgrowth of *Bacillus subtilis* spores. *J. Bacteriol.* **190**(6), 2031-2038 (2008).
30. R.Z. Zhao, S. Jiang, L. Zhang, Z.B. Yu, Mitochondrial electron transport chain, ROS generation and uncoupling. *Int. J. Mol. Med.* **44**, 3–15 (2019).
31. M.M. Weber, D.A. Broadbent, “Electron transport in membranes from spores and from vegetative and mother cells of *Bacillus subtilis*” in Spores VI, P. Gerhardt, R.N. Costilow, H.L. Sadoff, Eds. (American Society for Microbiology, 1975), pp. 411-417.
32. D.L. Nelson, A. Kornberg. Biochemical studies of bacterial sporulation and germination. XIX. Phosphate metabolism during sporulation. *J. Biol. Chem.* **245**, 1137-1145 (1970).
33. L. Sinai, A. Rosenberg, Y. Smith, E. Segev, S. Ben-Yehuda, The molecular timeline of a reviving bacterial spore. *Mol. Cell* **57**, 695–707 (2015).
34. D. B. Trentini, M.J. Suskiewicz, A. Heuck, R. Kurzbauer, L. Deszcz, K. Mechtler, T. Clausen, Arginine phosphorylation marks proteins for degradation by a Clp protease. *Nature* **539**, 48–53 (2016).

## Chapter V

### Conclusions and outlook

#### **Novel approaches to study spore formation**

*Bacillus subtilis* sporulation constitutes an incredibly powerful model system to advance our understanding of fundamental biological principles. In few systems are the processes of membrane biogenesis, cell envelope remodeling, signal transduction, cell-fate determination, and subcellular protein localization so amenable to study. In this present work, we have leveraged sporulation as a means of understanding cellular dormancy and metabolic differentiation, two important phenomena that underlie diverse pathologies, ranging from persistent bacterial infections to oncogenesis.

The process of spore formation has been intensively studied at the molecular level for the past half-century, rendering it one of the most thoroughly characterized developmental pathways in biology. One of the enduring limitations confronting the field has been the fact that proteins required for vegetative growth or sporulation initiation have thus far been inaccessible to study with current genetic approaches. To overcome these limitations, we developed a system that supports the rapid degradation of target proteins in a spatiotemporally regulated manner, allowing the developmental role of this class of proteins to be evaluated for the first time. We have termed this conceptual framework spatiotemporally regulated proteolysis (STRP). The STRP methodology is particularly well suited for use during sporulation, as it functions at the post-translational level, thereby allowing the rapid depletion of target proteins<sup>1,2</sup>. This represents a tremendous advantage over other techniques, such as CRISPR interference, which act pre-translationally to inhibit new protein synthesis and, therefore, rely on growth and cell division to deplete protein levels<sup>3</sup>.

As part of this research, we rigorously surveyed a series of cell-specific sporulation promoters, genetic loci, and –ssrA\* tags to optimize the degradation of target

proteins during sporulation, finding that the STRP-induced degradation of proteins is highly specific, rapid, and effective. In fact, using STRP to deplete proteins known to be essential for spore formation resulted in phenotypes equivalent to those of the null mutants. We also applied our methodology to understand the spatiotemporal requirement of two vegetative sigma factors, the stationary phase sigma factor,  $\sigma^H$ , and the essential housekeeping sigma factor,  $\sigma^A$ . Although several genes under the control of  $\sigma^H$  are required for the initiation of sporulation, we found that  $\sigma^H$  activity is dispensable following polar septation. Therefore, our results suggest that  $\sigma^H$  activity is only required acutely, in contrast to the master regulator of spore formation, Spo0A, which continues to function in the mother cell following polar septation<sup>4</sup>.

Our research revealed previously uncharacterized roles for  $\sigma^A$  during sporulation, and demonstrated that this  $\sigma$  factor plays disparate roles in the mother cell and forespore, though its activity is not required for gross spore morphogenesis in either cell.  $\sigma^A$  appears to play only a minor role in the mother cell, replenishing important housekeeping functions where required. On the other hand,  $\sigma^A$  seems to play a far more complex and critical role in the forespore. Our results demonstrate that  $\sigma^A$  activity during sporulation is required for efficient spore revival. While depletion of  $\sigma^A$  from the forespore during late stages of sporulation blocked outgrowth, the early depletion of  $\sigma^A$  additionally compromised spore germination. Taken together, these data suggest that  $\sigma^A$ -directed gene expression during sporulation is required to prepare the developing spore for germination and outgrowth, rather than orchestrating the morphogenetic process itself. Although our results provide compelling evidence that  $\sigma^A$ -directed gene expression is required to mediate the process of outgrowth, it remains unknown whether  $\sigma^A$  activity is needed early during spore formation to produce germination receptors, either directly or indirectly through the synthesis of metabolic building blocks, or if  $\sigma^A$ -dependent gene expression simply helps the developing spore attain a metabolic state conducive to

germination. It will be interesting to identify the specific housekeeping functions that are required in the forespore to promote spore revival, and the reason why the forespore line of gene expression does not regulate these functions, as appears to be the case for the mother cell<sup>5,6,7</sup>.

An important discovery stemming from this research is the fact that STRP can be used to deplete the spore of key metabolic enzymes and essential proteins, without significantly affecting the process of development, by inducing the degradation of target proteins in the forespore during late stages of sporulation. Traditionally, the study of germination has been relatively intractable using genetic techniques. The tremendous resistance properties of the spore have rendered chemical genetic approaches largely unviable. Furthermore, the germination machinery is produced during sporulation, making it difficult to genetically disentangle the processes of germination and spore formation. Therefore, researchers have generally pursued an understanding of germination from a biochemical standpoint. Innovative approaches, such as STRP, are therefore needed to thoroughly interrogate the processes of germination and outgrowth from a genetic and cell biological perspective. STRP allows the depletion of enzymes functioning in different biosynthetic pathways from the spore while only minimally perturbing the process of spore formation.

Our efforts using STRP have enabled us to address a controversy that has recently emerged in the germination field. Although research spanning decades has demonstrated that germination proceeds in the absence of macromolecular synthesis<sup>8,9</sup>, a recent study suggested that new protein synthesis is required for germination, challenging the long-held model of this process<sup>10</sup>. Our work provides compelling evidence that germination does not require macromolecular synthesis, and that the process is purely mechanical. Thus, STRP constitutes a powerful new approach to studying processes that have previously been neglected due to intractability.

Overall, the development of STRP represents a tremendous advancement that will allow a much more thorough dissection of the processes of spore formation and revival. The regulatory program of sporulation makes this process an ideal platform for the application of the STRP methodology, however, STRP can theoretically be used as a framework to study any transcriptionally regulated pathway such as stress responses, pathogenesis, stationary phase, and other developmental pathways. STRP is an incredibly versatile tool that can be used to inhibit cellular processes for which no drugs exist<sup>11</sup>, or as a more specific alternative to small molecule inhibitors, which frequently exhibit pleiotropic effects<sup>12</sup>. We are currently using STRP to undertake a systematic, genome-wide effort to compile a list of cellular parts required at every stage of spore formation and spore revival. Altogether, our work illustrates the potential of STRP to illuminate many facets of sporulation, from initiation to germination and outgrowth.

### **Metabolic nurturing during spore formation**

The prevailing model in the sporulation field proposed that the mother cell nurtures the forespore during its transition to dormancy, but the nature and extent of this nurturing relationship had never been established. Although it was known that the mother cell physically sequesters the developing spore, protecting it from the external environment following engulfment, molecular instances of nurturing had been limited to the endowment of resistance properties to the spore, such as coat deposition<sup>13</sup>, cortex synthesis<sup>14</sup>, and dipicolinic acid transport<sup>15,16</sup>. It was not clear whether the mother cell nurtures the forespore in a more profound, metabolic capacity by providing metabolic building blocks to sustain biosynthesis as the spore prepared for dormancy.

The few pieces of empirical evidence suggesting that the mother cell metabolically nurtures the forespore stemmed from research on a transenvelope complex, consisting of the mother cell-encoded SpoIIIA and the forespore-encoded SpoIIQ (hereafter, A-Q), that had been advanced as a feeding tube apparatus

connecting the cytoplasms of two cells<sup>17</sup>. Components of the A-Q complex have homology to bacterial secretion systems and had been found to assemble ring-like structures *in vitro*<sup>18,19</sup>. Furthermore, the A-Q transenvelope complex was known to be required for the maintenance of forespore gene expression and physiology<sup>20,21</sup>. Given these findings, A-Q had come to be accepted as a metabolic conduit, despite the absence of direct empirical evidence implicating A-Q in the intercellular transport of metabolites.

STRP allowed us to empirically test the longstanding nurturing model for the first time by enabling the inactivation of essential biosynthetic pathways in a cell-specific manner. Our results clearly indicate that the mother cell and forespore become functionally differentiated shortly after polar septation, and that forespore macromolecular synthesis requires mother cell-derived metabolic building blocks. Our findings also provide the first documentation that metabolically relevant molecules are trafficked between the mother cell and forespore during sporulation and that A-Q is required for the intercellular transport of small molecules. Therefore, our work has been instrumental in offering the first empirical evidence that the mother cell nurtures the forespore in a fundamental, metabolic capacity. Although metabolic specialization and cross-feeding are quite common in multispecies communities<sup>22</sup> and multicellular organisms<sup>23</sup>, our findings constitute one of the few instances of these behaviors in genetically identical bacterial sister cells<sup>24,25</sup>.

Our work demonstrates that arginine is transported from the mother cell to the forespore to support biosynthesis, but also suggests that arginine is likely to be just one of the many metabolites that are trafficked between the two cells. Future work will focus on identifying the full repertoire of substrates that are used to nourish the forespore. Genome-scale metabolic models can be used in conjunction with our STRP methodology to guide the identification of additional candidates to test for transport<sup>26</sup>.

Our current assay to evaluate transport depends on the availability of stable isotopes and known uptake systems, however, substrate-specific transport assays can be developed as needed to monitor the flow of nutrients between the two cells.

Another remaining challenge is deciphering how the A-Q dependent transport of small molecules is regulated. Our results suggest that intercellular transport is bidirectional and that A-Q is required for transport in both directions, which together argue against active transport. It remains unclear how directionality is achieved, however, we speculate that the downregulation of forespore metabolism and the polymerization of metabolic building blocks into final products generates a concentration gradient that reinforces the directional flow of nutrients from the mother cell to the forespore. Forespore to mother cell transport could be a physiologically relevant phenomenon, as it could be a means of preventing the accumulation of toxic metabolic byproducts in the small forespore<sup>27</sup>. It will be interesting to characterize the mechanism of A-Q mediated transport, using temperature dependence as an assay to distinguish between simple and facilitated diffusion<sup>28</sup>. One lingering question is how does the mature spore prevent the leakage of cellular contents via these channels once liberated through mother cell lysis? SpoIIQ has been shown to undergo proteolytic processing following the completion of engulfment, which results in the reorganization of the A-Q complex<sup>29</sup>. This structural reorganization could guarantee the termination of intercellular metabolic exchange, once the forespore has been endowed with sufficient levels of metabolic building blocks to complete the process of development. Finally, it remains formally possible that although A-Q is required for transport, it does not function as the transporter itself. The ultimate demonstration of the role of A-Q in transport will be to reconstitute the system in vegetative protoplasts and observe whether it can support the exchange of small molecules.

Although our work revolved around intercellular transport, it would be equally interesting to use stable isotopic labeling and mass spectrometry to explore the intracellular flow of metabolites through different biosynthetic pathways in the mother cell and forespore during sporulation. STRP could be employed here to validate metabolic models by blocking flux through different metabolic pathways and evaluating whether the predicted intermediates accumulate. Altogether, these strategies could achieve a comprehensive view of metabolic flux in the mother cell and forespore, and an understanding of the metabolic transformations that underpin spore formation.

We focused our efforts on pathways feeding directly into protein synthesis, but there are a multitude of other metabolic pathways that play critical roles during spore formation, including energy production, lipid metabolism, and peptidoglycan synthesis. At the onset of spore formation, cells exhibit a pronounced shift from a fermentative regime to an oxidative regime, and begin to produce energy through oxidative phosphorylation rather than substrate-level phosphorylation<sup>30</sup>. This presents a complication for the forespore, which our data indicate lacks its own tricarboxylic acid (TCA) cycle, a major source of electrons to sustain oxidative phosphorylation. Thus, the means by which the forespore produces the energy required to sustain anabolism remain enigmatic.

We can conceive of three models to account for how the forespore acquires the energy to power macromolecular synthesis: (1) the forespore produces reduced electron carriers to feed the electron transport chain independent of the TCA cycle, (2) the forespore is able to harness a proton motive force produced by the mother cell in the intermembrane space between the inner and outer forespore membranes, (3) the mother cell directly transports high energy compounds into the forespore. In accordance with the first model outlined above, malic enzyme, a major source of reduced electron carriers, is one of the few enzymes retained at high levels in the forespore following



polar septation. In support of the second model, our unpublished results and those of Magill et al. indicate that the intermembrane space surrounding the forespore becomes highly acidified following the completion of engulfment, suggesting that a powerful proton motive force to drive ATP synthesis could be at the forespore's disposal<sup>31</sup>. In favor of the third model, our data suggest that nucleoside triphosphate synthesis and the TCA cycle become mother cell-specific during spore formation. Furthermore, ATP synthase appears to be removed from the forespore membranes during engulfment, suggesting that the forespore loses its ability to harness the proton motive force as a means for energy production (Amy Camp, personal communication). Unfortunately, it is difficult to distinguish between these possibilities since many components of the electron transport chain have extracytoplasmic C-termini, making them incompatible with our STRP methodology, and all efforts to tag subunits of ATP synthase have thus far failed. In light of our limited data, however, we favor the model in which the mother cell feeds the forespore high-energy compounds to sustain biosynthesis from an energetic perspective. Clearly, further research is needed to fully elucidate the means by which the forespore derives its energy.

Perhaps one of the more intriguing pathways to study in the context of spore formation is lipid metabolism. Both the mother cell and the forespore require membrane synthesis to support engulfment and forespore growth<sup>32</sup>, respectively, but previous research has suggested that fatty acid synthesis becomes mother cell-specific following polar septation<sup>33</sup>. After engulfment completion, the forespore is surrounded by two lipid bilayers sandwiching a thin layer of peptidoglycan, a configuration that is highly reminiscent of the Gram (-) cell envelope. Since the inner and outer forespore membranes interface with the cytoplasm of different cells, there are likely mechanisms to ensure their coordinated growth. Consistent with this hypothesis, we have found that *Bacillus subtilis* encodes maintenance of outer membrane lipid asymmetry (Mla)

homologs. The Mla system in the Gram (-) bacterium *Escherichia coli* prevents the aberrant accumulation of phospholipids in the outer membrane by shuttling excess phospholipids back to the inner membrane<sup>34</sup>. Therefore, we can easily test the role of these homologs in lipid transport by blocking phospholipid synthesis using STRP and testing whether null mutants exhibit uncoupled membrane growth. Thus, sporulation could represent a powerful and non-essential model system in which to study membrane trafficking, a process common to Gram (-) bacteria, the eukaryotic nucleus, the mitochondrion, and the chloroplast. The manner in which membrane synthesis is coordinated between the mother cell and forespore is therefore a rich source of future inquiry.

### **Mechanisms of metabolic differentiation during spore formation**

Our results demonstrate that the metabolism of the forespore is dramatically reprogrammed during the transition to dormancy, leading to a profound metabolic differentiation of the mother cell and forespore shortly after polar septation. This finding constitutes one of the few examples of a large-scale metabolic differentiation of two genetically identical sister cells in bacteria, with heterocysts serving as the paradigmatic example<sup>35</sup>. We have identified two distinct processes that reduce the levels of metabolic enzymes in the forespore: dilution by forespore growth and degradation by YjbA-mediated proteolysis. Thus, it appears as though the sporangium has evolved redundant mechanisms to ensure the depletion of metabolic enzymes in the forespore, making forespore metabolic downregulation a highly robust process.

The extent of the proteolytic reprogramming of forespore metabolism remains to be determined. The only substrate of this pathway identified thus far is citrate synthase, however, it could be highly economical to only deplete the spore of enzymes functioning at critical metabolic junctions to facilitate the transition to and exit from dormancy. This strategy would allow metabolic flux into specific pathways to be blocked during

sporulation, but would also allow metabolism to be easily reconstituted through the synthesis of select metabolic enzymes when favorable conditions return. One candidate that fulfills these criteria and could be a potential substrate is MurAA, the enzyme that catalyzes the first committed step in peptidoglycan biosynthesis. Previous work has demonstrated that MurAA is subjected to ClpCP-mediated proteolysis under conditions of nutrient limitation, but degradation has not been observed using in vitro reconstitutions<sup>36</sup>. Therefore, it is possible that YjbA or another adaptor protein is required to stimulate ClpCP activity under these circumstances. Intriguingly, ClpCP has also been shown to mediate the proteolysis of several enzymes functioning at critical metabolic branch points, but the requirement of YjbA for this activity has never been tested<sup>37</sup>. Ultimately, trapping approaches will be useful in identifying a comprehensive list of substrates targeted for ClpCP-mediated proteolysis by YjbA, and to evaluate our model of targeting highly regulated metabolic junctions via this pathway<sup>38</sup>. Spores are also known to accumulate certain metabolic precursors, such as 3-phosphoglycerate<sup>39</sup>. It will be interesting to test whether metabolic models recapitulate the accumulation of these precursors in the absence of enzymes depleted from the forespore by YjbA and ClpCP.

The identification of a comprehensive list of substrates could allow for a bioinformatics-based elucidation of the signal eliciting YjbA recognition. Our preliminary work suggests that determinants at the N-terminus of CitZ might be required for degradation. The crystal structure of the *Pyrococcus furiosus* citrate synthase indicates that N-terminus is highly flexible, so it is possible that this could be a docking site for YjbA<sup>40</sup>. Additionally, our unpublished work indicates that substrate binding is required for citrate synthase to avoid proteolysis. Citrate synthase undergoes a pronounced conformational change upon substrate binding, opening up the possibility that the level of this enzyme, like many others, is regulated by substrate availability<sup>41,42</sup>. Much more

work is needed to fully elaborate the complex signals that target unwanted metabolic enzymes for proteolysis in the forespore.

Our results suggest that the lack of YjbA renders spores sensitive to oxidative stress. As the TCA cycle is a major source of electrons to drive the electron transport chain, spores may employ a strategy of inactivating the TCA cycle and oxidative metabolism until the cell is equipped to handle the burden of oxidative stress<sup>43,44</sup>. Consistent with this hypothesis, oxidative stress has been shown to exert its effects on the inner forespore membrane, where the electron transport chain resides<sup>45</sup>. It will be interesting to evaluate whether spores lacking YjbA evoke a stronger reactive oxygen species response than wild type. A clearer understanding of this phenotype will likely be achieved once a more comprehensive list of substrates is identified.

Altogether, the development of STRP represents a critical innovation to the study of spore formation, making longstanding hypotheses in the field finally accessible to empirical evaluation, and enabling the generation of countless new hypotheses. Our work with STRP has demonstrated that the mother cell and forespore rapidly become metabolically differentiated and that key metabolic enzymes are depleted from the forespore by ClpCP-mediated proteolysis, highlighting a set of fundamental principles governing the transition to and emergence from cellular dormancy. Since spore forming bacteria play critical roles in the rhizosphere and the human gut, understanding the processes of spore formation and spore revival at the molecular level will have long-ranging impacts on human health.

## References

1. Griffith, K. and Grossman, A. Inducible protein degradation in *Bacillus subtilis* using heterologous peptide tags and adaptor proteins to target substrates to the protease ClpXP. *Mol Microbiol.* **70**, 1012-1025 (2008).
2. Riley, E.P., Trinquier, A., Reilly, M.L., Durchon, M., Perera, V.R., Pogliano, K. & Lopez-Garrido, J. Spatiotemporally regulated proteolysis to dissect the role of vegetative proteins during *Bacillus subtilis* sporulation: cell-specific requirement of  $\sigma^H$  and  $\sigma^A$ . *Mol Microbiol.* **108**(1), 45-62 (2018).
3. Peters, J.M., Colavin, A., Shi, H., Czarny, T.L., Larson, M.H., Wong, S., Hawkins, J.S., Lu, C.H.S., Koo, B.M., Marta, E., Shiver, A.L., Whitehead, E.H., Weissman, J.S., Brown, E.D., Qi, L.S., Huang, K.C., and C.A. Gross. A comprehensive, CRISPR-based functional Analysis of Essential Genes in Bacteria. *Cell.* **165**(6), 1493-1506 (2016).
4. Fujita, M. and Losick, R. The master regulator for entry into sporulation in *Bacillus subtilis* becomes a cell-specific transcription factor after asymmetric division. *Genes Dev.* **17**, 1166–1174 (2003).
5. Eichenberger, P., Jensen, S.T., Conlon, E.M., Ooij, C., Van, Silvaggi, J., Gonzalez-Pastor, J.E., Fujita, M., Ben-Yehuda, S., Stragier, P., Liu, J.S., and Losick, R. The  $\sigma^E$  regulon and the identification of additional sporulation genes in *Bacillus subtilis*. *J Mol Biol.* **327**: 945–972 (2003).
6. Eichenberger, P., Fujita, M., Jensen, S.T., Conlon, E.M., Rudner, D.Z., and Wang, S.T. The program of gene transcription for a single differentiating cell type during sporulation in *Bacillus subtilis*. *PLoS Biol.* **2**: e328 (2004).
7. Vasudevan, P., Weaver, A., Reichert, E.D., Linnstaedt, S.D., and Popham, D.L. Spore cortex formation in *Bacillus subtilis* is regulated by accumulation of peptidoglycan precursors under the control of sigma K. *Mol Microbiol.* **65**: 1582–1594 (2007).
8. Setlow, P., and Kornberg, A. Biochemical studies of bacterial sporulation and germination. XXII. Energy metabolism in early stages of germination of *Bacillus megaterium* spores. *J Biol Chem.* **245**, 3637-3644 (1970).
9. Ghosh, S., Korza, G., Maciejewski, M., and Setlow, P. Analysis of Metabolism in Dormant Spores of *Bacillus* Species by  $^{31}\text{P}$  Nuclear Magnetic Resonance Analysis of Low-Molecular-Weight Compounds. *J Bacteriol.* **197**(5), 992-1001 (2015).
10. Sinai, L., Rosenberg, A., Smith, Y., Segev, E., and Ben-Yehuda, S. The molecular timeline of a reviving bacterial spore. *Mol Cell.* **57**(4), 695-707 (2015).
11. Yen Shin, J., Lopez-Garrido, J., Lee, S.-H., Diaz-Celis, C., Fleming, T., Bustamante, C., and Pogliano, K. Visualization and functional dissection of coaxial paired SpoIIIE channels across the sporulation septum. *eLife* **4**, e06474 (2015).
12. Choi, H., Kim, J.Y., Chang, Y.T., Nam, H.G. Forward chemical genetic screening. *Methods Mol Biol.* **1062**, 393-404 (2014).

13. Zheng, L. and Losick, R. Cascade regulation of spore coat gene expression in *Bacillus subtilis*. *J Mol Biol.* **212**(4), 645-660 (1990).
14. Daniel, R.A., Drake, S., Buchanan, C.E., Scholle, R., and Errington, J. The *Bacillus subtilis spoVD* gene encodes a mother-cell-specific penicillin-binding protein required for spore morphogenesis. *J Mol Biol.* **235**(1), 209-220 (1994).
15. Chen, N., Jiang, S., Klein, D., and Paulus, H. Organization and nucleotide sequence of the *Bacillus subtilis* diaminopimelate operon, a cluster of genes encoding the first three enzymes of diaminopimelate synthesis and dipicolinate synthase. *J Biol Chem.* **268**(13), 9448-9465 (1993).
16. Ramírez-Guadiana, F.H., Meeske, A.J., Rodrigues, C.D.A., Barajas-Orenlas, R.D.C., Kruse, A.C., and Rudner, D.Z. A two-step transport pathway allows the mother cell to nurture the developing spore in *Bacillus subtilis*. *PLoS Genet.* **13**(9), e1007015 (2017).
17. Meisner, J., Wang, X., Serrano, M., Henriques, A., and Moran, C. A channel connecting the mother cell and forespore during bacterial endospore formation. *Proc Natl Acad Sci.* **105**(39), 15100-15105 (2008).
18. Zeytuni, N., Hong, C., Flanagan, K.A., Worrall, L.J., Theiltges, K.A., Vuckovic, M., Huang, R.K., Massoni, S.C., Camp, A.H., Yu, Z., and Strynadka, N.C. Near-atomic resolution cryoelectron microscopy structure of the 30-fold homooligomeric SpoIIIAG channel essential to spore formation in *Bacillus subtilis*. *Proc Natl Acad Sci.* **114**(34), E7073-E7081 (2017).
19. Rodrigues, C.D., Henry, X., Neumann, E., Kurauskas, V., Bellard, L., Fichou, Y., Schanda, P., Schoehn, G., Rudner, D.Z., and Morlot, C. A ring-shaped conduit connects the mother cell and forespore during sporulation in *Bacillus subtilis*. *Proc Natl Acad Sci U.S.A.*, **113**, 11585–11590 (2016).
20. Camp, A. and Losick, R. A feeding tube model for activation of a cell-specific transcription factor during sporulation in *Bacillus subtilis*. *Genes Dev.* **23**, 1014-1024 (2009).
21. Doan, T., Morlot, C., Meisner, J., Serrano, M., Henriques, A., Moran, C., and Rudner, D.Z. Novel secretion apparatus maintains spore integrity and developmental gene expression in *Bacillus subtilis*. *PLoS Genet.* **5**(7), e1000566 (2009).
22. Pande, S., Merker, H., Bohl, K., Reichelt, M., Schuster, S., de Figueiredo, L. F., Kaleta, C., and Kost, C. Fitness and stability of obligate cross-feeding interactions that emerge upon gene loss in bacteria. *ISME J.* **8**(5), 953–962 (2014).
23. Volkenhoff, A., Weiler, A., Letzel, M., Stehling, M., Klämbt, C., and Schirmeier, S. Glial glycolysis is essential for neuronal survival in *Drosophila*. *Cell Metab.* **22**(3), 437–447 (2015).
24. Cumino, A.C., Marcozzi, C., Barreiro, R., and Salerno, G.L. Carbon cycling in *Anabaena* sp. PCC 7120 – Sucrose synthesis in the heterocysts and possible role in nitrogen fixation. *Plant physiol.* **143**(3), 1385-1397 (2007).

25. Martín-Figueroa, E., Navarro, F., and Florencio, F.J. The GS-GOGAT pathway is not operative in the heterocysts. Cloning and expression of *glsF* gene from the cyanobacterium *Anabaena* sp. PCC 7120. *FEBS Lett.* **476**(3), 282-286 (2000).
26. Henry, C.S., Zinner, J.F., Cohoon, M.P. and Stevens, R.L. iBsu1103: a new genome-scale metabolic model of *Bacillus subtilis* based on SEED annotations. *Genome Biol.* **10**(6), R69 (2009).
27. Kroos, L. Bacterial development: evidence for very short umbilical cords. *Curr Biol.* **19**(11), R452-3 (2009).
28. Nieves-Mori3n, M., Mullineaux, C.W., and Flores, E. Molecular diffusion through Cyanobacterial septal junctions. *MBio.* **8**(1), (2017).
29. Chiba, S., Coleman, K., and Pogliano, K. Impact of membrane fusion and proteolysis on SpoIIQ dynamics and interaction with SpoIIAH. *J Biol Chem.* **282**(4), 2576–2586 (2007).
30. Ireton, K. Jin, S., Grossman, A.D., and Sonenshein, A.L. Krebs cycle function is required for the activation of the Spo0A transcription factor in *Bacillus subtilis*. *Proc Natl Acad Sci USA.* **92**(7), 2845-2849 (1995).
31. Magill, N.G., Cowan, A.E., Koppel, D.E., and Setlow P. The internal pH of the forespore compartment of *Bacillus megaterium* decreases by about 1 pH unit during sporulation. *J Bacteriol.* **176**(8), 2252–2258 (1994).
32. Lopez-Garrido, J., Ojkic, N., Khanna, K., Wagner, F.R., Villa, E., Endres, R.G., and Pogliano, K. Chromosome translocation inflates *Bacillus subtilis* forespores and impacts cellular morphology. *Cell.* **172**(4), 758-770 (2018).
33. Pedrido, M.E., de Ona, P., Ramirez, W., Lenini, C., Goni, A., and Grau, R. Spo0A links *de novo* fatty acid synthesis to sporulation and biofilm development in *Bacillus subtilis*. *Mol Microbiol.* **87**(2), 348–367 (2013).
34. Malinverni, J.C., and Silhavy, T.J. An ABC transport system that maintains lipid asymmetry in the Gram-negative outer membrane. *Proc Natl Acad Sci USA.* **106**(19), 8009–8014 (2009).
35. Wood, N.B., and Haselkorn R., Control of phycobiliprotein proteolysis and heterocyst differentiation in *Anabaena*. *J. Bacteriol.* **141**(3), 1375-85 (1980).
36. Kock, H., Gerth, U., and Hecker, M. MurAA, catalysing the first committed step in peptidoglycan biosynthesis, is a target of Clp-dependent proteolysis in *Bacillus subtilis*. *Mol. Microbiol.* **51**(4), 1087-1102 (2004).
37. Gerth, U., Kock, H., Kusters, I., Michalik, S., Switzer, R.L., and Hecker, M. Clp-dependent proteolysis down-regulates central metabolic pathways in glucose-starved *Bacillus subtilis*. *J Bacteriol.* **190**(1), 321–331 (2008).

38. Trentini, D.B., Suskiewicz, M.J., Heuck, A., Kurzbauer, R., Deszcz, L., Mechtler, K., and Clausen, T. Arginine phosphorylation marks proteins for degradation by a Clp protease. *Nature*. **539**(7627), 48-53 (2016).
39. Nelson, D.L., and Kornberg, A. Biochemical studies of bacterial sporulation and germination. XIX. Phosphate metabolism during sporulation. *J. Biol. Chem.* **245**, 1137-1145 (1970).
40. Russell, R.J., Ferguson, J.M., Hough, D.W., Danson, M.J., and Taylor, G.L. The crystal structure of citrate synthase from the hyperthermophilic archaeon *Pyrococcus furiosus* at 1.9 Å resolution. *Biochemistry*. **36**(33), 9983-9994 (1997).
41. Bond, R.W., Field, A.S., and Switzer, R.L. Nutritional regulation of degradation of aspartate transcarbamylase and of bulk protein in exponentially growing *Bacillus subtilis* cells. *J Bacteriol.* **153**(1), 253-258 (1983).
42. Hu, P., and Switzer, R.L. Evidence for substrate stabilization in regulation of the degradation of *Bacillus subtilis* aspartate transcarbamylase in vivo. *Arch Biochem Biophys.* **316**(1), 260-266 (1995).
43. Sinai L., Rosenberg, A., Smith, Y., Segev, E., and Ben-Yehuda, S. The molecular timeline of a reviving bacterial spore. *Mol. Cell* **57**(4), 695–707 (2015).
44. Ibarra, J.R., Orozco, A.D., Rojas, J.A., López, K., Setlow, P., Yasbin, R.E., and Pedraza-Reyes, M. The Nfo and ExoA apurinic/aprimidinic endonucleases in repair of DNA damage during outgrowth of *Bacillus subtilis* spores. *J. Bacteriol.* **190**(6), 2031-2038 (2008).
45. Young, S.B., and Setlow, P. Mechanisms of killing of *Bacillus subtilis* spores by hypochlorite and chlorine dioxide. *J Appl Microbiol.* **95**(1): 54-67 (2003).